NASA CONTRACTOR REPORT

NASA CR-245

NASA CR-245

ANALYTICAL INVESTIGATION OF FLUID AMPLIFIER DYNAMIC CHARACTERISTICS VOLUME II

Prepared under Contract No. NAS 8-11236 *by*

SPERRY UTAH COMPANY

Salt Lake City, Utah

for

NATIONAL AERONAUTICS AND SPACE ADMINISTRATION • WASHINGTON, D. C. • JULY 1965

NASA CR-245

ANALYTICAL INVESTIGATION OF FLUID AMPLIFIER DYNAMIC CHARACTERISTICS

VOLUME II

Prepared under Contract No. NAS 8-11236 by
SPERRY UTAH COMPANY
Salt Lake City, Utah

for

NATIONAL AERONAUTICS AND SPACE ADMINISTRATION

For sale by the Clearinghouse for Federal Scientific and Technical Information
Springfield, Virginia 22151 - Price $6.00

28692

ABSTRACT
(VOLUME II)

Those aspects of dimensional analysis and similarity which are of most pertinence to fluid circuitry are discussed. The equations of fluid flow through both orifices and circular tubes are given and discussed. The equivalent parameters of passive fluid elements are presented, both steady-state and small-signal.

The instrumentation of fluids is discussed both for steady-state and time dependent measurements. Typical active devices are described, discussed, and compared. Specific attention is given to the impact modulator and its use in operational amplifiers. An equivalent circuit for the impact modulator is found.

The subject of circuit synthesis, and particularly transfer function synthesis, is discussed. The requirements of proportional fluid circuitry is discussed, and the use of equivalent circuits in the analysis of fluid circuits is presented through the discussion of specific circuits. Both steady-state and time varying examples are given.

The loop transfer function of an idealized, but typical, fluid control circuit is presented and analysed by the use of a Bode plot.

author

AUTHOR LIST

Author	Section
F. R. Goldschmied	All of Section 1.
H. L. Fox	All of Section 3. Part of Sections 4.2 and 4.3
D. L. Letham	All of Sections 2, 4.4, 4.5, 4.6 and 5. Part of Sections 4.2 and 4.3

TABLE OF CONTENTS

References
(Volume II)

1. Prandtl, L. and Tietjens, O. G. Applied Hydro- and Aeromechanics. Dover Publications, Inc.

2. Shearer, et al. Basic Research and Development in Fluid Power Control for the United States Air Force. Dynamic Analysis and Control Laboratory, Mechanical Engineering Laboratory. Massachusetts Institute of Technology, Cambridge, Mass. Progress Report No. 1. 1 Oct.-31 Jan. 1962

3. Streeter, Victor L. Handbook of Fluid Dynamics. McGraw Hill. 1961

4. Crane Company. Flow of Fluids Through Valves, Fittings, and Pipe. Technical Paper No. 410.

5. Raber, R. A. and Shinn. Fluid Amplifier Manual. Prepared for the Astrionics Laboratory, Marshall Space Flight Center, NASA, Huntsville, Alabama. Contract NAS 8-5408. September 1964.

6. Johnson Service Company. Final Report, Impact Modulator Amplifiers with Feedback, and Systems Applications. Contract No. DA 49-186-AMC-28(X) Prepared for Harry Diamond Laboratories.

7. Langhaar, H. L. Dimensional Analysis and Theory of Models. Wiley, 1951.

8. Sedov, L. I. Similarity and Dimensional Methods in Mechanics. Academic Press, 1959.

9. Patterson, John L. A Miniature Electrical Gage Utilizing a Stretched Flat Diaphragm. NACA Technical Note 2659.

10. Elrod, H. G. The Theory of Pulsating Flow in Conical Nozzles. ASME Paper 62-WA-221 1962

11. Belsterling and Tsui, Application Techniques for Proportional Pure Fluid Amplifiers. Proceedings of the Fluid Amplification Symposium, May 1964, Vol. II, page 163

12. Boothe, Willis A. A Lumped Parameter Technique for Predicting Analog Fluid Amplifier Dynamics. General Electric Co.

13. Zisfein and Curtiss: "A High Gain Proportional Fluid State Flow Amplifier," Proceedings of the Fluid Amplification Symposium, May 1964, Vol. 1, page 375.

14. Otsap, B. A.: Experimental Study of a Proportional Vortex Fluid Amplifier, Proceedings of the Fluid Amplification Symposium, May 1964, Vol. II, page 85.

Symbol List for Volume II

a	constant
A	Gain constant
b	constant
B	Constant
C	constant, flow coefficient, capacity, velocity of sound
D	orifice diameter, tube diameter
D_o	tube diameter
g	acceleration of gravity
f	frequency
f_c	break frequency
$G(s)$	transfer function
H	Fluid inductance
I	fluid current
I_r	reference current
k	ratio of specific heats
K	constant
K_1, K_2, K_3	gain constants
L	length
ΔL	length
M_a	Mach Number
n	polytropic exponent
P	pressure
P^*	critical pressure
P_o	mean pressure
P_1	upstream pressure
P_2	downstream pressure
P_t	throat pressure
ΔP	pressure drop
Q	volume flow
Q_o	mean volume flow
R_g	gas constant
R_e	Reynolds number
R_{eA}	Acoustic Reynolds Number
R	Resistance (general)
R_r	reference resistance
R_x	specific resistances
s	Laplace variable
S	Stokes Number
S_t	Strouhal Number
St_{LA}	Longitudinal Acoustic Strouhal Number
St_{TA}	Transverse Acoustic Strouhal Number
T_o	mean temperature
T	reference time
U	reference fluid velocity

u,v	general fluid velocities
u^*,v^*	dimensionless fluid velocities
$\bar{u}$	average fluid velocity
V	Fluid Velocity
x	distance
y	distance
Y	expansion coefficient
V	volume
ρ	mass density
γ	weight density
μ	viscosity
λ	dimensionless parameter
τ	time constant
θ	angle
ω	angular frequency
Ω	reference frequency

FLUID DYNAMICS FUNDAMENTALS

1.1 Introduction

A rapid growth has been seen in the past few years in the new technology of pure fluid amplifiers and pure fluid servo controls.

Pure fluid technology is based on some of the most sophisticated fluid dynamics phenomena encountered by the aerodynamicist, not to mention the control engineer, i.e. the problem of transient flow in a complex fluid network. As the response of the fluid amplifier is made faster and the circuit frequencies increase, these problems will become more and more acute.

The basic equations of motion of a viscous time-dependent flow, the Navier-Stokes eqs., are strongly non-linear and intractable analytically, even in the two-dimensional incompressible case.

In Volume I, Section 1.1, computational techniques are developed for the numerical solution of the equations for a limited flow field. Large computers will be needed to extend the flow field to the dimensions required by practical problems.

Furthermore, the Navier-Stokes equations are applicable strictly only to the laminar flow case, i.e., to such flows where the Reynolds Number remains below some limiting value (depending on the flow geometry).

Above this value, turbulent flow prevails, for which there is no exact mathematical description, because the number of unknowns exceed the number of available equations; additional empirical relationships have been formulated by many research workers to fit a variety of flow configurations, with varying success.

In view of the difficulties (even the impossibility, in case of turbulent flow) of adequate analytical treatment and since numerical solutions are not yet obtainable for flow fields of practical size, the aerodynamicist has relied heavily on experimental data and empirical investigations; this will also hold true, to an even higher degree, for the workers in the new pure fluid technology.

The purpose of this chapter is to discuss the necessity of employing dimensional analysis when relying on the empirical approach in fluid problems and in particular to present the Stokes-Reynolds Similarity Laws for dynamic flow circuits.

1.2 Dimensional Analysis.

1.2.1 General.

All phenomena in mechanics are determined by a series of variables, such as energy, velocity and mass, which take definite numerical values in given cases. Problems in dynamics or statics reduce to the determination of certain functions and characteristic parameters; the relevant laws of nature and geometrical relations are represented as functional equations, usually differential equations. In purely theoretical investigations, we use these equations to establish the general qualitative properties of the motion and to calculate the unknown physical variables by means of mathematical analysis. However, it is not always possible to solve a mechanics problem solely by the process of analysis and calculation. Sometimes the mathematical difficulties are too great, as in the case of laminar flow, and sometimes the problem cannot be formulated mathematically because the phenomenon to be investigated is much too complex to be described by a satisfactory theoretical model, as in the case of turbulent flow. In these cases, we have to rely mainly on experimental methods of investigation, to establish the essential physical features of the problem.

In general, we begin investigations of a natural phenomenon by finding out which physical properties are important and seeking relationships between such properties which govern the phenomenon.

Many phenomena cannot be investigated directly for practical reasons and therefore to determine the laws governing them we must perform experiments on similar phenomena which are easier and more convenient to handle. To set up the most suitable experiments, we must make a general qualitative analysis and bring out the essentials of the phenomenon in question; it is very important (and time-saving) to select the dimensionless parameters correctly. They should be as few as possible, while still reflecting all the fundamental effects.

The preliminary analysis of the phenomenon and the choice of a system of definite dimensionless parameters is made possible by the technique of dimensional analysis and similarity theory. These techniques have been developed to a high degree and have been presented by many authors, Langhaar[7], Sedov[8], etc.

In order to bring out the essential techniques and parameters in the most concise manner, a simple pipe flow will be investigated, comprising both a mean flow and an oscillatory component of small amplitude.

1.2.2 Dynamic and Steady-State Fluid Motion in a Pipe.

Let us consider a round pipe of diameter D and length L with a sinusoidal oscillatory flow of small amplitude and frequency ω over a mean flow Q_o; let the fluid be a viscous compressible gas.

All the parameters which seem pertinent to the problem will be listed below.

1.2.2.1 List of Physical Factors.

Gas Characteristics:

1.	Mass density, mean	ρ_o	$[\text{lb sec}^2/\text{ft}^4]$
2.	Absolute viscosity, mean	μ_o	$[\text{lb sec}/\text{ft}^2]$
3.	Ratio of specific heats	k	[0]
4.	Gas constant	R_g	$[\text{ft}/^\circ\text{R}]$

Heat Transfer Conditions:

5.	Polytropic exponent	n	[0]

Geometric Conditions:

6.	Pipe diameter	D	[ft]
7.	Pipe length	L	[ft]

Flow Conditions:

8.	Volumetric flow, mean	Q_o	$[\text{ft}^3/\text{sec}]$
9.	Pressure, mean (absolute)	P_o	$[\text{lb}/\text{ft}^2]$
10.	Temperature, mean (absolute)	T_o	$[^\circ\text{R}]$

Dynamic Conditions:

11.	Oscillatory frequency	ω	[rad/sec]

The lb notation refers to pounds force.

There are eleven parameters listed above; it is quite clear that the number of combinations and permutations of parameters will be extremely large, so that it is quite unproductive to undertake experimental work for a sufficient variation of each parameter to cover a meaningful range.

As this problem is a basically simple one in the fluid technology field, matters will be worse when complex fluid circuits will have to be studied experimentally and understood. Fluids employed will range from air at std. conditions to gaseous hydrogen at -250°F to hot combustion gases at 2000°F, in a pressure range from .1 PSIA to 1000 PSIA.

In this very confusing situation, in the absence of an adequate theoretical treatment, the aerodynamicist looks for his first basic tool, the Laws of Dynamic Similarity. The laws of similarity will allow building up an experimental solution of the problem with data from experiments under different sets of conditions.

The laws of similarity will allow the extrapolation of data under one set of conditions to another and different set of conditions, and will prescribe the correct conditions for a model experiment to be valid for a prototype.

The laws of similarity will also serve to classify quantitatively dynamic fluid regimes for generalized application to complex fluid circuits.

1.2.2.2 List of Dimensionless Parameters.

The following three dimensionless parameters have been found to be of basic importance for our problem:

1. Reynolds Number $R_e = \frac{U D \rho_o}{\mu_o}$

2. Acoustic Reynolds Number $R_{e_A} = \frac{C D \rho_o}{\mu_o}$

3. Stokes Number $S = \frac{\omega D^2 \rho_o}{\mu_o}$

where velocity of sound $C = \sqrt{k R_g T_g}$ or $\sqrt{n R_g T_g}$ (depending on heat transfer)

reference flow velocity $U = \frac{Q_o}{\frac{\pi}{4} D^2}$

Other dimensionless parameters, which can all be derived from the first three, have been found useful in particular ways:

4. Strouhal Number $St = \frac{S}{R_e} = \frac{\omega D}{U}$

5. Longitudinal Acoustic Strouhal Number $St_{LA} = \frac{S}{R_{e_A}} \cdot \frac{L}{D} = \frac{\omega L}{C}$

6. Transverse Acoustic Strouhal Number $St_{TA} = \frac{S}{R_{e_A}} = \frac{\omega D}{C}$

Finally, if the mean pipe flow velocity is sufficiently high, fluid compressibility effect must be accounted for by the mock number.

7. Mach Number $M_a = \frac{U}{C}$

Fortunately in fluid control technology, pipe velocities are generally low.

Seven dimensionless parameters are listed above; this number is still too high for indiscriminate application to practical experimental work. Previous aerodynamic experience, both theoretical and experimental, will serve to demonstrate the particular usefulness of each parameter to the experimenter.

If the Mach Number is neglected, there are only three basic parameters, the classical Reynolds and Stokes Numbers and another version of the Reynolds Number comprising the acoustical velocity in the pipe (instead of the flow velocity).

A discussion will be given below for each parameter, with supporting experimental evidence and physical interpretation as required.

1.2.3 The Reynolds Number.

The Reynolds Number may be derived from dimensional analysis

$$R_e = \frac{U D}{\nu} \left[\frac{\text{ft} \quad \text{ft sec}}{\text{sec ft}^2}\right] = \left[0\right]$$

Furthermore, it acquires fundamental significance from the fact that it can be derived from the steady-state Navier-Stokes eqs. of viscous fluid motion.

The steady-state Navier-Stokes eqs. are written in cylinderical coordinates r and x, with axial flow symmetry, for pipe flow below:

$$\rho\left(v\frac{\partial v}{\partial r} + u\frac{\partial v}{\partial x}\right) = -\frac{\partial p}{\partial r} + \mu\left(\frac{\partial^2 v}{\partial r^2} + \frac{1}{r}\frac{\partial v}{\partial r} - \frac{v}{r^2} + \frac{\partial^2 v}{\partial x^2}\right)$$

$$\rho\left(v\frac{\partial u}{\partial r} + u\frac{\partial u}{\partial x}\right) = \frac{\partial p}{\partial x} + \mu\left(\frac{\partial^2 u}{\partial r^2} + \frac{1}{r}\frac{\partial u}{\partial r} + \frac{\partial^2 u}{\partial x^2}\right)$$

where v is the velocity in the r direction

u is the velocity in the x direction

If now U, D and P are taken as references of velocity, length and pressure:

$$v^* = \frac{v}{U_o} \quad \text{and} \quad u^* = \frac{u}{U_o}$$

$$r^* = \frac{r}{D} \quad \text{and} \quad z^* = \frac{z}{D}$$

$$p^* = \frac{p}{P}$$

Then it is obtained for the steady-state Naview-Stokes eqs. after dividing each term by $\rho\frac{U^2}{D}$:

$$v^*\frac{\partial v^*}{\partial r^*} + u\frac{\partial v^*}{\partial x^*} = -\left[\frac{P}{\rho U^2}\right]\frac{\partial p^*}{\partial r} + \left[\frac{\mu}{\rho UD}\right]\left(\frac{\partial^2 v^*}{\partial r^{*2}} + \frac{1}{r^*}\frac{\partial v^*}{\partial r^*} - \frac{v^*}{r^{*2}} + \frac{\partial^2 v^*}{\partial x^{*2}}\right)$$

$$v^* \frac{\partial u^*}{\partial r^*} + u^* \frac{\partial u^*}{\partial x^*} = -\left[\frac{P}{\rho U^2}\right] \frac{\partial p^*}{\partial x^*} + \left[\frac{\mu}{\rho UD}\right] \left(\frac{\partial^2 u^*}{\partial r^{*2}} + \frac{1}{r^*} \frac{\partial u^*}{\partial r^*} + \frac{\partial^2 u^*}{\partial x^{*2}}\right)$$

The pipe flows can become similar only if the solutions expressed in terms of the coefficients $\left[\frac{P}{\rho U^2}\right]$ and $\left[\frac{\mu}{\rho U D}\right]$ are identical.

The first coefficient $\left[\frac{P}{\rho U^2}\right]$ is automatically satisfied in incompressible flow, leaving the coefficient $\left[\frac{\mu}{\rho U D}\right]$ as the criterion of similarity. This coefficient is the inverse of the Reynolds Number.

For our pipe problem, the Reynolds Number has been found indispensable for the correlation of steady-state pressure-loss data, regardless of pipe size, fluid velocity (flow rate) and fluid density and viscosity.

A pressure-loss coefficient may be defined as follows:

$$\frac{\Delta P}{\frac{1}{2}\rho U^2} = \lambda \frac{L}{D}$$

Figures 1.2.3-1 and 1.2.3-2 show the plot of λ against R_e.

A "laminar" fluid regime may be defined up to $R_e = 2000$ and a "turbulent" fluid regime may be defined from $R_e = 3300$. In the "transitional" area $2000 < R_e < 3300$ there is no clear correlation between λ and R_e.

Analitically, for the laminar case the Hagen-Poiseuille law holds:

$$\lambda = \frac{64}{R_e}$$

and for the turbulent case the Blasius law holds up to $R_e = 50{,}000$:

$$\lambda = \frac{0.316}{R_e^{\frac{1}{4}}}$$

For both cases, λ is a function of R_e alone.

Of interest in fluid technology instrumentation is the ratio of mean pipe velocity to center velocity, because in many cases a center measurement in a pipe must be made to yield total flow rate.

Again this ratio is <u>only</u> a function of R_e, as shown in Figures 1.2.3-3 and 1.2.3-4. There is to be noted that in the laminar regime this ratio is constant and equal to 0.5, and that the transitional area is wider, from $R_e = 1500$ to $R_e = 4500$.

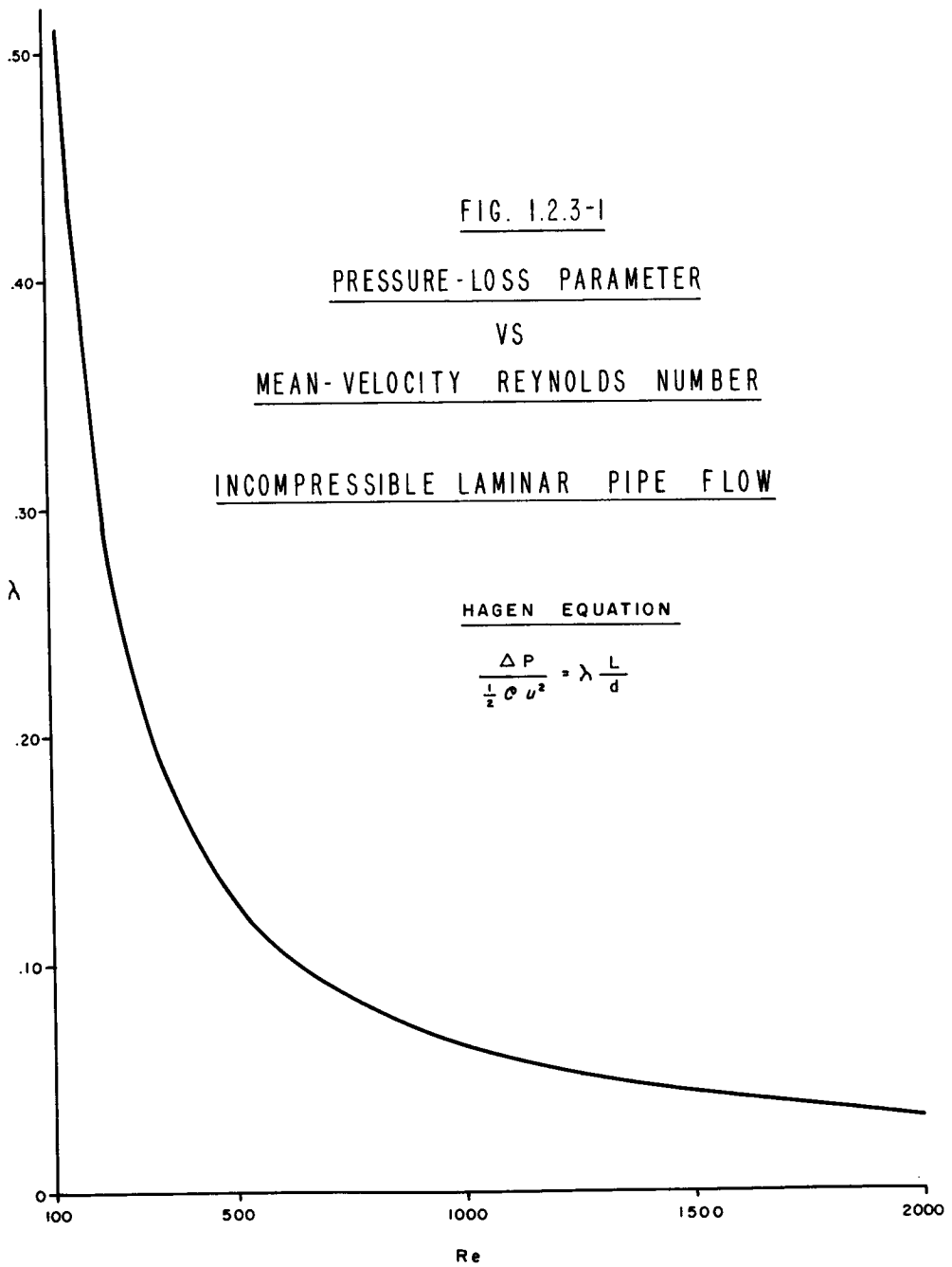

FIG. 1.2.3-1

PRESSURE-LOSS PARAMETER

VS

MEAN-VELOCITY REYNOLDS NUMBER

INCOMPRESSIBLE LAMINAR PIPE FLOW

HAGEN EQUATION

$$\frac{\Delta P}{\frac{1}{2}\rho u^2} = \lambda \frac{L}{d}$$

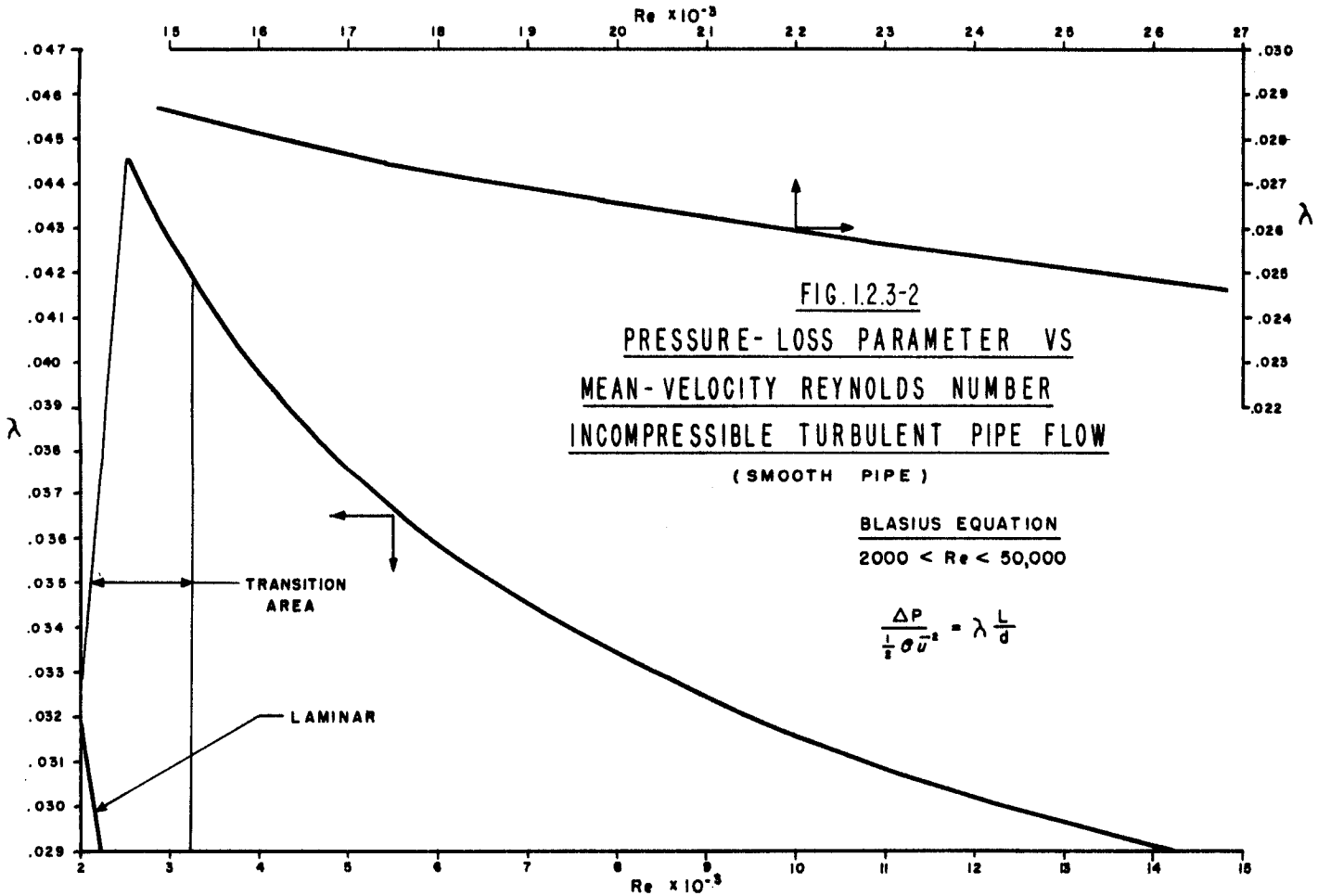

FIG. 1.2.3-2

PRESSURE-LOSS PARAMETER VS MEAN-VELOCITY REYNOLDS NUMBER INCOMPRESSIBLE TURBULENT PIPE FLOW

(SMOOTH PIPE)

BLASIUS EQUATION

$2000 < Re < 50{,}000$

$$\frac{\Delta P}{\frac{1}{2}\rho \bar{U}^2} = \lambda \frac{L}{d}$$

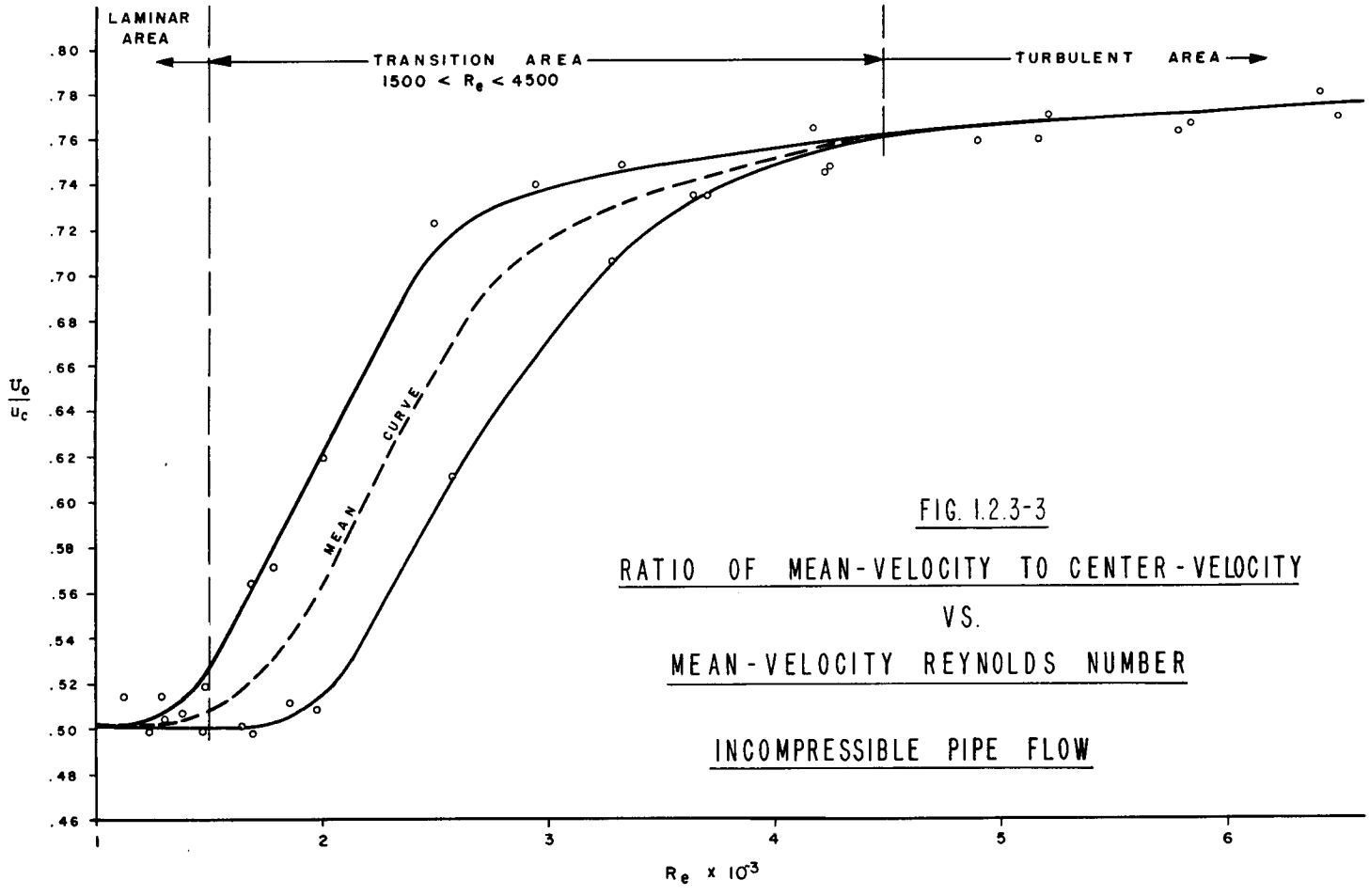

FIG. 1.2.3-3

RATIO OF MEAN-VELOCITY TO CENTER-VELOCITY

VS.

MEAN-VELOCITY REYNOLDS NUMBER

INCOMPRESSIBLE PIPE FLOW

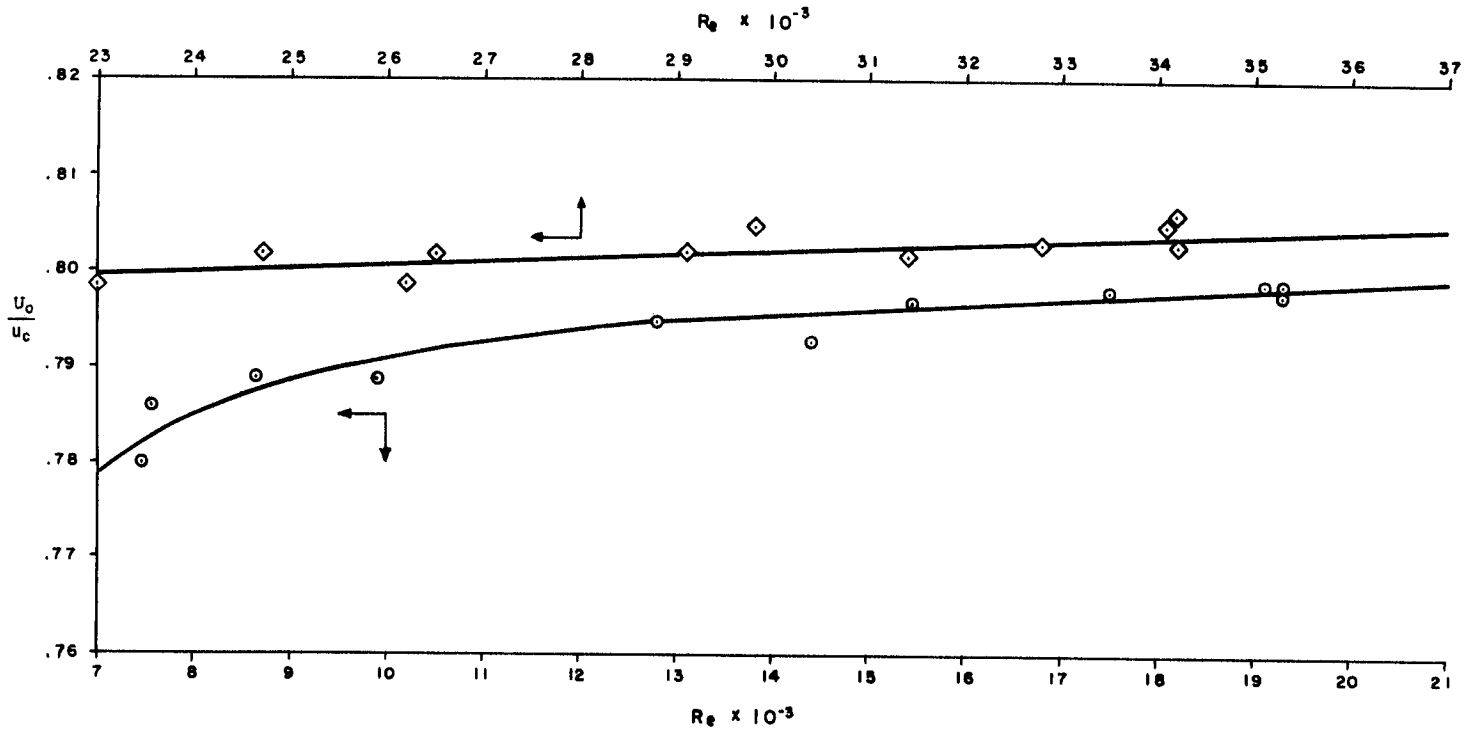

FIG. 1.2.3-4

RATIO OF MEAN-VELOCITY TO CENTER-VELOCITY VS MEAN-VELOCITY REYNOLDS NUMBER

INCOMPRESSIBLE TURBULENT PIPE FLOW

1.2.4 The Acoustical Reynolds Number

The Acoustical Reynolds Number may be derived from dimensional analysis:

$$R_{e_A} = \frac{CD}{\nu} \qquad \left[\frac{ft \quad ft\ sec}{sec \quad ft^2}\right] = \left[0\right]$$

It deviates from the classical Reynolds Number only by the use of the acoustical velocity C instead of the flow velocity U . Physically it can be interpreted as the ratio of acoustic inertia to viscous damping or as the limiting value of R_e.

It generally appears in dynamic fluid analysis only as a modifier of the Stokes Number, in the form $\frac{S}{R_{e_A}}$ and $\frac{S}{R_{e_A}^2}$.

1.2.5 The Stokes Number.

The Stokes Number may be derived from dimensional analysis:

$$S = \frac{\omega D^2}{\nu} \quad \left[\frac{ft^2\ sec}{sec\ ft^2}\right] = [0]$$

Furthermore, it acquires fundamental significance from the fact that it can be derived from the time-dependent vorticity transport equations.

These equations are transformations of the Navier-Stokes eqs. in term of the vorticity vector. Physically the vorticity ω is the angular velocity of a fluid element. In cartesian coordinates x and y, with velocity components u and v:

$$\omega = \tfrac{1}{2}\left(\frac{\partial v}{\partial x} - \frac{\partial u}{\partial y}\right)$$

The two-dimensional time-dependent Navier-Stokes equs. are reduced to:

$$\frac{\partial \omega}{\partial t} + u\frac{\partial \omega}{\partial x} + v\frac{\partial \omega}{\partial y} = \frac{\mu}{\rho}\left(\frac{\partial^2 \omega}{\partial x^2} + \frac{\partial^2 \omega}{\partial y^2}\right)$$

If the vorticity ω, the time t, the coordinates x and y and the velocities u and v are reduced to dimensionless ω^*, t^*, x^*, y^*, u^* and v^* by the introduction of reference quantities of frequency Ω, time T, length D and velocity V, then the vorticity equation will be governed by two dimensionless coefficients:

$$\frac{U}{\Omega D}$$

and

$$\frac{\nu}{D^2 \Omega}$$

The first coefficient is satisfied automatically while the second coefficient is the inverse of the Stokes Number.

Stokes' work antedates Reynolds' by more than thirty years, but for some reason the Stokes Number never achieved the popularity of the Reynolds Number. This is perhaps due to the fact that most fluid work has been directed toward steady-state phenomena.

For our pipe problem, the Stokes Number allows a physical interpretation as a dynamic damping index; it serves to classify dynamic fluid processes into arbitrary high-damping, intermediate-damping and low-damping regimes.

Experimentally, the Stokes Number will tell the investigator which frequency parameter to use to obtain a workable correlation for the amplitude attenuation ratio and the phase angle.

In conclusion, the Stokes Number is as basic to dynamic flows as the Reynolds Number is to steady-state flows.

1.2.6 The Strouhal Number.

The Strouhal Number may be derived from dimensional analysis:

$$St = \frac{\omega D}{U} \quad \left[\frac{\text{ft sec}}{\text{sec ft}}\right] = [0]$$

It is not a primary parameter because it can be derived as the ratio S/Re.

It does not contain viscosity and therefore it must be used either for theoretical "inviscid" flows or for conditions where the viscosity is negligible (as when the frequency is quite high). Also it has been found useful to correlate the frequency of self-oscillating fluid phenomena with the characteristics of the parent steady-state flow; here it would be plotted against Re.

An example of "inviscid" flow application is given in Figure 1.2.6-1, from the theoretical work of H. G. Elrod (Ref. 10), for pulsating flows in conical nozzles. The Strouhal Number is plotted against amplitude attenuation factor and phase angle for several subsonic Mach Numbers.

Obviously here the Stokes Number would not be applicable because of the absence of fluid viscosity from the analysis.

Two examples of self-oscillating fluid phenomena arising from steady-state flows are given in Figure 1.2.6-2 (the Karman Vortex Street) and in Figure 1.2.6-3 (typical Edge-tone). In both figures the Strouhal Number is plotted against the Reynolds Number.

A third example of self-oscillating fluid phenomenon arising from steady-state flows is given in Figure 1.2.6-4 (acoustic gap radiation). Here the Strouhal Number is plotted against Mach Number, for a given range of Reynolds Number (laminar boundary-layer flow over the plate), because the Mach effect predominates.

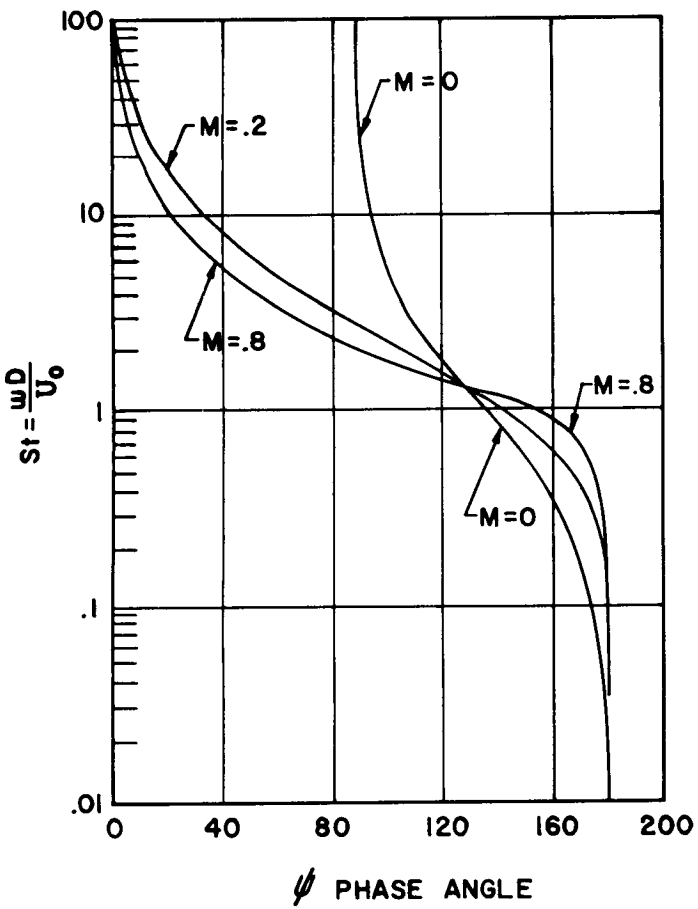

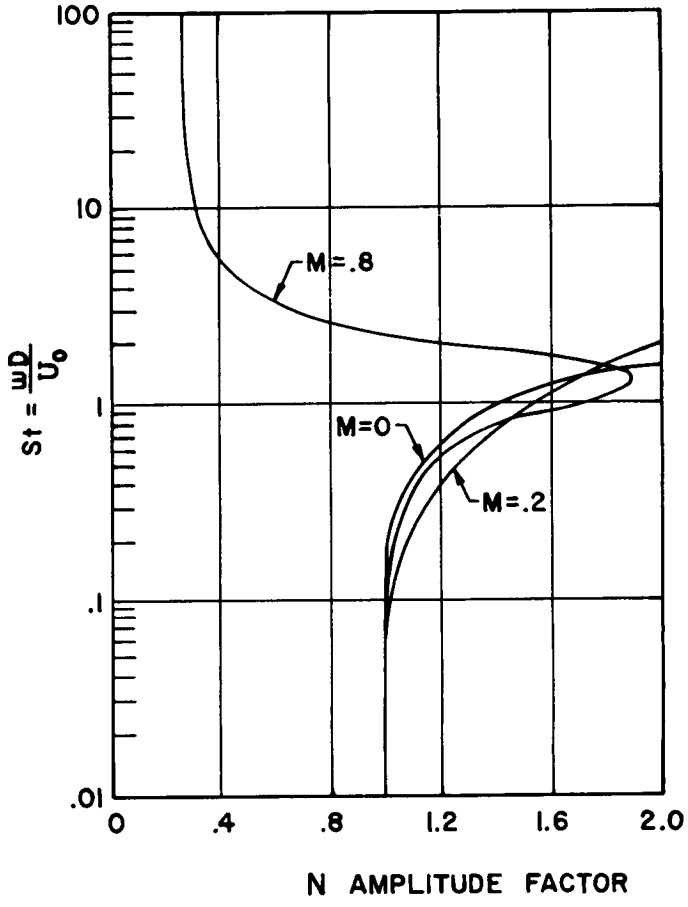

Figure 1.2.6-1 Conical nozzle with sinusoidally fluctuating exit pressure

Where P_{exit} is some P(ω)

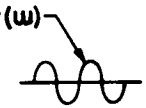

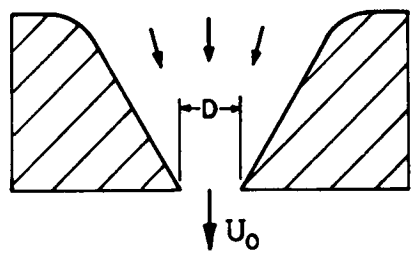

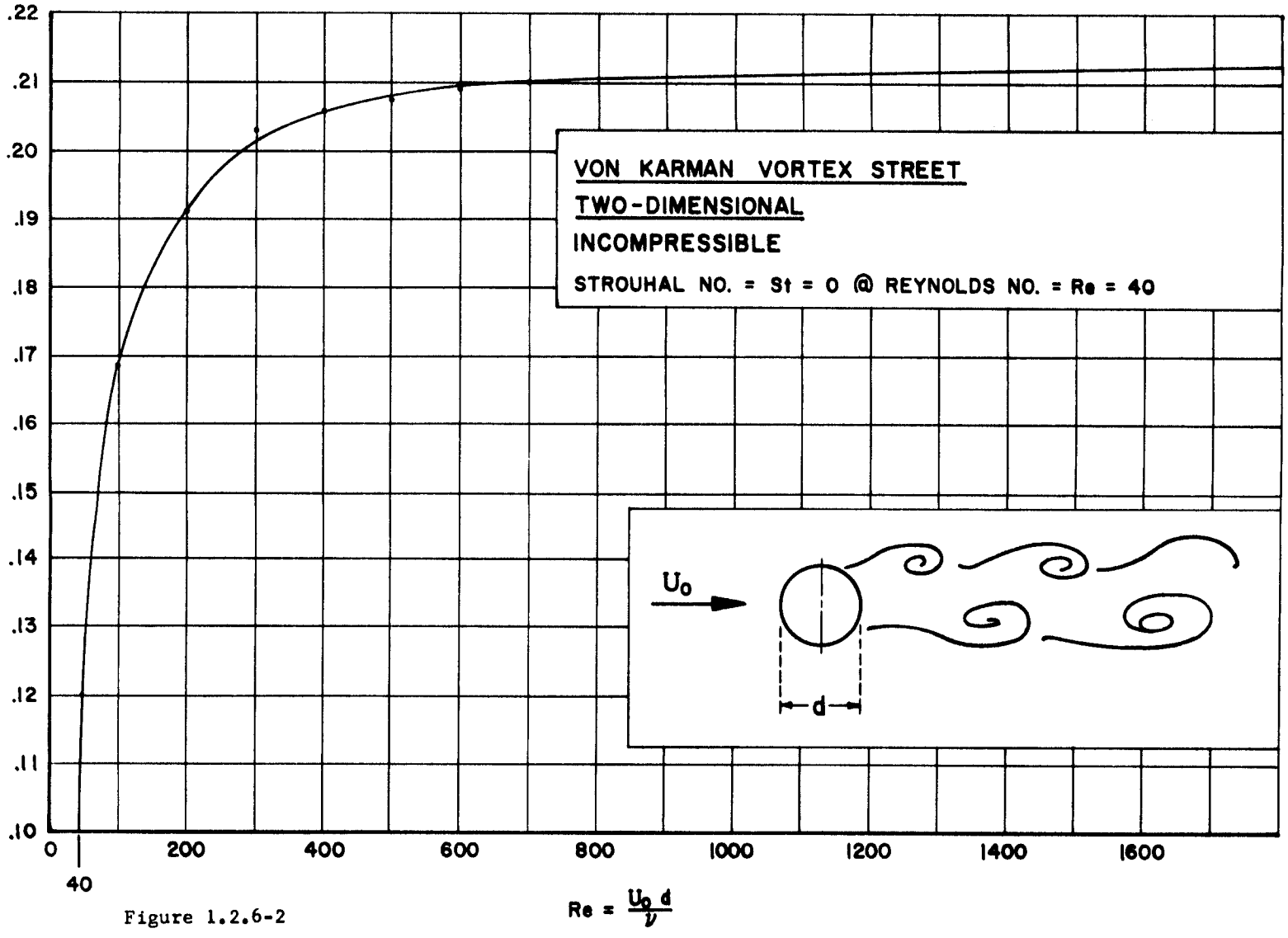
VON KARMAN VORTEX STREET
TWO-DIMENSIONAL
INCOMPRESSIBLE
STROUHAL NO. = St = 0 @ REYNOLDS NO. = Re = 40
U_o
d
$St = \frac{f d}{U_o}$
$Re = \frac{U_o d}{\nu}$
.22
.21
.20
.19
.18
.17
.16
.15
.14
.13
.12
.11
.10
0
40
200
400
600
800
1000
1200
1400
1600

Figure 1.2.6-2

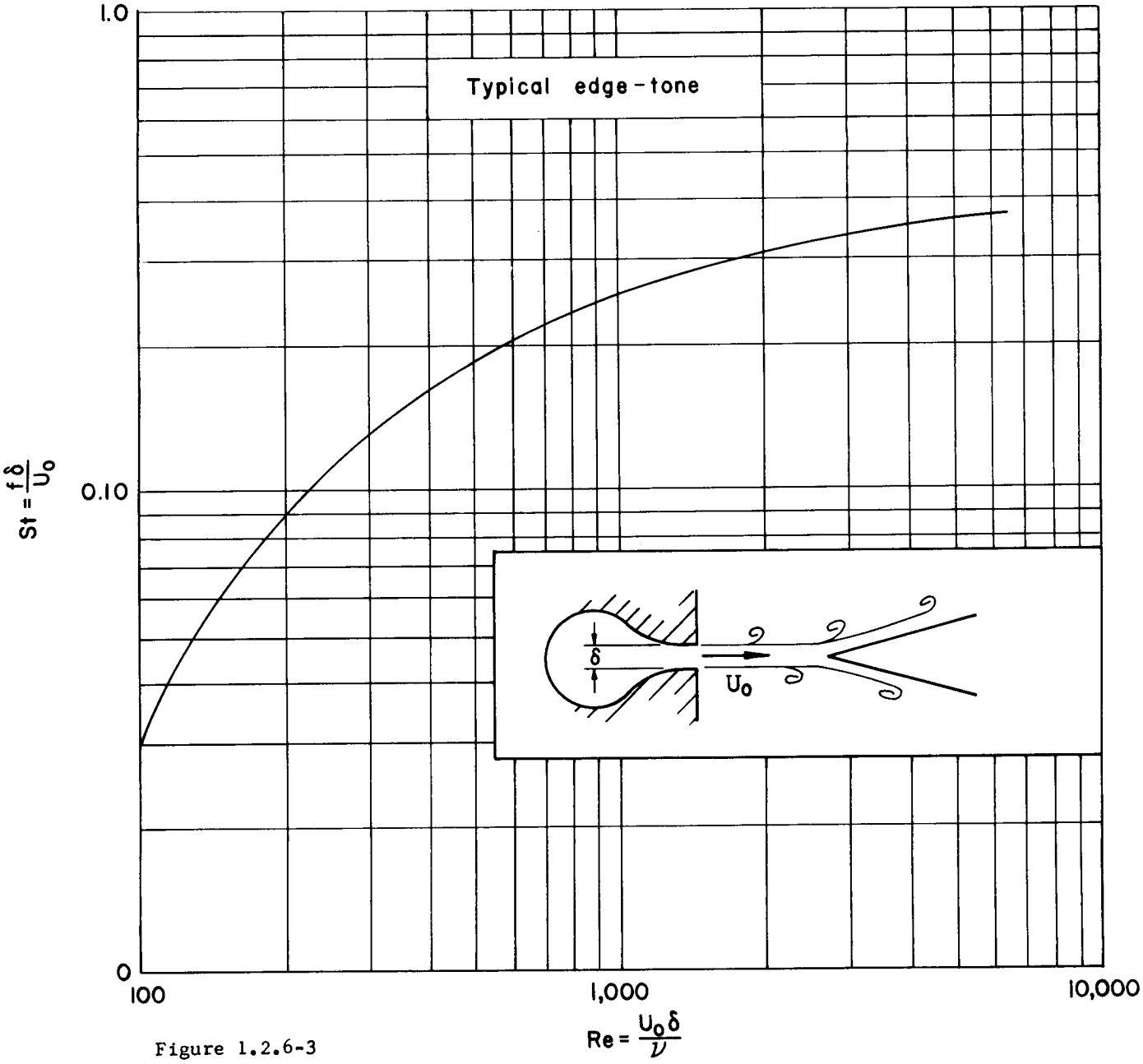
Typical edge-tone
1.0
0.10
0
100
1,000
10,000
$St = \frac{f\delta}{U_o}$
$Re = \frac{U_o \delta}{\nu}$
δ
U_o

Figure 1.2.6-3

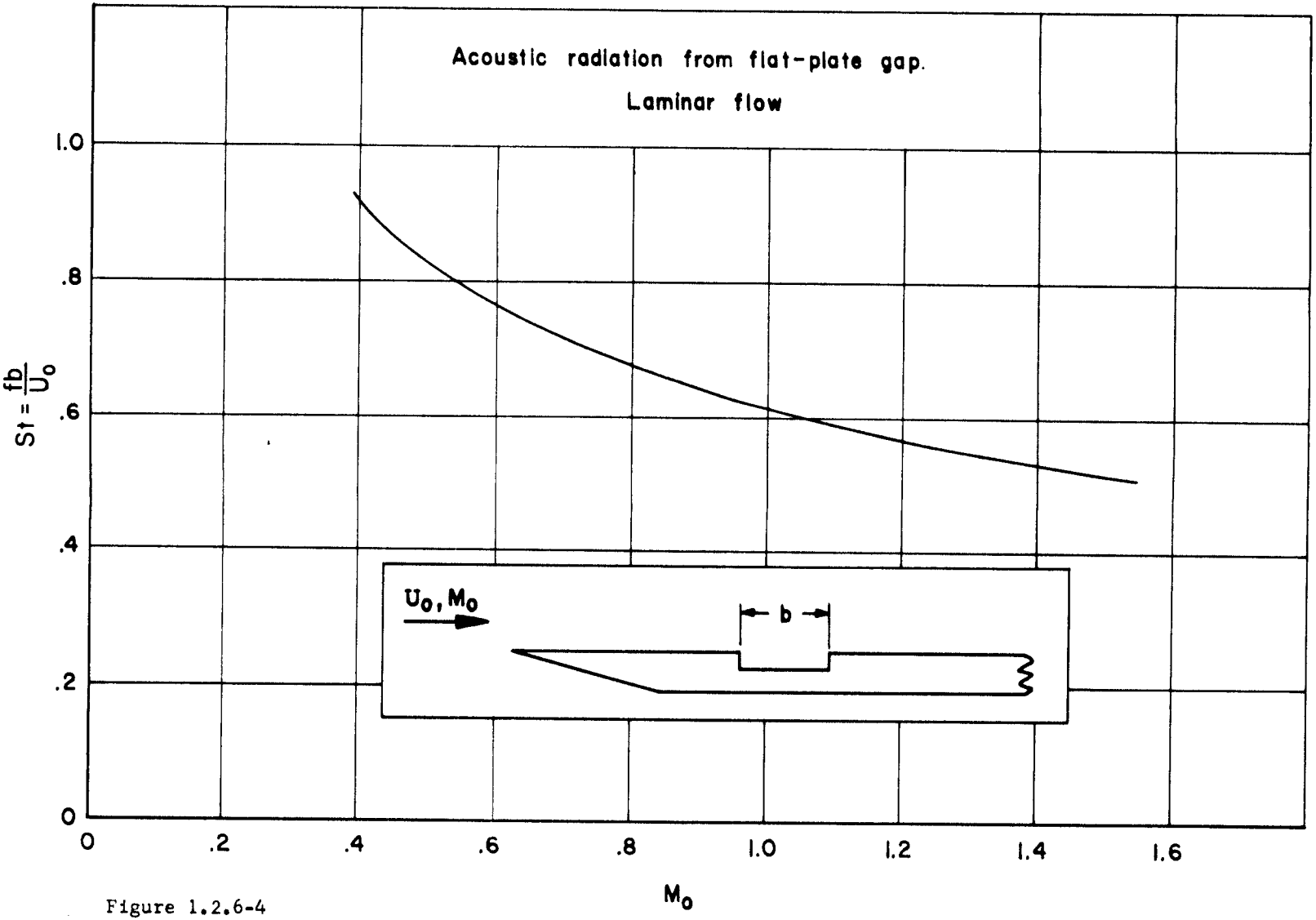
Acoustic radiation from flat-plate gap.
Laminar flow
St = fb/U0
1.0
.8
.6
.4
.2
0
0
.2
.4
.6
.8
1.0
1.2
1.4
1.6
M0
U0, M0
b

Figure 1.2.6-4

1.2.7 The Longitudinal Acoustic Strouhal Number.

The longitudinal acoustic Strouhal Number is a special form of the Strouhal Number, where the pipe length L is used, rather than the diameter D, and the velocity of sound C is used, rather than the flow velocity U.

$$St_{LA} = \frac{\omega L}{C}$$

It can be derived from the Stokes Number, the Acoustic Reynolds Number, and the pipe aspect ratio.

$$St_{LA} = \frac{S}{Re_A} \cdot \frac{L}{D}$$

It is used as the frequency parameter in the low-damping regime, where the acoustic effects become predominant.

1.2.8 The Transverse Acoustic Strouhal Number.

The Transverse Acoustic Strouhal Number is a special form of the Strouhal Number, where the velocity of sound C is used, rather than the flow velocity U.

$$St_{TA} = \frac{\omega D}{C}$$

It can be derived from the Stokes Number and the Acoustic Reynolds Number:

$$St_{TA} = \frac{S}{R_{e_A}}$$

It is used as a limiting criterion for the application of simple longitudinal-wave acoustic theory in a pipe because it predicts the onset of transverse acoustic waves.

The lowest transverse acoustical mode in a pipe is the first asymmetrical mode, which occurs at:

$$St_{TA} = 3.68$$

1.2.9 The Mach Number.

The Mach Number is the ratio of flow velocity U to the velocity of sound C. Above a Mach Number value of 0.2 to 0.3, the flow pattern will begin to change because of the fluid compressibility. In general pipe flow velocities are kept low ($M < 0.2$) to reduce pressure losses.

In the active amplifiers, however, analysis of the jet may require the application of Mach Number because velocities may be high, even supersonic.

1.3 Laws of Stokes - Reynolds Similarity.

For two pipe flows of equal $\frac{L}{D}$ ratio to be equivalent in both steady and dynamic states, the three basic dimensionless parameters #1, #2 and #3 must be equal. This, of course, applies if the flow velocity is low enough that Mach Number effects can be neglected. Otherwise four parameters must be kept equal.

Using subscript 1 for the one flow and subscript 2 for the other flow, it can be written:

$$R_e = \frac{U_1 D_1 \rho_1}{\mu_1} = \frac{U_2 D_2 \rho_2}{\mu_2} \tag{1}$$

$$R_{e_A} = \frac{C_1 D_1 \rho_1}{\mu_1} = \frac{C_2 D_2 \rho_2}{\mu_2} \tag{2}$$

$$S = \frac{\omega_1 D_1^2 \rho_1}{\mu_1} = \frac{\omega_2 D_2^2 \rho_2}{\mu_2} \tag{3}$$

From eq. (1):

$$\frac{\mu_2}{\mu_1} = \frac{U_2}{U_1} \frac{D_2}{D_1} \frac{\rho_2}{\rho_1} \tag{4}$$

From eq. (2):

$$\frac{\mu_2}{\mu_1} = \frac{C_2}{C_1} \frac{D_2}{D_1} \frac{\rho_2}{\rho_1} \tag{5}$$

From eq. (3):

$$\frac{\mu_2}{\mu_1} = \frac{\omega_2}{\omega_1} \frac{D_2^2}{D_1^2} \frac{\rho_2}{\rho_1} \tag{6}$$

Since all three eqs. must be valid by definition:

$$\frac{U_2}{U_1} \frac{D_2}{D_1} \frac{\rho_2}{\rho_1} = \frac{C_2}{C_1} \frac{D_2}{D_1} \frac{\rho_2}{\rho_1} = \frac{\omega_2}{\omega_1} \frac{D_2^2}{D_1^2} \frac{\rho_2}{\rho_1} \tag{7}$$

Therefore: $$\frac{U_2}{U_1} = \frac{C_2}{C_1} = \frac{\omega_2}{\omega_1}\,\frac{D_2}{D_1} \qquad (8)$$

and

$$\frac{U_2}{U_1} = \frac{C_2}{C_1} = \frac{\omega_2}{\omega_1}\,\frac{D_2}{D_1}$$

$$\frac{C_2}{C_1} = \frac{U_2}{U_1} = \frac{\omega_2}{\omega_1}\,\frac{D_2}{D_1}$$

$$\frac{\omega_2}{\omega_1} = \frac{C_2}{C_1}\,\frac{D_1}{D_2} = \frac{U_2}{U_1}\,\frac{D_1}{D_2}$$

$$\frac{D_2}{D_1} = \frac{U_2}{U_1}\,\frac{\omega_1}{\omega_2} = \frac{C_2}{C_1}\,\frac{\omega_1}{\omega_2}$$

Stokes-Reynolds Similarity Laws for Constant Fluid Viscosity (9)

Again from eq. (1):

$$\frac{D_2}{D_1} = \frac{U_1 \rho_1 \mu_2}{\mu_1 U_2 \rho_2} = \frac{U_1}{U_2}\,\frac{\rho_1}{\rho_2}\,\frac{\mu_2}{\mu_1} \qquad (10)$$

and from eq. (2):

$$\frac{D_2}{D_1} = \frac{C_1 \rho_1 \mu_2}{\mu_1 C_2 \rho_2} = \frac{C_1}{C_2}\,\frac{\rho_1}{\rho_2}\,\frac{\mu_2}{\mu_1} \qquad (11)$$

and from eq. (3):

$$\frac{D_2^2}{D_1^2} = \frac{\omega_1 \rho_1 \mu_2}{\mu_1 \omega_2 \rho_2} = \frac{\omega_1}{\omega_2}\,\frac{\rho_1}{\rho_2}\,\frac{\mu_2}{\mu_1} \qquad (12)$$

Since all three must be valid by definition:

$$\frac{U_1}{U_2}\,\frac{\rho_1}{\rho_2}\,\frac{\mu_2}{\mu_1} = \frac{C_1}{C_2}\,\frac{\rho_1}{\rho_2}\,\frac{\mu_2}{\mu_1} = \left(\frac{\omega_1}{\omega_2}\right)^{\frac{1}{2}} \left(\frac{\rho_1}{\rho_2}\right)^{\frac{1}{2}} \left(\frac{\mu_2}{\mu_1}\right)^{\frac{1}{2}} \qquad (13)$$

Therefore:

$$\frac{U_1}{U_2} \left(\frac{\rho_1}{\rho_2}\right)^{\frac{1}{2}} \left(\frac{\mu_2}{\mu_1}\right)^{\frac{1}{2}} = \frac{C_1}{C_2} \left(\frac{\rho_1}{\rho_2}\right)^{\frac{1}{2}} \left(\frac{\mu_2}{\mu_1}\right)^{\frac{1}{2}} = \left(\frac{\omega_1}{\omega_2}\right)^{\frac{1}{2}} \qquad (14)$$

Thus:

$$\left.\begin{aligned}
&\frac{U_2}{U_1} = \frac{C_2}{C_1} = \left(\frac{\omega_2}{\omega_1}\right)^{\frac{1}{2}} \left(\frac{\rho_1}{\rho_2}\right)^{\frac{1}{2}} \left(\frac{\mu_2}{\mu_1}\right)^{\frac{1}{2}} \\
&\frac{C_2}{C_1} = \frac{U_2}{U_1} = \left(\frac{\omega_2}{\omega_1}\right)^{\frac{1}{2}} \left(\frac{\rho_1}{\rho_2}\right)^{\frac{1}{2}} \left(\frac{\mu_2}{\mu_1}\right)^{\frac{1}{2}} \\
&\frac{\omega_2}{\omega_1} = \left(\frac{U_2}{U_1}\right)^2 \frac{\rho_2}{\rho_1} \frac{\mu_1}{\mu_2} = \left(\frac{C_2}{C_1}\right)^2 \frac{\rho_2}{\rho_1} \frac{\mu_1}{\mu_2} \\
&\frac{\mu_2}{\mu_1} = \left(\frac{U_2}{U_1}\right)^2 \frac{\omega_1}{\omega_2} \frac{\rho_2}{\rho_1} = \left(\frac{C_2}{C_1}\right)^2 \frac{\omega_1}{\omega_2} \frac{\rho_2}{\rho_1} \\
&\frac{\rho_2}{\rho_1} = \left(\frac{U_1}{U_2}\right)^2 \frac{\omega_2}{\omega_1} \frac{\mu_2}{\mu_1} = \left(\frac{C_1}{C_2}\right)^2 \frac{\omega_2}{\omega_1} \frac{\mu_2}{\mu_1}
\end{aligned}\right\} \begin{array}{l}\underline{\text{Stokes-Reynolds}} \\ \underline{\text{Similarity Laws}} \\ \underline{\text{for}} \\ \underline{\text{Constant}} \\ \underline{\text{Pipe Diameter}}\end{array} \qquad (15)$$

Interpreting the results of eq. (9), it is seen that scaling procedures are prescribed for the velocity U, the velocity of sound C, the frequency ω and the pipe diameter D if the fluid viscosity μ is kept constant. The mass density ρ does not appear in the similarity laws for constant fluid viscosity and therefore it does not need to be considered.

The absolute temperature T enters into the problem through the velocity of sound $C = \sqrt{R_g T g}$. The thermodynamic fluid properties k and R_g enter only through the velocity of sound, as shown above.

Interpreting the results of equation (15), it is seen that scaling procedures are prescribed for the velocity U, the velocity of sound C, the frequency ω, the fluid viscosity μ and the fluid mass density ρ if the pipe diameter D is kept constant.

The absolute temperature T enters into the problem through the velocity of sound $C = \sqrt{R_g T g}$, through the temperature-dependent fluid viscosity μ and through the fluid mass density ρ.

The thermodynamic fluid properties γ and R enter the problem through the velocity of sound, as shown above, and through the fluid mass density ρ.

The absolute pressure does not enter the problem except for a minor influence on μ.

It remains to demonstrate explicity that both the steady-state characteristics (pressure-loss coefficient and transverse velocity distribution) and the dynamic characteristics (amplitude attenuation ratio and phase angle) are maintained between a model pipe flow (subscript 1) and a prototype pipe flow (subscript 2) if the Reynolds Number, the Acoustic Reynolds Number and the Stokes Number are kept constant.

It is well known and it has been summarized in Section 2.2.1 that all steady-state characteristics are dependent only on the Reynolds Number (in the absence of Mach Number effects). In Chapter 2, Volume I it has been shown theoretically that the amplitude attenuation ratio and the phase angle are functions (for a given geometry) of a parameter χ_{To} or Z and of the Stokes Number. The choice of χ_{To} or Z depends on the range of the Stokes Number.

Now $$\chi_{To} = \omega \frac{\mu_o}{np_o} \left(\frac{L}{D}\right)^2$$

However $$\mu_o = \rho_o \nu_o$$

and $$\frac{np_o}{\rho_o} = nR_g Tg = C^2 \quad \text{(polytropic velocity of sound)}$$

Thus $$\chi_{To} = \omega \frac{\nu_o}{C^2} \left(\frac{L}{D}\right)^2$$

and $$\chi_{To} = \left(\frac{\omega D^2}{\nu_o}\right) \left(\frac{\nu^2}{C^2 D^2}\right) \left(\frac{L}{D}\right)^2 = \frac{S}{R_{eA}^2} \left(\frac{L}{D}\right)^2$$

It is seen that, since the $\frac{L}{D}$ ratio is constant by definition of geometric pipe similarity, then the parameter χ_{To} depends only the the Stokes Number and the Acoustic Reynolds Number.

If these two numbers are constant, then χ_{To} will be constant.

Furthermore $$Z = \frac{\omega L}{C} = St_{LA} \text{ (the Longitudinal Acoustic Stroubal Number)}$$

and $$Z = \frac{\omega L D^2 \nu}{C\ D^2 \nu} = \left(\frac{\omega D^2}{\nu}\right) \left(\frac{\nu}{CD}\right) \left(\frac{L}{D}\right)$$

thus $$Z = \frac{S}{R_{eA}} \left(\frac{L}{D}\right)$$

Again the parameter Z depends only on the Stokes Number and on the Acoustic Reynolds Number, the ratio $\frac{L}{D}$ being constant by definition of geometric pipe similarity.

Therefore, if the theory of Chapter 2, Volume I is even qualitatively correct, all the flow characteristics, both steady-state and dynamic, are maintained if the three basic dimensionless parameters, Reynolds Number, Acoustic Reynolds Number and Stokes Number, are constant.

For convenience of application of the Similarity Laws, the viscosity and mass density of air at 60^{o} F and of gaseous hydrogen at -250^{o} are given in Figure 1.3-1, plotted against absolute pressure. It is seen that the two gases have substantially different characteristics, which will be reflected in the scaling ratios.

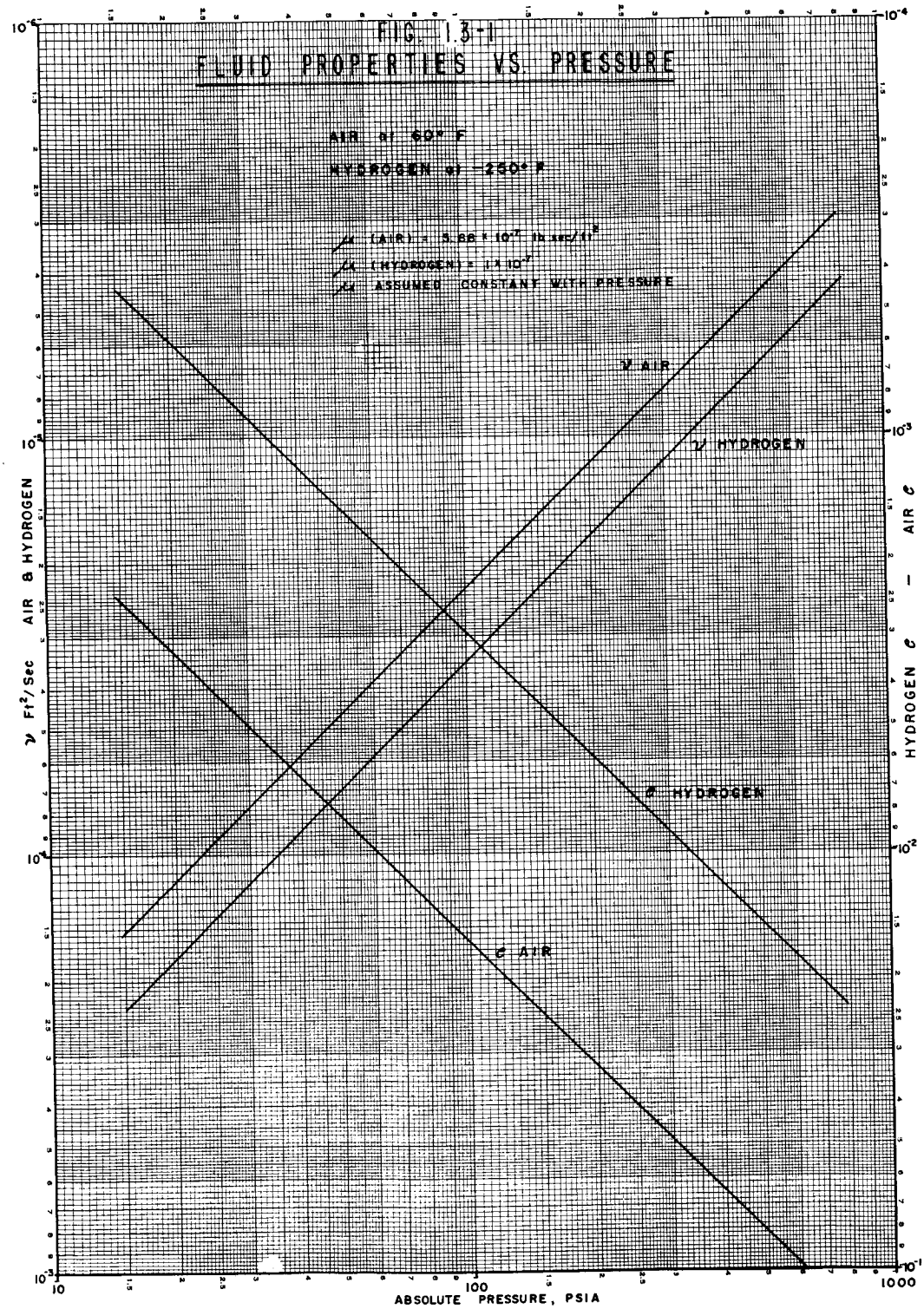
FIG. 1.3-1
FLUID PROPERTIES VS. PRESSURE
AIR @ 60° F
HYDROGEN @ -250° F
ν (AIR) = 5.88 × 10⁻⁴ in sec/(ft)²
ν (HYDROGEN) = 1.4 × 10⁻³
ρ ASSUMED CONSTANT WITH PRESSURE
ν AIR
ν HYDROGEN
ρ HYDROGEN
ρ AIR
ν Ft²/Sec AIR & HYDROGEN
HYDROGEN ρ — AIR ρ
ABSOLUTE PRESSURE, PSIA
10
100
1000

1.4 Conclusions.

It has been shown that the steady-state and dynamic flow of a viscous compressible fluid in a pipe depends only on three dimensionless fluid parameters, i.e. the Reynolds Number, the Acoustical Reynolds Number and the Stokes Number, plus the geometric pipe aspect ratio.

Similarity (scaling) laws have been derived for the case of constant fluid viscosity and for the case of constant pipe diameter. These will permit the extrapolation of experimental data, amplitude ratio and phase angle, to other sets of conditions.

2. PASSIVE CIRCUIT ELEMENTS

The passive fluid elements of most interest to the fluid circuit designer are tubes and orifices. The pressure-flow relations for these elements have been extensively investigated, both analytically and experimentally. In this section, these relations shall be presented and discussed. The general equations apply to any fluid. However, air is probably the most widely used control fluid, particularly in the pure fluid (no moving parts) control field. For this reason, specific examples of many of the general equations shall be given for air at room temperature.

2.1 Steady State Flow

2.1.1 Reynolds Number

In fluid control circuits, the pressure-flow relationship for fluid flow through a round tube is of interest. In this case, as in all fluid flows, the transition between laminar and turbulent flow depends upon the Reynolds number

$$R_e = \frac{\rho \bar{u} D}{\mu} \tag{1}$$

where

ρ = the fluid density

$\bar{u}$ = average fluid velocity

D = diameter of the pipe

μ = viscosity of the fluid

It has been found by experiment in a great many physical situations that for Reynold's numbers less than 2000 the flow is always laminar. For Reynolds numbers greater than 4000 the flow is always turbulent. In between Reynolds numbers of 2000 and 4000 the flow can be either laminar, turbulent, or in a transition stage, depending upon conditions. In the transition stage, no known law serves to describe the fluid behavior.

The fluid current, or the weight flow down a tube, is given by

$$I = \gamma Q \tag{2}$$

where γ is the specific weight of the fluid and Q is the volume flow through the tube. In terms of weight flow the Reynolds number becomes

$$R_e = \frac{4I}{\pi g \mu D} \tag{3}$$

where D is the diameter of the tube. This can be rewritten in terms of a reference current I_r as

$$R_e = \frac{I}{I_r} \tag{4}$$

Where

$$I_r = \frac{\pi g \mu D}{4} \tag{5}$$

For air, $g\mu = 10^{-6}$ lbf/sec-in. Therefore

$$I_r = 7.85 \times 10^{-7} D \qquad (6)$$

The flow through a tube enters the transition region between laminar and turbulent flow at 2000 I_r and leaves it at 4000 I_r. Plots of I versus D, showing the fluid flow regions is given in Figure 2.1.1-1.

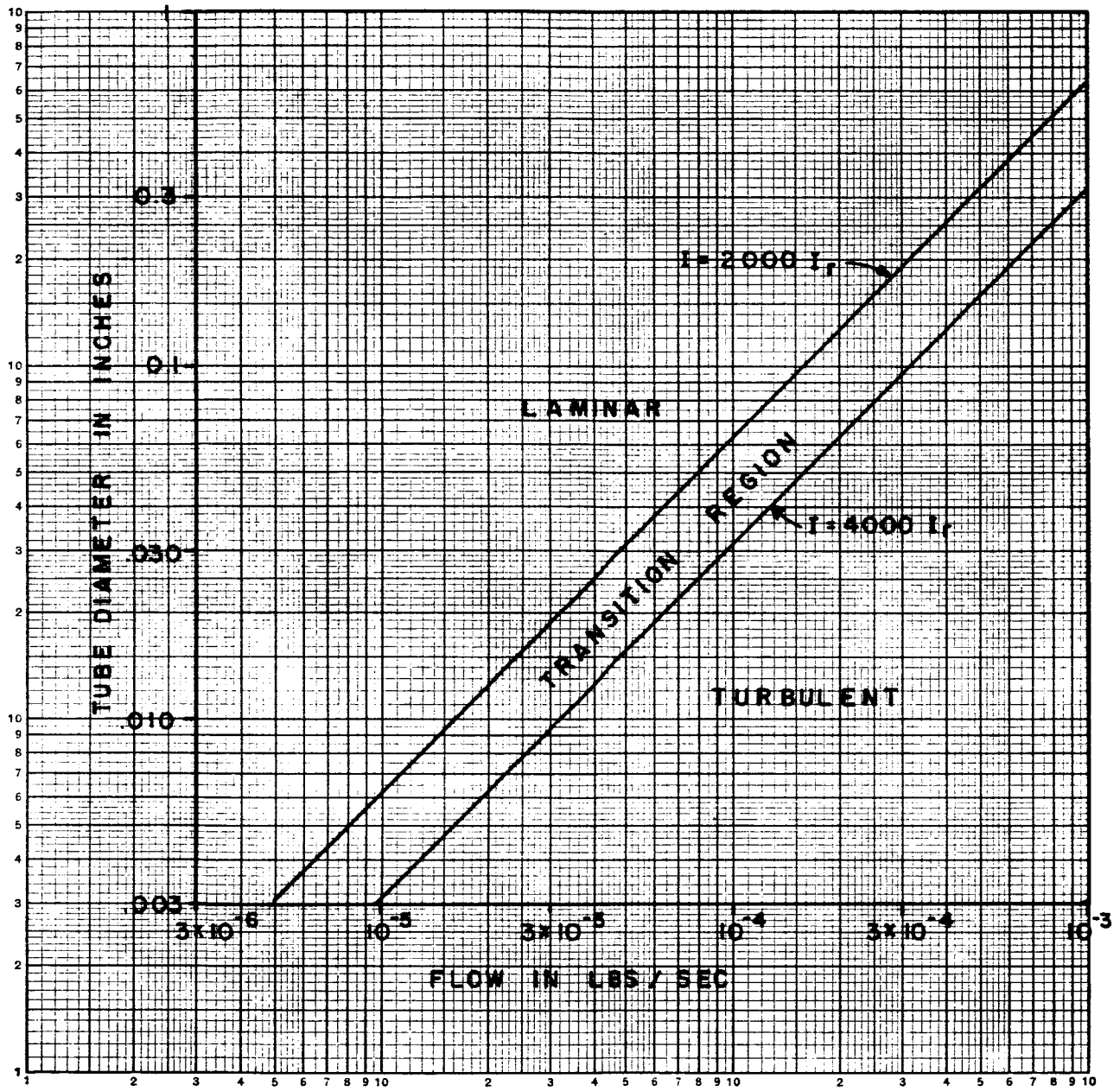

Figure 2.1.1-1 Laminar and turbulent regions for air flowing through tubes.

2.1.2 Flow Through Constant Cross Section Tubes

In the laminar flow region, the pressure drop, P, across a tube is given by (Reference 1).

$$\Delta P = a\bar{u} + b\bar{u}^2 \qquad (1)$$

where $\bar{u}$ is the average velocity of the fluid down the tube and 'a' and 'b' are constants. In this equation, it is assumed either that the fluid is a liquid and has a constant density, or that the pressure drop across the tube is so low that the fluid has a negligible density change in flowing through the tube.

The term $b\bar{u}^2$ is a kinetic energy term and represents the energy required to accelerate the fluid from zero velocity to the average velocity within the tube. For long tubes this term will be small compared with the term $a\bar{u}$ and can be neglected. Neglecting the kinetic energy term the pressure velocity relationship is (Reference 1)

$$\Delta P = \frac{32\,\mu L\bar{u}}{D^2} \qquad (2)$$

where

ΔP = Pressure across tube drop in psi

μ = Viscosity in lbf-sec/in^2

L = Length of tube in inches

$\bar{u}$ = Average fluid velocity in inches/sec

D = diameter of tube in inches

The pressure drop in a tube when the flow is turbulent is found to be proportional to

$$\frac{LP\bar{u}^2}{D} \qquad (3)$$

Although in laminar flow the pressure is proportional only to the first power of the velocity, the pressure drop is often considered as being proportional to the above expression. Under this assumption, the proportionality factor cannot be constant. The result is

$$\Delta P = \lambda\frac{LP\bar{u}^2}{2D} \qquad (4)$$

where λ is a dimensionless constant of proportionality.

In terms of the Reynold's number R_e this can be rewritten as:

$$\lambda = 64/R_e \qquad (5)$$

Hence the proportionality factor, λ, when plotted as a function of the Reynold's number yields a straight line. The same result is obtained in the turbulent region only the straight line has a different slope. Plots of versus R_e in these regions is shown in Figure 2.1.2-1. This figure, with appropriate values of density, viscosity, and tube diameter applies to the flow of any fluid

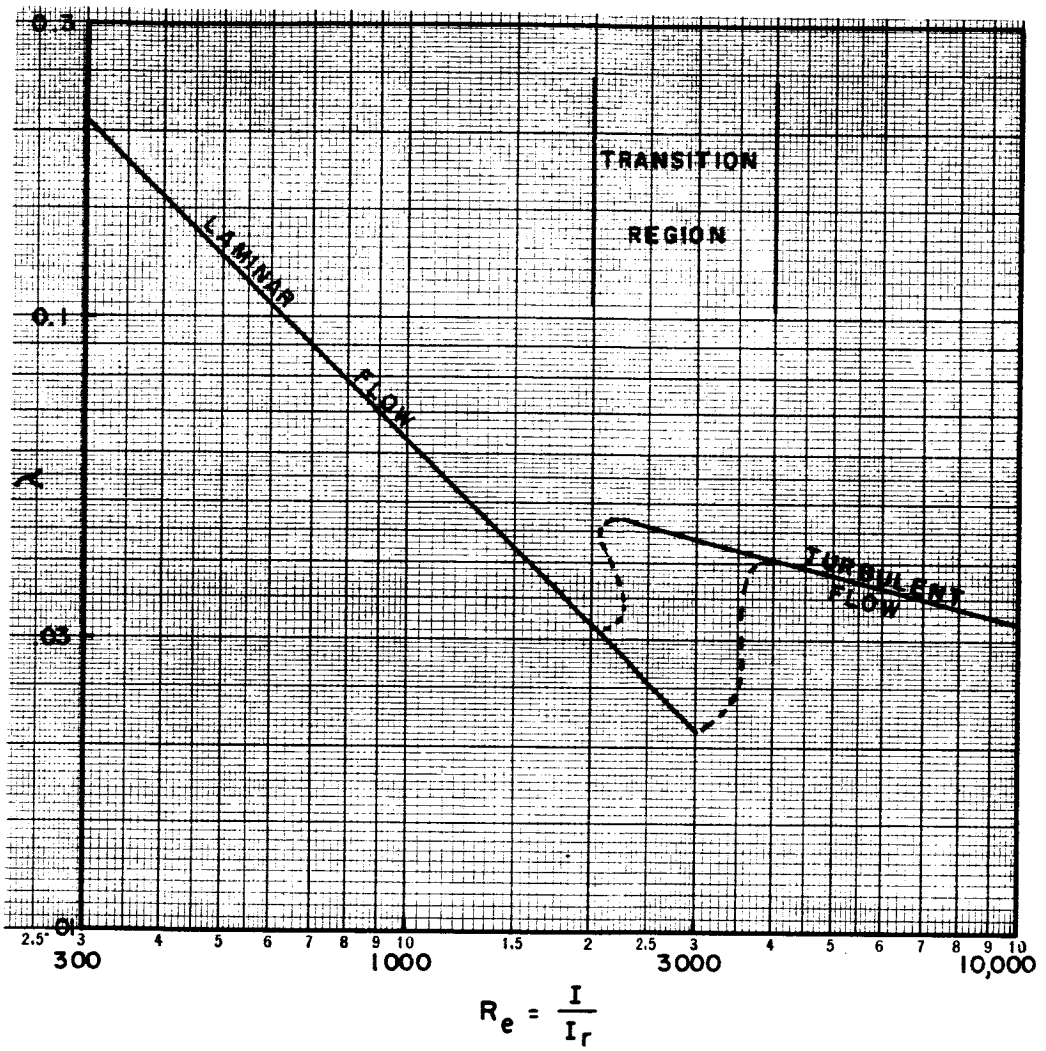

Figure 2.1.2-1 R_e versus λ for fluid flow through round tubes.

through any pipe. In this figure, it has been assumed that the pipe is smooth on the inside. Under this assumption, the resistance properties of tubes to fluid flow can be determined.

In terms of the fluid current I, the pressure-flow relation of equation (2) becomes

$$\Delta P = \frac{128\,\mu L I}{\pi D^4 \gamma} \tag{6}$$

where: I = fluid current in lbs/sec

γ = specific weight of the fluid in lbf/in^3

Solving for I gives

$$I = \frac{\pi D^4 \gamma}{128\,\mu L} \Delta P \tag{7}$$

Equations (6) and (7) are the expressions relating fluid current and pressure drop for a tube in the laminar flow region for an incompressible fluid.

For turbulent flow the equation relating λ and R_e is

$$\lambda = C/R_e^{\,1/4} \tag{8}$$

where the dimensionless constant C is experimentally found to be 0.316. Substituting for the equivalent of λ

$$\lambda = \frac{2\Delta P\, D}{\rho \bar{u}^2 L} \tag{9}$$

and R_e,

$$R_e = \frac{\rho \bar{u} D}{\mu} \tag{10}$$

in equation (8) and rearranging gives,

$$(\Delta P)^4 = \frac{C^4 \mu L^4 \rho^3 \bar{u}^{\,7}}{16\, D^5} \tag{11}$$

In terms of the fluid current I this becomes

$$\Delta P = \left(\frac{4}{\pi}\right)^{7/4} \left(\frac{CL}{2\gamma}\right) \left(\frac{\mu}{g^3 D^{19}}\right)^{1/4} (I)^{7/4} \tag{12}$$

solving for I this becomes

$$I = \left(\frac{\pi}{4}\right) \left(\frac{2\gamma}{CL}\right)^{4/7} \left(\frac{g^3 D^{19}}{\mu}\right)^{1/7} (\Delta P)^{4/7} \tag{13}$$

These equations can also be written in a dimenionless form.

Defining a reference fluid resistance R_r by

$$R_r = \frac{128\,\mu L}{\pi D^4 \gamma} \tag{14}$$

Equation (6), the pressure-flow relation for laminar conditions, reduces to

$$\Delta P = R_r I \tag{15}$$

In dimensionless form this becomes:

$$\frac{\Delta P}{R_r I_r} = \frac{I}{I_r} \tag{16}$$

The parameter λ can be written as

$$\lambda = \frac{\Delta P}{I} \cdot \frac{I_r}{I} \cdot \frac{64}{R_r} \tag{17}$$

From equation (8) and (17), the pressure-flow relation for the turbulent case becomes

$$\Delta P = \frac{C\, R_r (I)^{7/4}}{64\, (I_r)^{3/4}} \tag{18}$$

This can be rewritten as

$$\frac{\Delta P}{R_r I_r} = \frac{C}{64} \left(\frac{I}{I_r} \right)^{7/4} \tag{19}$$

since $C/64 = .00495$ this becomes

$$\frac{\Delta P}{R_r I_r} = .00495 \left(\frac{I}{I_r} \right)^{7/4} \tag{20}$$

Equations (16) and (20) are plotted in Figure 2.1.2-2. It is easily seen that Figure 2.1.2-2 is essentially the same plot as that of Figure 2.1.2-1.

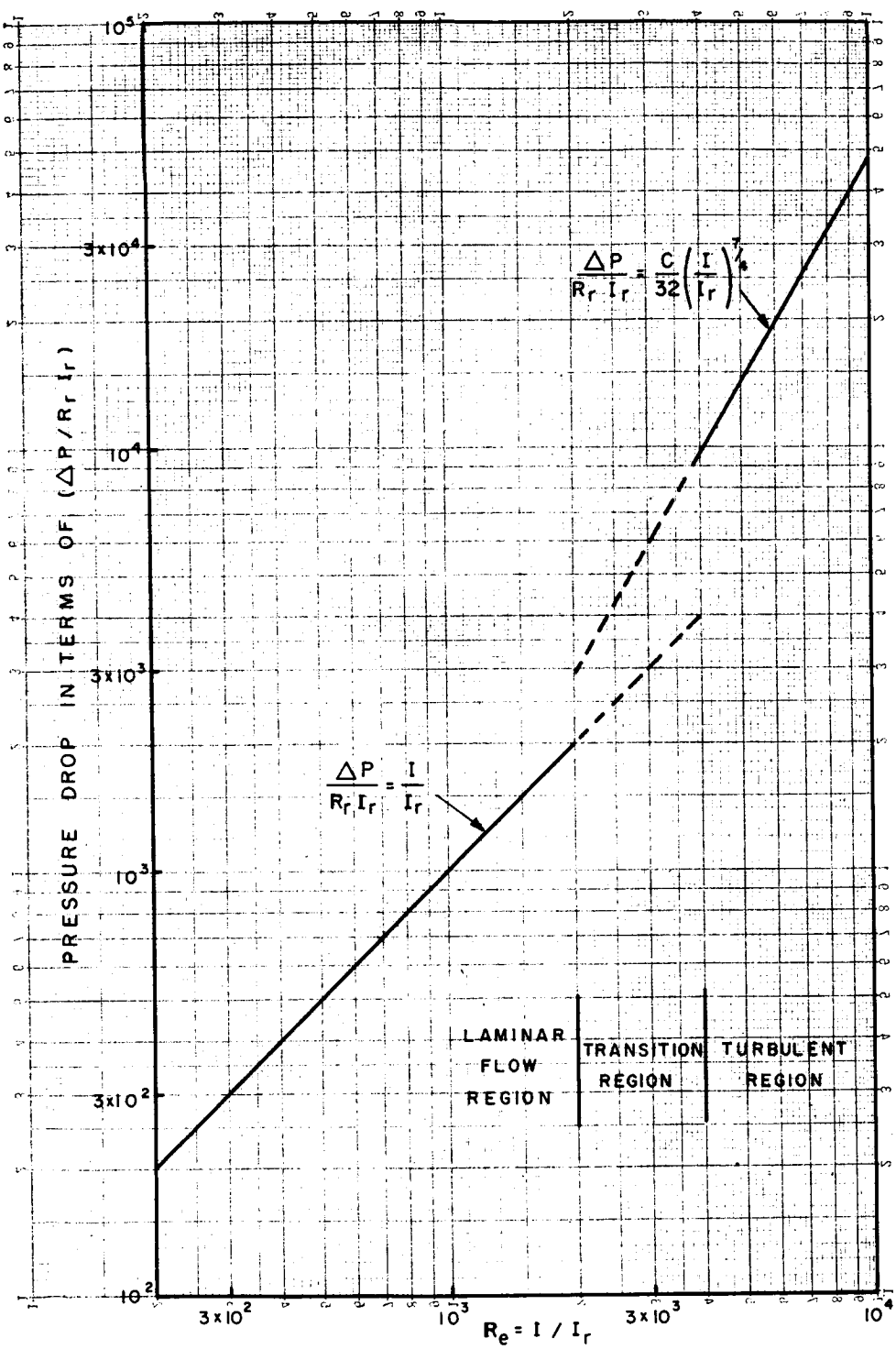

Figure 2.1.2-2 A dimensionless plot for flow through round tubes.

2.1.3 Flow Through Orifices and Nozzles

In fluid control circuits constrictions are used to impede the flow of fluid through a pipe. In this sense, they are the equavalent of electrical resistors which impede the flow of electrical current. Constrictions are termed either nozzles or orifices depending upon their construction. The distinction is that a nozzle has a smooth gradual transition from the line diameter down to the constriction diameter; whereas in the orifice, this transition is abrupt. A sketch showing this is given in Figure 2.1.3-1.

The construction of a nozzle usually requires careful shaping. The constrictions found in many fluid control systems are quite small - perhaps .010 to .075 inches in diameter. It would be difficult to machine nozzles of this size. Hence, the constrictions used in fluid circuitry are usually just drilled holes and are properly called orifices. The pressure-flow equations of orifices and nozzles are the same, and the equations for orifice flow can be used for nozzle flow with appropriate changes in the constants.

The fluid flow through an orifice depends, among other things, upon the pressure drop across the orifice. As shown in Figure 2.1.3-1., the higher pressure is termed the upstream or supply pressure, and is indicated by P_1; while the lower pressure is called the discharge, downstream, or back pressure, and is indicated by P_2.

The volume flow of an incompressible fluid through a nozzle or orifice is given by (Reference 3).

$$Q = C\,A\,\sqrt{\frac{2g(P_1 - P_2)}{\gamma}} \qquad (1)$$

where

Q = volume flow in inches^3/second

P_1 = pressure upstream from orifice in psi

P_2 = pressure downstream from orifice in psi

g = acceleration of gravity in inches/sec^2

γ = specific weight of fluid in lbf/inches^3

A = area of orifice in square inches

C = flow coefficient (dimensionless)

The weight flow rate, I, in pounds per second is given by γQ, or

$$I = C\,A\,\sqrt{2g\,\gamma(P_1 - P_2)} \qquad (2)$$

For compressible flow, the right hand side of (1) is multiplied by a dimensionless expansion factor Y. The compressible volume flow is then given by

$$Q = C\,Y\,A\,\sqrt{\frac{2g(P_1 - P_2)}{\gamma_1}}$$

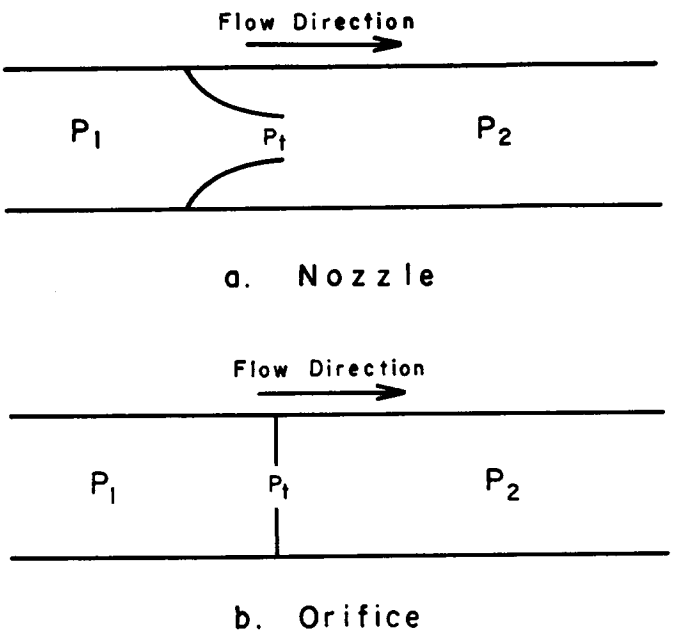

P_1 = Upstream or supply pressure

P_2 = Downstream, discharge or back pressure

P_t = Throat pressure

Figure 2.1.3-1 Cross sections of a nozzle and an orifice.

where $\gamma 1$ is the specific weight of the fluid at the inlet to the orifice. The mass flow is given by

$$I = C\ Y\ A \sqrt{2g\,\gamma 1(P_1 - P_2)} \qquad (3)$$

The flow coefficient C depends upon the Reynolds number and the ratio of the orifice diameter to the inlet tube diameter. The expansion factor Y is a function of the specific heat ratio k, the ratio of the orifice diameter to the inlet tube diameter, and the ratio of the downstream to upstream absolute pressures.

The equation for the compressible flow through a nozzle or orifice can be put in a more useful form by noting that

$$\gamma 1 = \gamma o \frac{P_1}{P_o} \qquad (4)$$

where γ_o is the specific weight of the fluid at atmospheric pressure, and P_o is atmospheric pressure. From equations (3) and (4),

$$I = Y\ C\ A \sqrt{\frac{2g\,\gamma_o P_1(P_1 - P_2)}{P_o}} \qquad (5)$$

For air, $\gamma_o = 4.34 \times 10^{-5}$ lbf/in^3, and

$$\left[\frac{2g\,\gamma_o}{P_o}\right]^{\frac{1}{2}} = .0477/\text{sec} \qquad (6)$$

Equation (5) then reduces to

$$I = .0477Y\ C\ A \sqrt{P_1(P_1 - P_2)} \qquad (7)$$

In terms of the orifice diameter D, this becomes

$$I = .0376\ Y\ C\ D^2 \sqrt{P_1(P_1 - P_2)} \qquad (8)$$

where D is in inches.

Consider the case where a compressible fluid at a supply pressure P_1 is discharging through an orifice or a nozzle into a region having a static pressure P_2. The pressure at the throat of the nozzle or at the orifice will be indicated by P_t.

Visualize starting out with the supply chamber pressure P_1 equal to P_2. Now decrease the discharge pressure P_2 keeping P_1 constant. The static pressure at the throat of the nozzle P_t remains equal to P_2 until P_2 reaches some critical pressure P*. At this point $P_t = P_2 = P^*$. When P_2 is lowered below the critical pressure, P*, it has no further influence upon the pressure at the throat. The throat pressure P_t remains equal to P*. The

ratio of the critical pressure P* and the supply pressure P_1 is given by,

$$\frac{P^*}{P_s} = \left(\frac{2}{k+1}\right)^{k/(k+1)} \qquad (9)$$

where k is the ratio of the specific heats.

As P_2 is first lowered, the velocity of the gas flow at the throat increases. When P_2 drops below P*, the velocity of gas issuing through the throat no longer increases, but remains equal to $\bar{u}^*$. The velocity $\bar{u}^*$ is equal to the speed of sound for the compressible fluid undergoing the flow and at the temperature and pressure conditions at the throat. The fluid flow through the orifice has the maximum value which is attainable for that particular orifice and supply pressure P_1. This is termed the critical flow or sonic limit.

2.1.4 Flow and Expansion Coefficients

Flow equations for orifices are often written in terms of a dischange coefficient C_d rather than the flow coefficient C. This is permissible only when the fluid velocity upstream from the orifice is negligible. This in turn depends on the ratio of the orifice diameter D to the diameter of the upstream tube D_o. The relationship between C and C_d is (Reference 4).

$$C = \frac{C_d}{\sqrt{1 - (D/D_o)^4}} \qquad (1)$$

For ratios of $D/D_o < 0.4$, C is found to be independent of D/D_o within a neglible error. A plot of C for Reynolds numbers of 10,000 and below Figure 2.1.4-1 for $D/D_o < 0.4$. Above this range, and for the same range of D/D_o the flow coefficient is nearly equal to 0.6.

The expansion factor Y is experimentally determined, and when plotted as a function of the ratio of the pressure drop across the orifice to the pressure upstream to the orifice is a series of straight lines. A plot of Y for air is shown in Figure 2.1.4-2. In many cases it is convenient to have a plot of the expansion factor as a function of pressure drop acrossed the orifice when the downstream pressure remains constant at atmospheric pressure. A plot of Y for air under these conditions is shown in Figure 2.1.4-3.

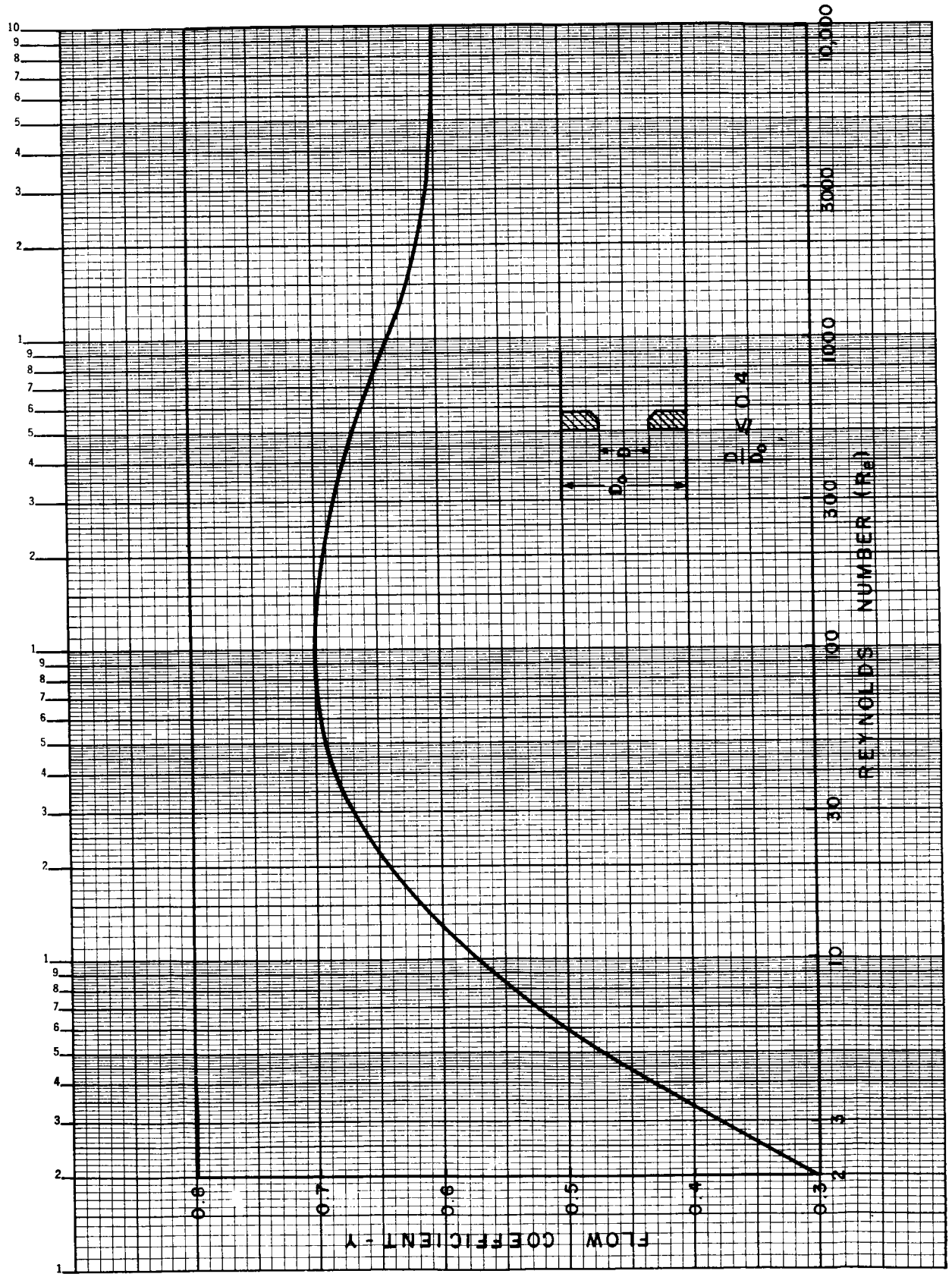

Figure 2.1.4-1 Flow coefficient for an orifice.

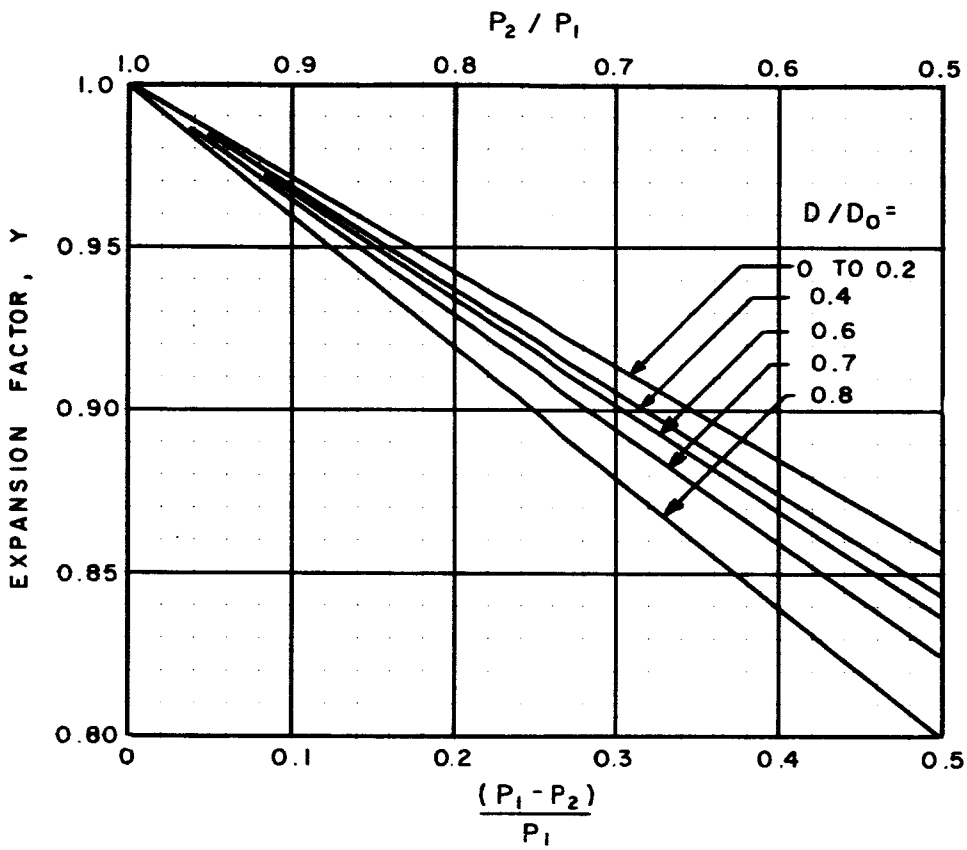

Figure 2.1.4-2 Expansion factor for air.

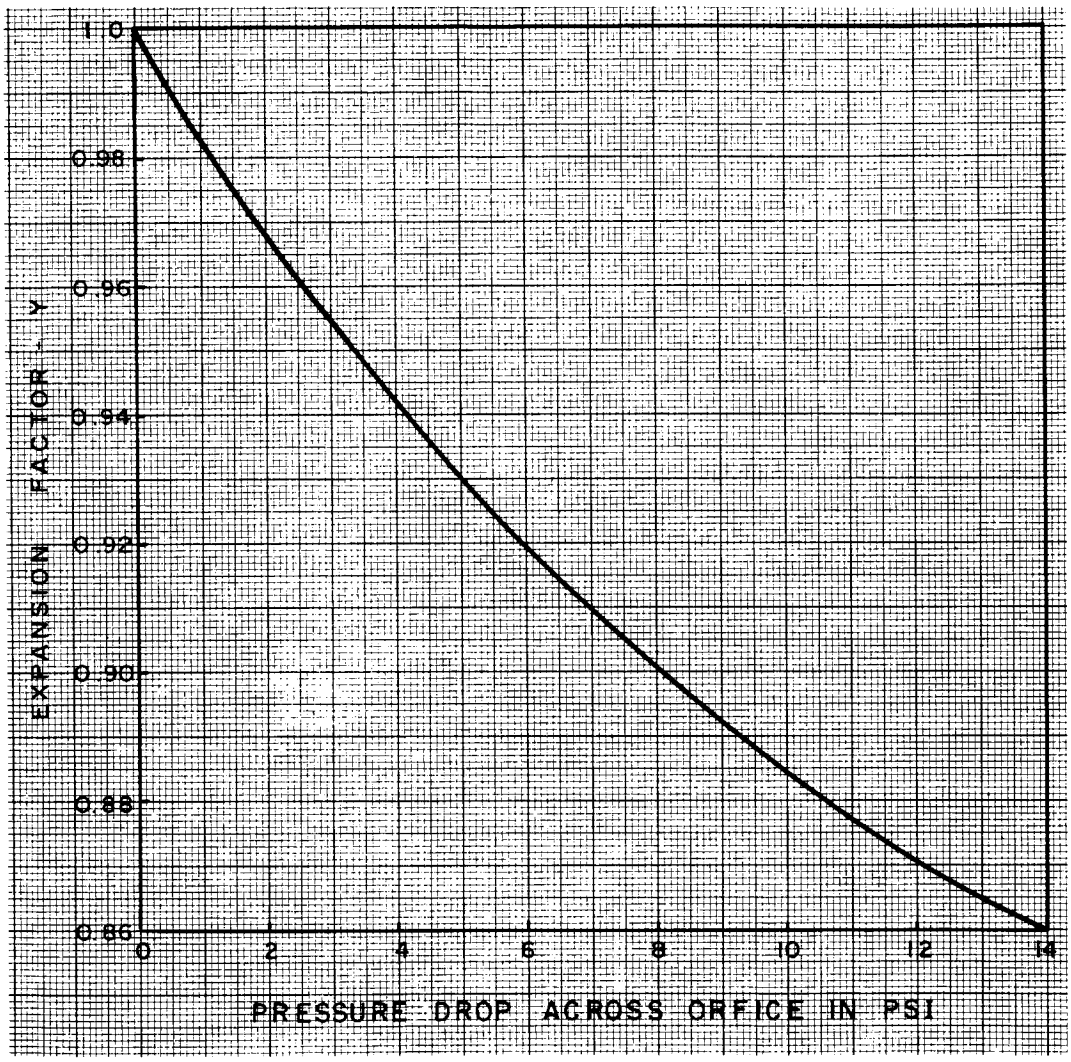

Figure 2.1.4-3 Expansion factor for an orifice discharging to atmosphere.

2.1.5 Flow Through Short Tubes

The previous discussions on orifice flow are derived for and have been experimentally verified for orifices which have sharp edges. In fluid circuitry and control systems many of the orifices are quite small and are made simply by drilling a hole through a plate having some thickness.

Consider 0.015 inch diameter hole drilled through, a 1/32 inch plate. This is no longer a sharp edged orifice but a short tube. Experiments have been performed upon elements in this range (Reference 3). It was shown in the study that the same law holds as for the sharp edge orifice. To use the data, the appropriate discharge coefficient must be known.

The flow through a tube has been shown to depend upon two dimensionless numbers (Reference 2)

$$\frac{\rho \Delta P D^2}{\mu^2} \qquad (1)$$

and

$$\frac{\rho Q}{D \mu} \qquad (2)$$

A plot of experimental results is shown in Figure 2.1.5-1. The slope of the line in this log-log plot is very nearly 2. Consequently the relationship between the dimensionless numbers (1) and (2) can be expressed as

$$\rho \Delta P D^2 / \mu^2 = K(\rho Q / D \mu)^2 \qquad (3)$$

From examination of Figure 2.1.5-1, it is seen that the constant k in equation (3) is very nearly equal to 1. The equation then reduces to

$$Q = D^2 \sqrt{\frac{\Delta P}{\rho}}$$

which can be expressed in standard form as

$$Q = \frac{A}{\pi} \sqrt{2 \Delta P / \rho} \qquad (5)$$

For an in compressible fluid,

$$Q = C\ A \sqrt{2 \Delta P / \rho} \qquad (6)$$

It can be seen from equations (5) and (6) that the flow coefficient C is approximately equal to

$$C = \frac{1}{\pi} = .32 \qquad (7)$$

For a compressible gas, equation (6) would become

$$Q = C\ Y\ A \sqrt{2 \Delta P / \rho} \qquad (8)$$

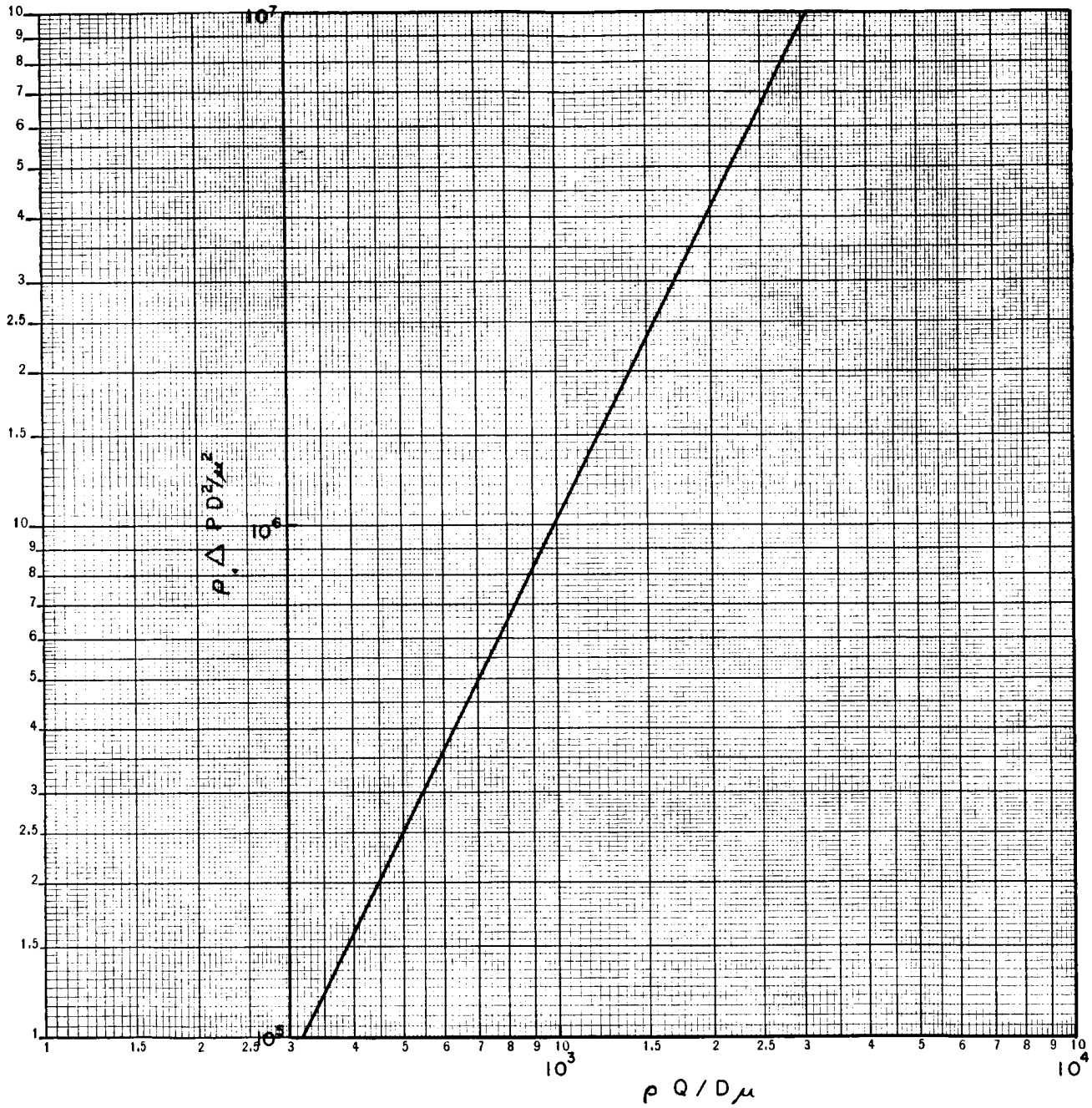

Figure 2.1.5-1 Dimensionless plot for flow through a short tube.

the weight flow is then

$$I = C\ Y\ A\ \sqrt{2g\ \gamma_1 \Delta P}$$

Where γ_1 is the specific weight at the inlet to the short tube.

From this it is seen that short tubes can be treated as orifices.

2.1.7 Laminar fluid jets

Laminar, free, fluid jets are useful in fluid circuitry. Consider the arrangement shown in Figure 2.1.7-1. A jet of fluid emerges from the left hand supply pipe and flows into the collection pipe on the right hand side. As long as the fluid jet emerging from the supply pipe is laminar, most of the flow and pressure can be recovered in the collection pipe. To obtain this condition it is necessary to carefully smooth the exit of the supply pipe so that turbulence is not introduced into the free jet, say by a burr or other irregularity on the supply pipe exit. Under proper conditions the free jet can remain laminar for a distance of over 100 times the inside diameter of the supply pipe.

The free jet can be acted upon in the region between the two pipes by either mechanical means or by other fluid streams. This is the basis for the turbulence amplifier.

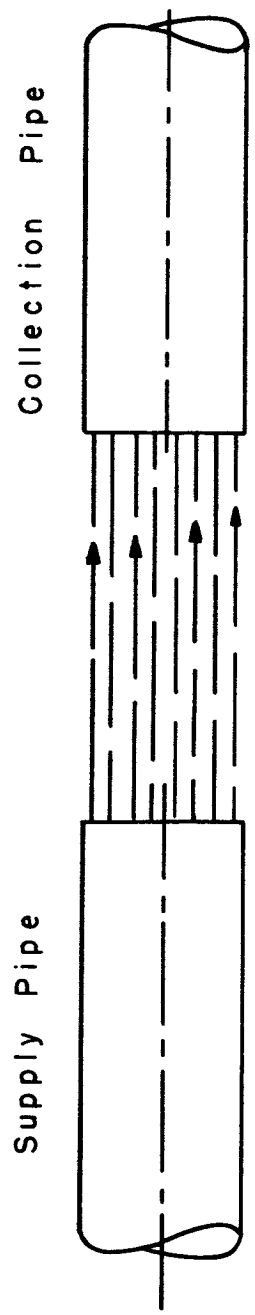

Figure 2.1.7-1 A free laminar jet.

2.2 Circuit Parameters of Passive Fluid Elements

2.2.1 Electrical Analogy and Equivalent Parameters

The analysis of pure fluid circuits is readily handled by using electrical equivalent circuits of the fluid circuit. In making this analogy the pressure drop is analogous to voltage and the fluid flow corresponds to electrical current. The resistance of a fluid element is defined as the pressure drop across the fluid element divided by the flow through the element.

Probably the most common measurement of fluid flow is the volume of fluid which flows through the element per unit time. For hydraulic circuits, where the compressibility of the working fluid is negligible volume flow is an adequate definition of fluid current. However, for pneumatic or other gas circuits this definition will not always suffice. For example, the volume flow at different points along a long thin tube will be different. The fluid current should be a constant.

Since the changing volume flow at different points in the tube, or other device, would make the definition of the fluid resistance imprecise, if not impossible, it becomes necessary to use some other measure of fluid flow. The logical flow to use would be a mass flow since the mass flow at various points in a long, thin pipe, or any other fluid element, would be constant, assuming steady state conditions. Since the weight flow is proportional to mass flow, it is equally useful, and flow in lbs/sec has been selected as a standard in fluid control work (Reference 5).

The steady state fluid resistance, R, of a fluid element is the pressure drop ΔP across the element divided by the flow, I, through the element, or

$$R = \Delta P / I \qquad (1)$$

In any specific case, the static fluid resistance is readily found by measurement or from a plot of P versus I.

The graphical determination of the incremental, or small signal resistance, $\partial \Delta P / \partial I$, poses no problem as long as the plot of P versus I is on a linear scale, since then the slope of the tangent to the curve is the desired incremental resistance. However, it is often very convenient in fluid work to make pressure-flow plots on a log-log scale. In this type of plot, the geometrical slope of the P-I curve does not have such a direct relation to the desired incremental resistance. The relationship is simple, however, and is readily found.

At any given values of pressure drop, ΔP, and flow, I, the relationship between the two factors can be approximated by

$$\Delta P = kI^n \qquad (2)$$

On a log-log plot, this approximation will plot as a straight line, tangent to the P-I curve at the point under consideration.

The incremental resistance is

$$R_i = \frac{\partial \Delta P}{\partial I} = nkI^{n-1} \qquad (3)$$

The factor n is the slope of the tangent, in appropriate units, at the operating point. It is readily seen that if the length of the logarithmic cycle on each axis is the same, then n is the geometric slope of the tangent at the point at which the resistance is desired. Multiplying the top and bottom of right hand side of equation (3) by I and using equation (2), it is seen that

$$R_i = nR \qquad (4)$$

where R is the steady state fluid resistance defined above.

In working with fluid resistances, and particularly if the flow is compressible, it is often easier to find the resistance of any given element from plot of flow versus pressure rather than to calculate it.

It should be noted that the incremental or small signal resistance, as defined above, assumes that the steady state condition holds for small transient or cyclic deviations from the steady state. The small signal resistances could properly be labeled quasi steady state, and it should be reorganized that as the frequency becomes high, the above given definitions for small signal resistances are no longer valid. The frequency limitations are discussed in section 1 of this volume. The same discussion would apply to the capacitances and inductances to be defined later.

2.2.2 Resistance of Tubes - Incompressible Flow

The relation between the flow-through through a tube and the pressure drop across the tube in the laminar flow region is given by:

$$\triangle P = \frac{128\,\mu\,LI}{\pi D^4\,\gamma} \qquad (1)$$

Since the fluid resistance is the pressure drop across the tube divided by the fluid current, the resistance of a tube in the laminar flow region is seen to be:

$$R = \frac{128\,\mu\,L}{\pi D^4\,\gamma} \qquad (2)$$

It is seen from this expression that in the laminar flow region and for an incompressible fluid, tubes act as linear resistors, i.e., their resistance is independent of the pressure drop across the tube.

For small pressure drops, air can be considered as an incompressible fluid. For air at 68° and atmospheric pressure, $\mu = 2.6 \times 10^{-9}$ lbf-sec/in^2 and $\gamma_o = 4.35 \times 10^{-5}$ lbf/in^3. Putting these values in equation (2) gives

$$R = 2.44 \times 10^{-3}\ L/D^4 \quad \text{psi-sec/lb} \qquad (3)$$

for the resistance of tubes to an air flow. A plot of equation (3) is given in Figure 2.2.2-1 and 2.2.2-2.

In some instances the conductivity $Y = 1/R$ is more useful than the resistance itself. The expression for Y is

$$Y = 410\ D^4/L \quad \text{lb/psi-sec} \qquad (4)$$

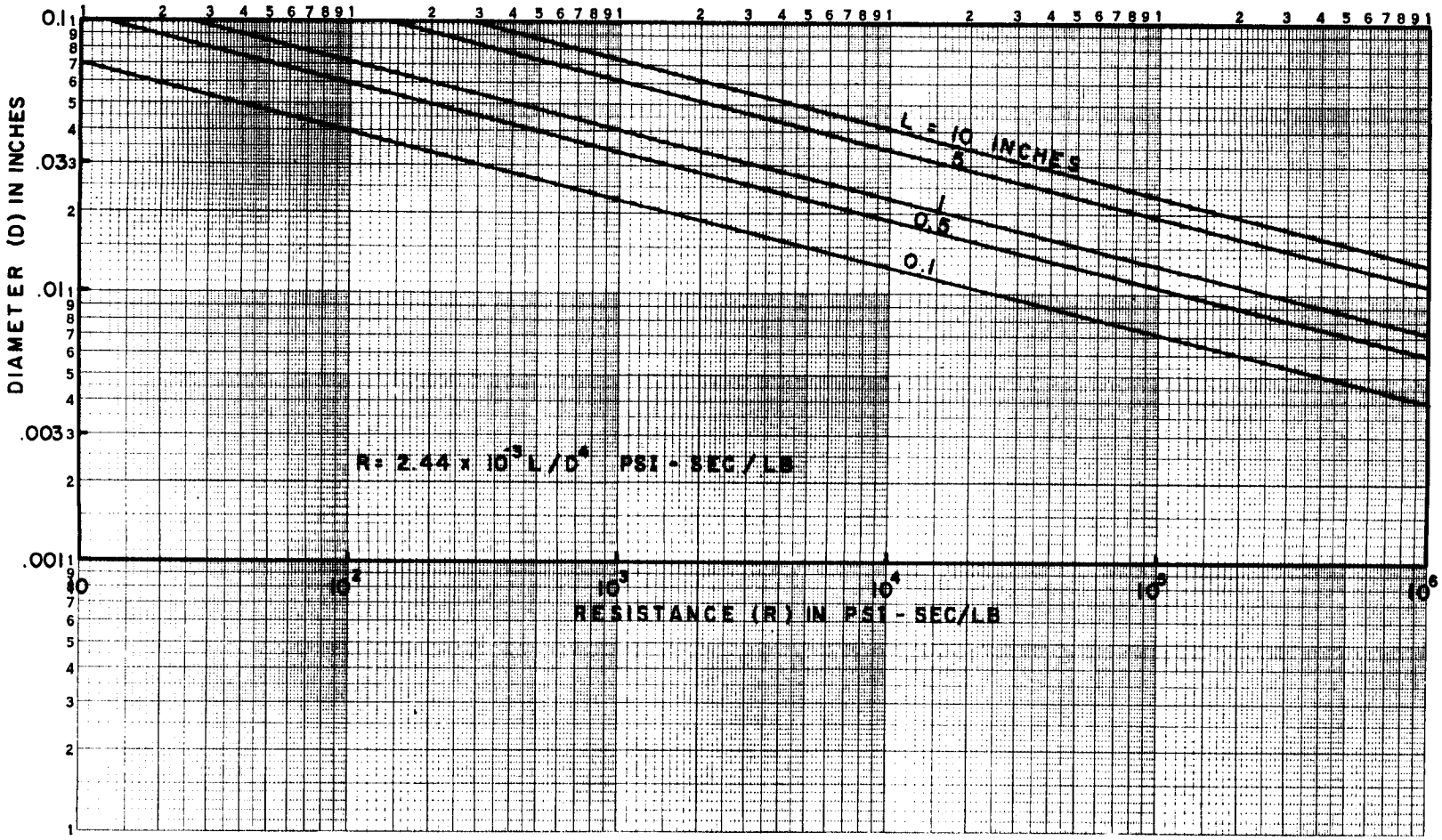

Figure 2.2.2-1 Resistance of round tubes to air flow.

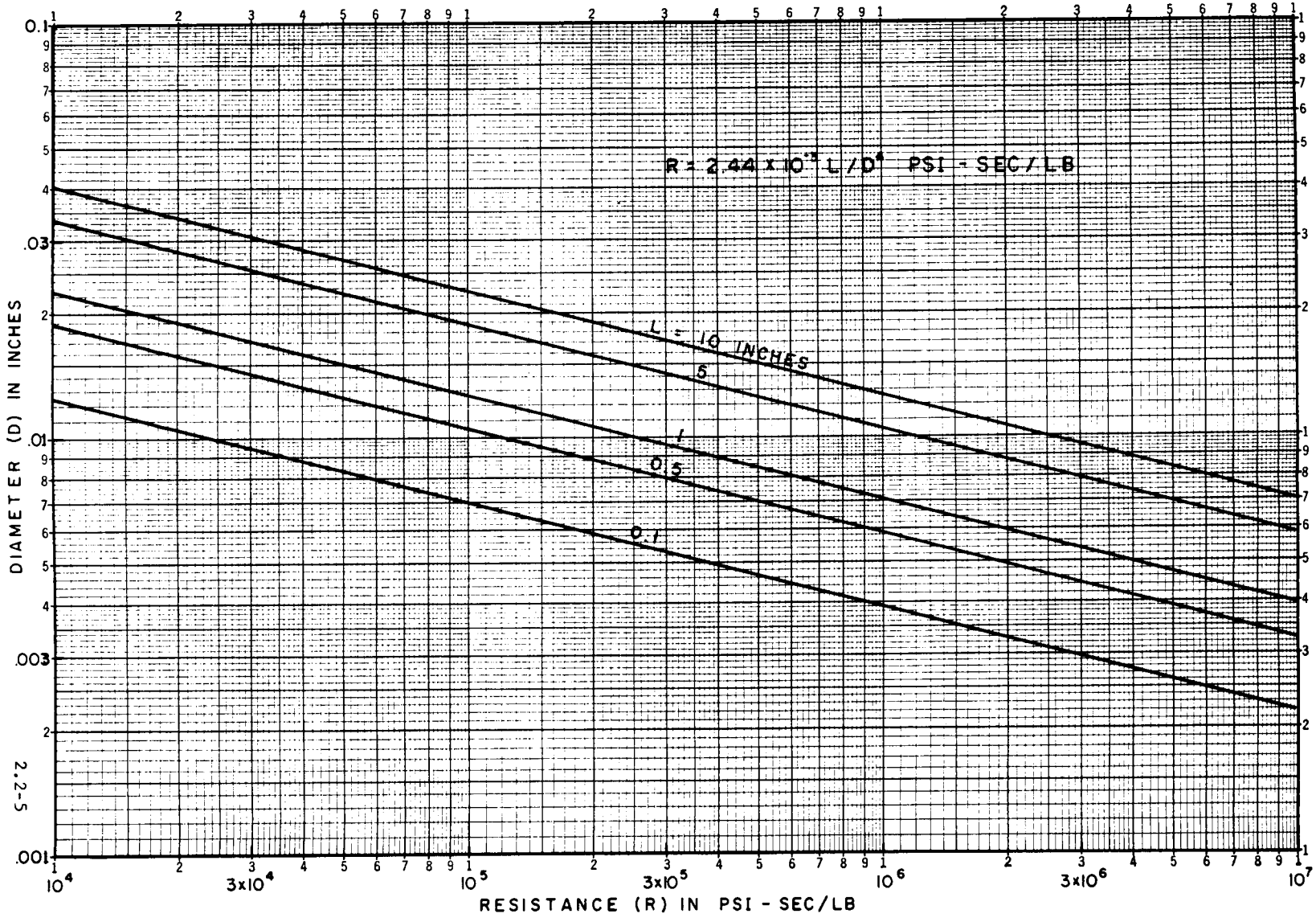

Figure 2.2.2-2 Resistance of round tubes to air flow.

2.2.3 Resistance of Tubes - Compressible Flow

In those cases where the density variation of the fluid from one end of the tube to the other is not negligible, equation (1) of Section 2.2.2 will be inapplicable and must be integrated in order to give the correct pressure-flow relationship for a tube.

Writing the specific weight as:

$$\gamma = \gamma_o P/P_o \qquad (1)$$

the expression for the pressure drop in the laminar flow region for a pipe ΔL inches in length becomes:

$$\Delta P = \frac{128 \mu P_o \, I \Delta L}{\pi D^4 \gamma_o P} \qquad (20$$

This equation, as it stands, is only valid for small ΔP. Now consider a section of a tube $\Delta L = dx$ in length, with a pressure drop $\Delta P = dP$ across it as shown in Figure 2.2.3-1. Applied to this section of tube, equation (2) becomes:

$$PdP = \frac{128 \mu P_o I}{\pi D^4 \gamma_o} \quad dx \qquad (3)$$

Defining R_o by

$$R_o = \frac{128 \mu L}{\pi D^4 \gamma_o} \qquad (4)$$

equation (3) becomes

$$PdP = \frac{R_o P_o I}{L} \quad dx \qquad (5)$$

In Figure 2.2.3-1, let the pressure at x_1 be P_1 and the pressure at x_2 be P_2, where the pressure P_1 is greater than the pressure P_2. Let x_1 and x_2 be the coordinates of the ends of the tube. Integrating equation (5) gives:

$$\frac{P_1^2 - P_2^2}{2} = \frac{R_o P_o I}{L} \quad (x_2 - x_1) \qquad (6)$$

The term $(x_2 - x_1)$ is simply L, the length of the tube. Noting that

$$P_1^2 - P_2^2 + (P_1 - P_2) \quad (P_1 + P_2) \qquad (7)$$

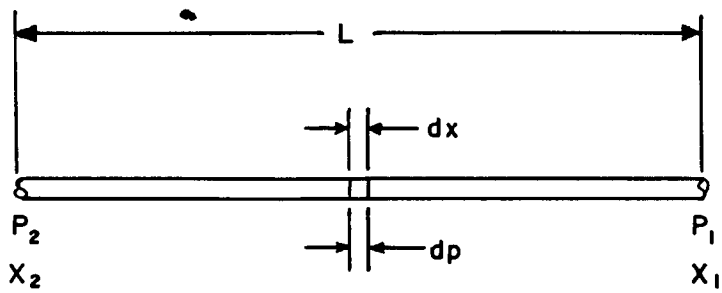

Figure 2.2.3-1 Parameters relating to compressible flow through a tube.

reduces equation (6) to

$$\Delta P(P_1 + P_2) = 2R_o P_o I \tag{8}$$

Solving for ΔP gives

$$\Delta P = R_o I \left(\frac{2 P_o}{P_1 + P_2} \right) \tag{9}$$

The current I is given by

$$I = \left(\frac{\Delta P}{R_o} \right) \left(\frac{P_1 + P_2}{2 P_o} \right) \tag{10}$$

Substituting for R_o gives

$$I = \frac{\pi D^4 \gamma_o}{128 \mu L} \Delta P \left(\frac{P_1 + P_2}{2 P_o} \right) \tag{11}$$

This is the expression for the fluid current which will flow through a tube of finite length L under a pressure drop across the tube of magnitude ΔP, where P_1 and P_2 are the absolute pressures at the input and the output ends of the tube respectively. As long as the flow remains laminar, the equation is valid whatever the density variation throughout the length of the tube.

From equation (11), the fluid resistance of a tube for laminar, compressible flow is found to be:

$$R = \frac{128 \mu L}{\pi D^4 \gamma_o} \cdot \left(\frac{2 P_o}{P_1 + P_2} \right) \tag{12}$$

or

$$R = R_o \left(\frac{2 P_o}{P_1 + P_2} \right) \tag{13}$$

R_o is seen to be the resistance the tube would have for the same fluid if it were incompressible. Since P_1 and P_2 are not constant, the resistance of a tube in the laminar flow region is not a constant for a compressible fluid.

In equation (11), an expression for the flow through a tube as a function of the pressure drop across the tube, the absolute pressures at the ends of the tube, the dimensions of the tube, and the fluid characteristics is given. Let us now specialize this equation to that case where the tube is always discharging to atmospheric pressure. In this case, $P_2 = P_o$. Then,

$$P_1 = P_o + \Delta P \tag{14}$$

The expression $\Delta P(P_1 + P_2)$ then becomes

$$\Delta P\ (P_1 + P_o) = \Delta P(\Delta P + 2P_o) \tag{15}$$

This can be factored to give

$$\Delta P(P_1 + P_o) = \Delta P\ 2P_o\ (1 + \Delta P/2P_o) \tag{16}$$

Applying this to equation (8) and solving for I results in

$$I = \frac{\Delta P}{R_o}\ (1 + \Delta P/2P_o) \tag{17}$$

In equation (16), $2P_o$, was factored out of the pressure expression. The resulting correction factor $(1 + \Delta P/2P_o)$ is seen to be useful for small pressure drops. If ΔP is factored out rather than $2P_o$, there results

$$\Delta P\ (P_1 + P_o) = \Delta P^2(1 + 2P_o/\Delta P) \tag{18}$$

This correction new factor is $(1 + 2P_o/\Delta P)$ and is useful for computation at high rather than low pressure drops.

Using equations (8) and (18), the pressure-flow relationship can be written as

$$I = \frac{\Delta P^2}{2\ R_o\ P_o}\ (1 + 2P_o/\Delta P) \tag{19}$$

In those regions where the pressure drop ΔP is large enough that the correction factor $(1 + 2P_o/\Delta P)$ becomes essentially one, it is seen that the current I is proportional to the square of the pressure drop.

Choosing units for I such that $R_o = 1$, neglecting the correction factors and noting that $1/2P_o = .034$ equations (17) and (19) become

$$I = \Delta P \tag{20}$$

and

$$I = .034\ \Delta P^2 \tag{21}$$

respectively. These two equations represent asymptotic limits for the flow.

The behavior and slopes of the two asymptotic lines are given by lines-a and b in Figure 2.2.3-2. The exact value of the current can be obtained from either equation (17) or (19), and is given as curve -c in Figure 2.2.3-2. The equation of curve-c is

$$I = \Delta P(1 + \Delta P/2P_0) \tag{22}$$

or

$$I = .034\Delta P^2(1 + 2P_0/\Delta P) \tag{23}$$

From curve -c, the flow through any tube can be found by the use of appropriate multiplying factors.

Curve -c of Figure 2.2.3-2 indicates that the flow is approximately proportional to the pressure drop, i.e., the resistance is linear, up to pressure drops of 2 or 3 psi. These results were derived for smooth tubes. In actual practice, the linearity usually holds for a much higher pressure drop. An example is shown in Figure 2.2.3-3 for a capillary tube 0.008 inches in diameter and 1.78 inches long.

In fluid circuits, one consideration which limits the allowable length of small-tube, laminar resistors is that of transit time. In situations where it is necessary to limit this, the laminar resistors should be kept as short as possible.

Let us consider one-inch lengths of small tubes (.005 to .015 inches in diameter) used as laminar resistors. Considering the fluid as incompressible, the flow as of function of pressure drop is given in Figure 2.2.3-4. Noting that the resistors become nonlinear when the flow leaves the laminar region, it can be concluded from Figure 2.2.3-4 that the larger diameter tubes become nonlinear at very small pressure drops. Stated in other words, the larger the tube, the smaller the allowable pressure drop above which the resistance becomes nonlinear.

In the turbulent flow region, the pressure-flow relation for small density variations is

$$\Delta P = \frac{CR_r I_r}{32} \left(\frac{I}{I_r}\right)^{7/4} \tag{24}$$

Considering a small element of tube dx in length this becomes

$$P\ dp = \frac{CR_0 I_r}{32} \left(\frac{I}{I_r}\right)^{7/4} dx \tag{25}$$

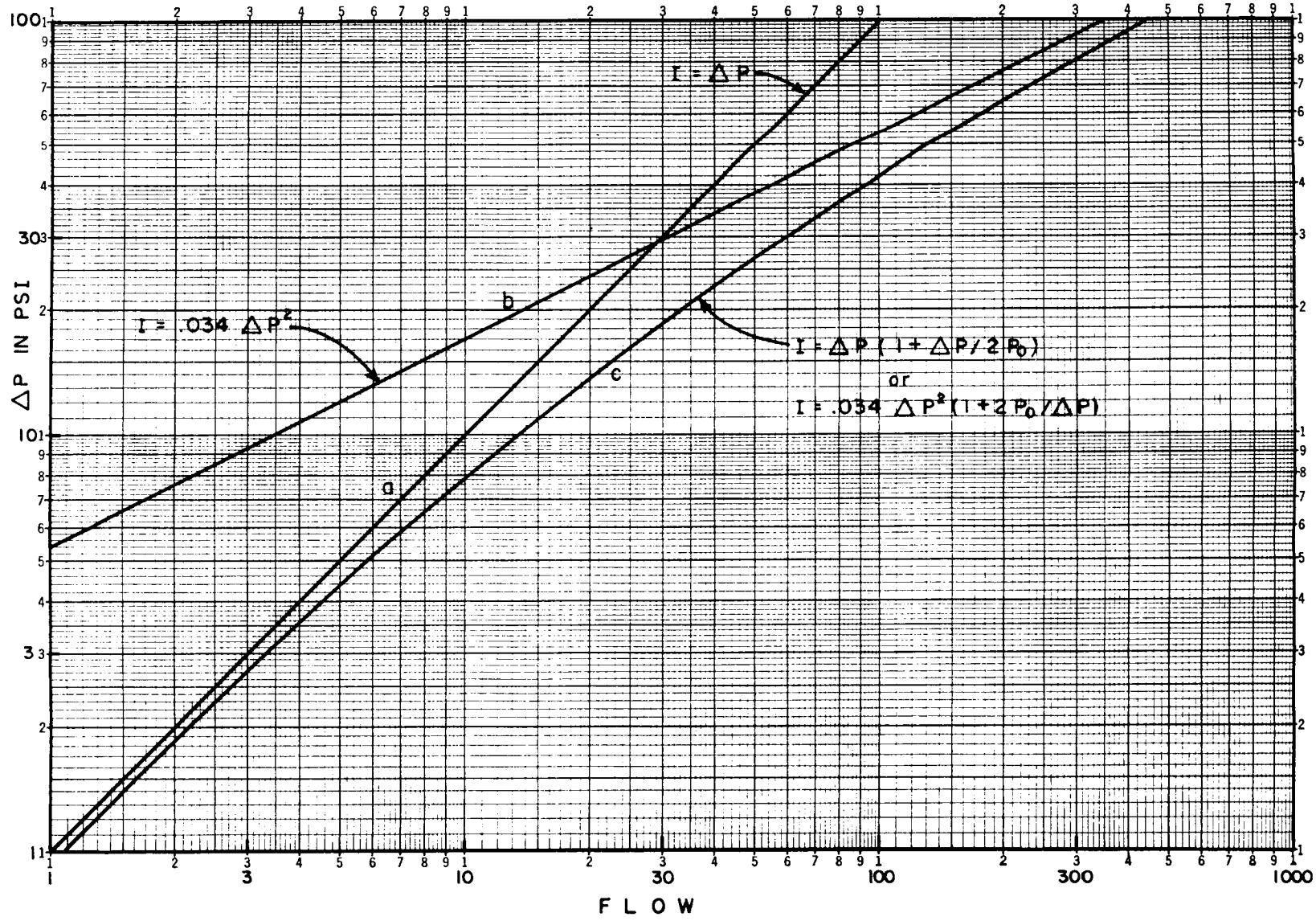

Figure 2.2.3-2 Flow of a compressible fluid through a round tube.

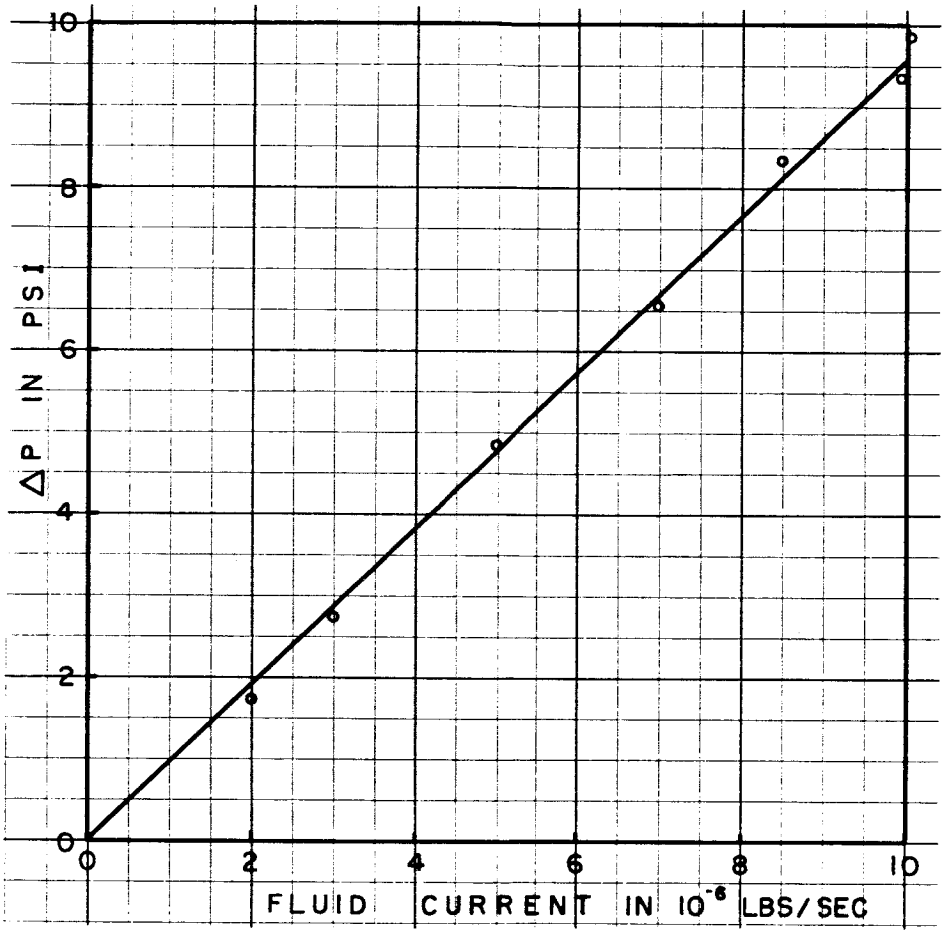

Figure 2.2.3-3 Experimental data for a tube resistor.

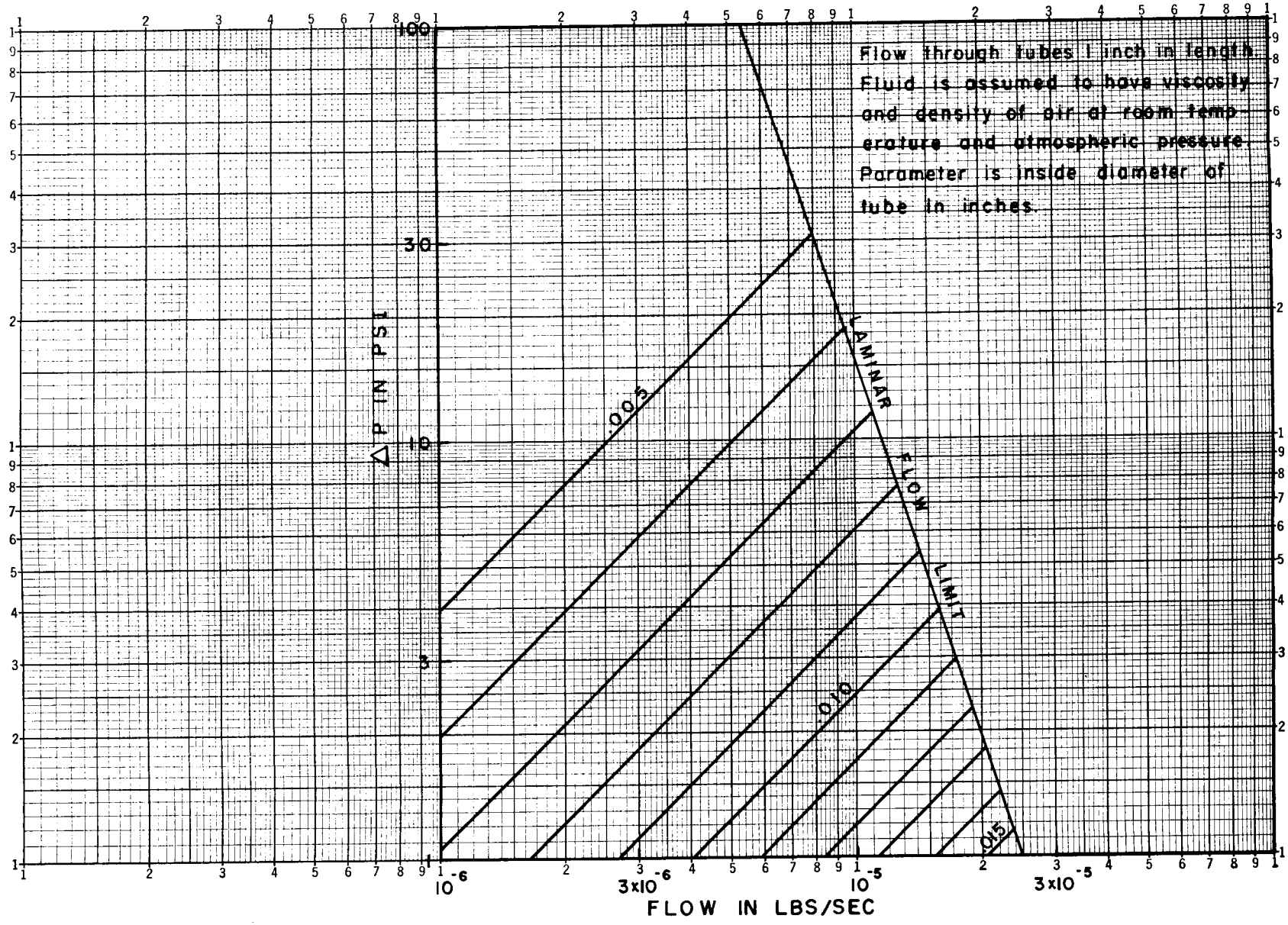

Figure 2.2.3-4 Flow through tubes.

Integrating and rearranging gives

$$\Delta P(P_1 + P_2) = \frac{2CR_oI_rP_o}{32} \left(\frac{I}{I_r}\right)^{7/4} \qquad (26)$$

solving for ΔP gives

$$\Delta P = \frac{CR_oI_r}{32} \left(\frac{I}{I_r}\right)^{7/4} \left(\frac{2\ P_o}{P_1 + P_2}\right) \qquad (27)$$

The expression for I is

$$I = I_r \left[\left(\frac{32\Delta P}{CR_oI_r}\right) \cdot \left(\frac{P_1 + P_2}{2\ P_o}\right)\right]^{4/7} \qquad (28)$$

2.2.4 Resistance of Orifices - Incompressible Flow

The weight flow of an incomprssible fluid through an orifice is given by

$$I = CA\sqrt{2g\gamma(P_1 - P_2)} \qquad (1)$$

or setting $P_1 - P_2 = \Delta P$,

$$I = CA\sqrt{2g\gamma\Delta P} \qquad (2)$$

Lumping the constants together,

$$I = B\sqrt{\Delta P} \qquad (3)$$

where $B = C\,A\sqrt{2g\gamma}$. From equation (3), the orifice resistance $(\Delta P/I)$ is given by

$$R = \frac{\sqrt{\Delta P}}{B} \qquad (4)$$

The orifice resistance is seen to be nonlinear, increasing with the pressure drop across the orifice.

From equation (3), the incremental resistance $(\partial\Delta P/\partial I)$ is found to be

$$R_i = \frac{2\sqrt{\Delta P}}{B} \qquad (5)$$

or,

$$R_i = 2R \qquad (6)$$

Hence the incremental orifice resistance is twice the steady state value.

Both the steady state and the incremental resistance are independent of the absolute values of the supply and discharge pressures, depending only upon the pressure drop across the element.

2.2.5 Resistance of Orifices - Compressible Flow

The flow through an orifice is given by

$$I = YCA \sqrt{\frac{2g\,\gamma_o P_1 (P_1 - P_2)}{P_o}} \qquad (1)$$

The fluid resistance of an orifice is hence given by

$$R = \frac{\sqrt{\Delta P}}{\sqrt{YCA\,\gamma 2g_{\,o} P_1 / P_o}} \qquad (2)$$

Where $\Delta P = P_1 - P_2$. The resistance of an orifice is seen to be highly nonlinear, and the best way to handle flow problems through orifices is through the use of pressure-flow plots. Two cases are of importance; a constant discharge-pressure with a variable upstream-pressure and a constant upstream-pressure with a variable discharge-pressure. They shall be discussed in that order.

In the case of air flow through an orifice where the orifice discharges to a pressure, P_2, the orifice flow equation is

$$I = .0376\ YCD^2 \sqrt{P_1\ (P_1 - P_2)} \qquad (3)$$

when P_2 is atmospheric pressure, this reduces to

$$I = .0376\ YCD^2 \sqrt{14.7} \sqrt{\Delta P}\ \sqrt{1 + \Delta P/14.7} \qquad (4)$$

or

$$I = .144\ YCD^2 \sqrt{\Delta P}\ \sqrt{1 + \Delta P/14.7} \qquad (5)$$

This equation can be considered to be the product of two expressions

$$I = .144\ \ CD^2 \sqrt{\Delta P} \qquad (6)$$

and a correction factor

$$Y \sqrt{1 + \Delta P/14.7} \qquad (7)$$

Equation (6) is plotted as line-a in Figure 2.2.5-1 for C = D = 1. When the correlation factor of equation (7) is applied, the line is shifted to the right as indicated by line-b in Figure 2.2.5-1. These equations are only valid to the sonic limit, that is, they are only valid up to the pressure drop at which the flow through the orifice becomes choked. Above this a different expression must be used.

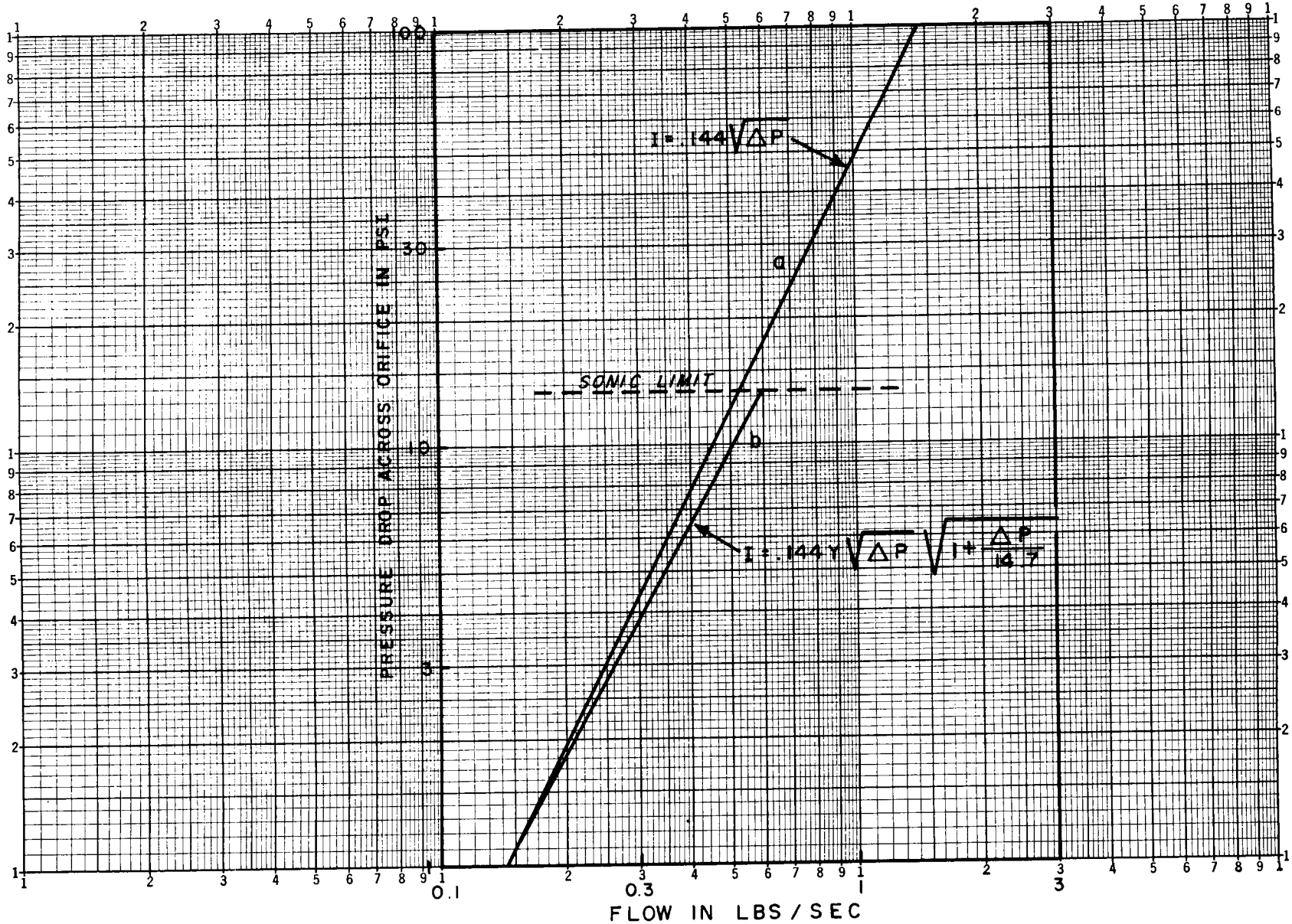

Figure 2.2.5-1 Air flow through an orifice.

For small pressure drops, equation (6) suffices to describe the flow through an orifice. A plot of equation (6) for C = 1 and a variety of diameters is given in Figure 2.2.5-2.

For choked flow through an orifice which is discharging air to atmospheric pressure, P^* is

$$P^* = .524\ P_1 \tag{8}$$

where P^* is the throat pressure and P_1 is the upstream pressure. When the orifice flow is choked the throat pressure will always remain at $.524\ P_1$. In this case the expression for the flow through the nozzle becomes

$$I = .0376\ YCD^2 \sqrt{P_1\ (P_1 - .524\ P_1)} \tag{9}$$

This in turn reduces to

$$I = .026\ YCD^2\ P_1 \tag{10}$$

Since the ratio P^*/P, is a constant for choked flow, the expansion factor for the orifice will remain a constant. For the conditions considered here and for small D/D_0 ratios, the expansion factor Y is found to be equal to 0.86. In this case, equation (10) reduces to

$$I = .0224\ CD^2\ P_1 \tag{11}$$

Now, writing P_1 as

$$P_1 = \Delta P + 14.7 \tag{12}$$

equation (11) can be written as

$$I = CD^2\ \left[.0224\ (\Delta P + 14.7)\right] \tag{13}$$

which reduces to

$$I = CD^2\ (.33 + .0224\Delta P) \tag{14}$$

The choked flow through an orifice can be considered to be the sum of two expressions, a constant and an expression involving ΔP. Setting C = D = 1, the portion of the sum which is a function of ΔP is plotted as line-a in Figure 2.2.5-3. This factor plus the constant term is plotted as line-b in Figure 2.2.5-3, which gives the air flow through a choked orifice which is discharging to atmosphere for C = D = 1.

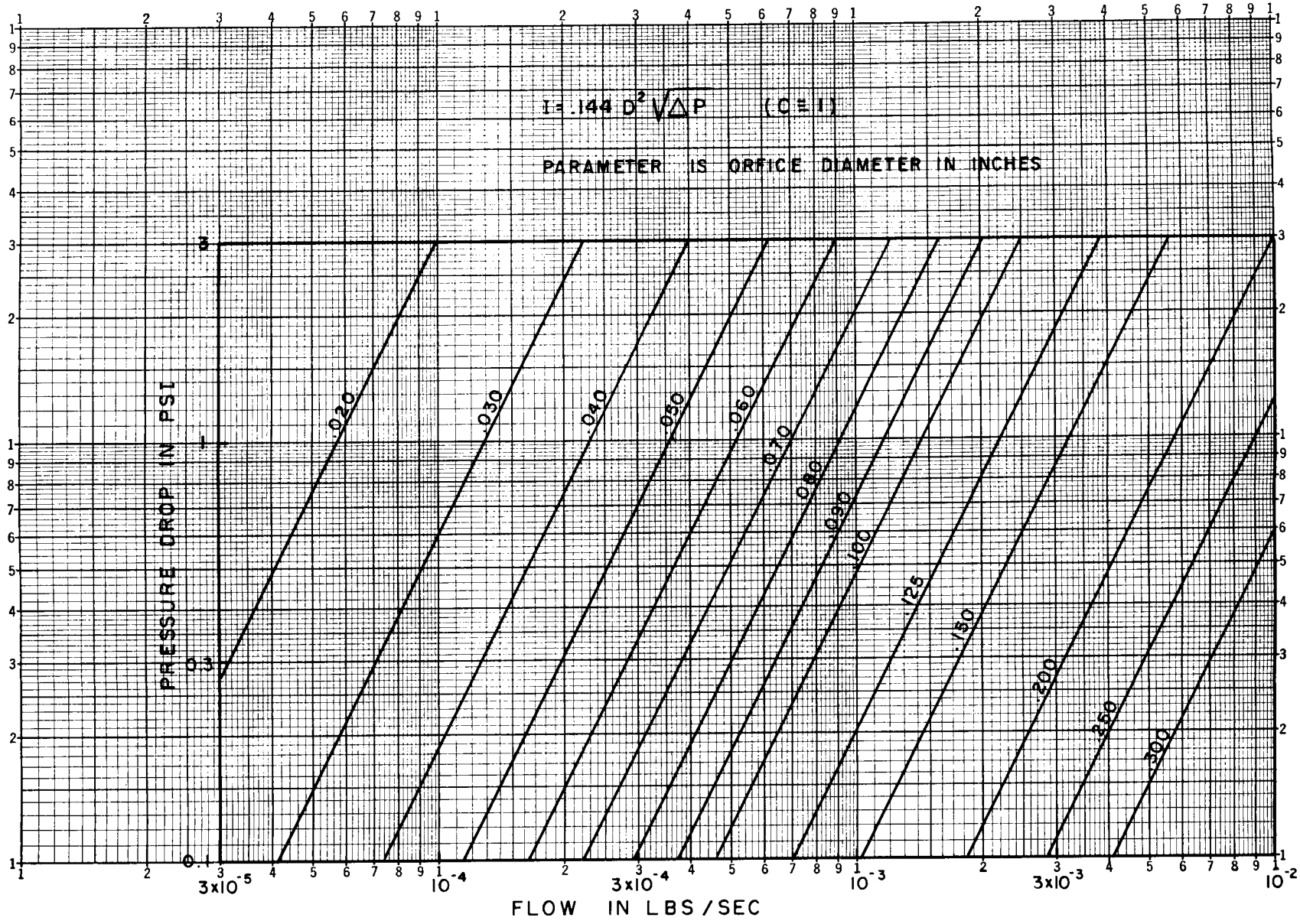

Figure 2.2.5-2 Air flow through orifices of various diameters.

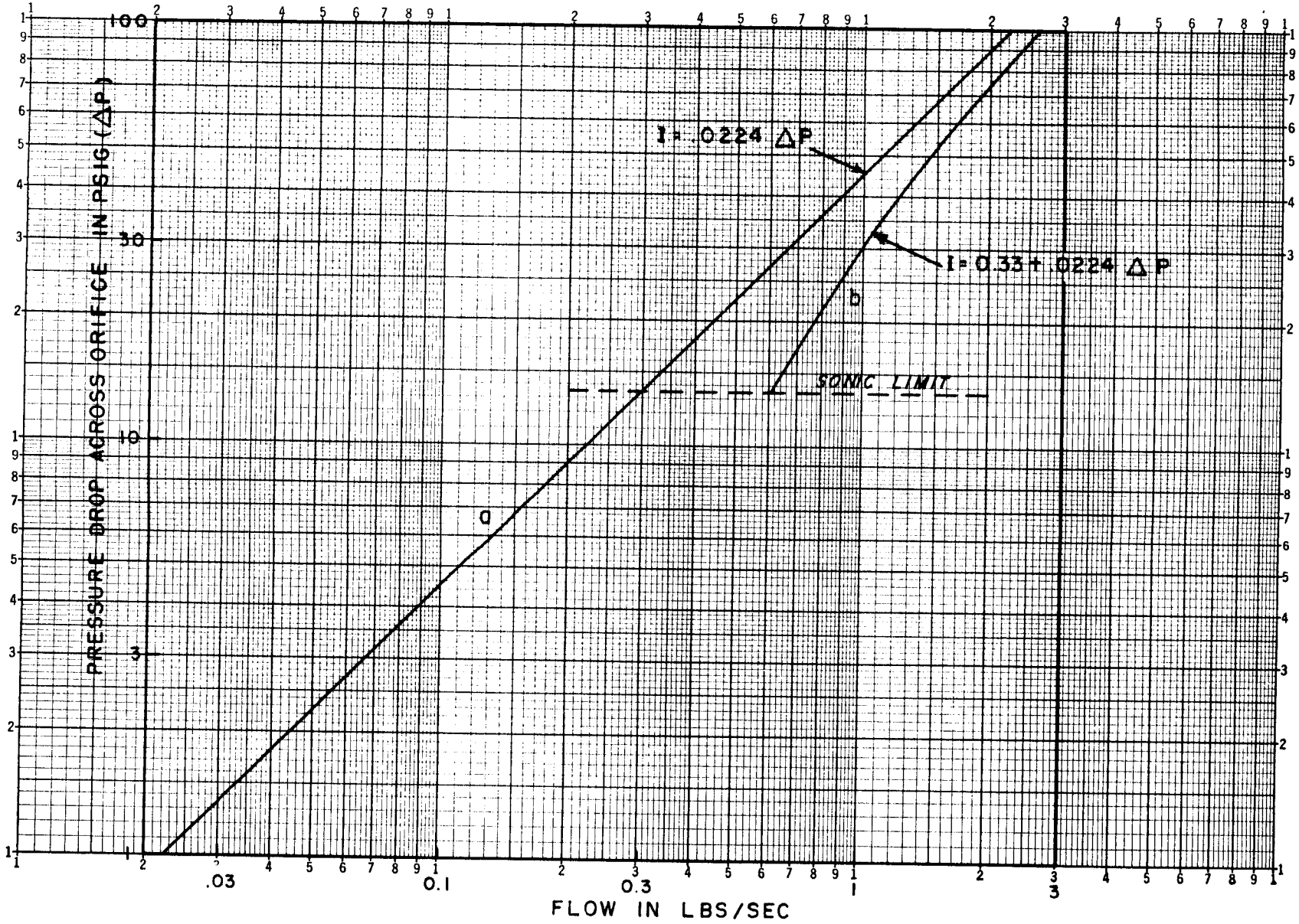

Figure 2.2.5-3 Choked air flow through an orifice.

The curve of the choked flow through an orifice, as given in Figure 2.2.5-3, and the curve of Figure 2.2.5-1 for the unchoked flow through an orifice, fit smoothly together, giving a complete curve of flow through an orifice which is discharging to atmospheric pressure. The complete curve is shown in Figure 2.2.5-4. In this figure it has again been assumed that C and D are both equal to 1. By applying appropriate multiplying factors to Figure 2.2.5-4, the flow through any sized orifice can be found for a wide range of pressure drops. Such a plot is given in Figure 2.2.5-5 for a value of C = 1 and a variety of orifice diameters.

The flow of air through an orifice of diameter D is given by equation (3). For the case where the upstream pressure P_1, is a constant this is conveniently factored as

$$I = .0376\ YCD^2\ \sqrt{P_1}\sqrt{\Delta P} \qquad (15)$$

Let us now consider the case where C = D = 1. Neglecting Y, that is setting Y equal to 1, and setting P_1 = to 114.7 psia (100 psig), equation (15) becomes

$$I = .376\ \Delta P \qquad (16)$$

This equation is plotted as line-a in Figure 2.2.5-6. Considering the expansion factor Y, the actual pressure-flow curve becomes that shown as line-b in Figure 2.2.5-6. Note that in line-b the flow continues to increase only up to the critical pressure 52.6 pounds. Above this the flow is a constant. Line-b of Figure 2.2.5-6 is as close as one can come to a universal flow curve for the orifice which has a constant upstream pressure.

By multiplying by appropriate constants, and calculating new critical pressures, the flow through a nozzle for any constant upstream pressure can be found from Figure 2.2.5-6. A family of curves so derived is given in Figure 2.2.5-7. These curves are more convenient to use than the curve in Figure 2.2.5-6.

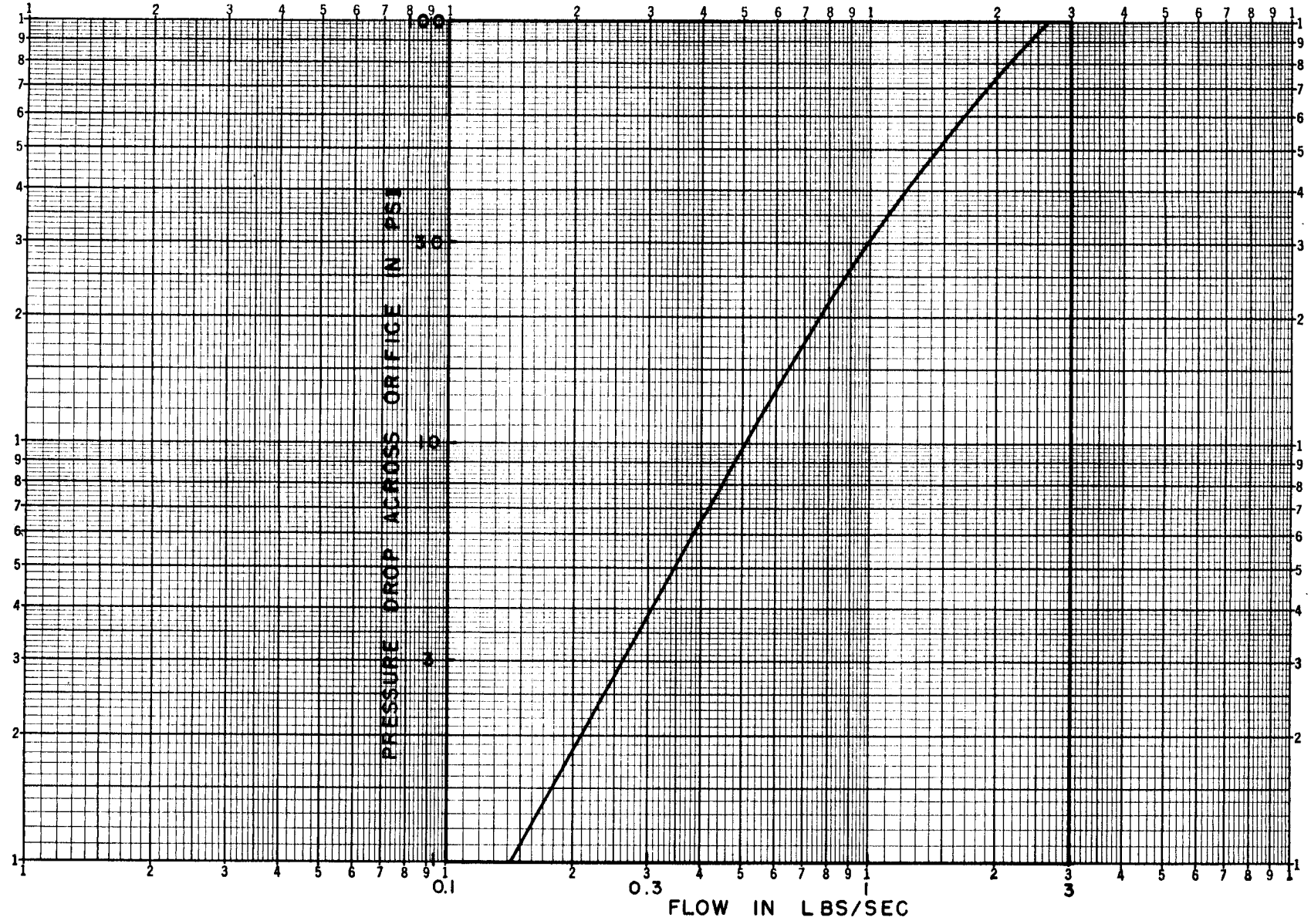

Figure 2.2.5-4 Complete flow curve for an orifice.

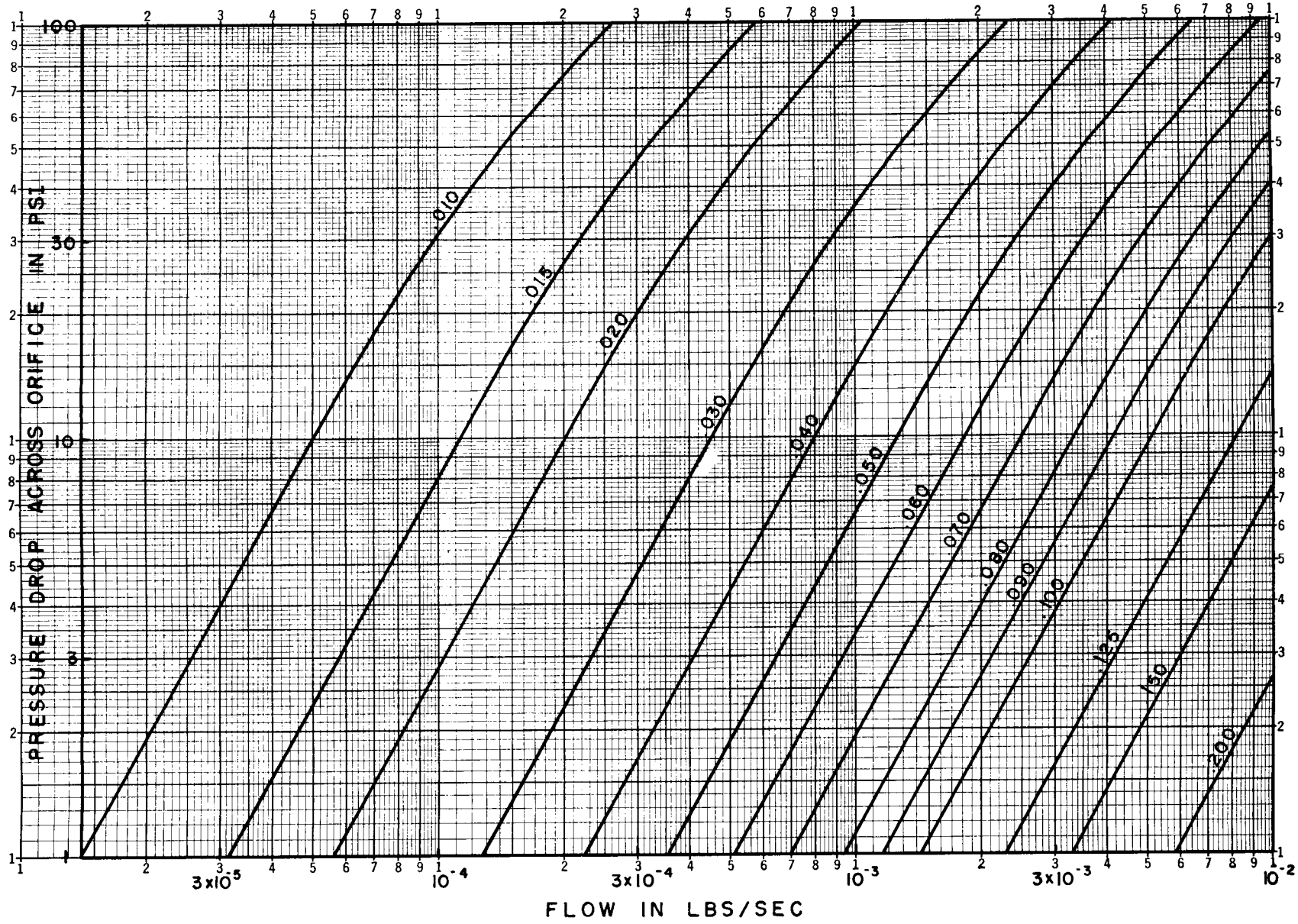

Figure 2.2.5-5 Flow of air through orifices of various diameters. (diameter is in inches)

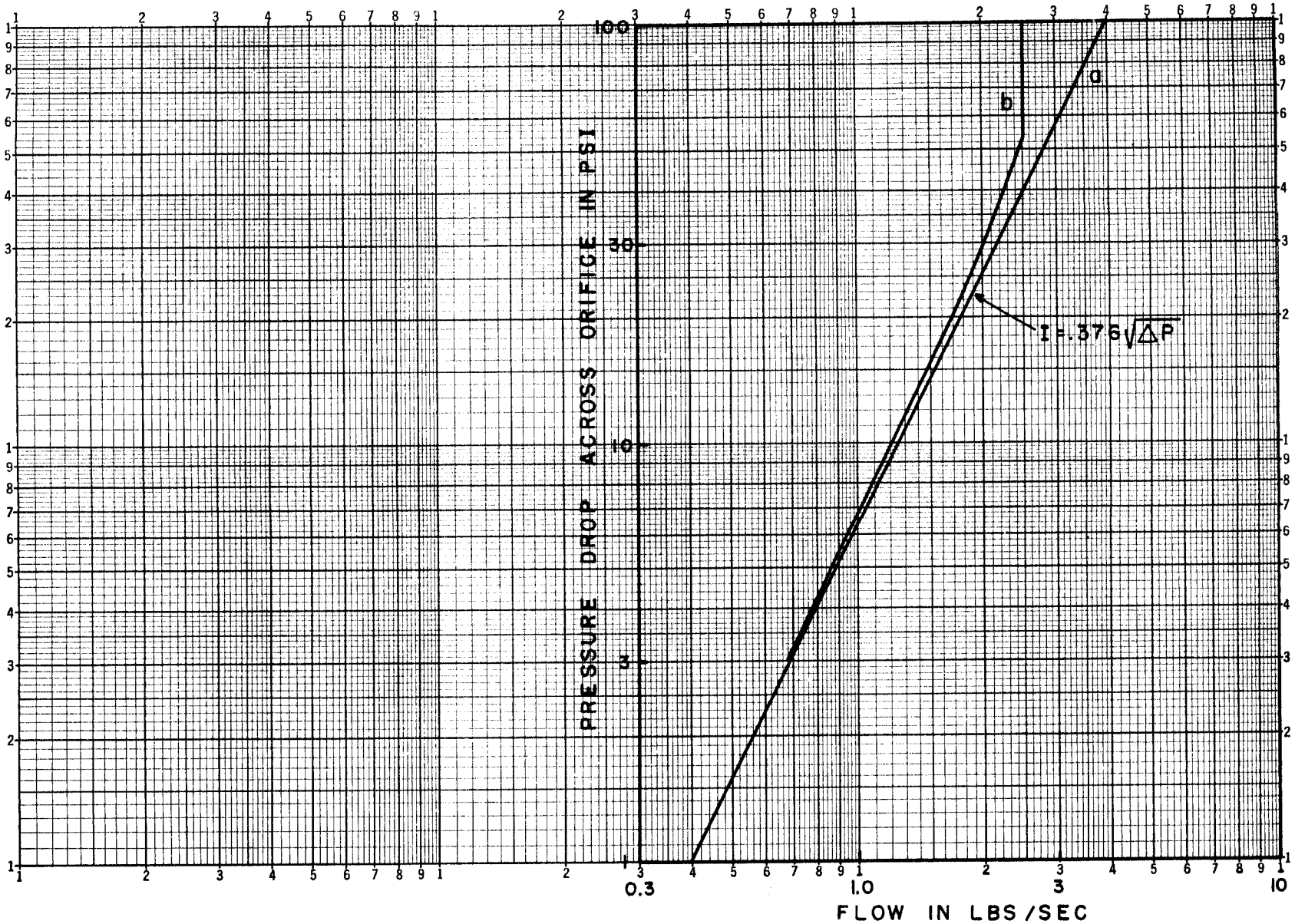

Figure 2.2.5-6 Flow of air through an orifice with constant upstream pressure.

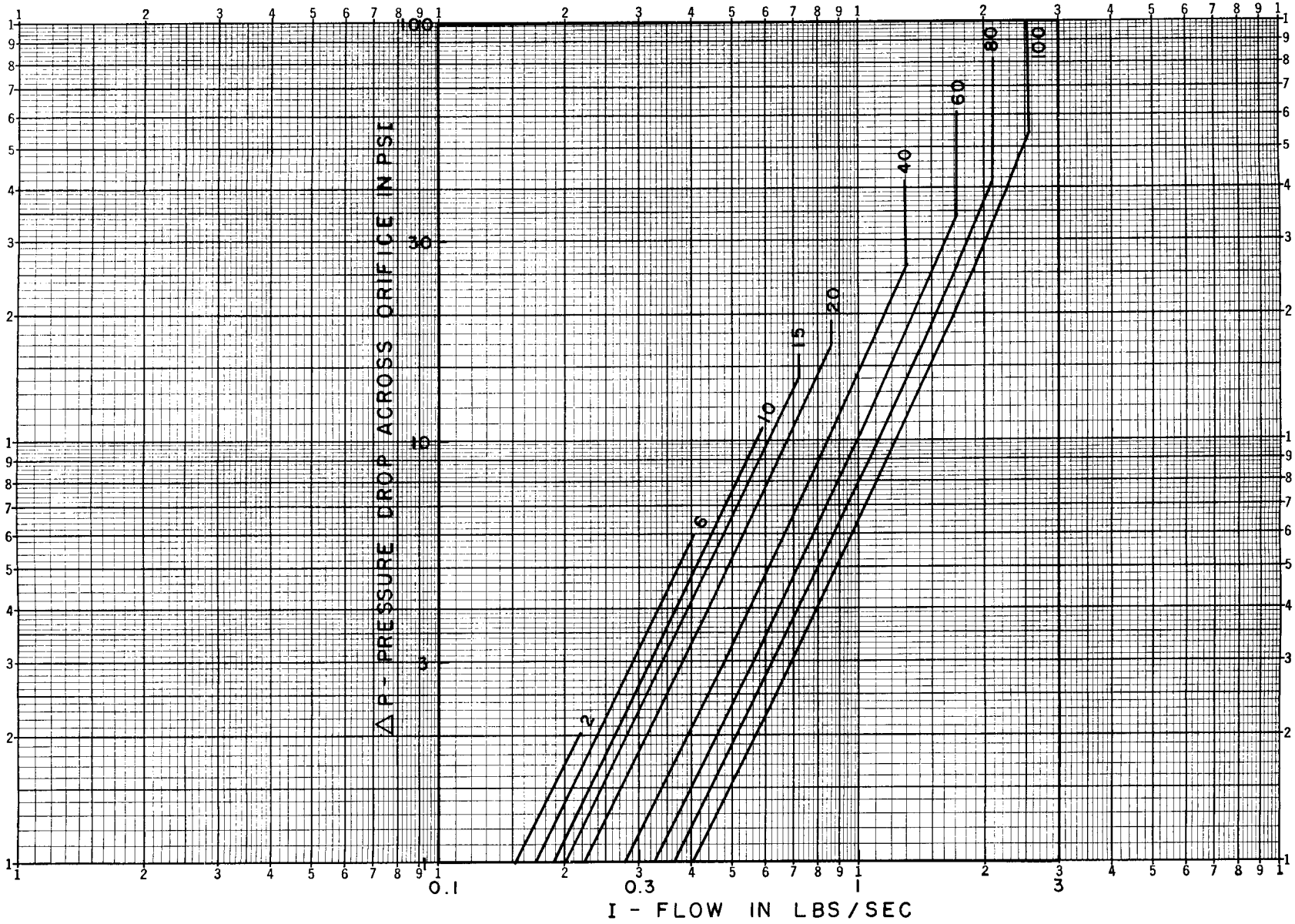

Figure 2.2.5-7 Air flow through an orifice for various, fixed upstream pressures.

2.2.6 Fluid Capacity

The fluid capacity, C, of a volume, V, is defined as the change in the weight of fluid contained within the volume divided by the associated pressure change, i.e.,

$$C = \frac{\int I dt}{\Delta P} \qquad (1)$$

For low frequencies the process will be isothermal and the capacity is given by

$$C = \frac{V}{RT} \qquad (2)$$

In general the flow of the fluid to and from the volume will be polytropic and obeys the law

$$PV^n = \text{constant} \qquad (3)$$

where n is the dimensionless polytropic exponent. When the polytropic law obtains, the capacity is given by

$$C = \frac{V}{nRT} \qquad (4)$$

where n can vary between 1 (the isothermal case) and k (the adiabatic case).

From equation (1) the units of capacity are seen to be lbf/psi = in^2. Hence, in^2 are the proper units of fluid capacity. However, the equivalent lbf/psi is more physically meaningful and shall often be used in place of in^2.

For air at room temperature, the isothermal capacity is found to be

$$C = 2.95 \times 10^{-6} \quad V \quad in^2 \qquad (5)$$

where V is in cubic inches. The polytrop capacity will be less than this by a factor of n, the maximum deviation being the adiabatic situation where n = k = 1.4. A plot of capacity for air as a function of volume is given in Figure 2.2.6-1.

In circuit analysis and synthesis, the capacitive reactance of the volume is of more interest than the actual value of the capacity itself.

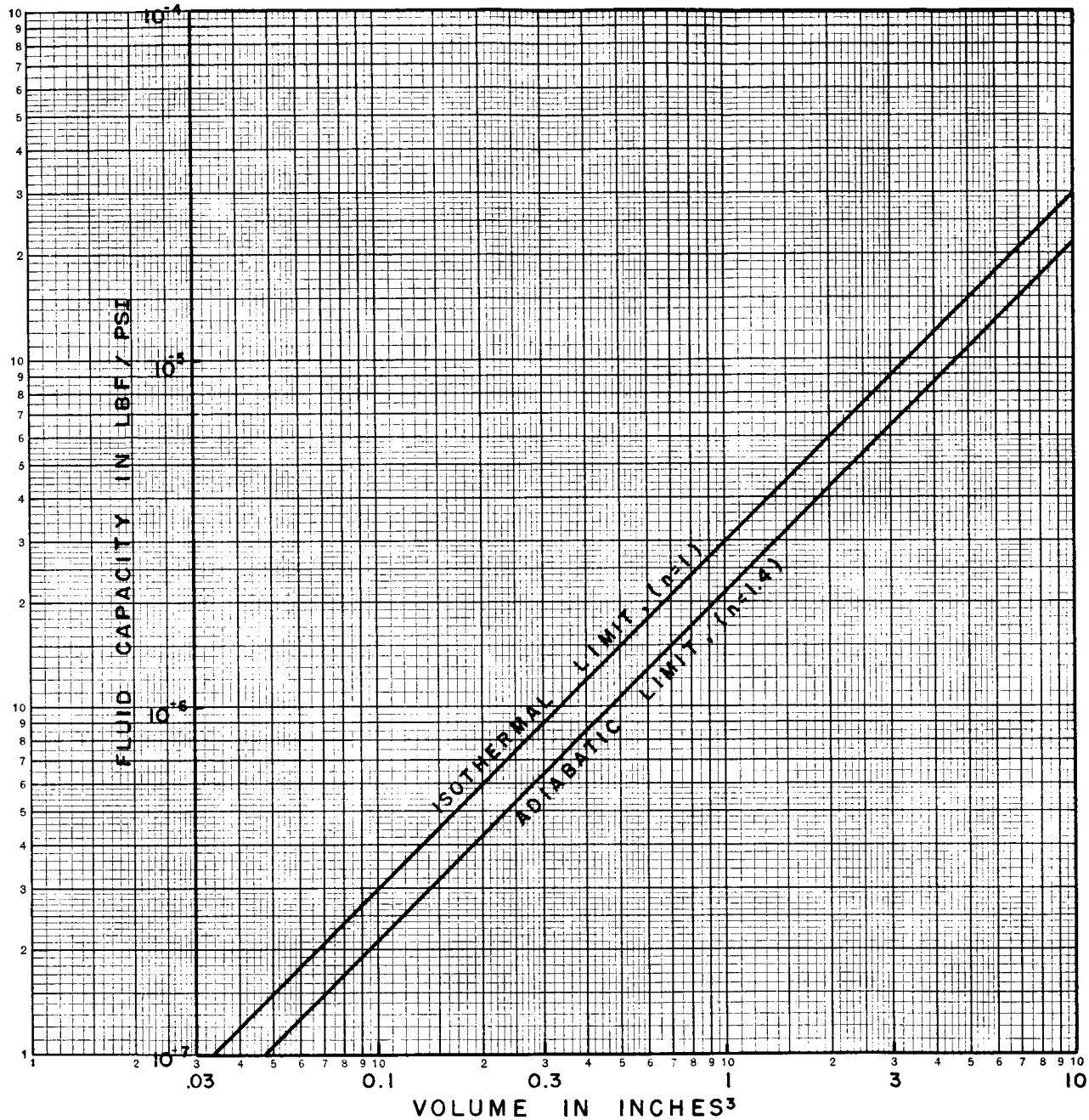

Figure 2.2.6-1 Fluid capacity of a volume.

Hence, a useful graph is a plot of capacitive reactance as a function of volume and frequency. Such a plot eliminates the intermediate step of calculating the capacity. One such plot for the isothermal capacity covering commonly used ranges of parameters is given in Figure 2.2.6-2. A larger plot, of a wider range of parameters, is given in Figure 2.2.6-3. A single cycle out of this larger plot is given in Figure 2.2.6-4. To find the isothermal capacitive reactance of any given volume outside the range of Figures 2.2.6-2, the approximate value can be found from Figure 2.2.6-3 and the more exact value from Figure 2.2.6-4.

In the literature, the fluid capacity of a volume is often given as

$$C' = V/P \tag{6}$$

This differs from the results found above in that the capacity is dependent not only upon the volume but also upon the pressure to which the volume is subjected. This discrepancy comes about from using the actual volume flow rather than a weight flow for the definition of fluid current. For a given fluid current, the actual volume flow at any point in a fluid circuit is dependent upon the pressure at that point.

Starting from the gas law

$$PV = m\,RT \tag{7}$$

and considering the isothermal case, the increment of mass Δm which flows into a volume V under an increment of pressure ΔP is given by

$$\Delta m = \frac{V}{RT}\,\Delta P \tag{8}$$

Define a fluid capacity as

$$C' = \Delta V'/\Delta P$$

where $\Delta V'$ is the actual volume of gas which flows into a fixed volume, V, under a pressure change ΔP. The volume $\Delta V'$ is related to the actual mass flow in by

$$\Delta V' = \Delta m\,RT/P \tag{9}$$

using equation (8) this becomes

$$\Delta V' = \frac{V}{P}\,\Delta P \tag{10}$$

or,

$$C' = V/P \tag{11}$$

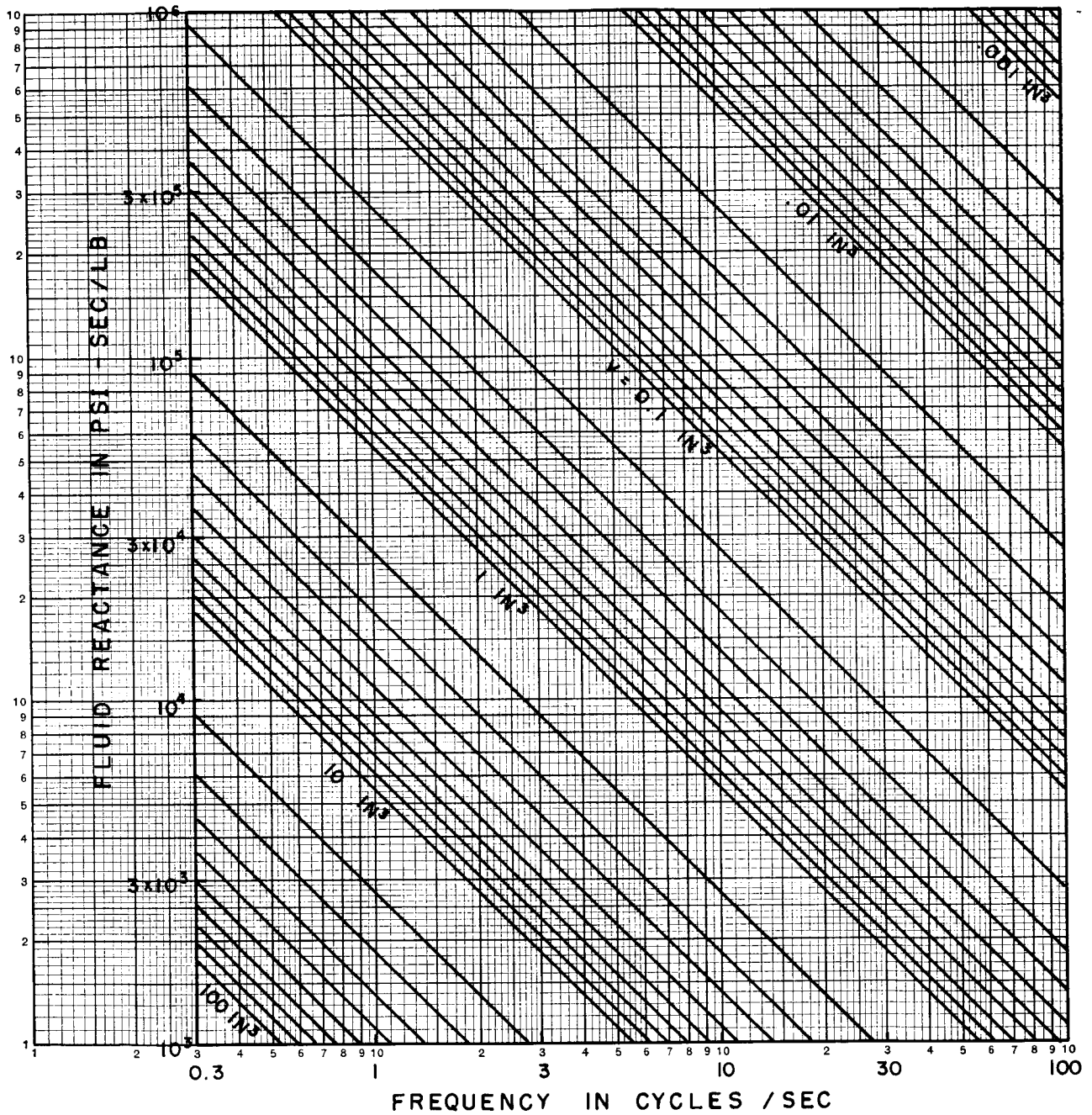

Figure 2.2.6-2 Isothermal capacitive reactance.

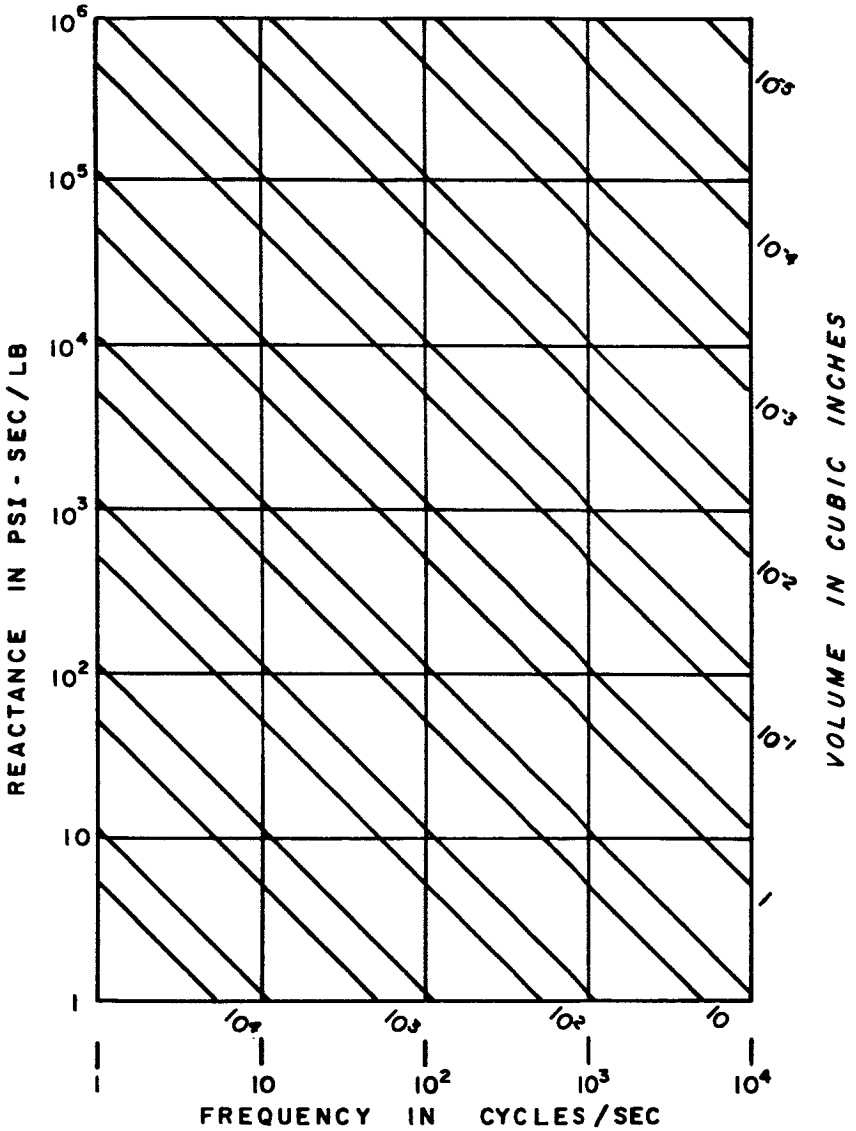

Figure 2.2.6-3 Isothermal capacitive reactance.

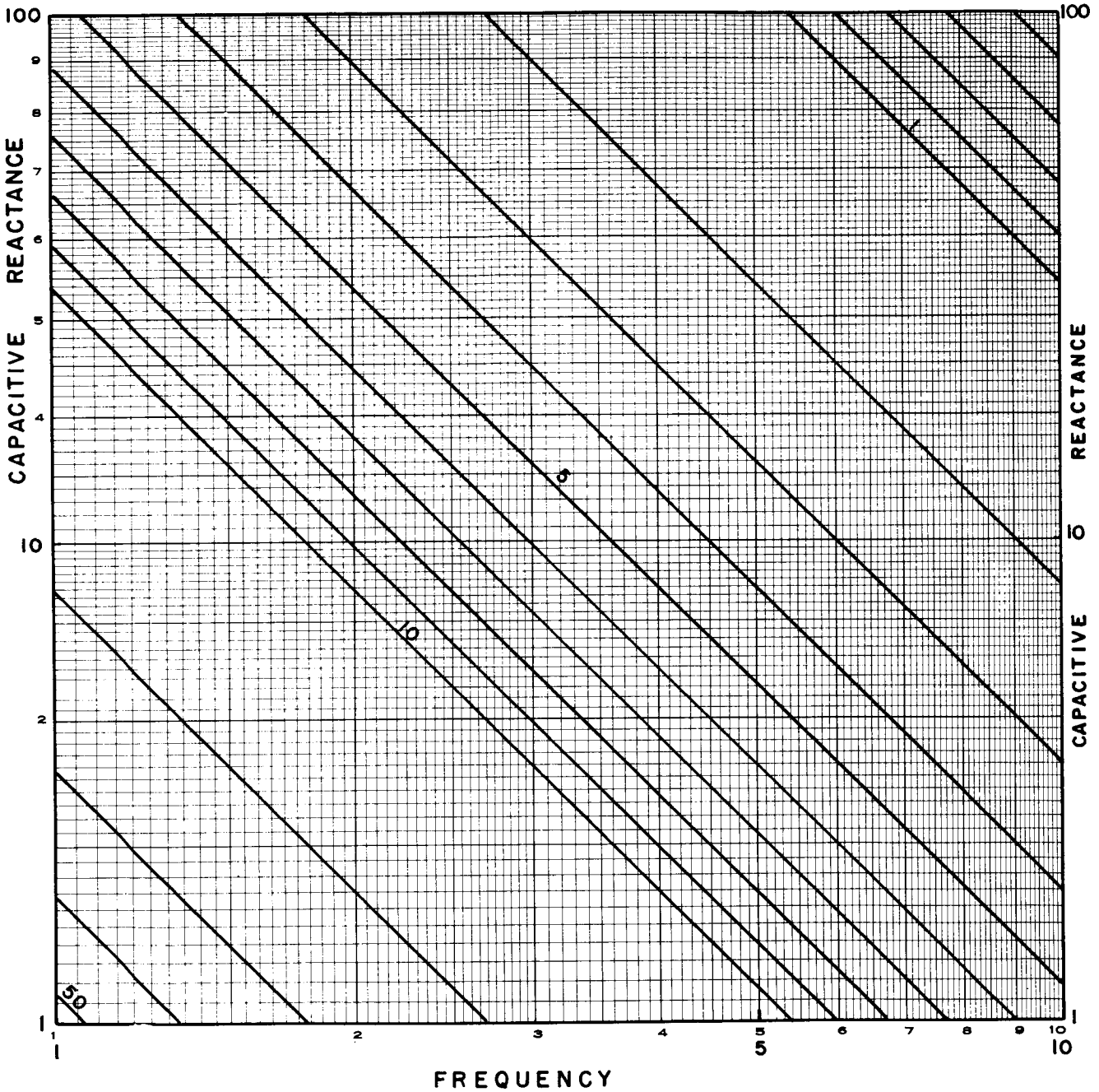

Figure 2.2.6-4 Isothermal capacitive reactance.

Hence, the introduction of P into the denominator of the capacitance equation is seen to come from the defining capacity in terms of the unreduced or actual volume flow rather than the more appropriate weight flow. This expression for the capacitance, while usable, makes the circuit analysis much more complex than the more straightforward definition of equation (1). We shall use the capacitance based upon weight flow in this volume.

2.2.7 Fluid Inductance

In fluid circuitry, a mass which is accelerating or de-accelerating will have the action of an inductance. In the pure fluid circuit, the only moving material will be the fluid itself. Hence, the fluid contained within the transmission lines and other components of the system will be the only inductances.

Consider a section of tubing with area A and length L. Let the tubing be of sufficient size that the resistance is negligible; although this need not necessarily be so. Whenever the fluid current through this section of tubing is increased a pressure drop across the tubing will be required to accelerate the fluid within the transmission lines. For purposes of analysis, the fluid within the section of line under consideration shall be assumed to be incompressible and to accelerate as a single mass. The inductance of this mass will be denoted by H

$$\Delta P = H \frac{dI}{dt} \tag{1}$$

The fluid current through the element is given by

$$I = \gamma Q = \gamma A \bar{u} \tag{2}$$

Combining (1) and (2), it follows that

$$\Delta P = H \gamma A \frac{d\bar{u}}{dt} \tag{3}$$

Applying Newtons' first law to the mass within the tube it is seen that

$$\Delta P A = AL \cdot \frac{\gamma}{g} \cdot \frac{d\bar{u}}{dt} \tag{4}$$

From equation (3) and equation (4) it follows that

$$H = L/Ag \tag{5}$$

Hence, it is seen that the inductance is a function of the dimensions of the fluid component under consideration only. As indicated in equation (5) the units of inductance are psi - $sec^2/lb. = sec^2/in^2$.

Consider now the inductance of a length of round tubing. The inductance in terms of the diameter D is given by

$$H = \frac{4L}{\pi g D^2} \tag{6}$$

The inductive reactance X_H, neglecting the j, is given by $2\pi fH$, or

$$X_H = \frac{8\ fL}{gD^2} \qquad (7)$$

where f is the frequency. Since $8/g = 0.0206$ $sec^2/inch$, this becomes

$$X_H = .0206\ fL/D^2 \quad (psi\text{-}sec/lb) \qquad (8)$$

Plots of inductive reactance for one inch lengths of tubes of various diameters are given in Figure 2.2.7-1.

It is interesting to compare the inductive reactance of tubing to the capacitive reactance of the same section of tubing considered to be a capacitor. Take air as the fluid, and consider a 1 inch length of tube with 0.1 inch diameter. From Figure 2.2.7-1, the inductive reactance of this section of tubing at 100 cycles/sec is 206 fluid ohms. The volume of this same piece of tubing is 0.008 cubic inches. From Figure 2.2.6-7 the capacitive reactance of this volume at 100 cycles/sec is 68,000 fluid ohms. Hence, it is seen that for even quite small sections of tubing the capacitive effects far outweigh the inductive effects.

Now consider a 1 inch length of tubing with a 0.010 inch diameter. The inductive reactance at 10 cycles is seen to be 2,060 fluid ohms. On the other hand it is seen from Figure 2.2.2-2 that the laminar fluid resistance of this same tubing is 240,000 fluid ohms.

In general it is seen that in an air circuit the inductive effects of the fluid can be neglected.

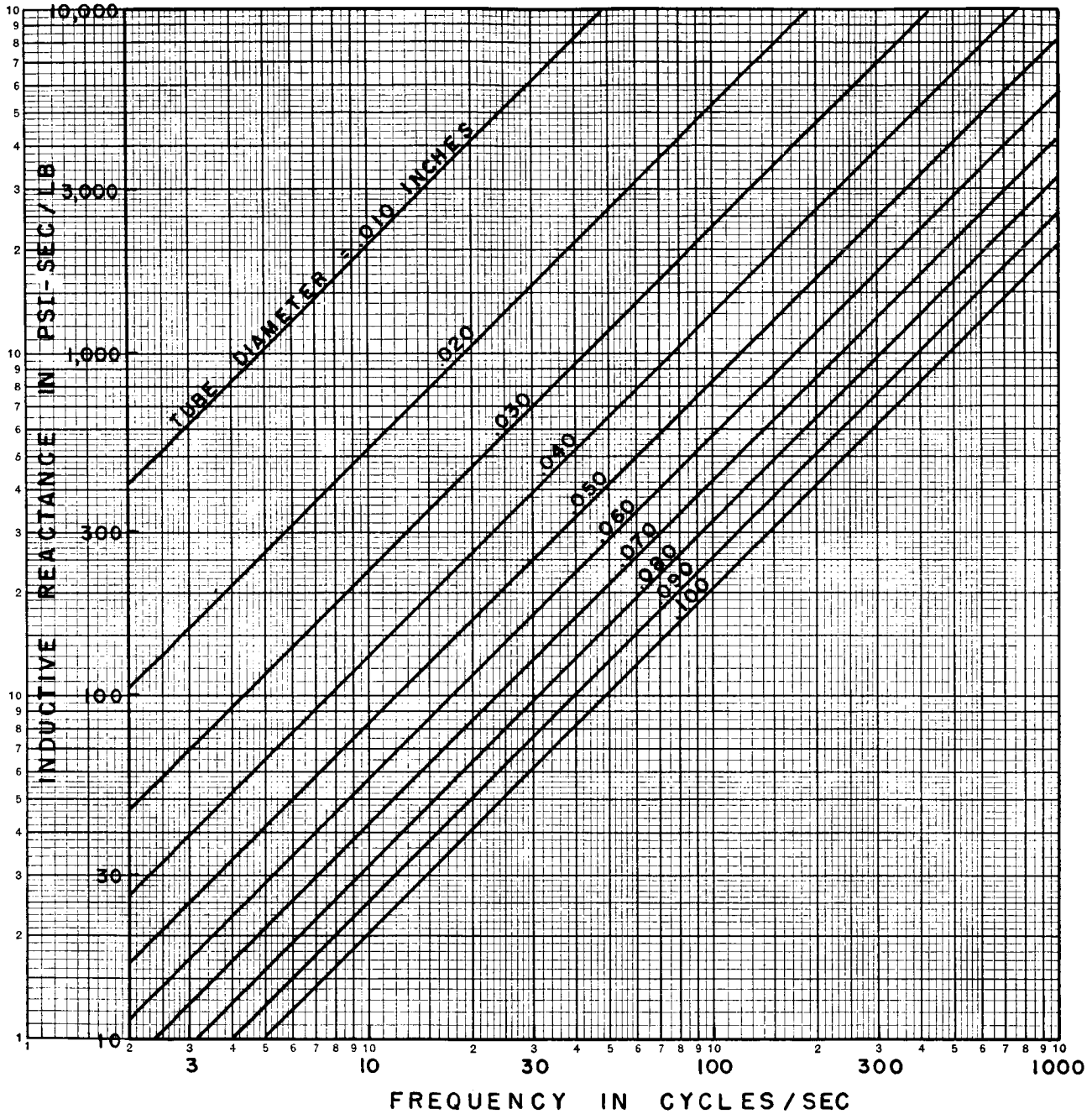

Figure 2.2.7-1 Inductive reactance of a tube one inch in length.

3. FLUID INSTRUMENTATION

As in any new technological field, so in the field of fluid amplification, there is a necessary contemporary development of instrumentation to meet the needs of the new technology. Most of the previous work in fluid dynamics has been concerned with steady-state flow. However, digital and proportional fluid circuitry require the measurements of time-dependent flow. Prior to the development of this new field of fluid amplification, the study of time-dependent flow was performed (for the most part) with fairly large size devices. The advent of fluid amplifiers and the desire to make small computer and control system circuitry created the need for small and time-dependent instrumentation. This portion of the report details some of the fluid instrumentation problems and current instrumentation developments. The instrumentation is covered in two parts: steady-state measurements and time-dependent measurements.

3.1 Steady-State Measurements

Steady-state or quasi steady-state fluid flow does not require instrumentation having any particularly frequency response. The bulk of the fluid dynamics literature (possibly 90%) is concerned with steady or slowly varying flow. This section will treat briefly the instrumentation available and used for such measurements.

3.1.1 Flow Measurements

Flow meters can be divided into two basic sub-divisions: meters to measure velocity of flow and meters to measure quantity of flow. A further breakdown into no-moving-parts, deformable-parts, and moving-part flow meters is useful. A list of the various types of flow meters divided into the above heads follow:

VELOCITY METERS (Rate of flow)

No Moving Parts

Meters utilizing an in-line restriction and providing a pressure difference across the restriction for the flow measurement:

- Venturi
- Elbow (or centrifugal type)
- Orifice
- Flow Nozzle
- Linear Resistance
  - Capillaries
  - Porous Plug
- Critical Flow Nozzles and Orifices
- Thermal Types
  - Hot Wire Anemometers
  - Hot Film Anemometers
  - Thermistor Type
  - Heat Transfer Type

Deformable Part Flow Meters

Force on body with known drag coefficient

- Rotates spring loaded arm
- Bends a flexible supporting arm

Moving Part Flow Meters

- Cup Anemometer
- Vane Anemometer
- Rotor Type Flowmeters
- Rotameters

QUANTITY METERS (Volumetric or Mass Flow)

No Moving Parts

Electromagnetic Flowmeter
Radioactive Tracers

Moving Parts

Wobble Plate or Nutating Disk
Rotary Type

Most of the meters listed above are steady-state type flow meters. The exceptions are the thermal types and these will be discussed later.

The work performed at Sperry Utah Company has in general made use of the "Vol-O-Flow" linear restriction type of flow meter (see Figure 3.1.1-1), the quantity or totalizing flowmeter which is a modified gas meter such as used to measure gas consumption in the home (see Figure 3.1.1-2), locally fabricated venturi and orifice types of flowmeters, and the hot-wire anemometer (Figure 3.1.1-3). (See discussion in Section 3.2.1.)

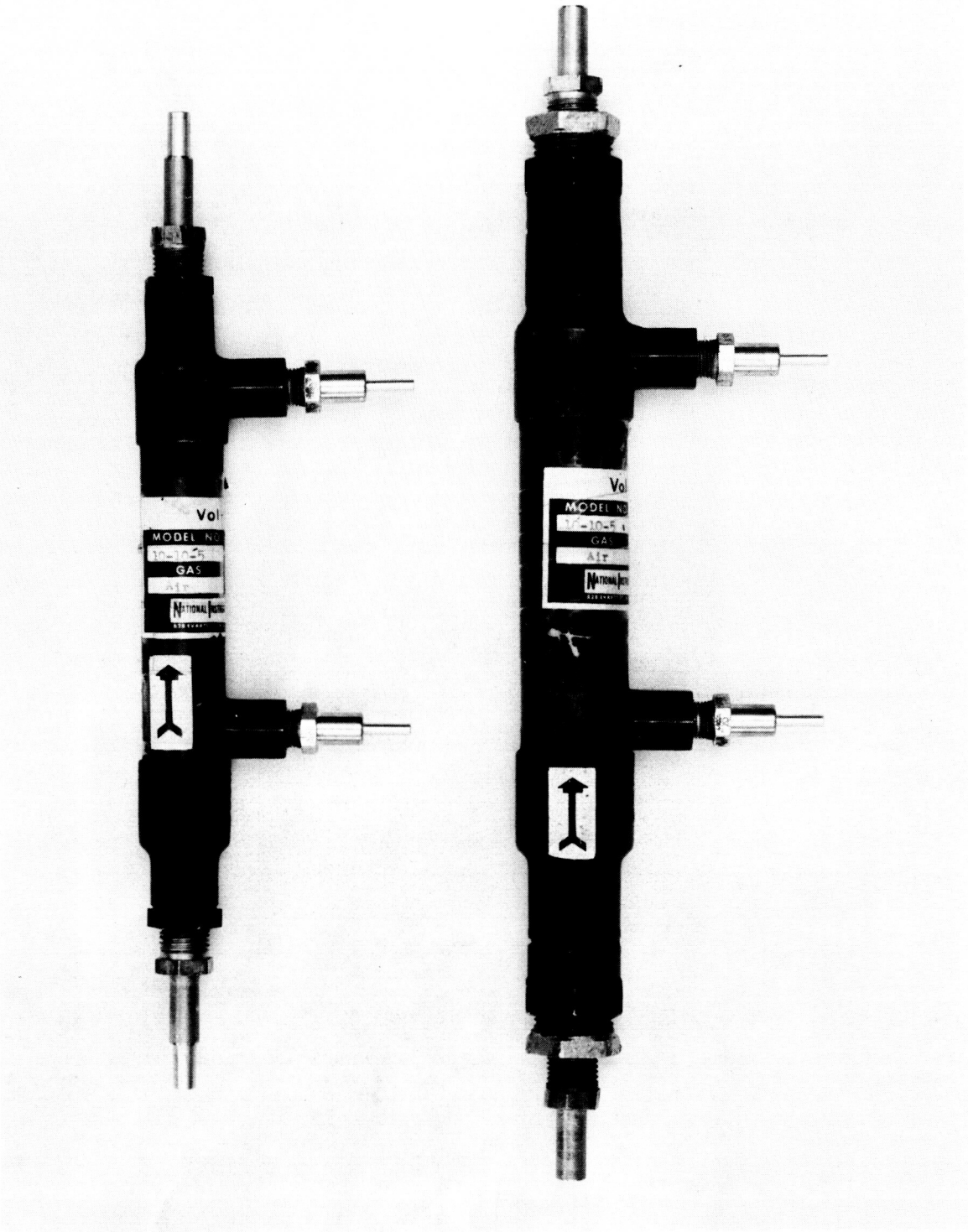

Figure 3.1.1-1

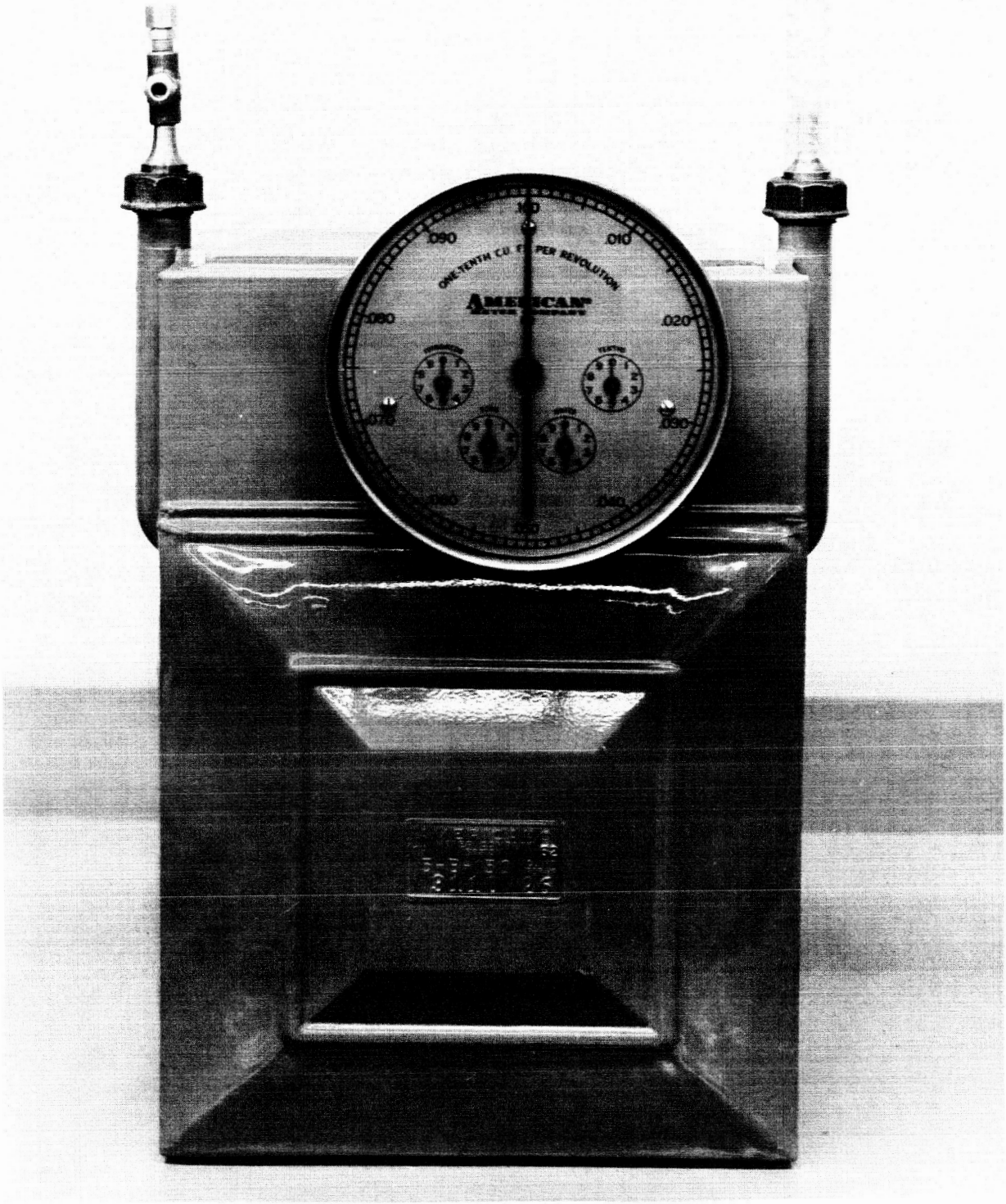

Figure 3.1.1-2 Totalizing Flowmeter

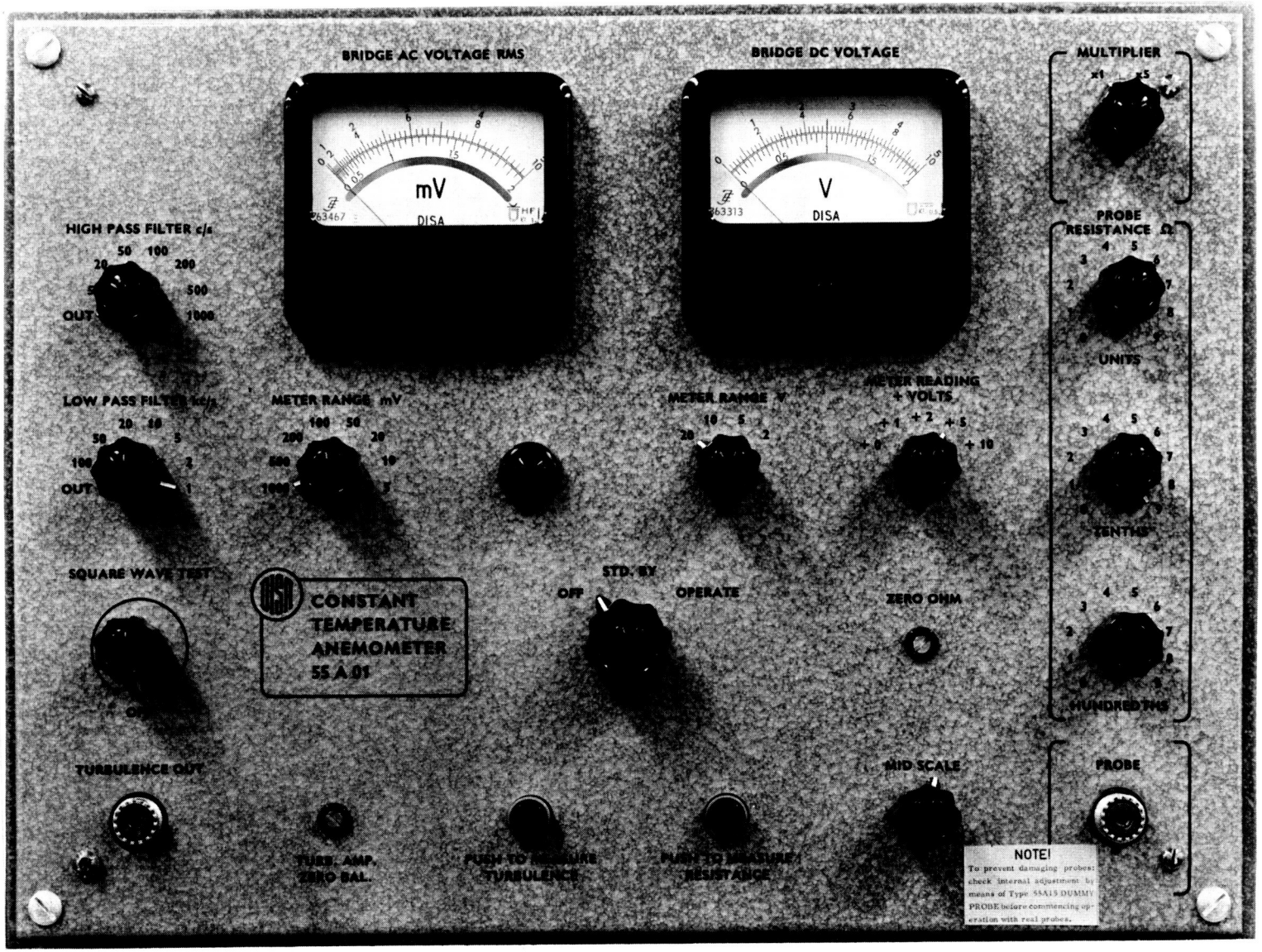

Figure 3.1.1-3 Constant temperature hot wire anemometer.

3.1.2 Pressure Measurements

Instruments to measure pressure can be subdivided into the no-moving-part, deformable-parts, and moving-parts types of devices. A list of most types of pressure measuring devices is presented under the above headings:

No Moving Parts

- Pilot Tubes
- Kiel Probes
- Claw Probes
- Wedge Probes
- Manometers
  - U-Tube
  - Well Type

Deformable Parts

- Diaphragm Types
  - Capacitive Pickoffs
  - Strain Gage Pickoff
  - Variable Reluctance
- Crystal Transducers
  - Quartz
  - Lead Zirconate Titanate

Moving Parts

- Gages (generally with moving part linkages)
  - Bourdon Tube
  - Bellows
  - Diaphragm

With the exception of the diaphragm type devices using some form of electrical pick-off and the Crystal-type pressure transducers all of the other pressure measuring devices are usable only for steady-state pressure measurements or for slowly varying flows.

At Sperry Utah Company, we have used the Pitot tubes, U-tube mercury and water manometers, piezo-electric pressure transducers, bourdon and bellows-type pressure gages, and a variable reluctance pressure gage.

The piezo-electric transducers and the variable reluctance pressure gage will be discussed under the Section 3.2.2.

For steady state flow, the pressure gage is the easiest piece of equipment to use. The only disadvantage to the pressure gage is the need for occasional calibration checks. Manometers are easy to use, work over a wide pressure range by using either water, oil, or mercury and are essentially always in calibration. However, the reading of manometers and conversion of the readings to desired units, the replacement of the water or mercury after an unexpected pressure change, and the bulkiness of a tall manometer are disadvantages which subtrace from their utility in the laboratory.

3.1.3 Flow Visualization Techniques

Three types of flow visualization techniques are of importance to the fluid system designer. The first of these is the use of colored fluids (liquids) and can be used both for steady-state flow visualization and slowly varying flows. For rapidly varying flows, difficulties arise due to turbulent mixing of the fluid.

Wind tunnel technology has long made use of plumes of smoke to show the steady-state or slowly varying flow patterns in the vicinity of an obstacle or model. With proper scaling, certain elements of fluid circuitry can be observed by an adaptation of this technique of observing the flow patterns by the use of smoke.

The most useful flow visualization tool used at Sperry Utah Company consists of a modified Preston Oil Smoke Generator together with a fume hood and transparent models of fluid devices. Figure 3.1.3-1 shows the smoke generator being used with some models. Figure 3.1.3-2 depicts a fluid vortex formed in a right circular cylinder. This flow visualization equipment was used to observe the formation of a fluid vortex and was found to be a great aid in solving the fluid equations necessary to analytically handle the vortex phenomena.

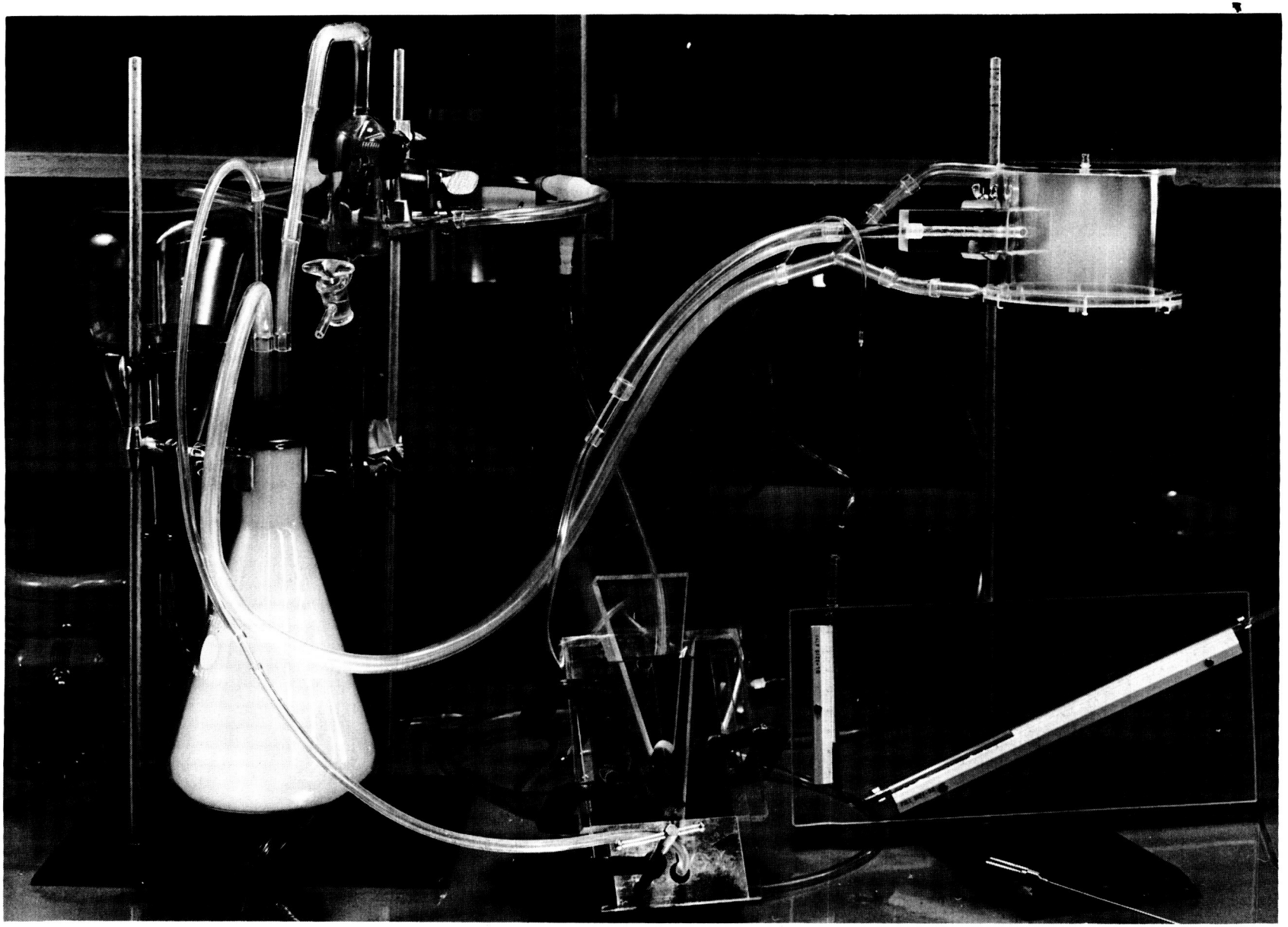

Figure 3.1.3-1 Vortex chamber, laboratory setup.

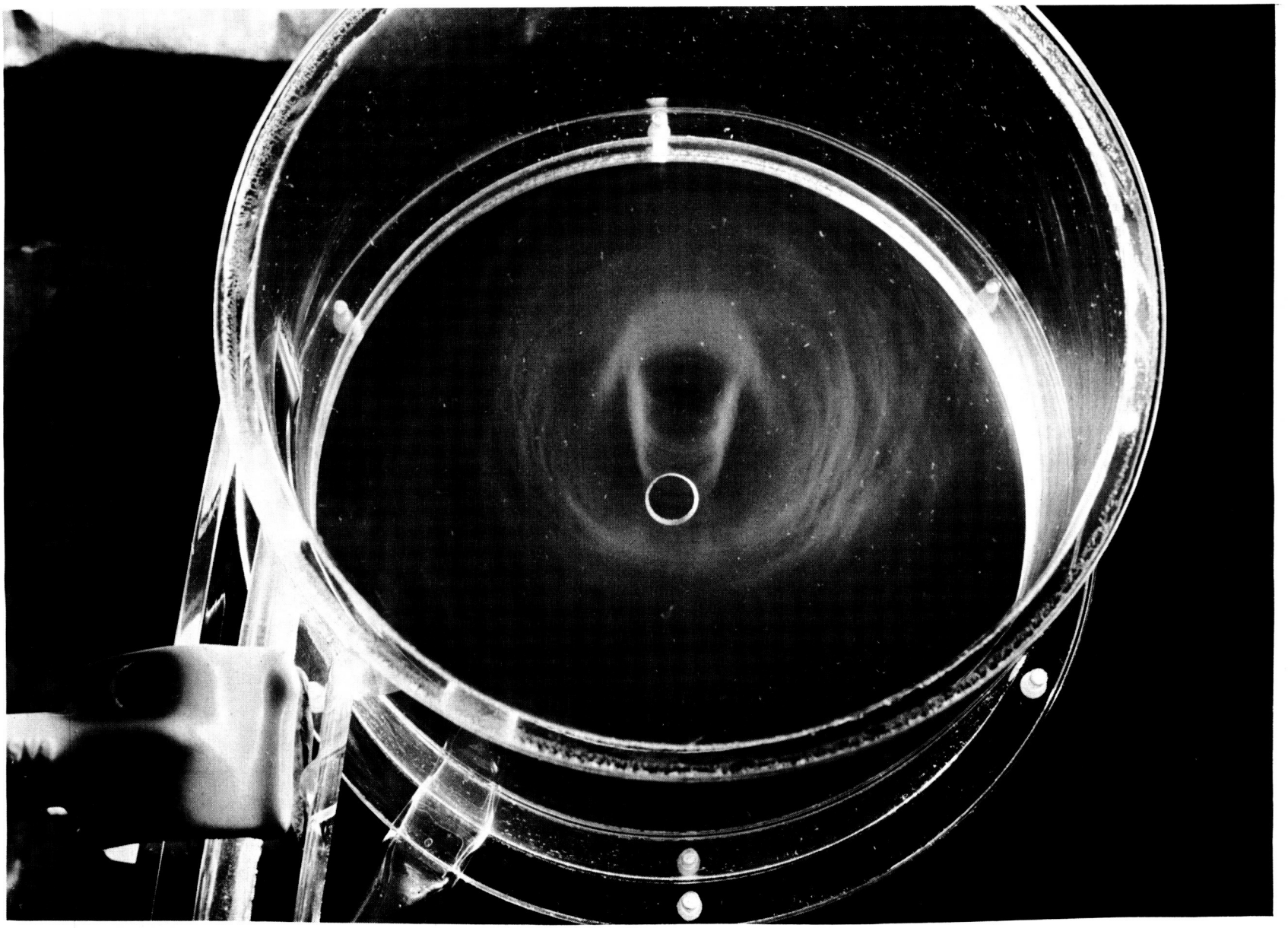

Figure 3.1.3-2 Photograph of experimental vortex chamber.

3.2 Time Dependent Measurements

For fluid measurements which vary with time, there are a limited number of devices which can provide adequate information. Any flow or pressure measuring device can, of course, provide information on slowly varying changes. In fact some gages will respond to changes up to a few cycles per second. For the purposes of fluid-control engineering, it is necessary to have instrumentation which has a frequency response of at least an order of magnitude higher than the signals being measured. Some such flow and pressure measuring instruments are discussed in this section.

3.2.1 Flow Measurements

The basic instrument for measuring rapidly fluctuating flows is the hot wire anemometer. Basically, this instrument utilizes the change in current through a resistance wire caused by a change in temperature. In operation a fine wire (such as Platinum or Tungsten Wire of less than 0.001" in diameter) or a thin film is heated by passing an electric current through the wire or film. Any change in the flow of a fluid (usually a gas) past a heated wire, or film, will result in a change in the temperature of the wire, or film. The faster the fluid flows, the greater the rate of heat removal.

As heat is removed from the wire, or film, electrical circuitry connected to the hot wire, or film, probe senses the change in resistance of the wire, or film. Two types of circuitry are utilized. One type of circuitry is designed to keep the temperature of the wire constant (Constant Temperature Hot Wire Anemometer). A second type of circuitry is designed to maintain the current through the wire at a constant value (Constant Current Hot Wire Anemometer).

At Sperry Utah Company, we have chosen to use the constant current type of hot wire anemometer because it has, in general, a higher frequency response than the constant temperature type device. Figure 3.1.1-3 depicts a Constant Temperature Anemometer made by DISA of Denmark.

The probes that are available with hot wire anemometers are not readily suited for making fluid measurements in small diameter ducts and pipes. SUCO has therefore designed special probes which can be placed directly in series with the line to be measured. Figure 3.2.1-1 depicts these special probes. Figure 3.2.1-1a also shows the ordinary miniature probe provided with the equipment. This probe is useful making flow measurements (or traverses) across relatively large devices or ducts. The delicate nature of the probe, because of the very fine wire welded across the probe tip, prevents it from being readily inserted into a tube or pipe. Figure 3.2.1-1b depicts the same type of probe in a different sort of mounting. Here the probe support is adapted for easy mounting of the hot wire directly in line with a circular duct or pipe. Figure 3.2.1-1c depicts a probe body which combines both the hot wire anemometer probe and the crystal pressure transducer. The insertion of this probe in the line permits the measurement of both the flow and the pressure fluctuations at the same time. For example of hot-wire data see Figure 3.2.1-2.

Figure 3.2.1-1

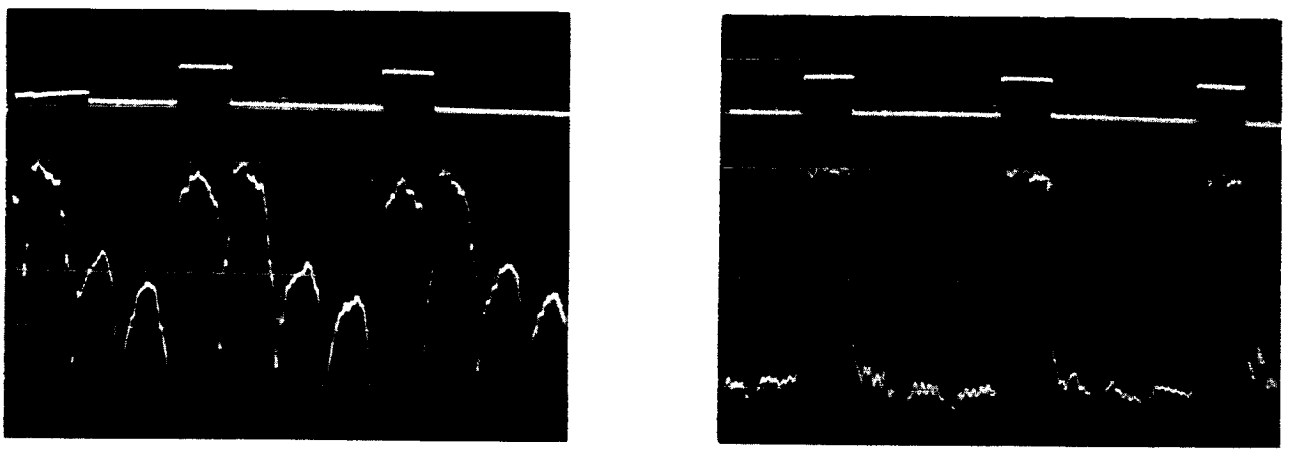

Figure 3.2.1-2 Acoustic effects in a pulse fed pipe.

LEFT: INPUT WAVEFORM WHEN SUPPLYING FLUID PULSES TO A FOUR FOOT PIPE (¼ in. I.D.)

RIGHT: INPUT WAVEFORM WHEN END OF FOUR FOOT PIPE HAS PROPER ACOUSTIC TERMINATION.

NOTE: UPPER TRACES FROM OPTICAL PICK-OFF; TIME 10 msec/cm, DISA HOT WIRE ANEMOMETER DATA.

Some difficulties should be noted in the use of a hot wire anemometer. The probes with their associated circuitry provide a fourth power curve as a function of flow (see Figure 3.2.1-3). Some manufacturers provide linearizing circuitry.

Due to the non-linear nature of the output, pulse shapes are considerably distorted. The non-linearity is such that the probe is most sensitive to small flows and less sensitive to large flow rates. If one is using the anemometer to observe fluctuations in flow superimposed on a given amount of flow, then the non-linearities are not greatly apparent. Under such conditions, however, another of the difficulties with some anemometer equipment becomes apparent.

Some of the anemometer circuitry uses a cathode follower circuit to couple to external indicating equipment (such as to an oscilloscope). A fluctuating signal superimposed on a steady-state flow represents a given voltage output plus a fluctuating voltage. To observe the details of the fluctuations on an oscilloscope, it is necessary to isolate the oscilloscope from ground and then provide a steady bias voltage between scope and ground to "float" the scope above the ground potential. When using two hot wire anemometers, this procedure can become very troublesome because of the difference in voltage outputs from two sets of anemometer circuitry and probes.

At least one manufacturer (Thermo-Systems, Inc.) provide for direct "biasing" of the output voltage on the control panel of the anemometer. This accomodation is of great advantage. The equipment made by DISA does have some filter circuits, which will remove the d.c. voltage from the output and leave just the fluctuations. There are some difficulties involved in using this circuitry for some of the flow measuring applications peculiar to pure fluid control systems.

The calibration of the ordinary probe (Figure 3.2.1-1a) requires a low turbulence wind tunnel such as is shown in Figure 3.2.1-4. However, the types of devices as shown in Figures 3.2.1-1b and 3.2.1-1c can easily be calibrated by using a length of tubing of the appropriate size and a totalizing flowmeter. If the length of the tubing preceding the probe is many times the diameter of the tubing, then there will be fully established "pipe flow" up to the probe and good results can be made in calibating the probes. The tubing after the probe need only be connected to the totalizing flowmeter (or to a rotameter of the correct size) and the flow determined. The totalizing flowmeter is desirable due to its low cost and high accuracy.

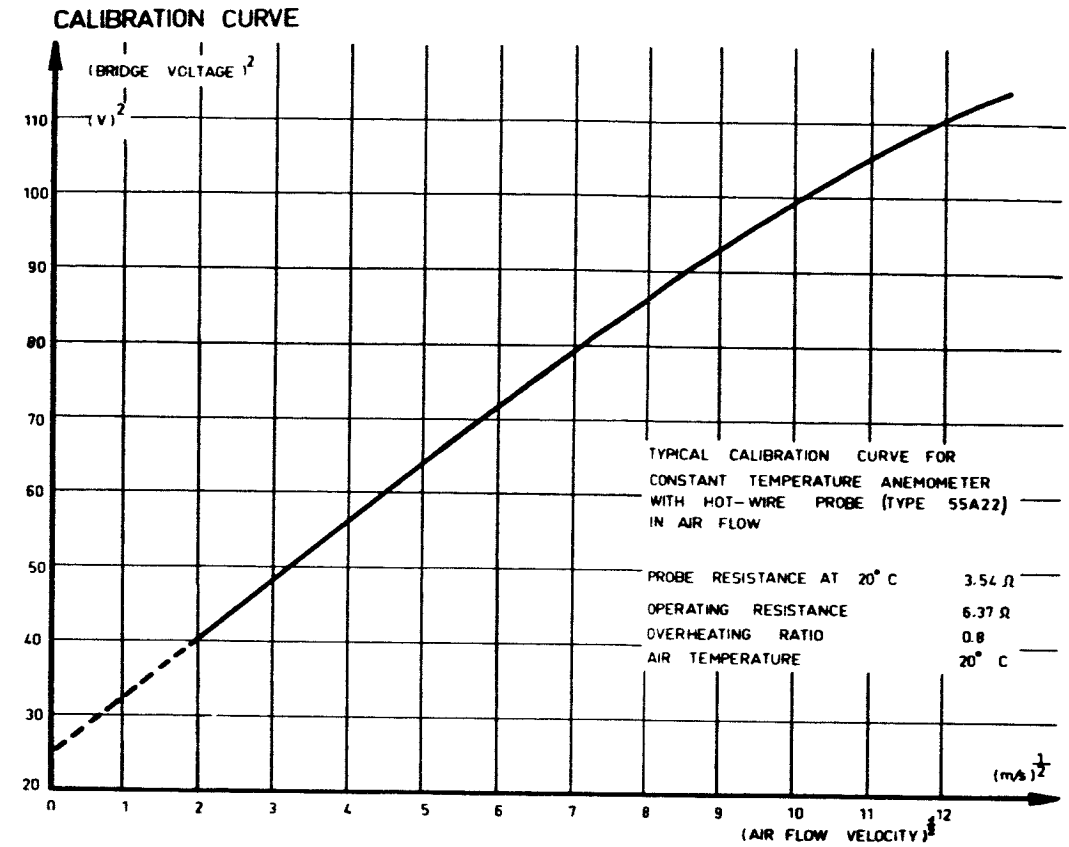

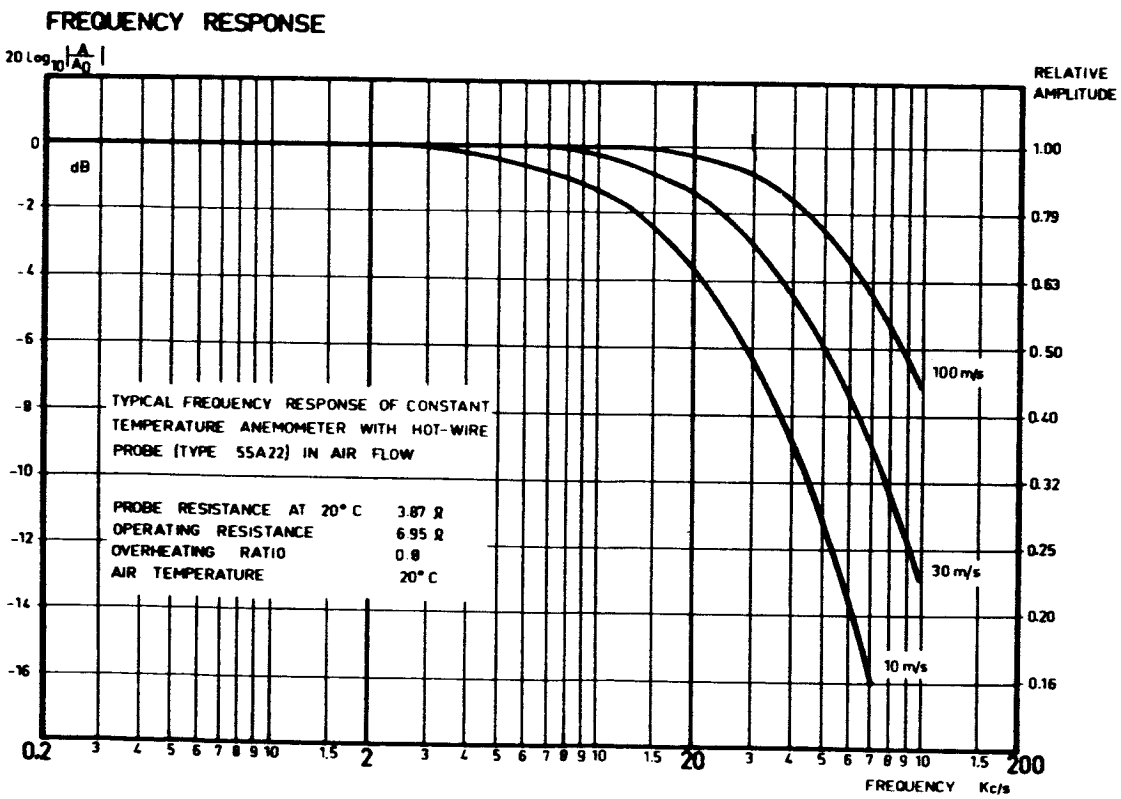

Figure 3.2.1-3 Typical calibration curves for anemometer probe.

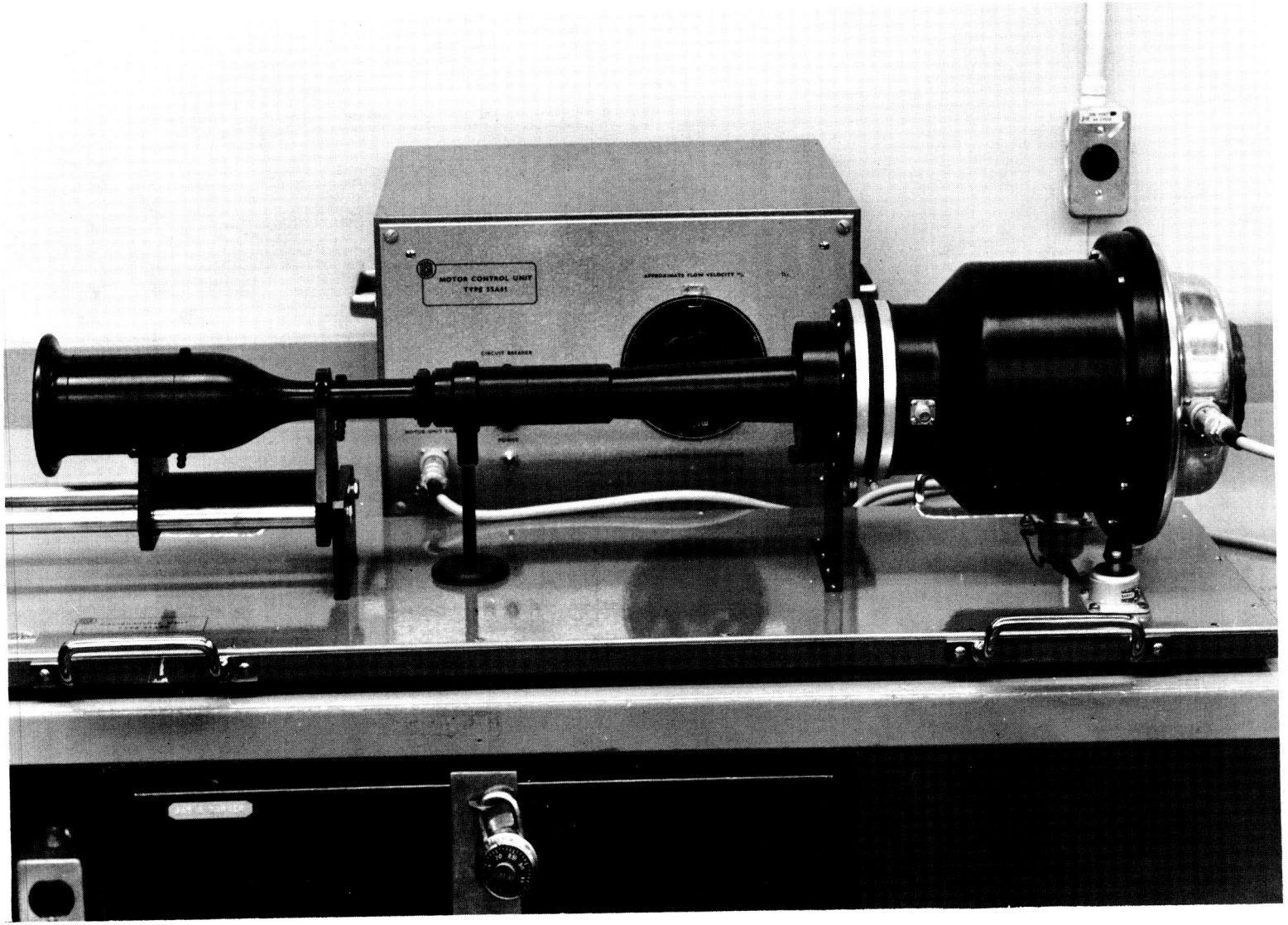

Figure 3.2.1-4 Calibration Wind Tunnel

3.2.2 Pressure Measurements

Time dependent pressure measurements at SUCO are made by one of two devices, the Sensonics "Variducer" and a locally fabricated variable reluctance pressure transducer.

Crystal Transducers. The "Variducer" made by Sensonics, Inc., of Kensington, Maryland utilizes a small lead zirconate titanate crystal as the sensing element. The crystal is pre-stressed for improved performance. The Variducer used at SUCO is the MC25-1 which has a pressure range from 0 to 100 psig with the useful minimum pressure being about 0.001 psig (although this minimum value depends on the circuitry to which the crystal is attached). The frequency response of the device is listed as 2 cps to 500 kcps.

The crystal type transducers (either the lead zirconate titanate or the quartz crystal) have two problems in use. The first problem is that the transducer is responsive only to changes in pressure and not to the mean value of the pressure. This may be compared to an electronic device which indicates only the a.c. component of the signal and not the d.c. component. This problem results in some difficulty in calibrating the transducer and associated circuitry. It is only fair to say that the manufacturers of these transducers do sell circuitry to resolve both of the above difficulties. Typical prices of the transducers are $200 to $250 each and the associated transducer amplifiers range from $300 and up.

Another difficulty in use of the crystal pressure transducer is in its very high frequency range. While this may appear to be an immediate advantage some consideration will show that high frequency response can be a limitation in pure fluid control circuitry work. In almost all fluid circuitry where there are active components there is some type of a free jet, submerged free jet, jet-edge combination, or impinging jets. In all of these cases a considerable amount of high frequency "noise" is produced. To the ear, this noise is a hissing sound. To the crystal transducer, this noise is a highly variable, high-frequency background, somewhat comparable to the "white noise," or thermal noise, in electron circuitry. Very often, the amplitude of this hissing noise is of the same order of magnitude as the signal when measurements are made close to the active element. However, almost none of the active devices which are coupled downstream are sensitive to this high frequency noise. In many cases the volumes of the interconnecting passages quickly damp out of the high frequency perturbations. Therefore, when measuring the output of an active component, the signal is often masked by the high frequency variations of this "noise." When using a crystal transducer, both the signal and the "noise" are present in the display output, unless the circuitry is modified to filter out the high frequency components.

Variable Reluctance Pressure Transducer. If it is desired to produce a linear pressure transducer which has an output which is a function of both steady-state and fluctuating pressures, then conceptually a small diaphragm pressure transducer will suffice. The details of some of the physical design problems are presented in Reference 9.

At SUCO, we have adapted the information contained in this reference and have fabricated a transducer which has proved most useful. Figure 3.2.1-1d

shows this variable reluctance pressure transducer. The solution to the response problem is to use a small thin pre-stressed diaphragm. Radially stressing the diaphragm acts to raise the natural frequency of the diaphragm to a level above those frequencies which are of primary interest.

Some of the biggest problems in the construction of this variable reluctance pressure transducer are found in the associated electronic circuitry. The pick-up coils must be supplied with alternating current excitation of a frequency well above the frequency which the transducer is expected to measure. Balancing means need to be provided to balance out the bridbe circuitry. Considerable amplification of the pick-off signal must be provided to obtain a useful output level. Near zero pressure, the transducer is also near zero output voltage so that any noise is amplified by the associated circuitry. Unless special care is used in the design and isolation of the circuitry, very low level signals may be masked by electronic noise.

In operation, the transducer functions in the following manner: The diaphragm is part of a magnetic circuit formed by the body of the transducer and excited by the two pick-off coils. With no pressure differential across the diaphragm, the electrical output of the transducer is zeroed. When pressure on one side of the transducer is larger than the opposite side, then the diaphragm will bend toward the lower pressure. The change is position of the diaphragm represents changes in the magnetic circuit of the transducer. Such a change in the magnetic circuit unbalances the pick-off coil portion of the bridge circuit with a resultant change in the output voltage. The output voltage from the bridge may vary from zero to fifty millivolts.

The voltage level from the bridge is too low to be rectified with diode circuitry so the output voltage is fed to an amplifier. The output of the electronic amplifier is supplied to a diode, bridge-rectifying circuit, and the resulting d.c. voltage is used to drive an output display device (oscilloscope or recorder). The d.c. output has a fairly good linear relationship with the input pressure to the transducer. Therefore, when the transducer is used with fluctuating signals, the output waveform is a fairly accurate representation of the pressure waveform.

The transducers as made and used at SUCO have been designed to provide a frequency response in the range of two to four kcs. This allows for the measurement of the signal frequencies without being responsive to the "hissing" high frequency noise. This results in a quite clean signal when viewed by the use of an oscilloscope.

Figure 3.2.2-1 shows a photograph of a typical input and output signal and measurement made with an "impact modulator."

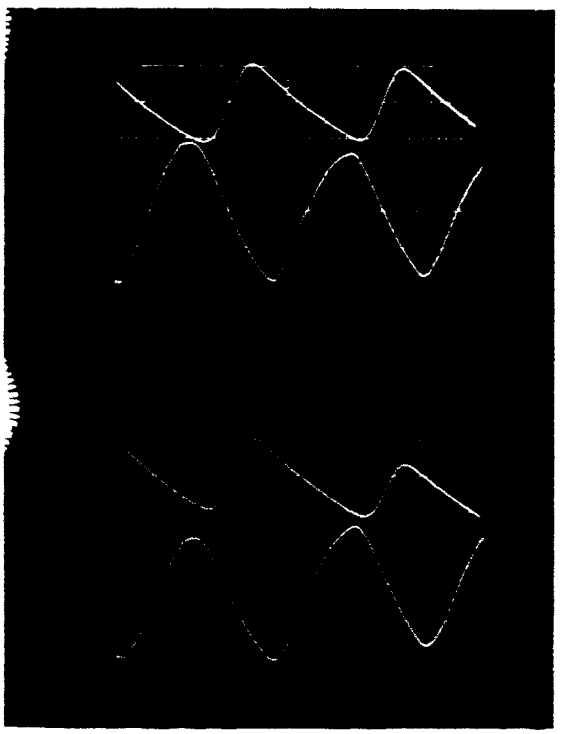

Figure 3.2.2-1 Impact Modulator Input Output Signals

3.2.3 Flow Visualization Techniques

Flow visualization techniques suitable for the study of time-dependent fluid phenomena exist. The most useful device for this approach is the oil smoke generator (see Figures 3.1.3-1 and 3.2.3-1) used together with either visual or photographic techniques. The problems in using smoke visualization techniques can be listed as follows:

a. Inhalation of oil smoke can cause respiratory ailments, therefore it is necessary to utilize a fume hood or at least a charcoal hood with ventilating fan to remove the smoke.

b. The oil smoke tends to condense in tubes and ducts. Condensation is particularly troublesome with small pipes and ducts. Therefore, it is sometimes necessary to scale up the experiment (using proper scaling laws) in order to study the flow patterns.

c. Even the best smoke is sometimes difficult to photograph. It takes some experience with lighting, smoke density control, and careful machining of transparent test devices to obtain the desired results.

d. Smoke visualization can best be used only up to a certain level of flow velocities. High speed air moving into a geometry where turbulence is no longer inhibited allows for rapid dispersal of the smoke. With care, however, flows as 250 feet per minute can be studied by smoke visualization.

Even with the above problems, the use of smoke visualization is one of the best methods of determining the nature of the fluid flow variations and leads to considerable improvement in device design.

Experimental work performed by Messrs. Goldschmied and Fox using a high speed motion picture camera and smoke for flow visualization made significant early contributions to the understanding of the nature of the flow in wide-angled rectangular diffusers and in the switching mechanisms of the wall-attachment amplifier. Photographs were taken of edgetone and switching phenomena at the rate of 8,000 frames per second. The slow motion projection of the movies which resulted were most helpful in understanding some of the basic fluid dynamics problems associated with the devices studied. Suffice to say that such efforts with flow visualization are credited with saving many manhours in work in cut-and-try empirical methods.

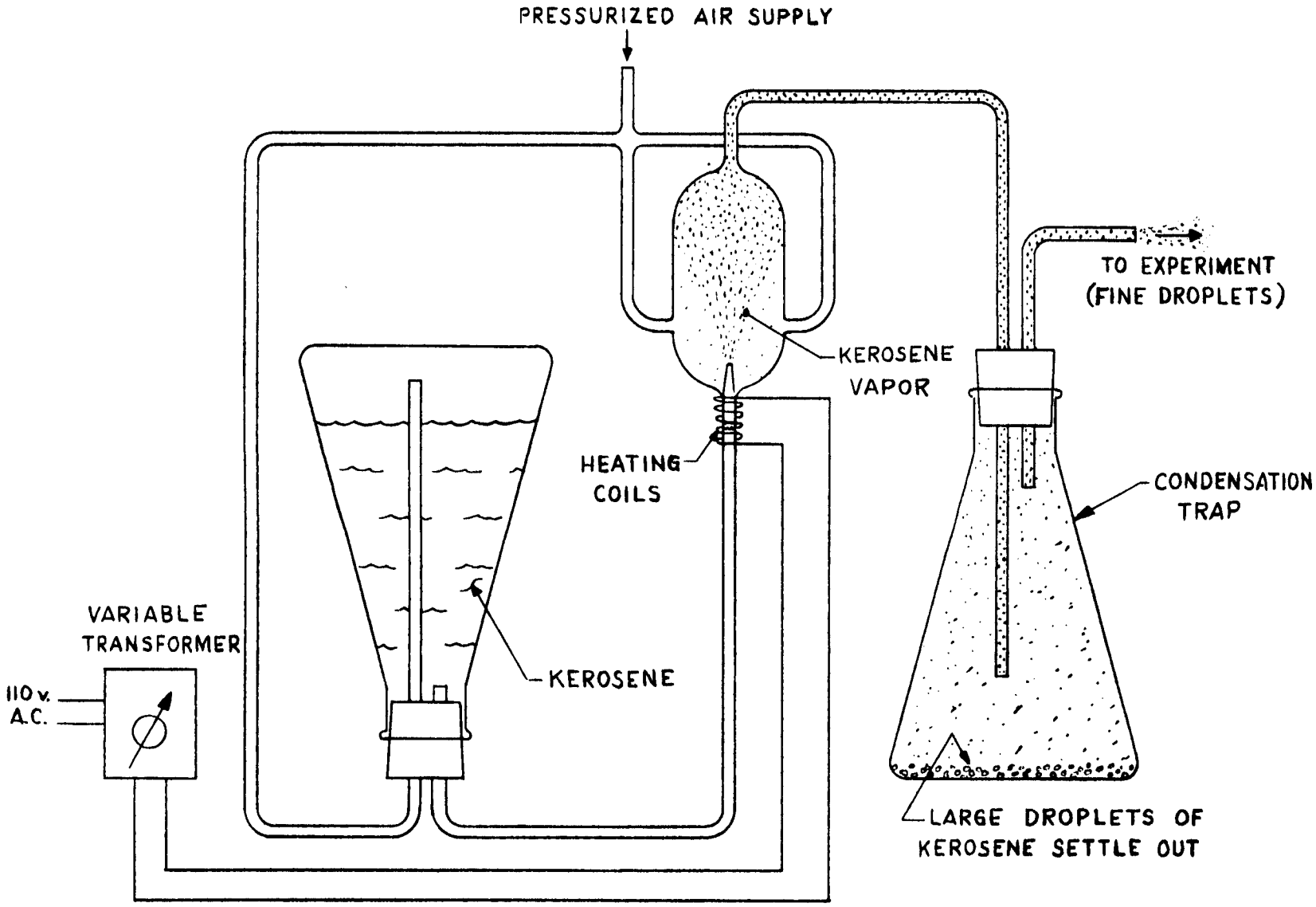

Figure 3.2.3-1 Kerosene smoke generator.

PROPORTIONAL ACTIVE DEVICES

4.1 Fluid Dynamics Fundamentals

The basic fluid phenomena underlying the proportional fluid amplifiers discussed in Section 4.2 are as follows:

a) Impacting and deflecting jets, axisymmetric and rectangular, subsonic.

b) Wall-jet separation from curved surfaces, rectangular, subsonic.

c) Spiral flow, rectangular, subsonic.

In all cases, the influence of viscosity is important, as measured by the Reynolds Number for the steady-state flow and by the Stokes Number for the dynamic flow.

In some cases, particularly for the impacting and deflecting jets, there will be fluid compressibility effects as measured by the Mach Number of the jet.

Both flow and pressure must be considered for the input and output of fluid amplifiers, because even ram-piston loads require an appreciable flow rate in the dynamic case.

In general, for proportional amplifiers it is assumed that at any instant the flow corresponds to the steady-state flow under similar conditions, i.e., the dynamic flow is assumed to be quasi-steady.

4.2 Typical Active Devices

4.2.1 Introduction

It is the purpose of this section to explore some of the design problems in the development and use of pure fluid proportional amplifiers. Four classes of proportional devices will be considered: the impact modulator, the beam deflection amplifier, the vortex amplifier, and the elbow amplifier. The operation of each type will be described. No attempt is made to discuss design parameters. Plots of phase and gain for a variety of proportional active devices are given in Figure 4.2.1-1.

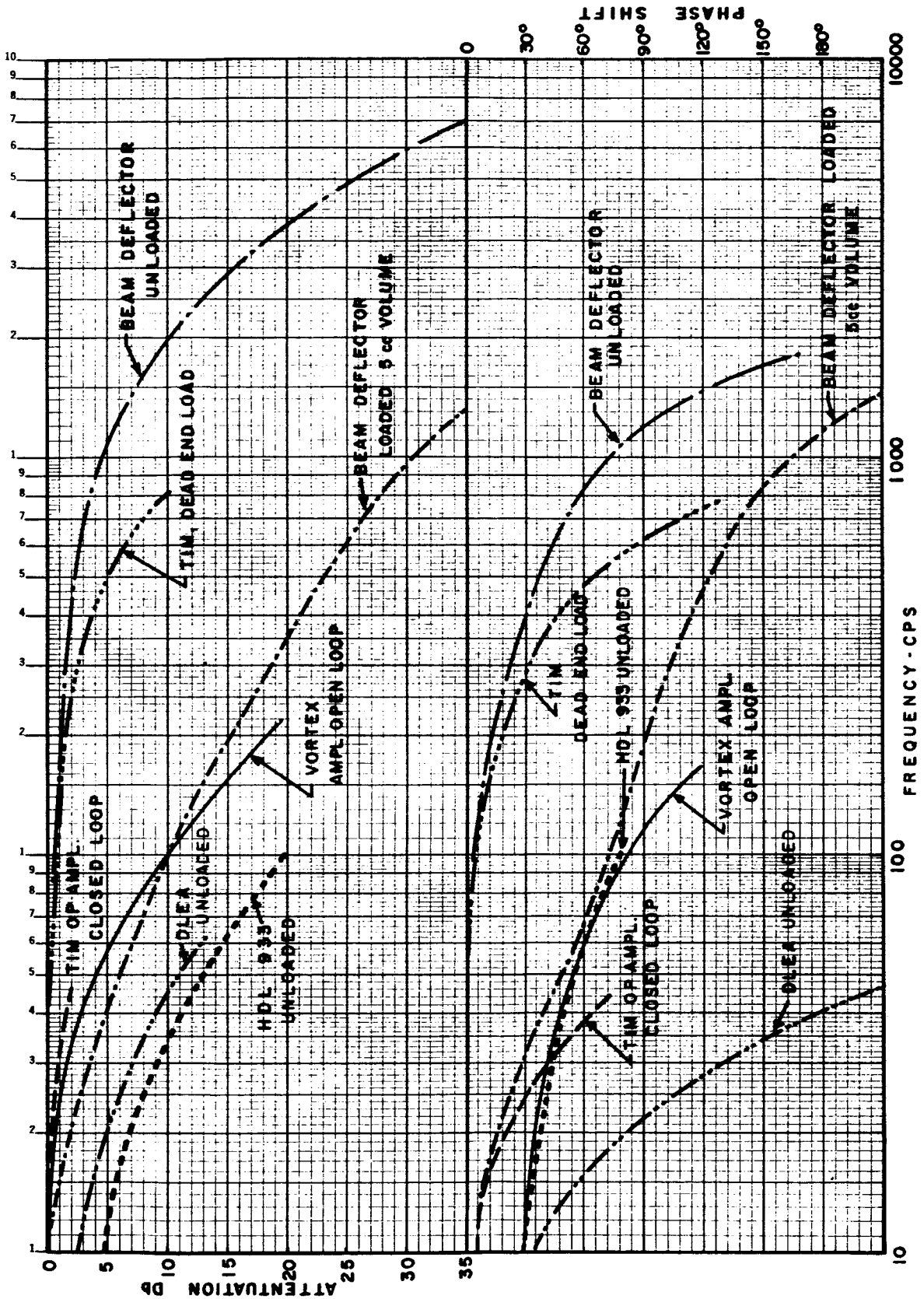

Figure 4.2.1-1 Bode plots.

4.2.2 Transverse Impact Modulator

The transverse impact modulator is a pure fluid amplifier which utilizes two impacting fluid jets. Figure 4.2.2-1 shows the direct impact of two fluid jets. The position of the line of impact depends upon the relative momentum in the two fluid streams. The momentum, in turn, depends upon the pressure in the two fluid reservoirs. Consequently, changes in one of the reservoir pressures changes the momentum of one of the jets. This results in a shift in the radial-jet position.

The pressure within the radial jet can be sampled with a pitot tube. For a fixed pitot tube location any change in the radial jet position is reflected in the pressure sensed by the pitot tube. Such changes can be considered as an output signal. In this case, the input signal would be the pressure change in the reservoir which caused the shift in the impact point of the two jets.

The flow available from a pitot tube pickup is small; and where a flow, as well as a pressure, output is required an annular collection chamber can be used. Such an arrangement is shown in Figure 4.2.2-2. A control orifice is also shown in the same Figure. The elements of Figure 4.2.2-2 constitute what is called the transverse impact modulator.

When pressure is applied to the control orifice of an impact modulator, the control jet interacts with the jet emerging from the left hand or emitter orifice (Figure 4.2.2-2). The interaction changes the momentum of this jet, and the impact plane of the two jets shifts to the left. The result is a reduction in the output-chamber pressure and flow. This effect constitutes the basic mechanism of the transverse impact modulator.

The sensitivity of the impact modulator is quite high, and pressure gains of 10 to 20 are readily obtainable. Input signals can be applied to either the control orifice or one of the main orifices. The gain is negative if the signal is applied to the control orifice.

A labeled, cross-sectional sketch of a transverse impact modulator and the symbol used to represent it is shown in Figure 4.3.2-2. Also shown in this figure is the terminology which shall be used. In general, the subscripts 1 and 2 refer to the emitter and collector jets respectively. The subscript "i" refers to the input or signal orifice while a subscript "o" relates to the output or collector chamber. Upper case letters refer to steady state values of flow and pressure, while lower case letters refer to incremental or small signal values.

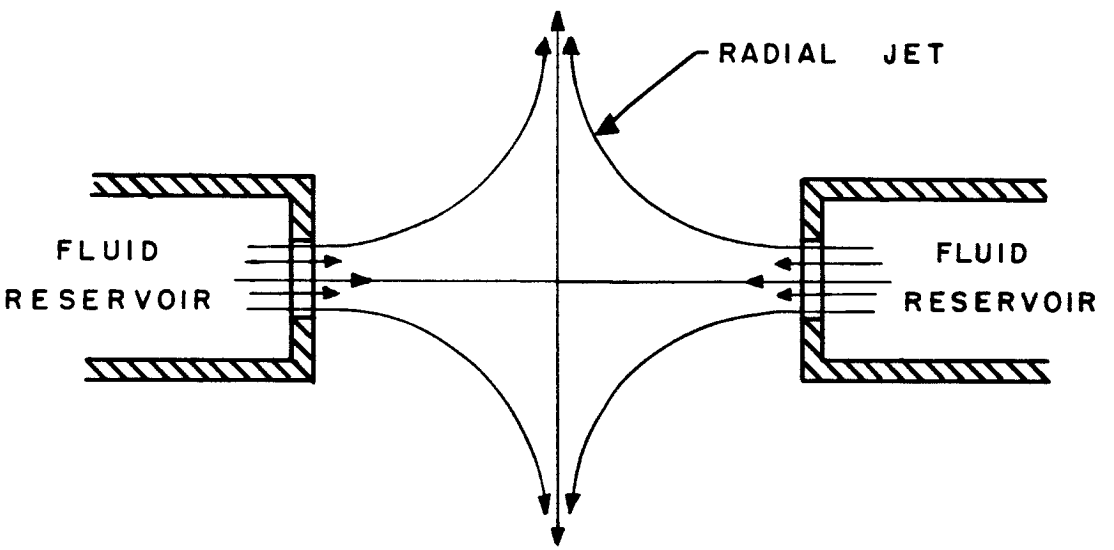

Figure 4.2.2-1 Impacting jets.

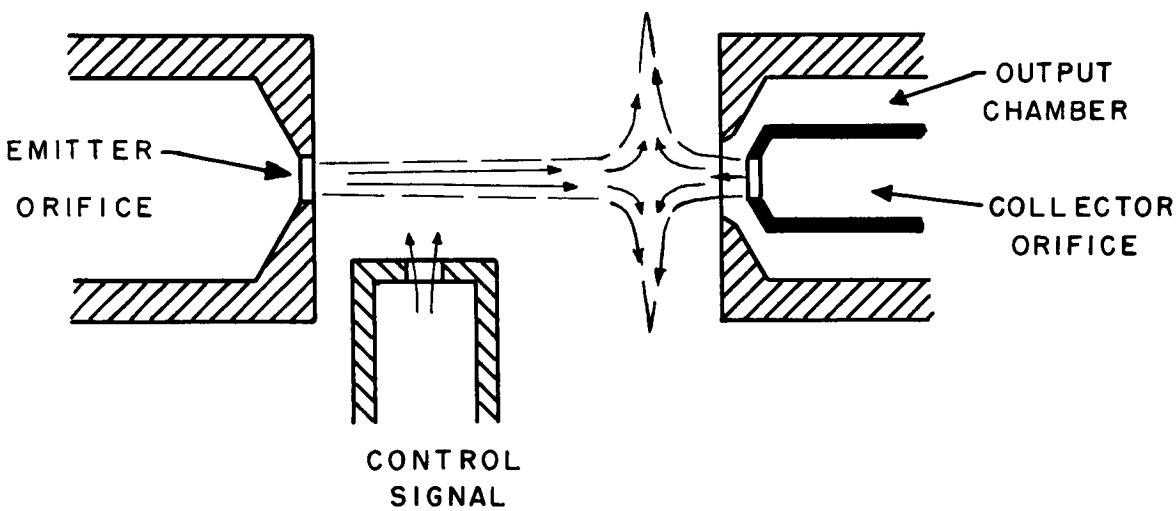

Figure 4.2.2-2 Transverse impact modulator.

4.2.3 Beam Deflection Amplifier

Historically, the beam deflection amplifier was the first of the pure fluid proportional amplifiers (Ref. 11, 12). Figure 4.2.3-1 depicts a typical stream interaction amplifier. Figure 4.2.3-2 shows typical device characteristics. This device makes use of the principle of momentum exchange between orthogonal fluid jets to provide proportional amplification.

Under conditions where no control flow is present, the power input stream flows out both the right and left output ducts in equal amounts. In the pressence of a differential flow across the two control ducts, there is a momentum exchange between the control flows and the power jet. The control flow with the greatest energy will deflect the power jet away from itself. A small amount of power jet deflection causes significant changes in differential flow from the two output ducts.

It should be noted that the interaction region in this proportional amplifier is designed in such a manner that the power jet does not flow near an adjacent wall in the vicinity of the power jet outlet. The presence of a wall can cause an adjacent jet to bend to and flow along such wall (Coanda effect). This effect is an important design consideration. Another necessary design feature is the providing of vents on each side of the power jet in the interaction region so that there is no differential pressure across the jet. Such a differential pressure would bend the jet even in the absence of control flows.

The "splitter" or wedge which divides the power stream into equal outputs constitutes a source of noise. In fact, the jet-edge system which exists in many variations of pure fluid devices constitutes a noise source or a source of instability. This jet-edge combination does not lend itself to easy analysis and therefore most of the design work has been done by empirical methods.

The biggest difficulty involved in the cascading of several beam deflection amplifiers is the lack of isolation between stages. The results of cascading is some considerable loss in gain per stage plus an upstream sensitivity to downstream loading. It has been reported that perturbations in the downstream portion of a control system have been reflected all the way upstream to the rate sensor.

Another difficulty which this fluid device shares with most other fluid devices is a signal to noise ratio which is much lower than those usually encountered in electronic equipment components. Currently there is no adequate published information on signal to noise ratios; nor, for that matter, is there a good agreement on what frequency spectrum should be considered in the noise measurements.

Figure 4.2.1-1 shows a Bode plot of the operational characteristics of both an unloaded and a loaded beam deflection amplifier. (Ref 12) Note that when the amplifier is loaded there is a marked change in the operational characteristics of the device. This charcteristic is probably the most

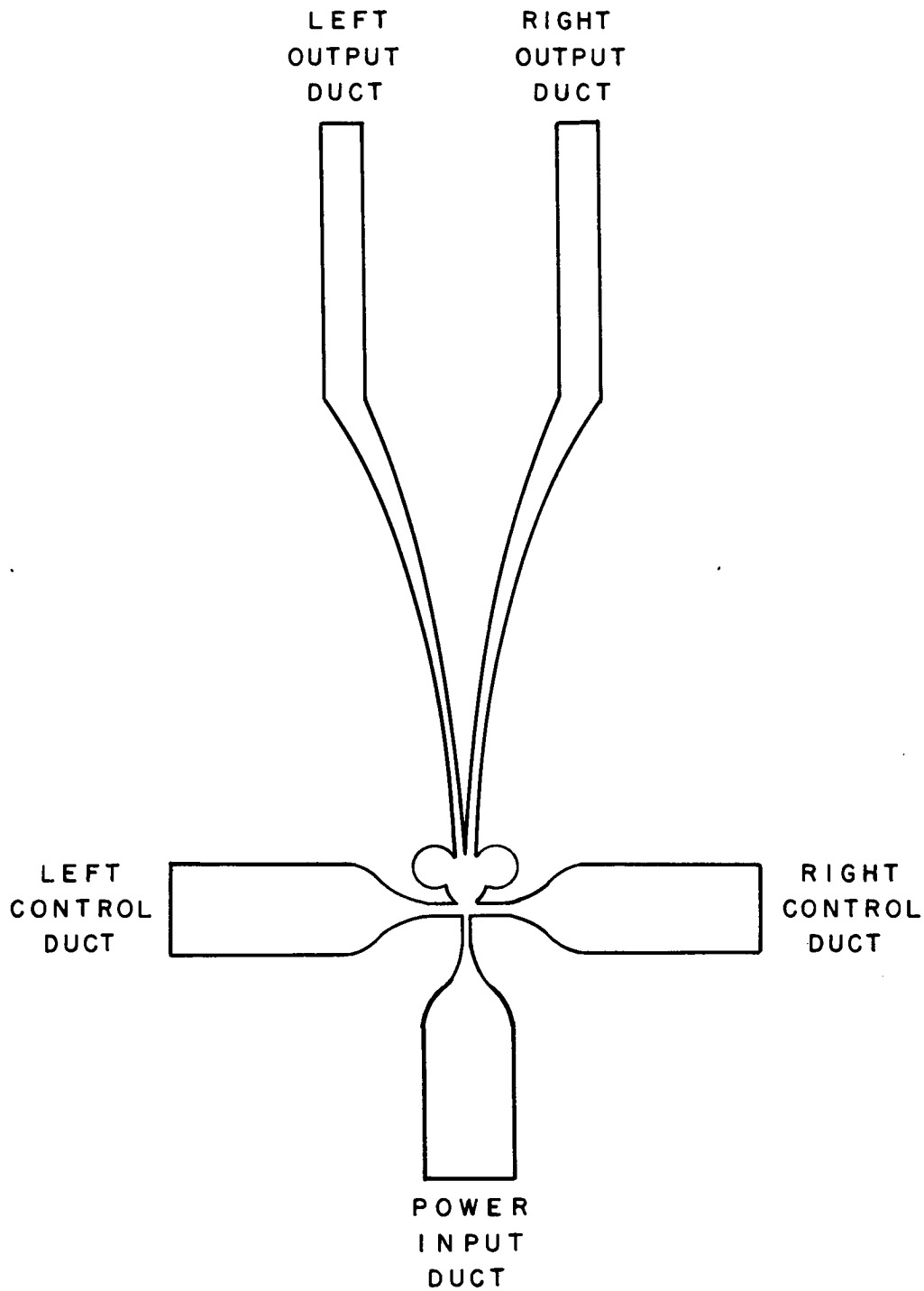

Figure 4.2.3-1 Beam deflection amplifier.

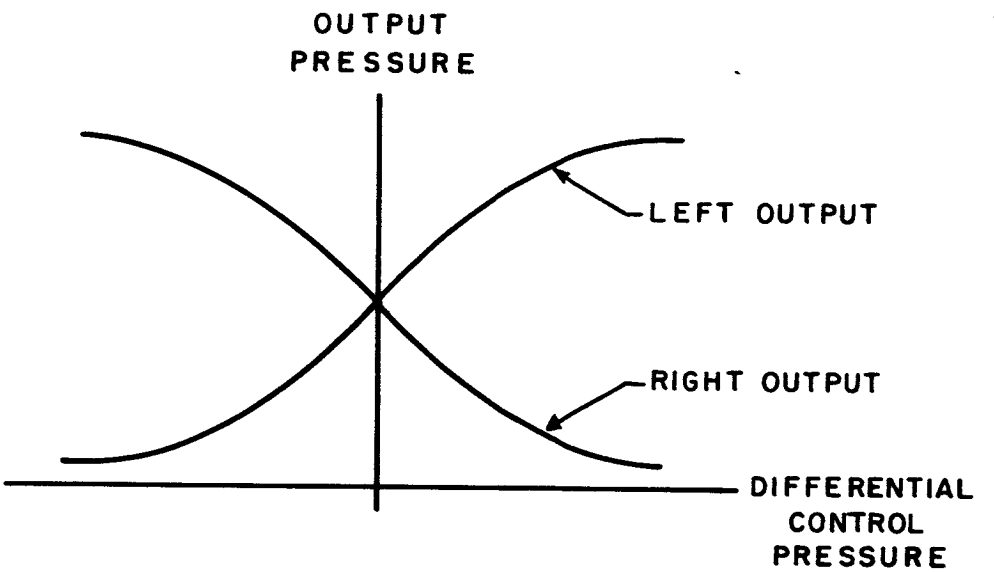

Figure 4.2.3-2 Characteristics of beam deflection amplifier.

important one to consider when designing circuits using these amplifiers. It must be pointed out that it is by no means a simple or trivial task to design proportional circuitry using beam deflection amplifiers.

4.2.4 Vortex Amplifier

A pure fluid amplifier, which operates in a sense as a variable restrictor, can be made by utilizing vortex flow in a right circular cylindrical chamber. As shown in Figure 4.2.4-1, the "power" or input flow is introduced into the chamber from the outer wall in such a manner that in the absence of control flow the power stream flows radially to the center of the chamber and out the output duct. Control flow is introduced in the manner depicted so that the momentum exchange between power and control flows will produce a tangential component to the power stream. As the interacting streams converge on the centrally located output, angular momentum is conserved with the resulting effect that the tangential component of velocity is greatly amplified and a vortex flow is established in the circular chamber.

Two effects are present in this device, both of which have potential for pure fluid amplification. The tangential velocity of the combined power and control streams is greatly amplified at the output (to a first approximation by a factor of the larger diameter of the chamber divided by the diameter of the output duct). Secondly, the creation of the vortex flow serves as a limiting effect or an established back pressure on the power flow. The first effect has been exploited in making proportional fluid rate sensors and the second effect is making a variable restrictor. The second effect has also been utilized in making a fluid diode.

Two major difficulties are found in utilizing the vortex amplifier for proportional amplification. The first difficulty is that the circuitry must be built using the device as a variable restrictor. The second difficulty is that the basic, restrictor device requires a large amount of control flow to approach a complete throttling of the power stream. Figure 4.2.4-2 shows curves for typical operation of the vortex amplifier.

One minor design difficulty is related to the relative low, frequency response of the device when used to modulate the upstream power stream. Another design restriction is related to the physical size of the vortex amplifier. These devices do not lend themselves to miniaturization, or to low pressure and low flow requirements, as easily as do other pure fluid devices.

One of the distinct advantages of the vortex amplifier is its high amplification factor. Most other pure fluid amplifiers have gains of the order of ten. Vortex amplifiers have potential of an order of magnitude better gain performance. Another advantage of the vortex amplifier is that it performs a distinct and unusual (to electronics) function -- that of being a variable restrictor.

In Appendix I of Volume I of this report there is contained a summary of the work done at Sperry Utah Company on the analytical investigation of the vortex phenomena. Figure 3.1.3-2 shows, visually, how complex the motion of a confined vortex can be. Such complexity has advantages for it allows for the discovery and exploitation of new fluid dynamics effects. At Sperry Utah some very interesting vortex effects were observed and noted during earlier fluid investigation. For example, a circular jet directed through a vortex is focused by the action of the vortex. Again, if the vortex is

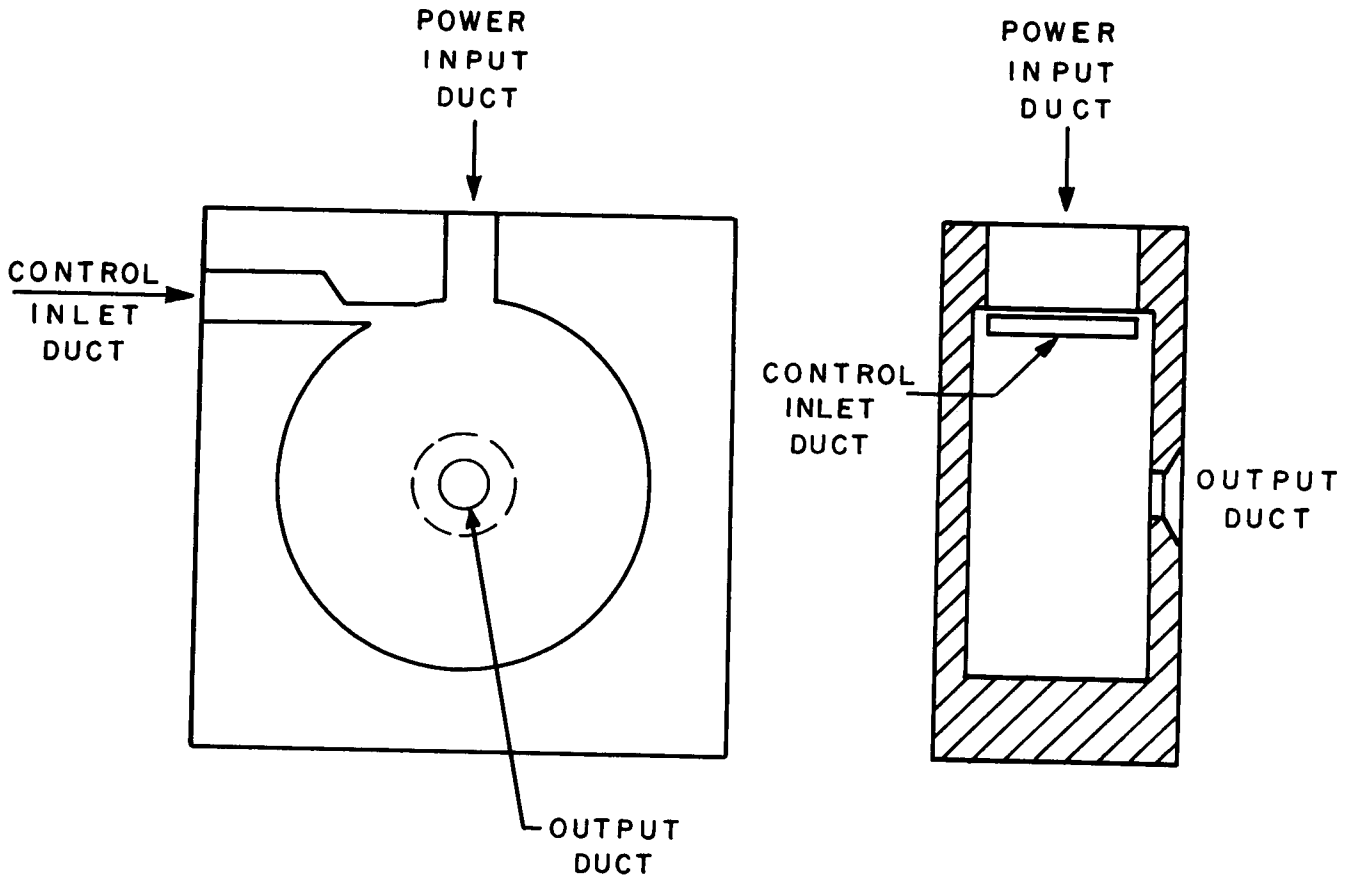

Figure 4.2.4-1 Vortex amplifier.

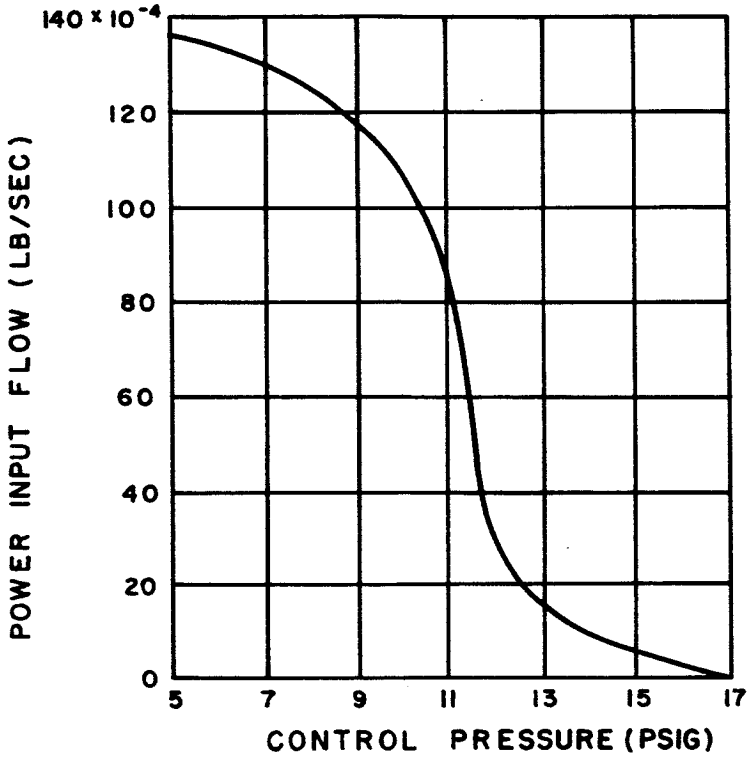

Figure 4.2.4-2 Characteristics of vortex amplifier.

formed in a spherical chamber, there are very interesting modes of oscillation which are not dependent on external feedback.

The greatest gain of the vortex amplifier is in the amplification of the tangential velocity of the spiral flow. If it were practical to utilize the full gain of this tangential velocity component of the flow in cascaded circuitry, extremely high gain circuitry would result. This procedure remains as a challenge to fluid experimenters.

4.2.5 Elbow Amplifier

The pure fluid proportional amplifier which apparently has the highest flow gain is the double leg elbow amplifier (DLEA) developed by Giannini Controls Corporation. Two basic fluid flow phenomena are used in this device: flow separation in a curved channel, and momentum exchange (or stream interaction) between two flows. Figure 4.2.5-1 depicts the phenomenon of flow separation from a curved surface in a rectangular elbow. The point of flow separation can be changed by the introduction of a counterflow as depicted in the drawing (Figure 4.2.5-1).

The velocity profile of the supply flow in the straight section of the elbow is symmetric about the center line of the elbow. However, after undergoing sufficient curvature, the velocity profile is skewed so that the higher flow velocities are near the outside of the curved section. With appropriate values of flow and curvature the flow tends to separate from the inner wall of the elbow.

With the addition of a control flow, the point of separation moves upstream. The result is a significant change in the flow momentum per unit area (momentum flux) of the flow downstream from the elbow, as depicted in the illustration by the dotted lines. By utilizing a downstream means of recapturing the flow, the change in flow per unit area results in a considerable flow change in the output duct.

The double leg elbow amplifier, which utilizes a further addition to the amplifier described above, is depicted in Figure 4.2.5-2. Coupled with the basic elbow flow separation is an additional "passive" leg which provides a second stream to interact with the stream in the "active" leg. As shown in Figure 4.2.5-2, the DLEA has two output ducts. With no control flow present, the magnitude of the momentum flux is low near the outlet of the passive leg because of the larger area that the flow occupies. The active leg flow is thus easily deflected to the left by the passive leg flow (utilizing the momentum exchange of stream interaction).

With control flow present, the magnitude of the momentum flux of the active leg flow is increased because of the smaller area that the flow occupies. The passive flow is now unable to "bend" the active stream as much and flow exits in the right output. A proportional control signal at the control duct will result in a similar but amplified signal at the right output duct. The remainder of the vents, and the splitter vane, are added to improve the performance of the device. For typical characteristics of the DLEA see Figure 4.2.5-3 and also Reference 13.

The disadvantages of the DLEA are the low pressure gains, complexity of the basic element, and somewhat slow response time (greater than 100^{o} phase shift at 25 cps). See the summary of operation of proportional devices, Figure 4.2.1-1 (data from References 11, 12, 13, 14). The low pressure gain of the device would suggest that the device would be difficult to interconnect due to a sensitivity to downstream loading. In fact, one might generalize and suggest that the better the pressure gain of a device, the more easily it can be interconnected in fluid circuitry.

The advantage of the DLEA are its excellent flow gain characteristics. This device is the best of the proportional devices in terms of flow gain.

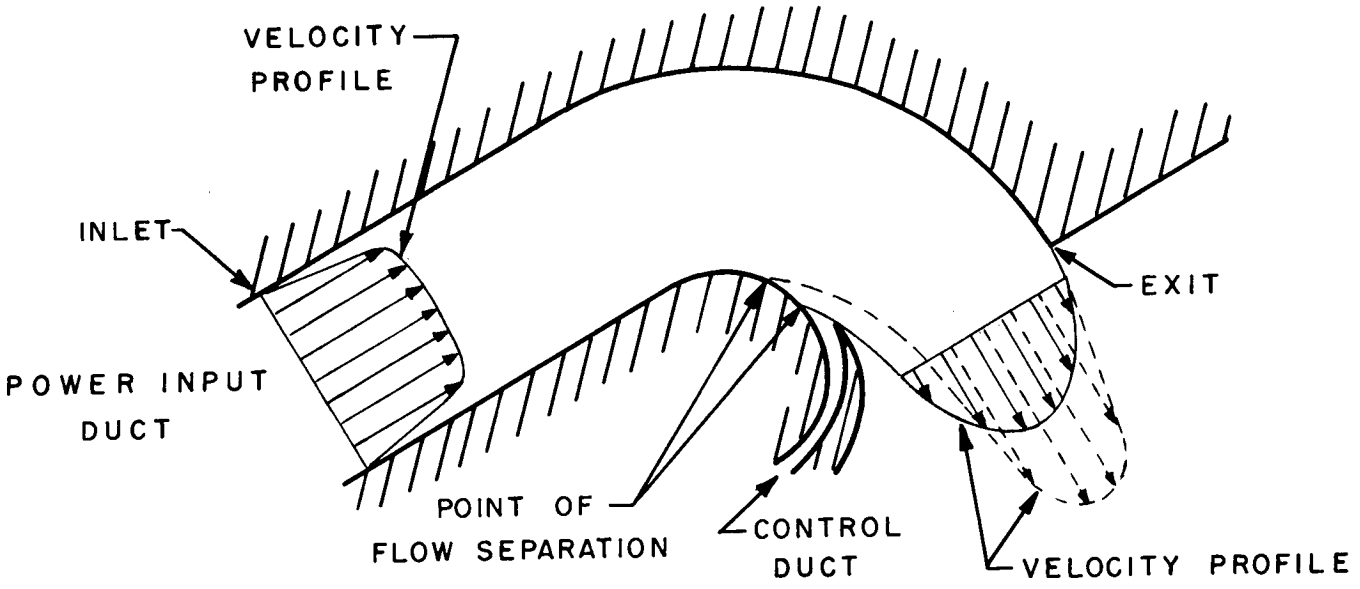

Figure 4.2.5-1 Elbow amplifier.

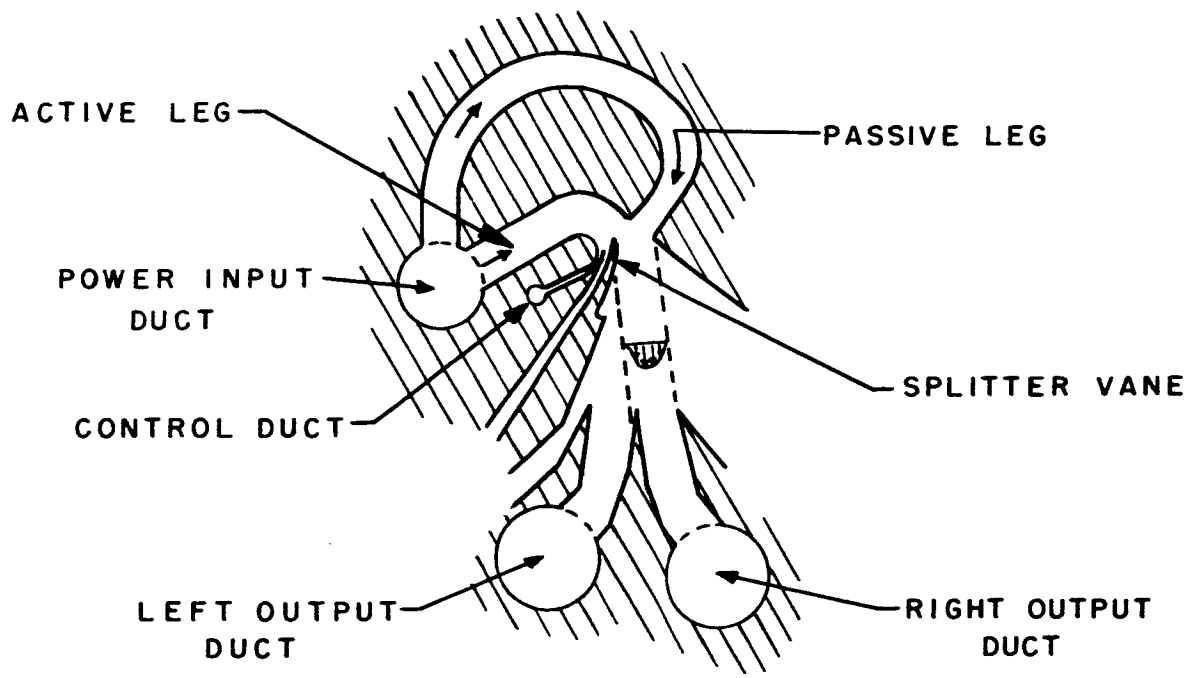

Figure 4.2.5-2 Double leg elbow amplifier.

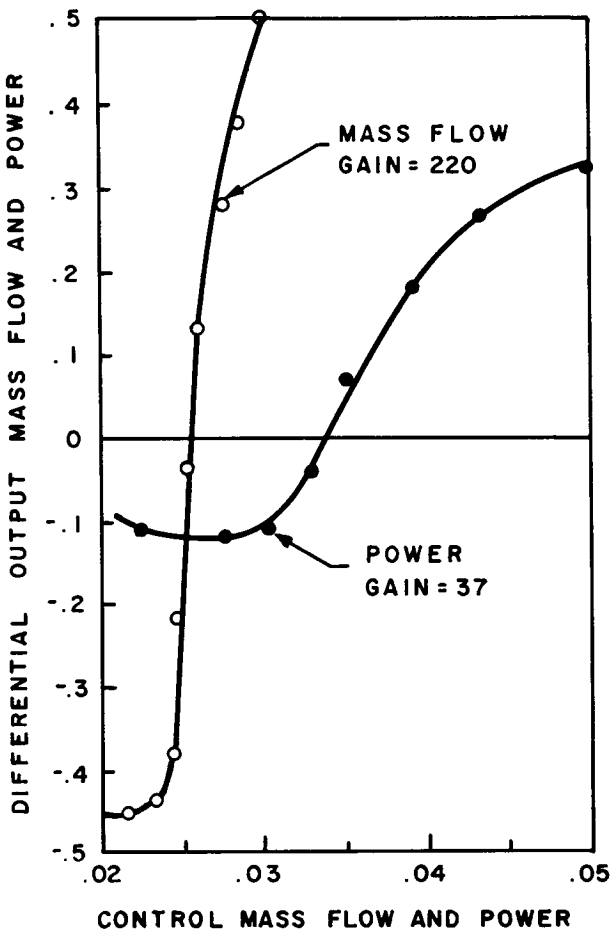

Figure 4.2.5-3 Characteristics of double leg elbow amplifier.

4.3 Impact Modulators

4.3.1 Introduction

Given any new active fluid device there are basic questions which require answers prior to utilizing it in circuits or systems. Of first concern is the performance of a single device under steady state conditions. Logically the next requirement is information concerning the device characteristics under dynamic conditions. If the element proves promising as a single component, further information is needed on the problems of interconnecting two or more devices. Both steady state and dynamic performance data will be needed. Information concerning such characteristics is input and output impedances, degree of isolation of stages, gain under load, and stability criteria will be useful.

It is the purpose of this section to provide the type of design information for typical impact modulators which will enable the control system designer to utilize them in fluid control circuits.

4.3.2 Impact Modulator Operation and Nomenclature

Figure 4.3.2-1 is a cross section of an impact modulator showing the basic features and typical dimensions. In Figure 4.3.2-2 is a sketch which is more nearly what the actual cross section might actually be in a production model impact modulator. Also shown in Figure 4.3.2-2 is the schematic symbol used for the transverse impact modulator and the letter symbols which are used for pressures and flows.

In the impact modulator two colinear opposing jets (P_1 and P_2) are connected to a fluid power source such that the impacting balance point is located within a collector chamber. An orthogonal control jet is located so as to affect the power jet opposite the collector chamber. Any flow through the control orifice will cause some weakening of the power jet P_1 with a resultant shift in the balance point between the two power jets. This shift will affect the output pressure P_o. Thus the output is a direct function of the control jet signal P_i.

The usual method for connecting the two power jets to the supply pressure shown in Figure 4.3.2-3. If the resistor between the two power jets, R_2, is linear over the range of variations of the supply pressure, then the impact point of the two jets, i.e. the balance point, will remain in the same relative location with respect to the collector chamber. This means that with the proper value for the resistor the designer need only to determine the required value of one supply pressure.

Inasmuch as any signal fed to the control jet tends to move the impact area out of the collector chamber, the output of the impact modulator is the negative of the input signal. In other words, the impact modulator has a negative gain.

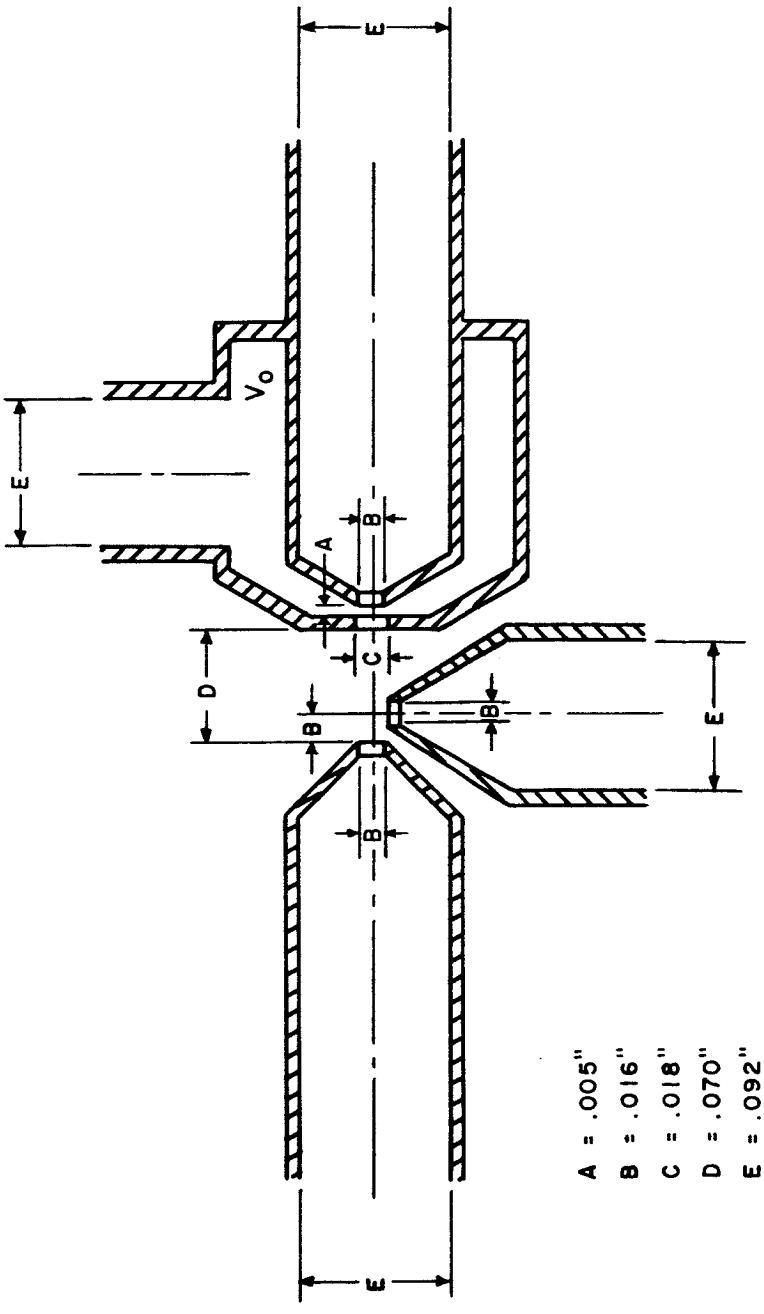

Figure 4.3.2-1 Typical dimensions for an impact modulator.

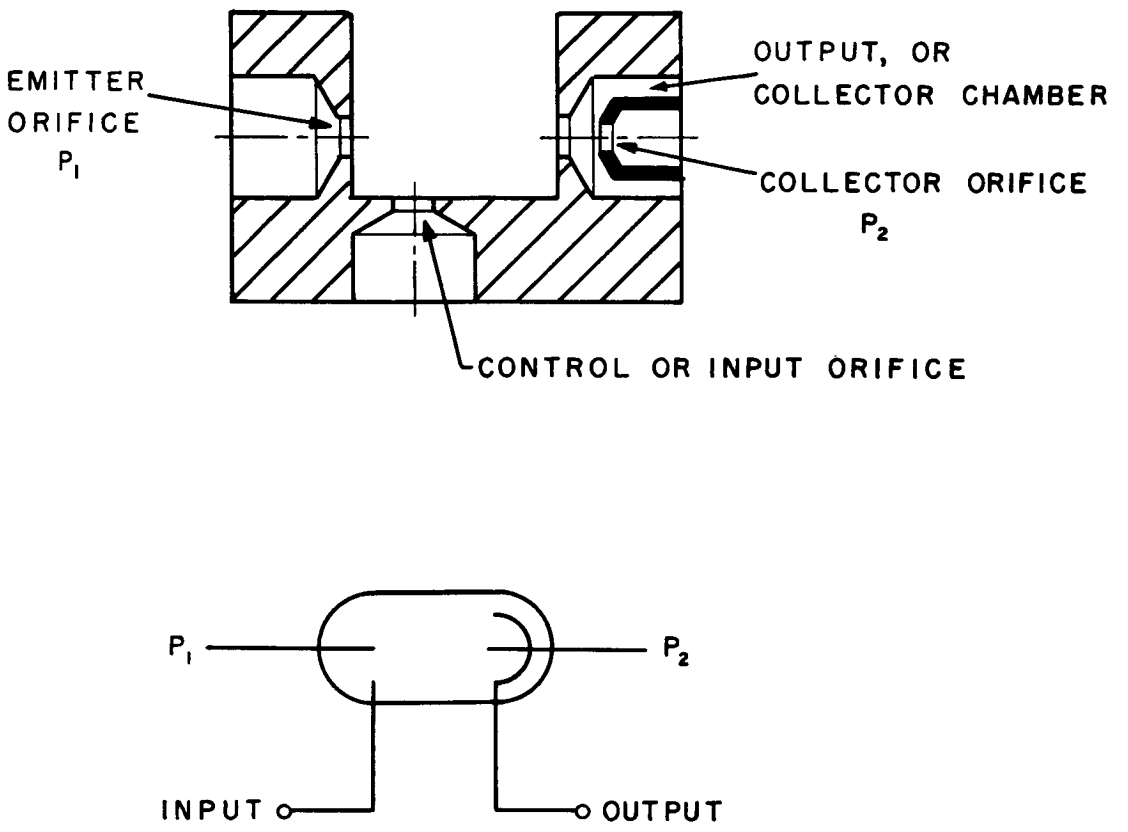

Figure 4.3.2-2 Schematic symbol for an impact modulator.

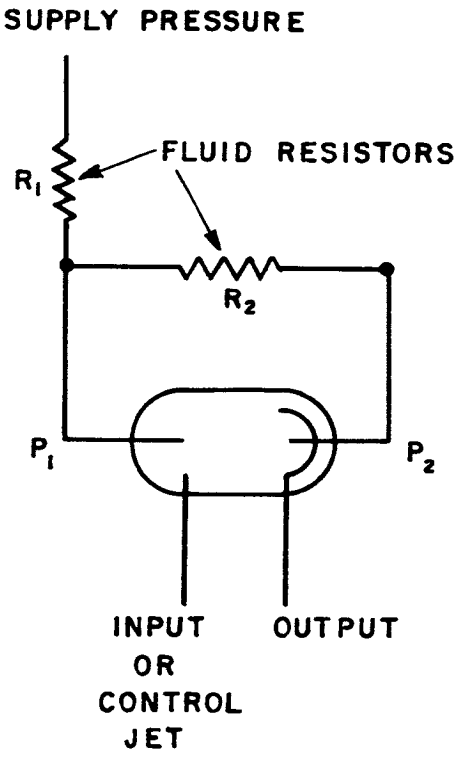

Figure 4.3.2-3 Connecting an impact modulator to the supply.

4.3.3 Steady-State Behavior

A family of typical pressure curves for an impact modulator are shown in Figure 4.3.3-1. These are curves of output pressure, P_o, plotted against emitter orifice pressure, P_1, with the collector orifice pressure, P_2, fixed, with no input signal. These curves depict the maximum output pressure range that can be achieved with any particular power jet supply pressures. The collector jet supply pressure, P_2, can be compared to the grid bias voltage of a vacuum tube, in that it biases the output flow to positive, zero, or negative values with no input signal. By this method the modulator output can be biased into the desired range.

Tests have shown that the steady state pressure gains (P_o/P_i) of various impact modulators vary from 20 to 50. However, due to the additional constraints added in interconnecting impact modulators in direct coupled circuitry, the pressure gain per stage drops to between 15 and 25.

Figure 4.3.3-2 is a tracing of an X-Y recorder plot of a two stage amplifier circuit with no feedback. As can be calculated by the slope of the curve, the gain is approximately 300 for two stages or an average gain of 17 per stage. Several stages can be cascaded in this manner so that four and five stage amplifiers can be used as the basic, high-gain, open-loop amplifiers for fluid "operational amplifiers."

One problem encountered in the steady-state circuit design is matching the impedance of the input transducer or circuit to the input impedance of the impact modulator. The input impedance of the impact modulator is just the impedance of the control or input orifice.

In many circuits, it is desirable to have a high input impedance. The pressure-flow equation for an orifice is

$$I_i = B\sqrt{P_i} \qquad (1)$$

where I_i and P_i are the input current and input pressure. The parameter B is a function of the orifice diameter and flow coefficient. The incremental input impedance (R_i) of the device becomes:

$$R_i = \frac{\partial P_i}{\partial I_i} = \frac{2\sqrt{P_i}}{B} \qquad (2)$$

and is seen to increase with increasing input pressure.

The conclusion is obvious: to increase the input impedance, increase the applied pressure. However, a very high pressure applied to the control orifice will put the impact modulator beyond its operating range. Typically, 0.25 psi is the maximum possible input pressure for an impact modulator. Hence, there is a definite limit to the input impedance which can be obtained with a given device used in the normal fashion.

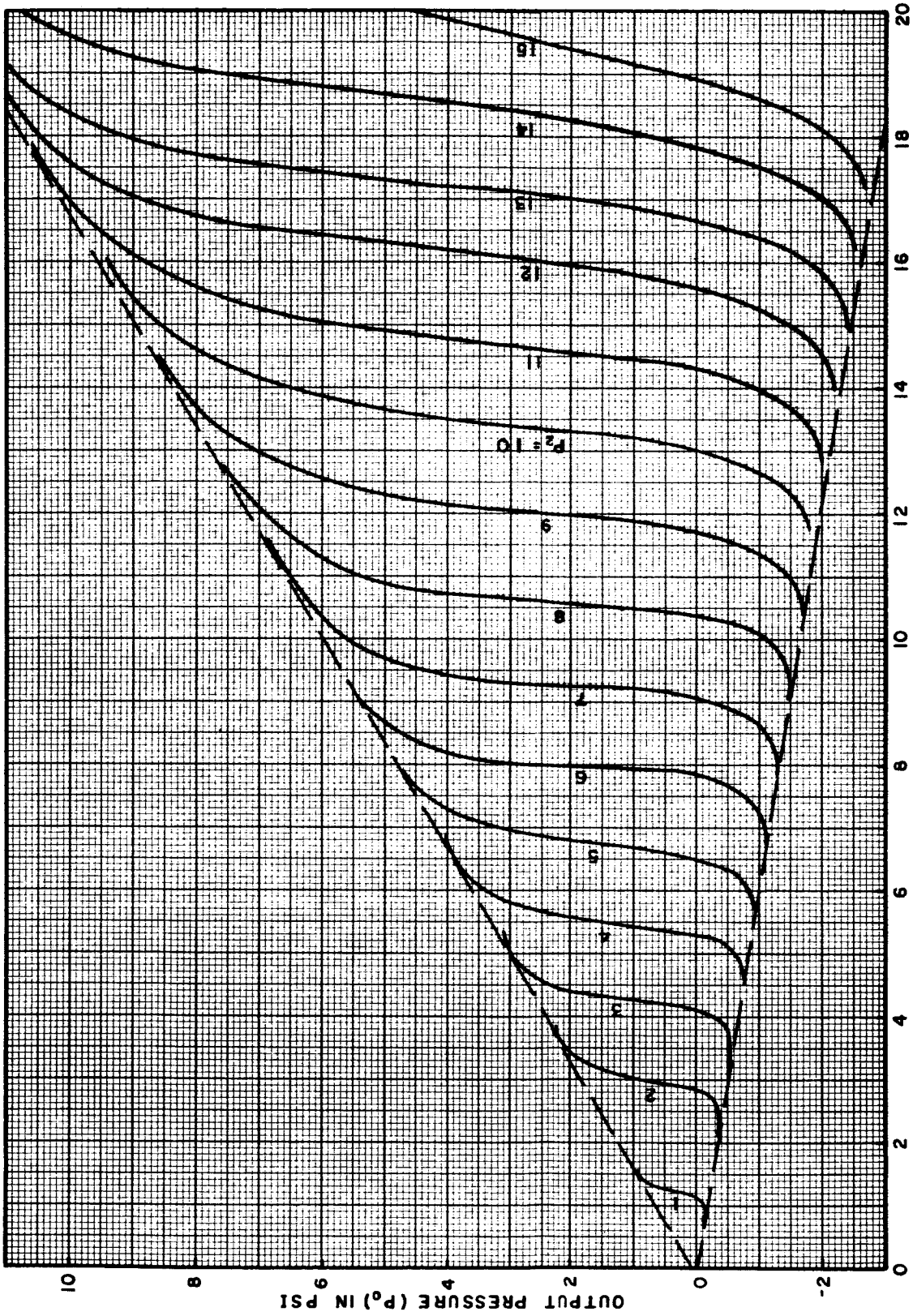

Figure 4.3.3-1 Typical characteristic curves for an impact modulator.

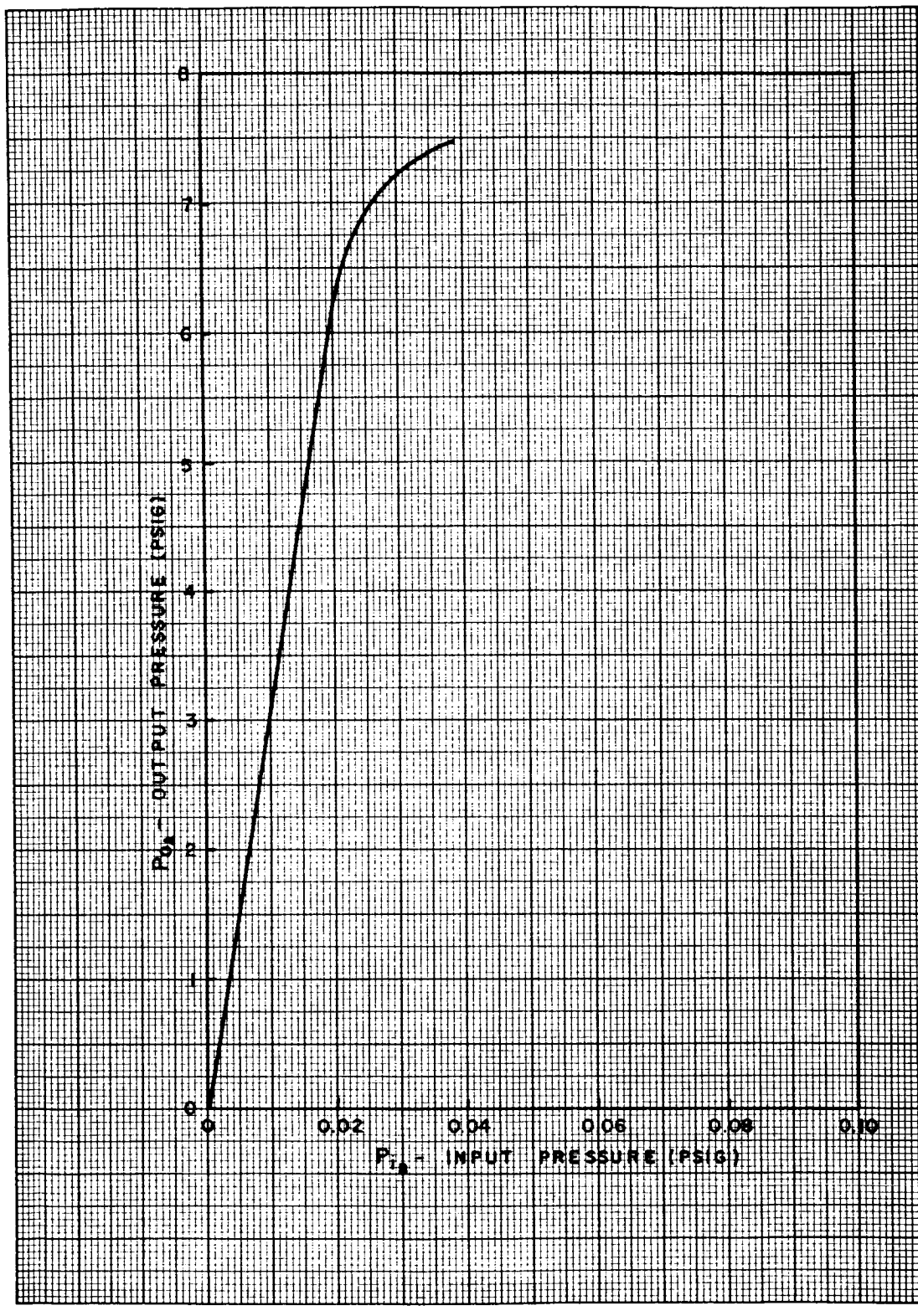

Figure 4.3.3-2 Input-output curve for a 2-stage amplifier.

Relatively large pressures can be applied to the power jets, and it has been found to be possible to obtain quite high input impedances by connecting the input or signal line to one of the power jets rather than the control jet. Either power jet can be used as the input orifice. The pressure at the other power jet is set so that the output pressure is in the desired range. A schematic showing the connections when the emitter jet is used as the input orifice is shown in Figure 4.3.3-3a.

A differential amplifier can be made by using both the emitter and the collector power jets as inputs as shown in Figure 4.3.3-3b. The output pressure in this arrangement is a linear function of the difference of the two inputs.

An equivalent circuit for the impact modulator is needed for circuit design and analysis. The values of the parameters in the equivalent circuit will depend greatly upon the power jet pressures, P_1 and P_2.

In arriving at an equivalent circuit, first note from Figure 4.3.2-2 that the control jet operates upon the fluid stream which issues from the emitter jet. This modulates the emitter jet, which in turn flows towards and interacts with the collection chamber and the collector jet. The important point to note is that there is no feedback from the collection chamber to the control jet. The input to the impact modulator can then be represented by a simple resistor equal to the resistance of the control jet orifice.

The static equivalent circuit of the output section of the impact modulator can be obtained through the use of well known circuit theory. The output, or collector, chamber can be considered to be a generator with a given voltage and a given internal, perhaps nonlinear, resistance. These parameters can be determined by connecting the various orifices to fixed pressures and measuring the output flow as a function of the pressure in the collection chamber.

The output-pressure versus output-flow measurement is obtained by connecting a variable resistor to the output such that the output flow can be varied from zero to the maximum obtainable. A series of plots of output flow versus output pressure are then made for a variety of control jet settings.

A plot of output-flow versus output-pressure for a typical impact modulator is shown in Figure 4.3.3-4. The signal pressure P_i varies from 0 to 0.25 psi. In the higher input pressure ranges the curves are seen to be linear. The collector chamber hence acts as a linear resistor in this area, and the internal resistance in the equivalent circuit will be a linear resistor. For the higher signal pressures the internal resistance, R_o, is found from the curves shown in Figure 4.3.3-4 to be about 10^5 psi-sec/lb.

For impact modulators, a wide range of power jet supply pressures are possible. This complexity increases the design problem; but in return, it allows a selection of various supply pressures P_1 and P_2 for a given output pressure. This is shown in Figure 4.3.3-5 which shows output flow-pressure curves for a typical device. Note that the three curves, each representing different supply pressures, all pass through a common operating point; P_o = 2.2 psi and I_o = 2×10^{-5} lbs/sec.

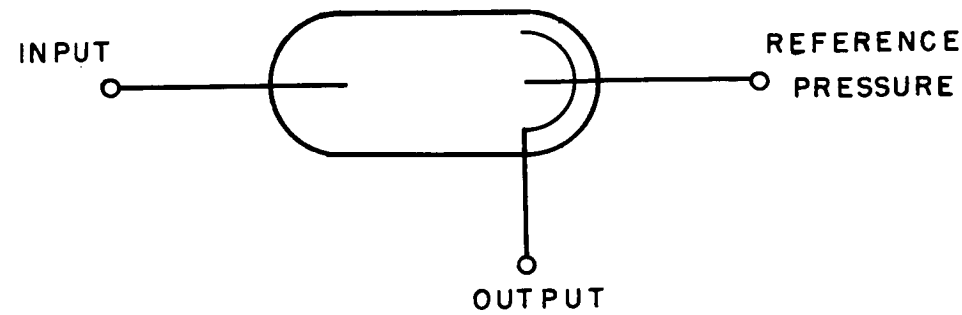

a. EMITTER JET USED AS INPUT ORIFICE

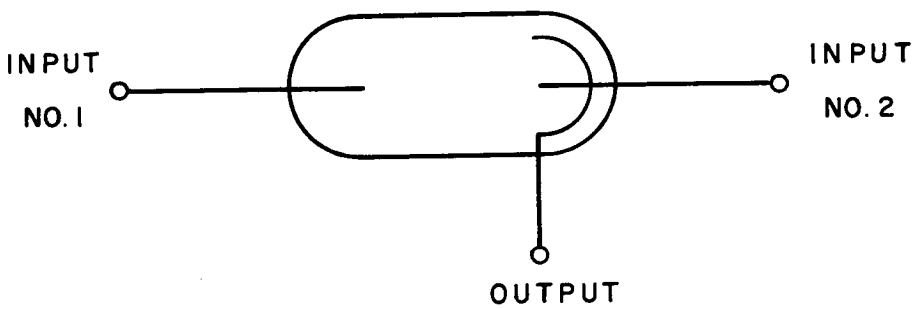

b. DIFFERENTIAL CIRCUIT

Figure 4.3.3-3 Use of power jets as inputs.

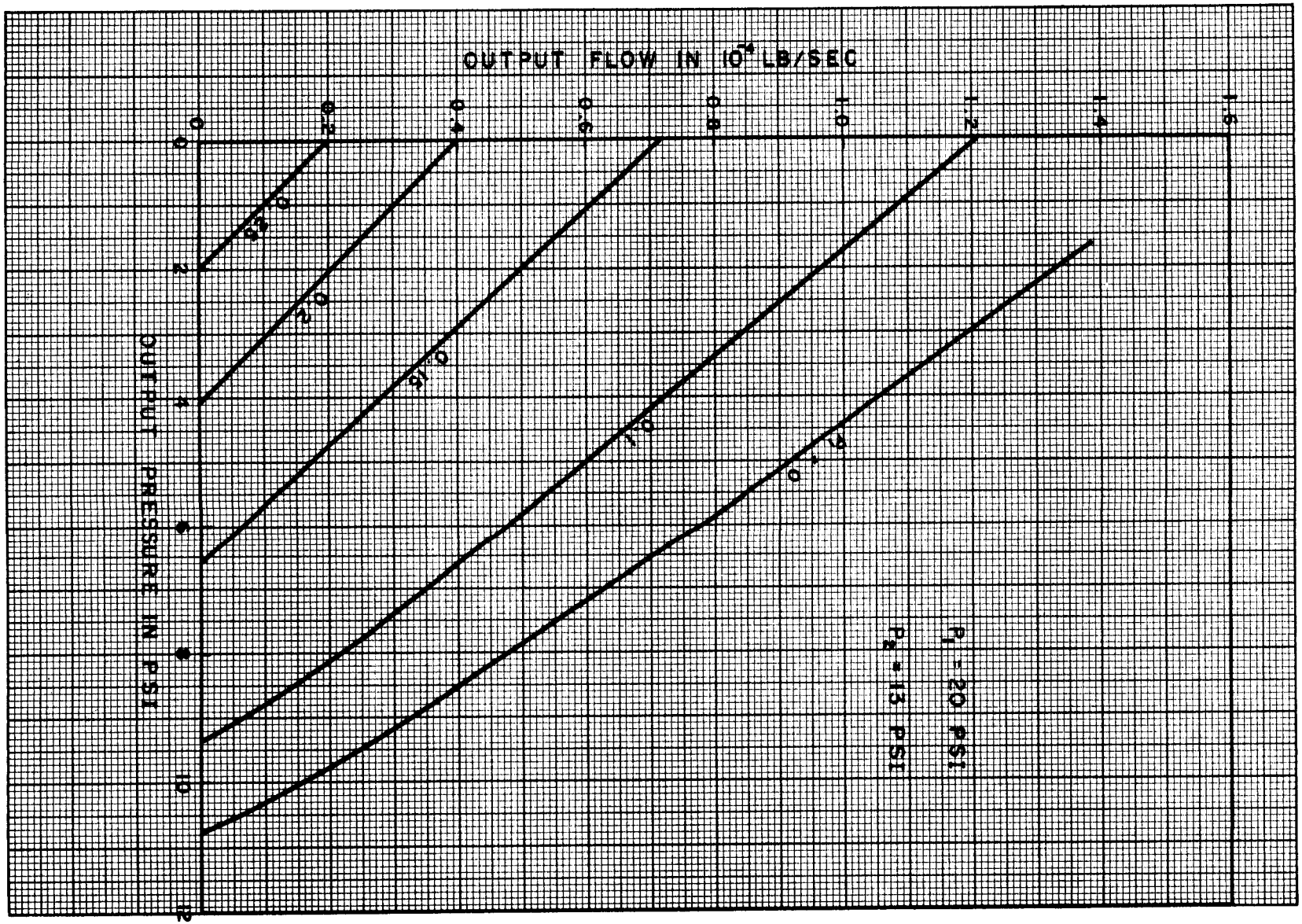

Figure 4.3.3-4 Typical output curves for an impact modulator.

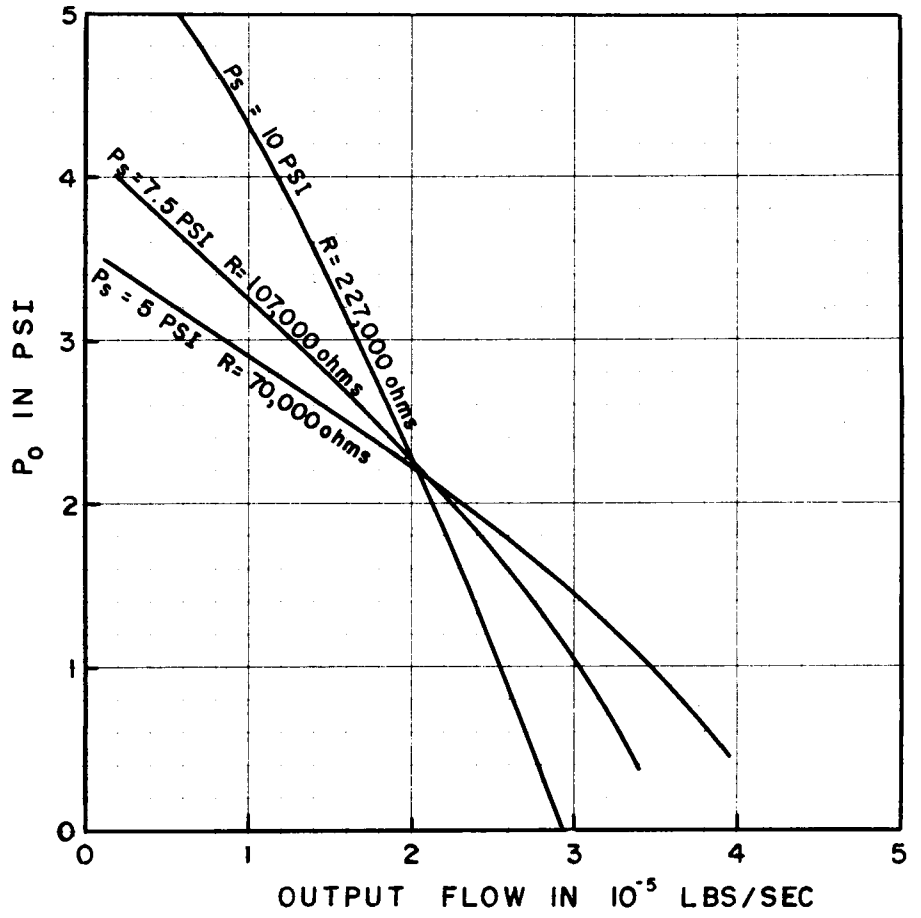

Figure 4.3.3-5 Output curves of an impact modulator for various supply pressures.

Note that the three curves all pass through the operating point with different slopes. This means that the incremental, or small signal, output impedance can be regulated by proper choice of supply pressures. This is also true of the transconductance and amplification factor of the device.

Returning to Figure 4.3.3-4, a plot of output pressure versus input pressure for zero output flow can be made from the intercept of the curve with the output pressure coordinate. This is shown in Figure 4.3.3-6 and is seen to have a quite linear region. In this linear region, the gain

$$A = \frac{\Delta P_o}{\Delta P_i} \Bigg|_{I_o = 0} \qquad (1)$$

is seen to be roughly -50.

The equivalent circuit of the impact modulator is given in Figure 4.3.3-7. For the device under consideration the gain A has been determined above to be roughly -50, at least in the straight line portions of Figure 4.3.3-4. In the low input pressure region, the gain is less than this and the internal impedance is nonlinear.

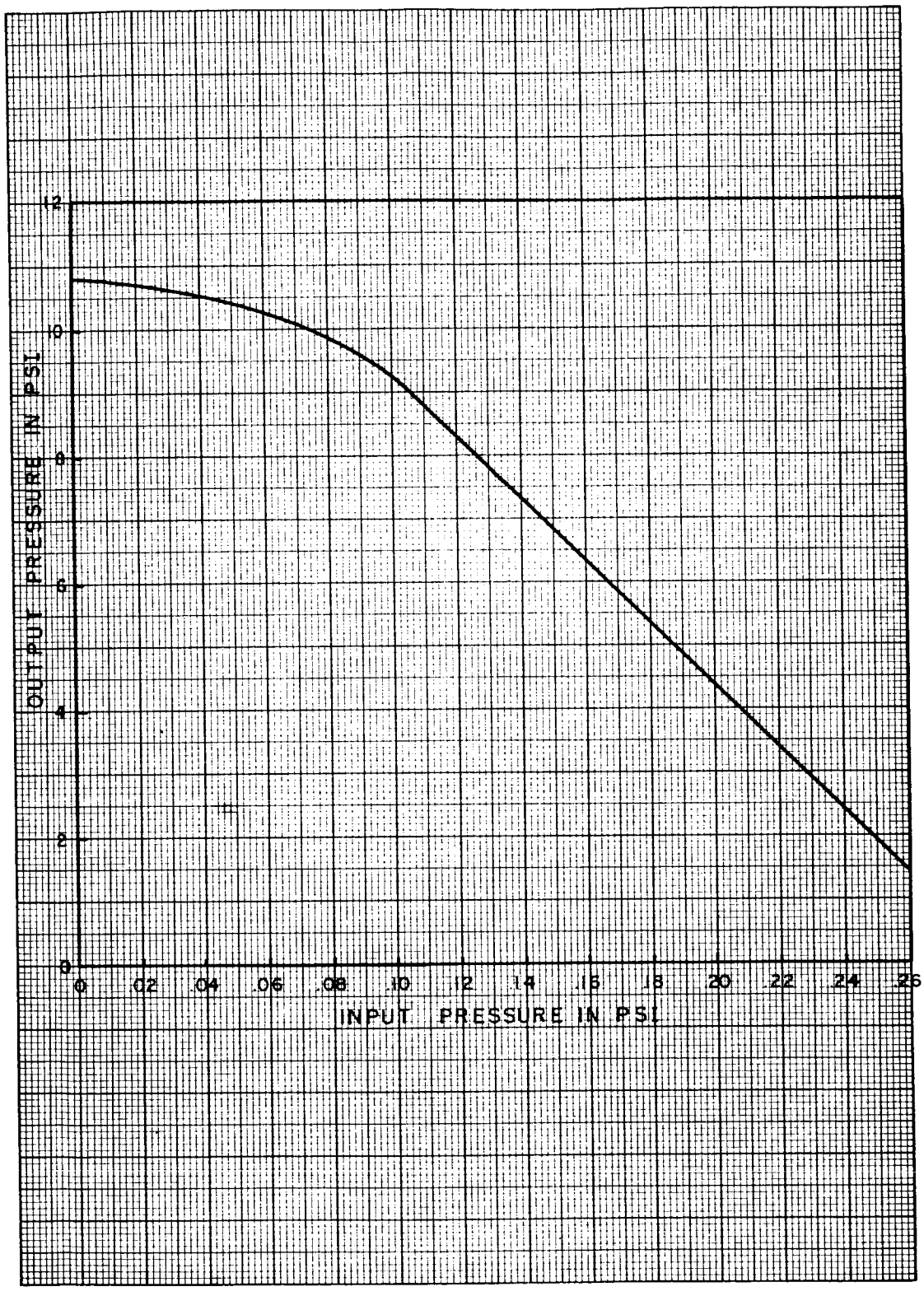

Figure 4.3.3-6 Input-output curve for a typical impact modulator.

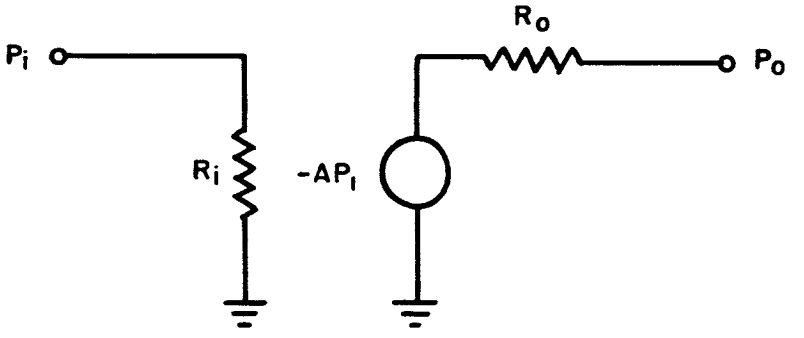

Figure 4.3.3-7 Low frequency equivalent circuit for an impact modulator.

4.3.4 Dynamic Characteristics

With slight changes, the incremental or small-signal, equivalent circuit is the same as the steady-state equivalent circuit. In the steady state equivalent circuit the resistor, R_o, represents both the resistance of the cylindrical orifice into the collection chamber and the resistance of the output tube. In the nonsteady-state case, the collection chamber volume acts as a capacity to ground, sandwiched between the input orifice resistance R_c and the output tube resistance R_t. This is shown in Figure 4.3.4-1. A typical value for the collection chamber volume is 0.01 cubic inch. In general, R_c will be much larger than R_t. The resistance R_t can be estimated from plots such as the one shown in Figure 2.2.2-1 and 2.2.2-2. A typical value would be 100 fluid ohms.

The input resistor R_i is an orifice; and, in general, the incremental resistance of an orifice is not the same as the steady state resistance, particularly at the low pressure drops which are customarily used in the control jets. As far as our analysis indicates, however, the gain A is the same in the steady state case as in the small signal case.

The transverse impact modulators are usually operated at such pressures that the emitter jet emerges from the nozzle at near sonic velocity. In a typical impact modulator, the maximum distance traveled by the emitter jet before interaction with the collection chamber is 0.100 of an inch. The distance from the location of the control jet to the collection chamber is still smaller, 0.084 inches. Considering even the larger distance of 0.100 inches, it is seen from Figure 4.5.5-1 that the phase delay associated with this distance of jet travel is less than 3 degrees at 1,000 cycles per second. The frequency must be increased to nearly 4,000 cycles per second before a phase delay of 10 degrees is achieved.

It is clear that the phase delay, or the phase shift, associated with transit time in the transverse impact modulator is negligible compared with the phase shift contributed by the resistance-capacitance circuits inherent in the modulator.

Let us know use the equivalent circuit of the impact modulator to calculate a gain of such a device in a circuit. Load the output of the modulator with an orifice, say one with a 0.015 inch diameter opening. Keep the frequency low enough that the capacity of the collection chamber can be ignored. Assuming a flow coefficient of 0.6 for the orifice and a pressure drop acrossed the orifice of roughly 3.5 psi the resistance of the orifice is approximately 90,000 ohms. The low frequencies equivalent circuit for this special case becomes that shown in Figure 4.3.4-2. The change in the output pressure divided by the change in the input pressure is given by:

$$\frac{\Delta P_o}{\Delta P_i} = \frac{(50)(100,000)}{90,\ 000 + 100,000}$$

which gives roughly 25 for the gain of the impact modulator stage with this particular loading, and at the specified pressure levels.

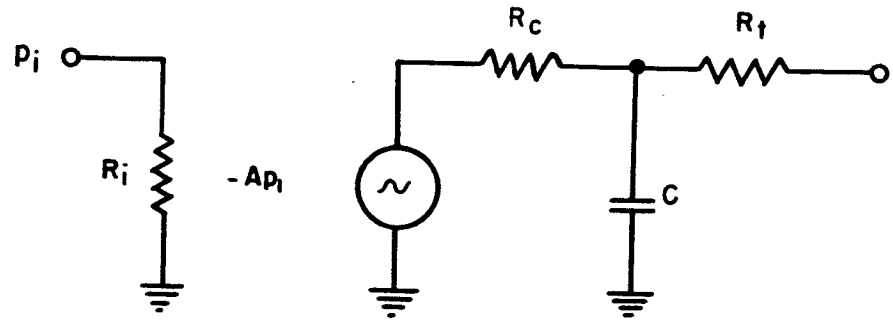

Figure 4.3.4-1 High frequency equivalent circuit for an impact modulator.

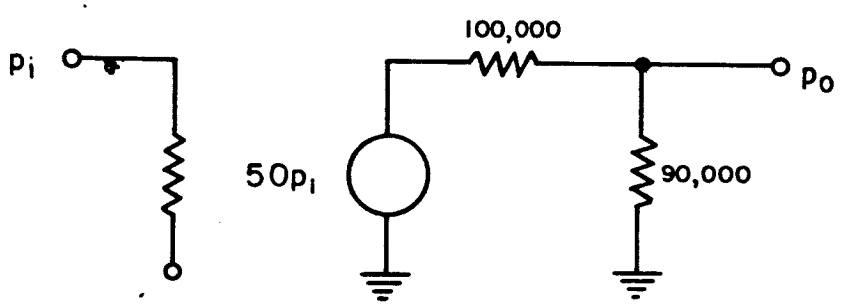

Figure 4.3.4-2 A loaded impact modulator.

For many commercial applications of the impact modulators a few cycles per second bandwidth is all that is needed. Measurements have shown that the present devices, which have been fabricated for the commercial market, work well to at least 30 cycles per second. Good results are obtained for smaller non-commercial devices up to 100 cycles per second. Little or no phase shift in signal is observed at these lower frequencies. These measurements are not adequate to verify the correctness of the small signal equivalent circuit presented above. The data is not inconsistent with the theoretical model however.

4.3.5 Interconnecting Impact Modulators

The construction of circuitry using impact modulators requires a technique for interconnecting the fluid amplifiers. This section provides a step-wise procedure for making such interconnections.

a. Determine the pressure required for the output of the final stage. Current limitations are that the impact modulator has been designed for subsonic operation. For air therefore, the power jet pressures are limited to less than 1.9 times ambient pressure. Output pressures will not exceed approximately 0.6 times the supply pressure).

b. Determine the output flow required from the last stage. From the transfer curves for available impact modulators, select the best one for the output requirements. The flow requirements may be met by paralleling two or more units in the final stage.

c. Having selected the unit, use the transfer curve, (P_o versus Q_o) to determine the "no control signal" operating point for the final stage. A typical set of curves is shown in Figure 4.3.5-1. The load line for the final stage will intersect this point (P_o, Q_o) and will go through the origin of the plot.

d. Using the plot of P_i (input control pressure) versus Q_o having lines of various P_o's, sketch in the load line points (this will provide a "dynamic transfer curve"). The range of P_i can be directly determined for any desired range of P_o (see Figure 4.3.5-1).

e. The maximum P_i needed to drive the final stage will now be the maximum P_o of the driver stage. The Q_o of the driver stage can be determined by using the data of Section 2.1. Having determined the P_o and Q_o of the driver stage, the design procedure continues for the next stage as in steps a, b and c above.

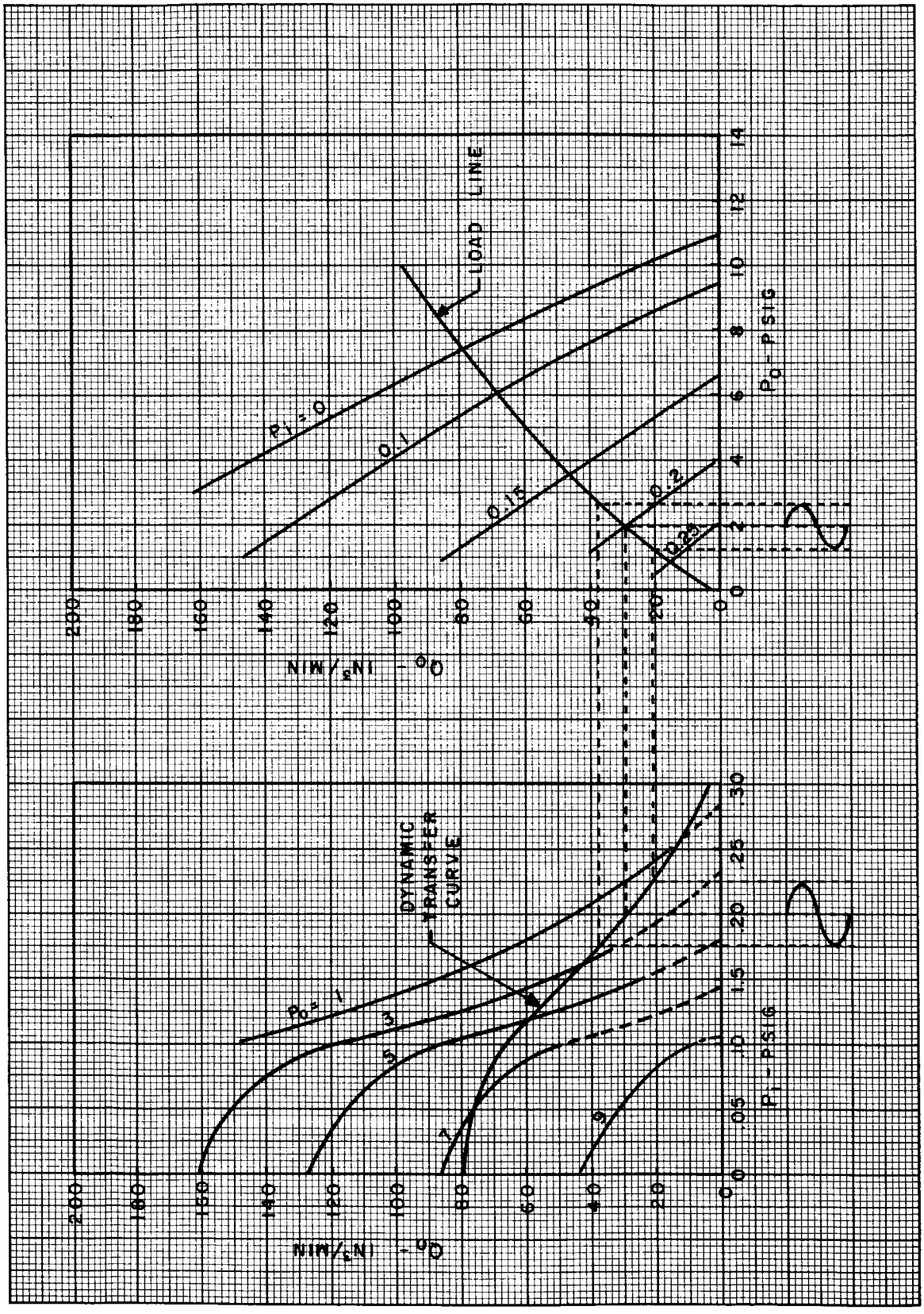

Figure 4.3.5-1 Transfer curve for an impact modulator.

4.3.6 Frequency Response and Noise

If a pressure or flow transducer having a high frequency response is connected to the output of a single impact modulator, it will be noted that there is considerable fluctuations in the output pressure and flow. These fluctuations constitute "noise". It has been observed that the "frequency of the noise" appears to be a function of the size of the impact modulator. However, the calculated resonant frequency of the collection chamber of the TIM16 impact modulator, for example, appears to be at least an order of magnitude higher than the observed fluctuations. There is little in the literature concerning the dynamics of impacting jets which would indicate the source of the noise. Therefore, an investigation of the mode of noise generation in impact modulators remains to be performed.

Optimizing the commercial, impact-modulator for higher frequency, control-system circuitry is expected to be accomplished in the near future. Paralleling the development of higher frequency response will be the development of amplifiers with a higher signal to noise ratio. Investigations are currently underway at Johnson Service Company to minimize the output noise.

The noise as well as the frequency characteristics of impact modulators seems to be size dependent. One small device tested (power orifice diameter of 0.005 inch) worked well up to 200 cycles per second and had a much better signal to noise ratio than the larger devices (.016 inch orifice). This same small device worked, with considerably reduced amplitude, up to 800 cycles per second. It must be pointed out, however, that there were problems with the signal generator at these higher frequencies and the device limitations have not been adequately determined.

In defining the signal to noise ratio for fluid devices, it is necessary to specify the bandwidth over which the noise is to be measured. For example, there may be considerable noise at 5 kc, but if this noise is incapable of modulating the downstream circuitry, it is of no interest to the area of concern.

Noise is a problem in the dynamic operation of both the single unit and the cascaded unit. However, it must be pointed out that the level of noise in the impact modulator is considerably less than most pure fluid devices. As a matter of interest, the noise level for the impact modulator circuitry is cited in Reference (6). Page 15 of this report states: "The noise encountered in the operational amplifiers varied somewhat, but was usually in the neighborhood of 0.003 psig, where the output range was 10 psig." Thus, if we define the signal to noise ratio as

$$S/N = \frac{\text{Output Range}}{\text{Output Noise}}$$

The signal to noise ratio of the above becomes 333.

In one case cited in the above reference, the noise was as high as 0.15 psig. This would give a S/N ratio of 67. This amount of noise was based upon a noisy first stage in an amplifier. Work presently being done by the Johnson Service Company is expected to improve the S/N ratio markedly.

In summary, it can be said that the impact modulator is adequate (even in its standard commercial design) for most fluid control-system applications. The major, device design-problem at present is to increase the signal to noise ratio.

4.3.7 Dynamic Tests of Impact Modulators

Conceptually, it is simple to test the dynamic response of a fluid component or of a fluid system. In actual practice, the dynamic testing becomes difficult. To test components which have a frequency response of a few hundred cycles requires the use of a signal generator to produce a sine wave of these frequencies. In addition, some type of a fluid to electrical transducer is needed which itself is responsive over the range of frequencies used. Since noise can mask a signal making it difficult to observe the phase shift, noise can be, in fact usually is, a problem in fluid circuits. These problems are typical of the instrumentation problems of a new technology.

Dynamic tests have been made on impact modulators and on operational amplifiers constructed from impact modulators. The test circuit is shown in Figure 4.3.7-1.

This same test approach can be used for pressure measurements as well as for flow measurements. The hot-wire probes are removed and pressure transducers (such as the variable reluctance pressure transducer) are put in their place. The hot-wire amplifier is then replaced by the transducer electronics. If it is desired, the oscilloscope can be replaced with a recording instrument. Dynamic measurements on an entire amplifier or fluid system can be using the same test circuit. It is only necessary to replace the device under test with the circuit to be tested.

Dynamic tests on the impact modulator were first tried using the hot wire anemometer, but the sensitivity of the hot wire to noise resulted in signals which masked the phase relationship. The dynamic tests were then repeated with the variable reluctance pressure transducers. This technique gave fair results.

Figure 4.3.7-2, shows typical test results in the form of reproductions of the tape from a Brush Recorder. In this Figure, the top pieces of tape show the calibration. The center piece shows the response to a 5 cps input. The bottom tape demonstrates device operation at 30 cps. It will be noted that at 30 cps there is no detectable phase shift between input and output waveforms. Separate tests were made using an oscilloscope in order to determine the device's characteristics at considerably higher frequencies. One device of a smaller size than the one tested above would operate up to 800 cycles per second. However, the gain of the device was markedly reduced at this frequency. This same device had a 90 degree phase shift at approximately 700 cps.

In general, the impact modulator having 0.016" diameter input orifices has a Bode plot approximately as shown in Figure 4.3.7-3. Exact valuation of the break frequency is difficult because of the noise at the output. The currently available devices are designed for commercial use with no particular frequency requirements above a few cycles per second.

The noise generated by the device is apparently related to the size of the output or collector chamber volume. The frequency of the noise is of the order of 1 to 2 thousand cps in the smaller devices and becomes

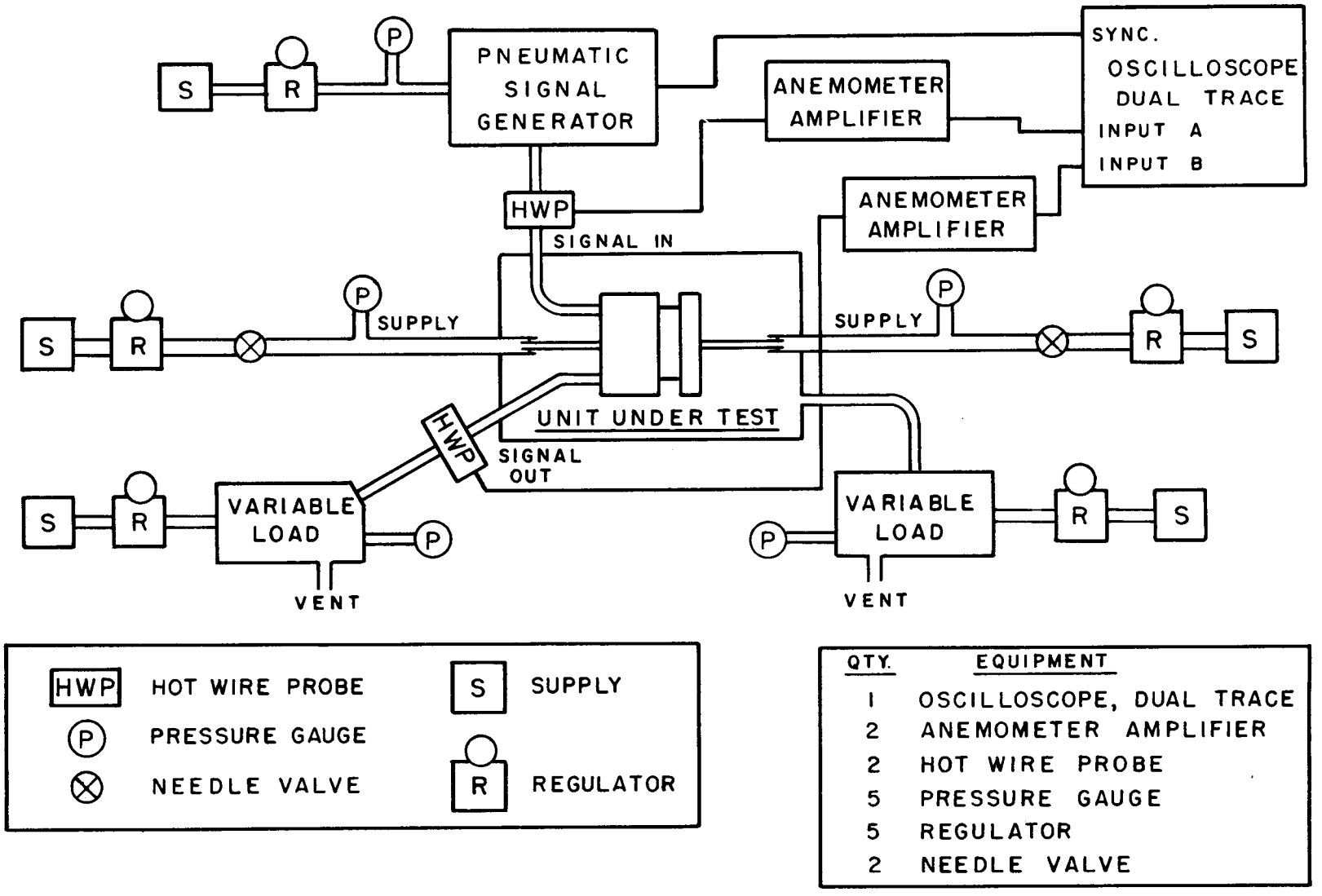

Figure 4.3.7-1 Dynamic test circuit.

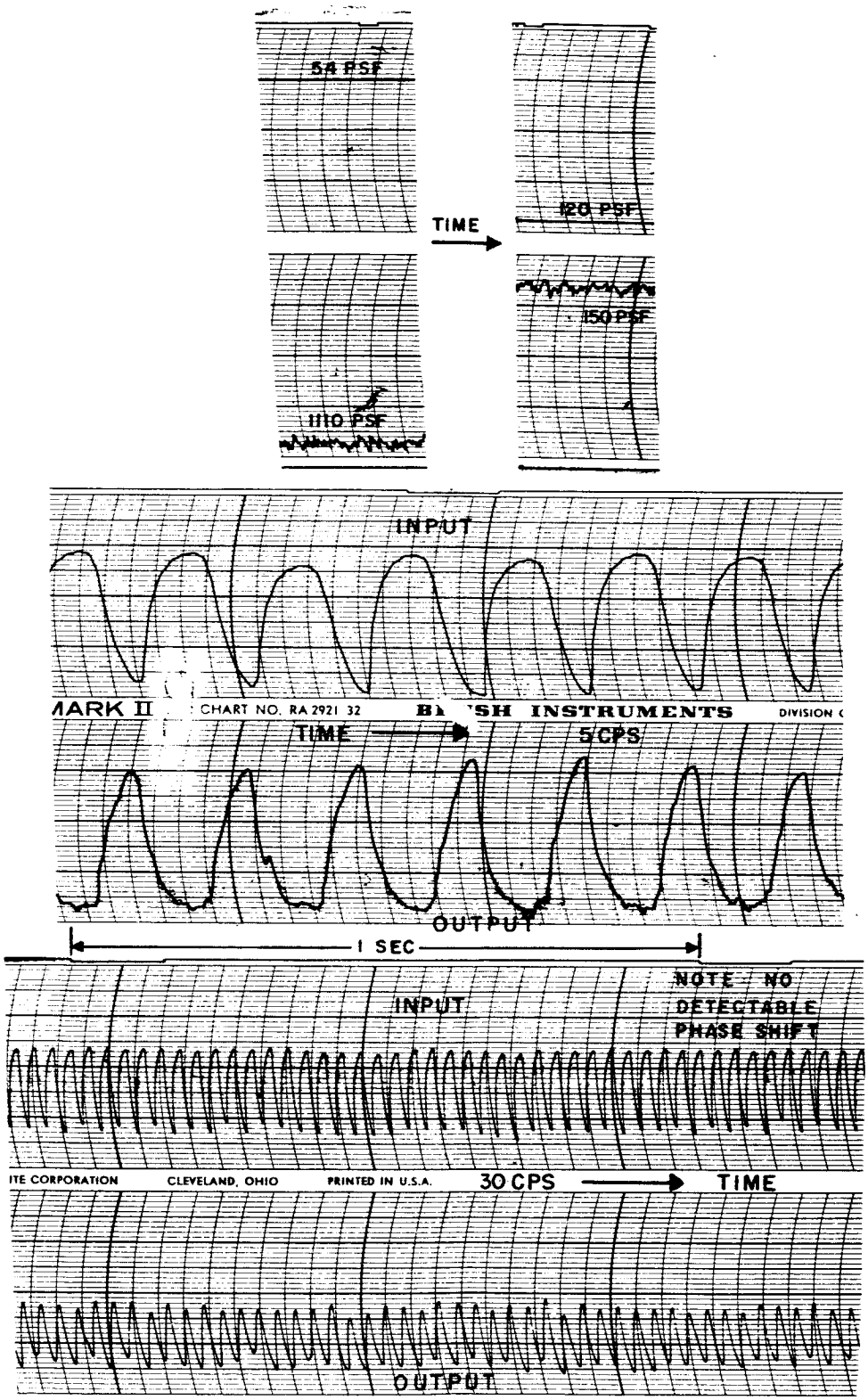

Figure 4.3.7-2 Input and output recordings for an impact modulator.

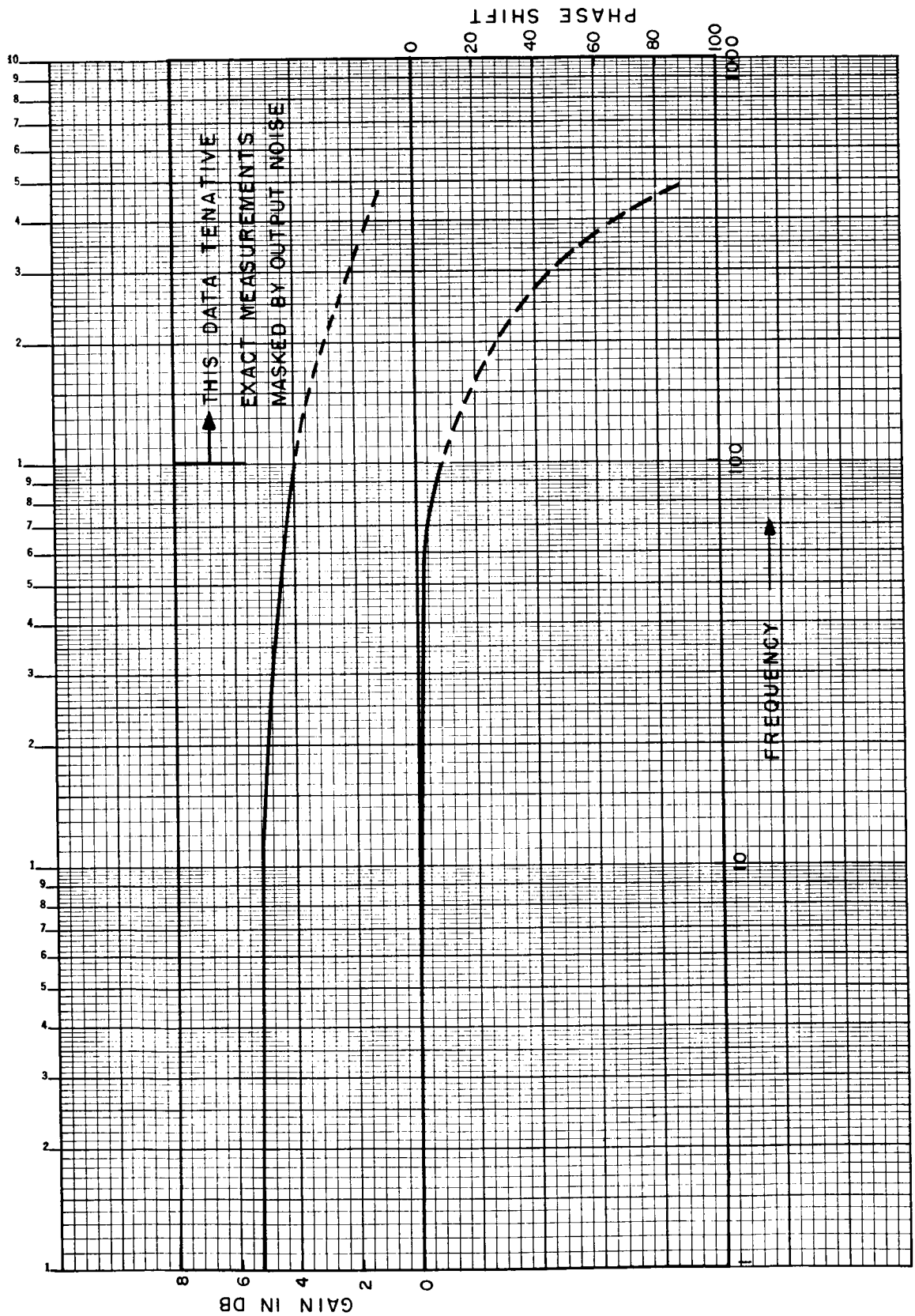

Figure 4.3.7-3 Bode plot for an impact modulator.

lower for somewhat larger devices. Future work planned by Johnson Services Company will optimize the device geometry to attain better high frequency performance and a better signal to noise ratio. As pointed out in the section on instrumentation, any jet-edge, or impacting jet systems, will create high frequency noise. The design goals are to insure that the noise is well above the desired frequency response of the device. Similarly, the transducers should be selected so as to be responsive only to those frequencies of interest to the experimenter.

Figure 4.3.7-4 shows the results of tests made at Johnson Service Co. An impact modulator was tested with various volumes added to the output (5, 10, and 20 in^3). The effect of the added volumes on the frequency response is to reduce the response to a few cycles per second.

As indicated previously, a complete operational amplifier employing impact modulators has been tested and shows excellent dynamic performance. The recorder charts reproduced as Figure 4.3.7-5 show that for 25 cycles/second input signal, the phase shift is approximately 30^o. This compares favorably to a single vortex amplifier where the phase shift is 25^o at a frequency of 10 cycles per second (See Reference 14). Recorder charts at 90 cycles/sec are shown in Figure 4.3.7-6.

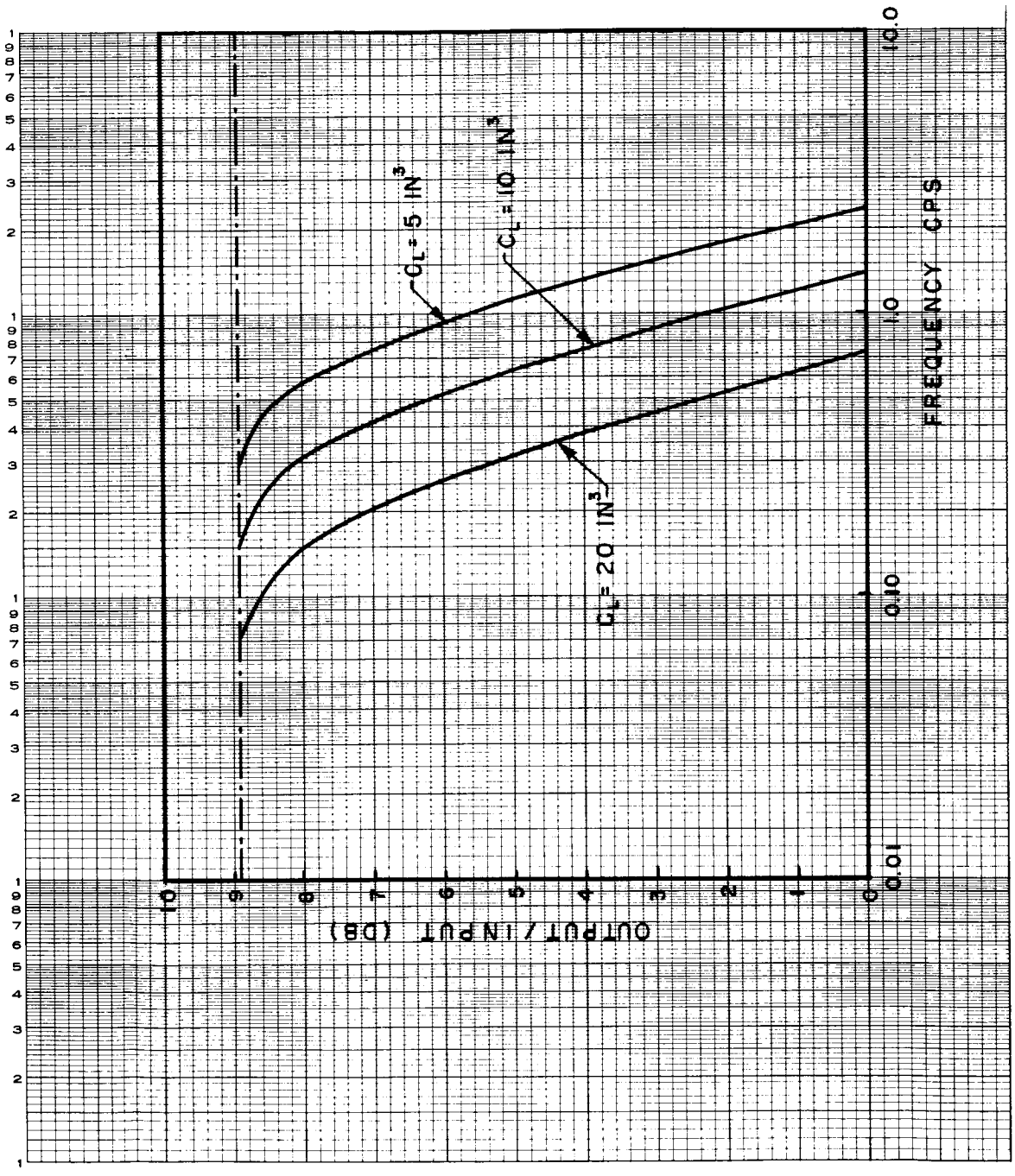

Figure 4.3.7-4 Bode plot for an impact modulator.

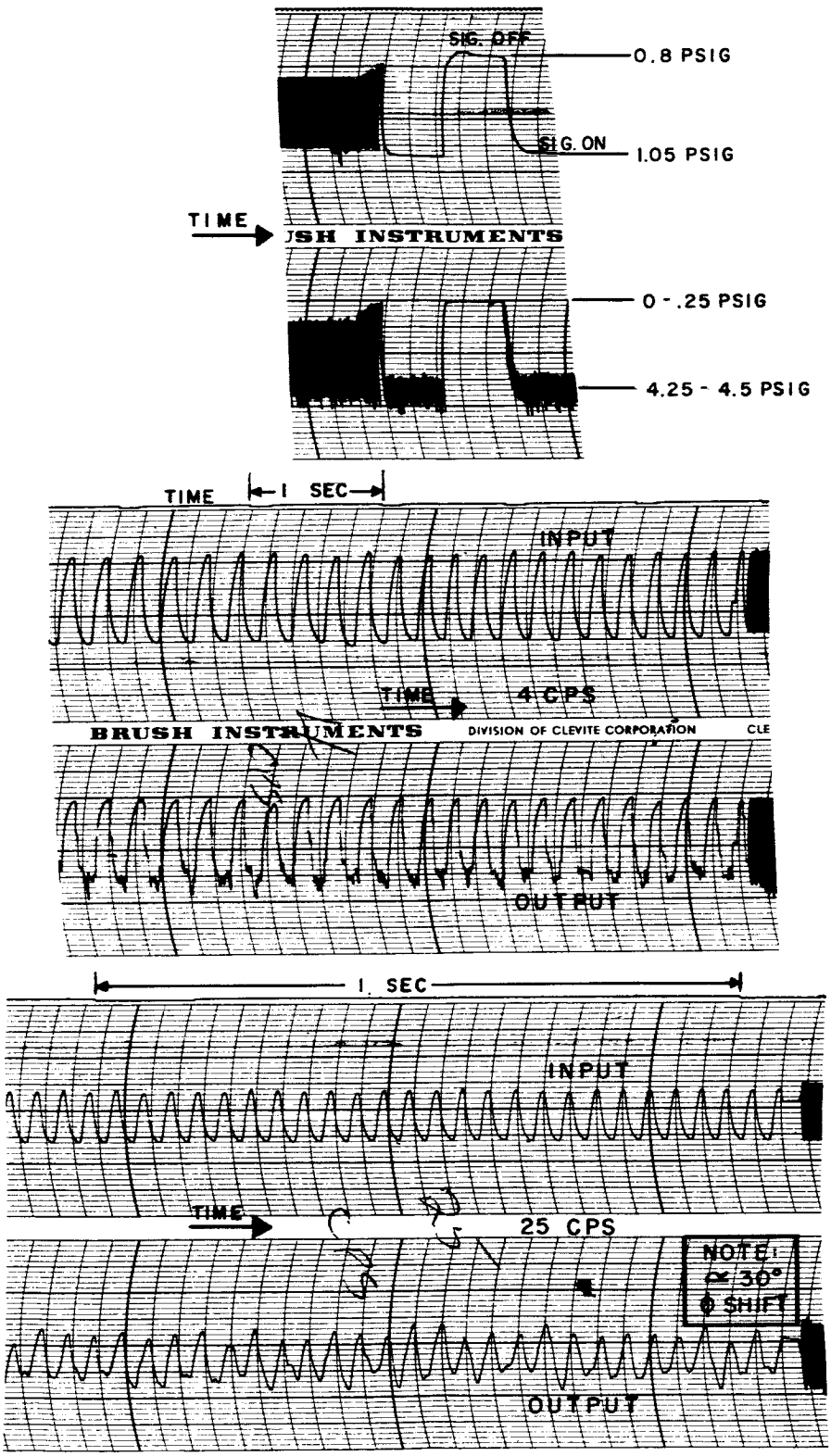

Figure 4.3.7-5 Dynamic Response Operational Amplifier (4 CPS-25 CPS)

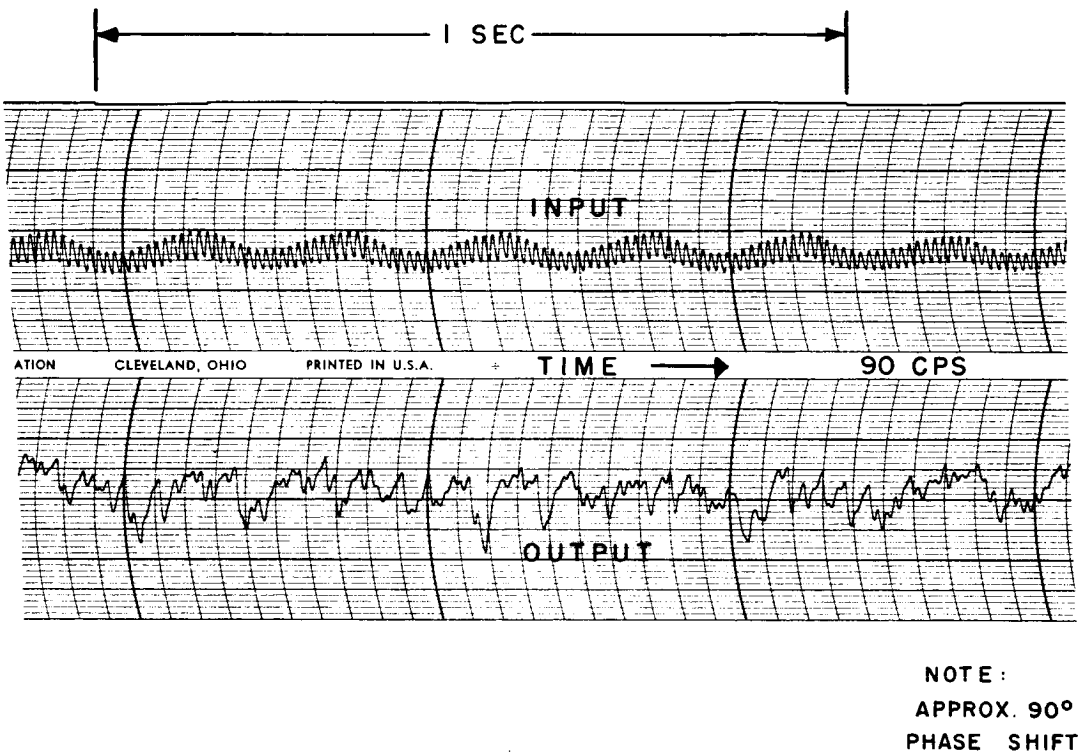

Figure 4.3.7-6 Dynamic Response Operational Amplifier (90 CPS)

4.4 Proportional Circuit Requirements

4.4.1 Linear Fluid-Resistors

In fluid amplifiers, and particularly in the feed-back circuit of operational amplifiers, it is desirable to have linear fluid-resistors. In liquid circuits linear resistors are readily obtained by the use of capillary tubes operating in the laminar flow region.

With gaseous amplifiers, however, the problem is more difficult. Capillary tubes, while linear for small pressure drops, are not linear for large pressure drops. Hence, in order to obtain linear resistors for gases using capillary tubes, it is necessary to ensure that the pressure drop across any given individual resistor is small. The term small is dependent upon the resistor, but for those resistors usually used in pure fluid control circuits, a pressure drop of 20 psi, or less, is small.

Non-linearity in a capillary resistor can arise from at least two sources; the finite compressibility of the fluid and the onset of turbulence. The onset of turbulence at the desired pressure drop can be eliminated by using sufficiently small tubing. This is shown in Figure 2.2.3-4. It is seen from this figure that the smaller the tubing, the larger the allowable pressure drop before the onset of turbulence.

The expected deviation from linearity due to compressibility is shown by line-c of Figure 2.2.3-2, where line-a of the same figure would represent the flow if the fluid were incompressible. Curve-c of Figure 2.2.3-2 is theoretical and was derived for smooth tubes. Fortunately, this theoretical law is not followed too closely for most practical fluid resistors. An example is shown in Figure 4.4.1-1 which shows the pressure-flow relationship for three Corning glass-resistors. They are quite linear up to 20 psi, the maximum pressure drop at which measurements were made.

One method of making fluid resistors is to flatten tubing until the opening is quite narrow. Pressure-flow curves for fluid resistors made by flattening .093 I.D. brass tubing is shown in Figure 4.4.1-2. The deviation from linearity at higher pressures is small but evident. The deviation is in the direction predicted by the smooth tube theory of Section 2.2.3, as shown in Figure 2.2.3-2.

Laminar resistors can also be made by casting fine wires in epoxy and then removing the wires. Pressure-flow plots for 3 such resistors made by casting epoxy around .008 inch diameter wires are given in Figure 4.4.1-3. Also shown in the figure are lines representing a linear resistor, labeled "theoretical laminar flow" and a line with the slope the pressure-flow curve would have if the flow were completely turbulent. The deviation of the experimental plots away from linearity and toward turbulence are evident at the higher pressure drops.

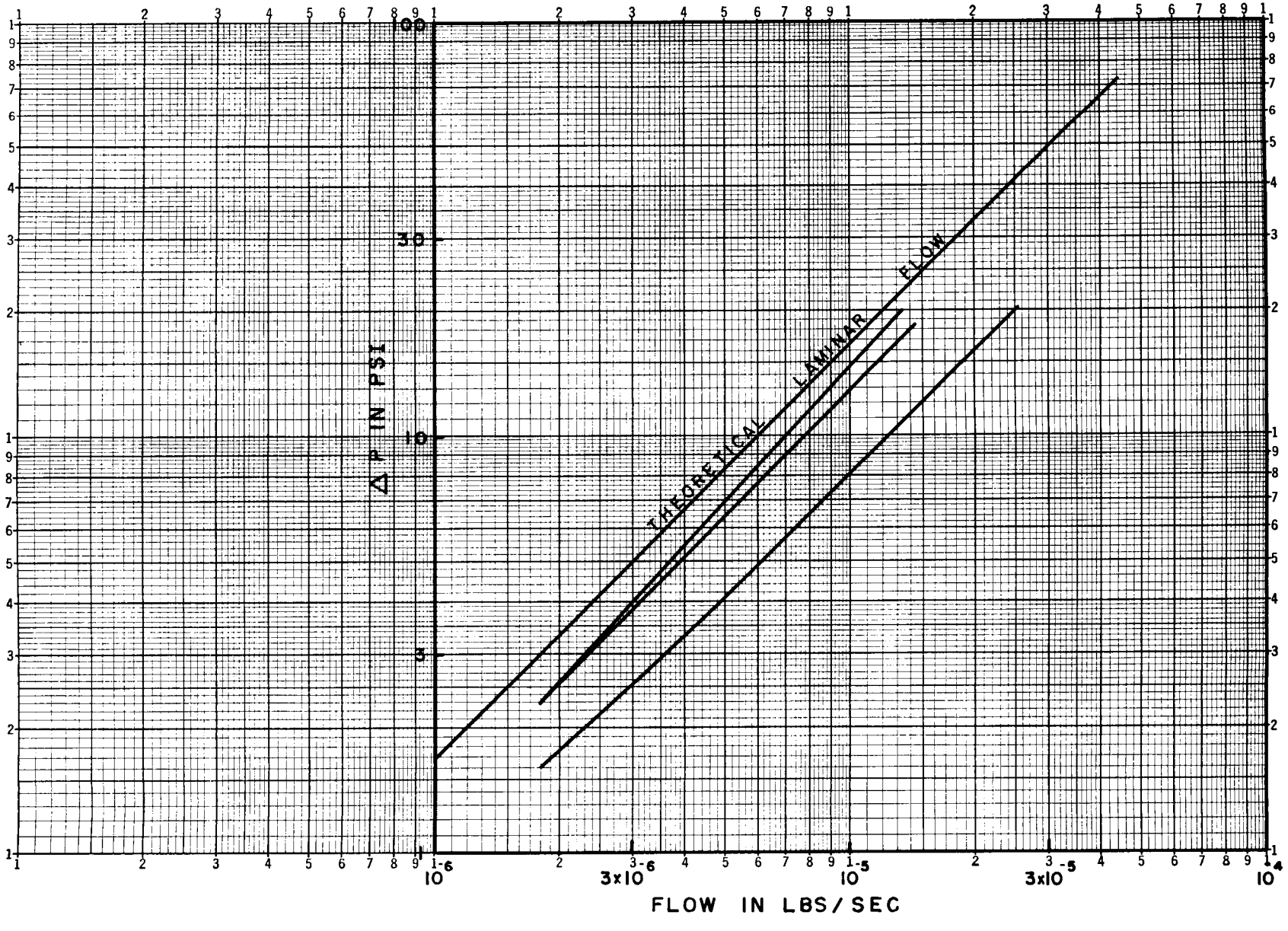

Figure 4.4.1-1 Flow data for three Corning glass-resistors.

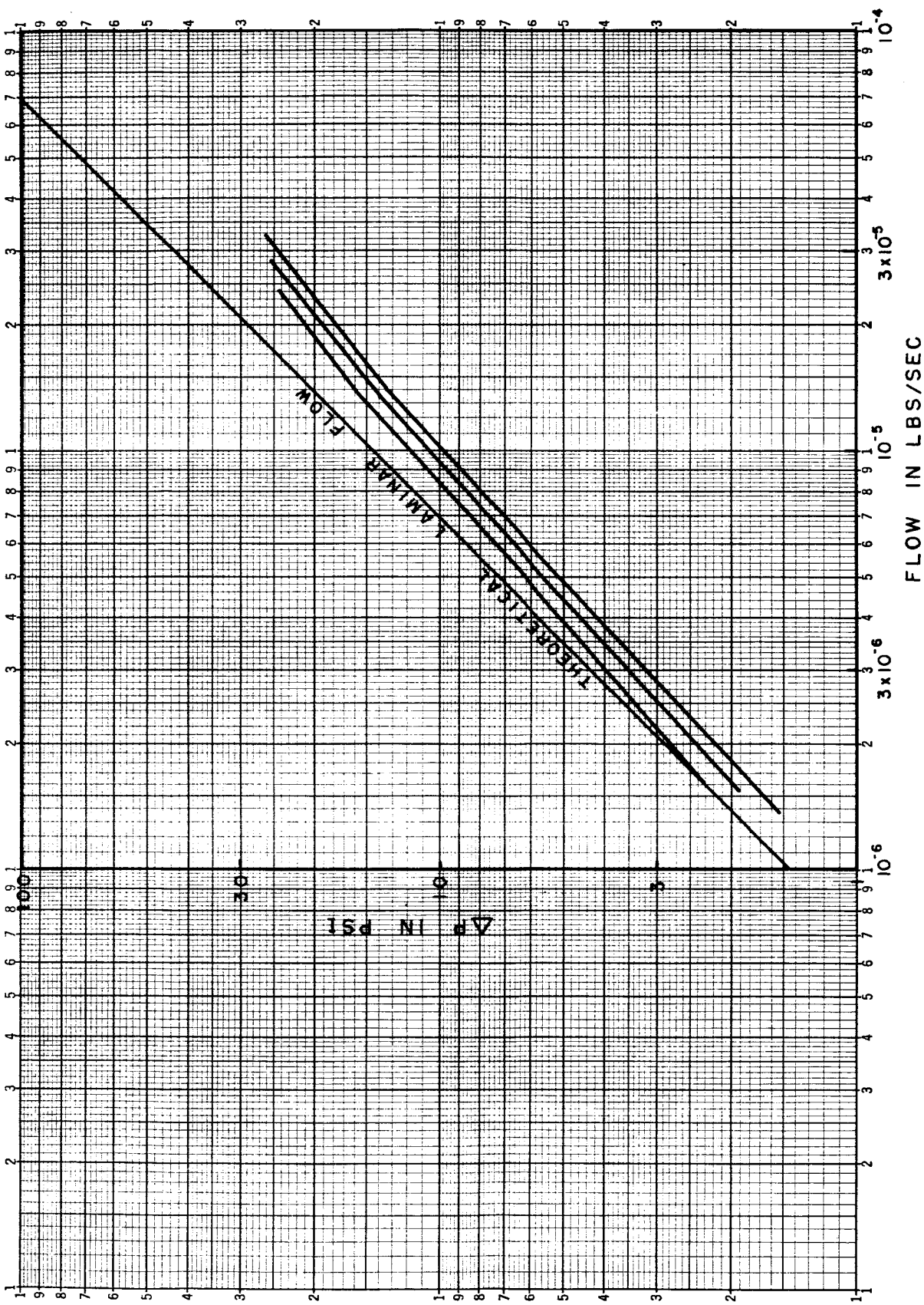

Figure 4.4.1-2 Flow for three flattened copper tube resistors.

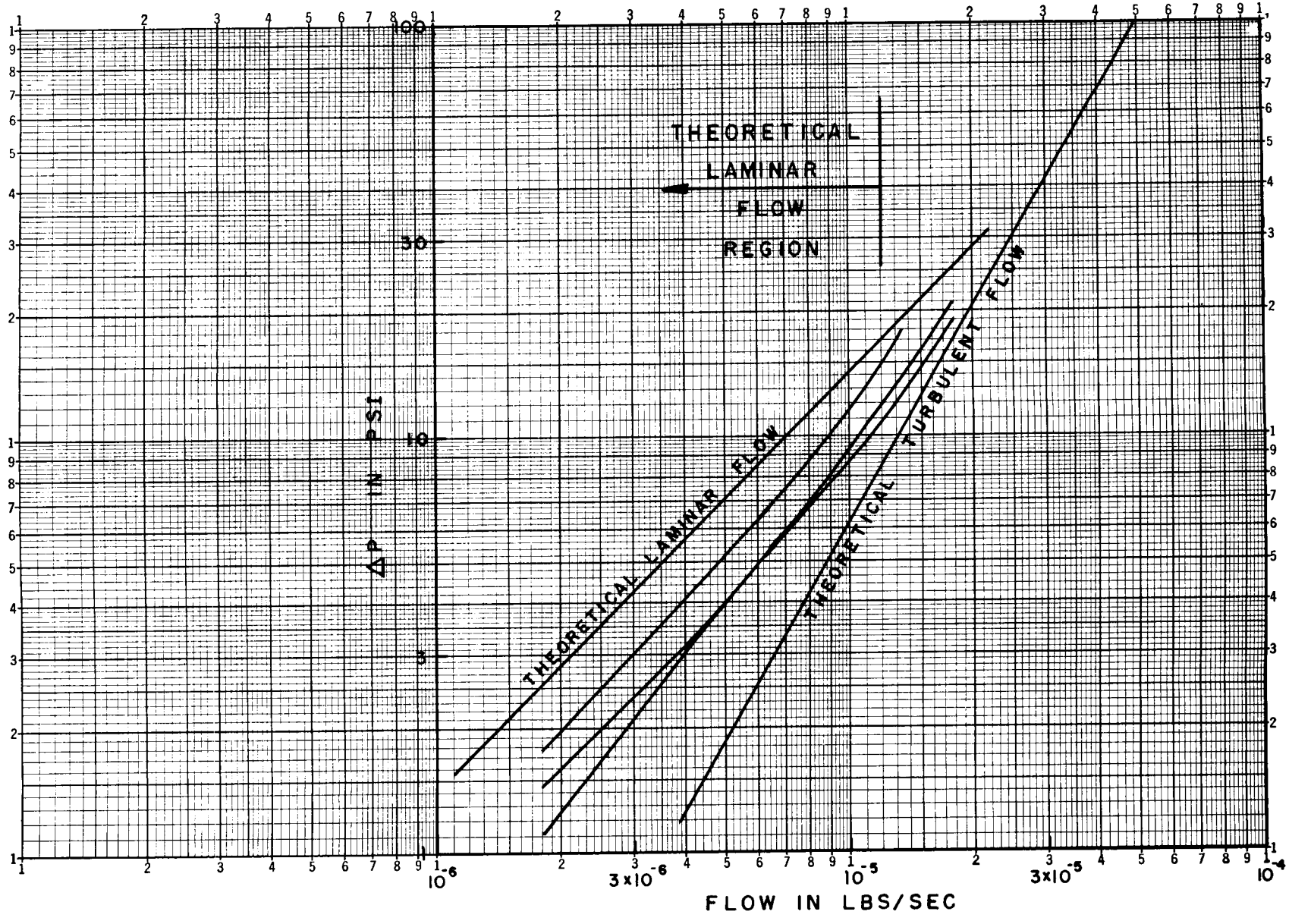

Figure 4.4.1-3 Flow for three resistors made by casting epoxy around fine wires.

4.4.2 Variable Fluid-Resistors

For a given fluid, the principal factors which determine the resistance of a laminar-flow resistor are the dimensions of the resistor. Hence, a variable resistor is obtained by changing some dimension of the resistor.

A tapped, or stepped, fluid-resistor can be made by simply taking a long capillary tube and putting taps along it at various points. The resistance can then be varied by changing taps. In contrast to electrical circuits where unwanted taps can simply be ignored, the unwanted taps in the fluid resistor must be carefully sealed off.

Completely satisfactory variable fluid-resistors are not available. One common method of constructing a variable fluid-resistor is through the use of a cylinder and loose fitting piston. The space between the cylinder and the piston is the constriction which gives the resistance. Pushing the cylinder in and out varies the length of the constricted area and therefore varies the resistance of the resistor. However, the variable volume at the end of the piston acts as a variable fluid capacitance which is often highly undesirable.

The lack of adequate variable linear-resistors does not hinder the experimental design of fluid circuits, at least on a D.C. basis. Where the size of a linear resistance must, or can, be found by experiment, a needle valve can be inserted into the circuit and adjusted to the optimum value. The value of the needle valve resistance is then measured and an equivalent linear resistor is substituted in the circuit for the valve. Needle valves are highly nonlinear. Therefore, when measuring the resistance of needle valves, it is important to make the measurements at the same pressure levels as those found in the circuit being developed.

4.4.3 Fluid Capacitors

Ideally, only compressible fluids show capacitive effects. Incompressible fluids do not show capacitive effects as such. Most liquids are sufficiently incompressible that capacity need not be concerned at least in most low pressure designs. In some cases the elastic properties of the fluid system must be considered. For example, in very high pressure hydraulics systems the walls of the fluid transmission lines elastically expand under the high pressure. These can feed energy back into the system giving the effect of a capacitance. However, for most low pressure control systems these effects can be neglected.

In circuits employing compressible fluids the analog of the electrical capacitor is simply a volume. Even small volumes are quite important in fluid circuitry, in that a volume is small as 1/10 cubic inch is a capacitance of sufficient size that it must be considered in many circuit designs.

Most often the problem is not to obtain a fluid capacitor, but rather to so design the system that the unwanted effects of capacitances are minimized.

One problem with fluid capacitors, and particularly in circuits where frequency shaping is desired, is that without moving, or deformable, parts fluid capacitors to ground are the only type which can be obtained. In order to obtain a series fluid capacitor it is necessary to use a moving part, a diaphram for example. Where it is necessary to have the equivalent of the series capacitor for some desired shaping function, the effect this can be accomplished by the use of differentiating circuits employing operational amplifiers. This technique is discussed in Section 4.6.

4.4.4 Electro-Pneumatic Transducers

The transducers of fluid circuitry fall into two classifications; transducers which convert some quality such as voltage, current, position or force into a fluid pressure or flow, and those transducers which convert a pressure or flow into a position or force or some other quantity.

Transducers are readily available which convert an electrical signal into a pressure. Static test results on one type produced by the Johnson Service Company has shown it to be quite linear over an output pressure range of 0-20 psig. The bandwidth of this particular transducer is roughly 6-cycles/second. Developments are underway which should increase the bandwidth by a factor of 10.

4.4.5 Flapper-Valve Transducer

A flapper valve can be used as a position-to-pressure transducer in fluid circuitry. A cross-sectional drawing of a flapper valve is shown in Figure 4.4.5-1. The flapper valve consists of a volume, V, which is connected with a constant supply pressure, P_s, through an orifice or constriction. Also connected to the volume is a downstream orifice or nozzle. The free jet which emerges from this opening impinges upon a flat plate of "flapper." The movement of this flat surface is the input signal to the valve. The output signal is taken through a tube connected to the volume, V.

The operation of the flapper valve is as follows: the supply pressure, p_s, forces a fluid flow through the upstream orifice. A portion of this flow goes out through the downstream orifice to the atmosphere. As a result, the pressure, P, in the volume, V, will lie between atmospheric pressure and the supply pressure. The resistance of the downstream orifice is dependent upon the distance, x, between the end of the nozzle and the flat surface. As x is decreased the resistance of this orifice increases and the pressure within the chamber will increase.

A set of typical curves showing the chamber pressure for a flapper valve as a function of the displacement, of the flapper is shown is shown in Figure 4.4.5-2. These curves are seen to be highly non-linear. A linear relationship between the input and the output of a transducer is highly desirable and can be obtained in the flapper valve by replacing the flat surface by a cam as shown in Figure 4.4.5-3. As the cam is moved laterally, the distance x changes. By properly shaping the cam, the chamber pressure, and consequently the pressure output signal, can be made to vary linearly with the lateral movement, y, of the cam. It is evident that the cam need not be of the type showing in Figure 4.4.5-3 but could be a rotary cam. The pressure output would then be a linear function of the angle of rotation of the cam. A set of curves for a typical valve cam combination is shown in Figure 4.4.5-4.

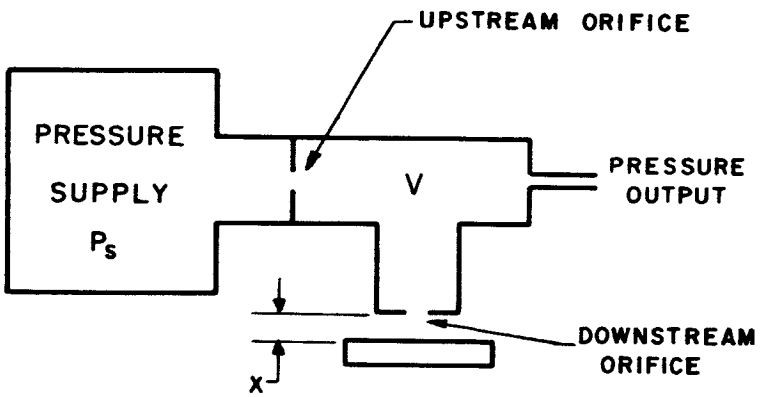

Figure 4.4.5-1 Flapper valve.

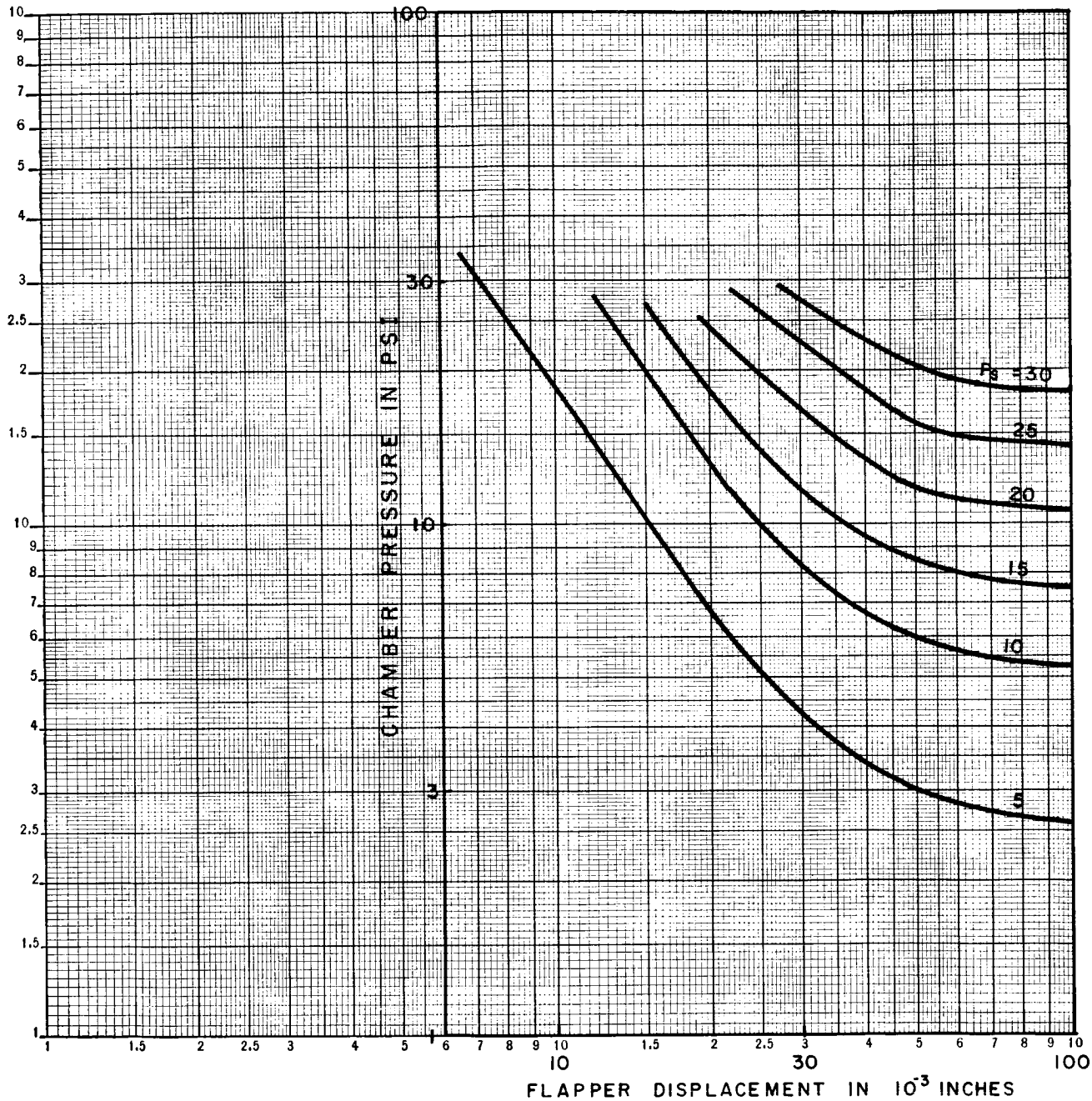

Figure 4.4.5-2 Chamber pressure for a flapper valve.

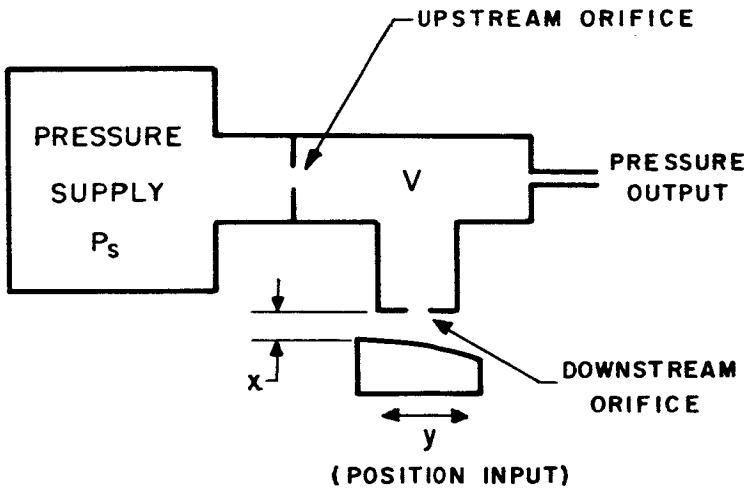

Figure 4.4.5-3 A flapper valve modified to transduce the position of a cam into an output pressure.

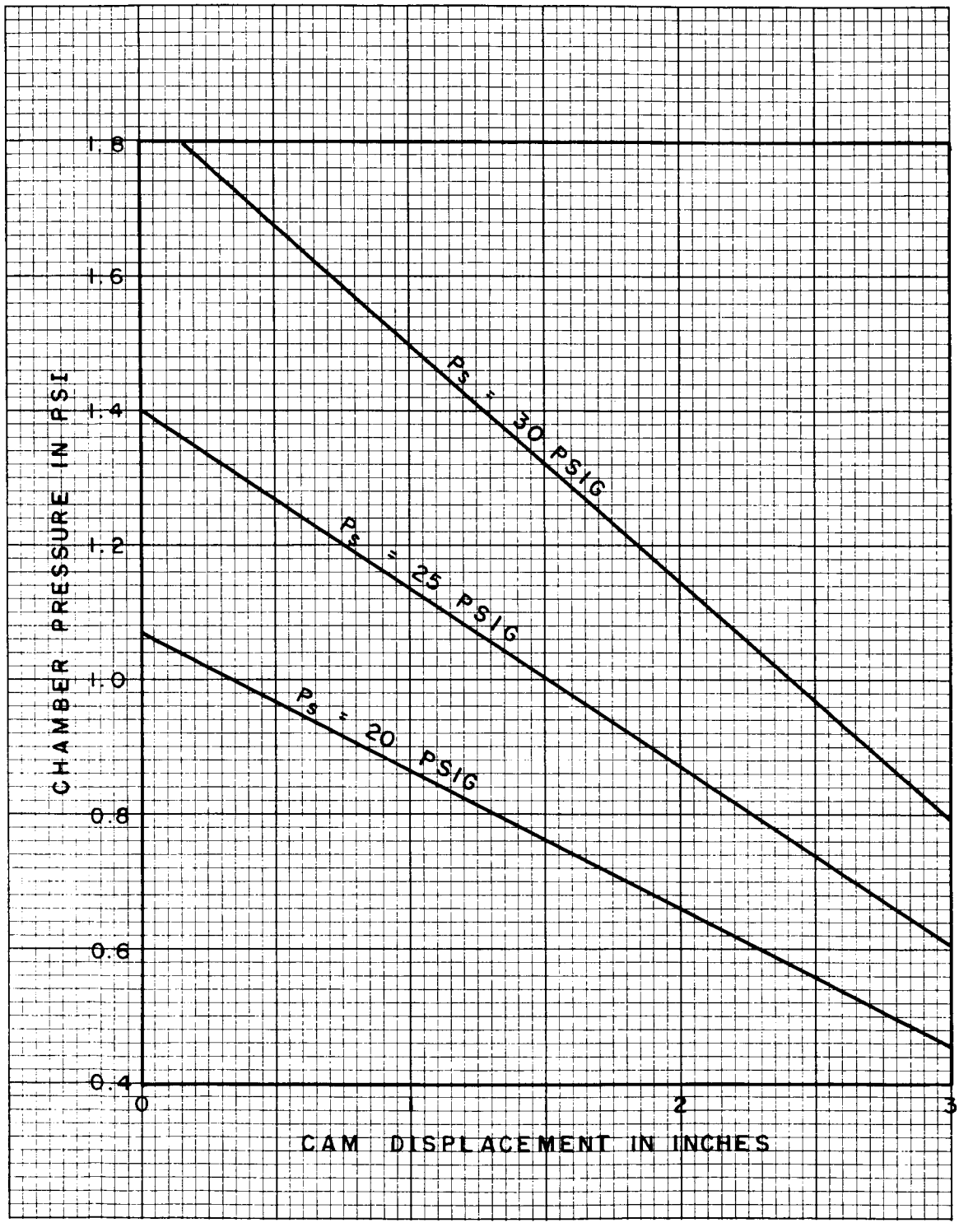

Figure 4.4.5-4 Chamber pressure as function of the cam displacement for a flapper-valve transducer.

4.4.6 Pressure-Position Transducers

A pressure to position transducer, or a pressure to force transducer, is readily obtained by the use of bellows. Metal bellows are available in a wide range of sizes and force constants, and as long as the elastic limit of the bellows material is not exceeded, the transducer is linear.

In order to reduce the fluid capacity of the transducers, the bellows are usually constructed so as to minimize the inside volume. This is often done merely by plugging the bellows with a solid cylinder. Where bellows expansion is large, the change in fluid capacity with expansion will have to be considered in the circuit design.

4.5 Circuit Analysis

4.5.1 Introduction

The analysis of fluid circuits falls into two areas; steady state and dynamic. The steady state analysis is relatively simple and straight forward. The expressions describing the pressure-flow relationships are well known, have been experimentally verified, and have been or can easily be supplemented by empirical data where necessary.

The dynamic behavior of fluid circuits is more difficult to analyse and is not completely understood. A great deal of work has been done, particularly in the small signal region and fairly good treatments are available. Large signal and transient behavior of fluid circuits is not amenable to analysis at present. Consequently our dynamic analysis of fluid circuitry shall be limited to small signals and shall further be limited to a lumped-parameter, low frequency, equivalent circuit.

4.5.2 Orifices in Series

As an example of steady state flow calculations, consider the problem of finding the flow through, and pressure division between, two orifices in series. As a special case, assume that the two orifices each have an orifice diameter of 0.030 inches and a flow coefficient of 0.6. Further let us consider the case of a constant pressure of 20 psi applied to the upper orifice and let the lower orifice discharge to atmosphere.

Denote the pressure drop across the first, or upstream, orifice by ΔP_1 and the pressure drop across the second, or downstream orifice by ΔP_2. Then, for a given ΔP_1, the drop across the lower orifice is given by $20-\Delta P_1$.

The flow through the upstream orifice as a function of pressure drop across the orifice can be found from Figure 2.2.5-7. This flow is plotted in Figure 4.5.2-1. Since the pressure drop across the second orifice, ΔP_2, is directly related to ΔP_1, the flow through this orifice is a function of ΔP_1. This can be found from Figure 2.2.5-4 or, more easily, from Figure 2.2.5-5.

In Figure 4.5.2-1, the flow through the upper orifice increases with increasing ΔP_1, while the flow through the lower orifice decreases. The point where the flow lines cross gives the actual flow through the series combination. This is seen to be roughly 3.1×10^{-5} lbs/sec. Of the 20 psi supply pressure, 7.3 psi will be dropped across the upper orifice and 12.7 psi across the lower orifice.

It is seen from this simple example, that although two series orifices are the same size and have the same flow coefficient the pressure does not divide itself equally across them. This is do to the nonlinearity of the orifice resistance.

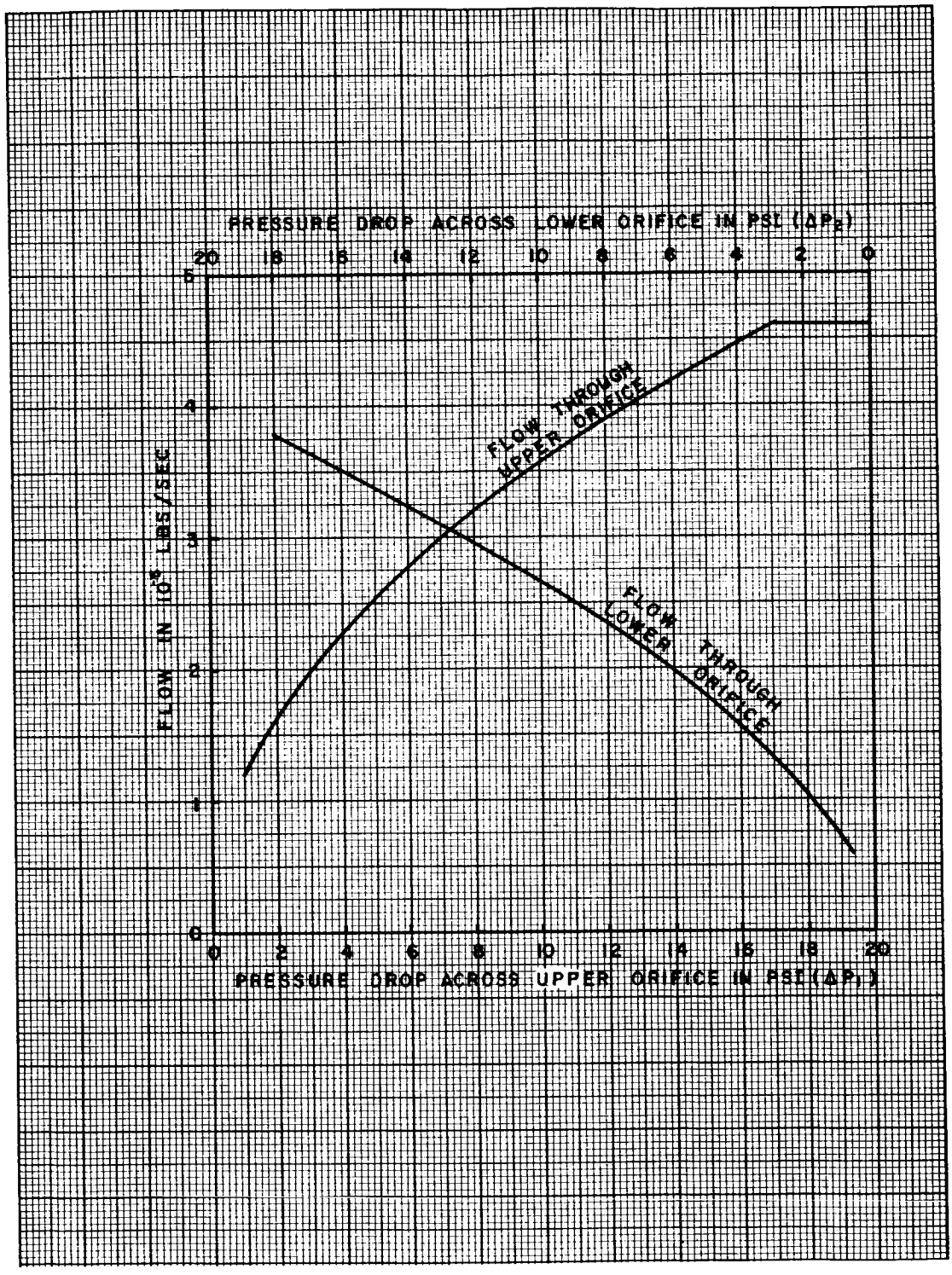

Figure 4.5.2-1 Flow through two equal sized orifices connected in series, with an upstream pressure of 20 psig and an atmospheric downstream pressure.

4.5.3 Flapper Valve

As an example of dynamic analysis, consider a cam-operated, flapper valve which linearly translates a cam movement into an output pressure. Such a transducer is shown in Figure 4.4.5-3.

In a lumped parameter equivalent circuit, volumes become capacities and restrictions become resistors. In the flapper-valve transducer shown in Figure 4.4.5-3, C will represent the electrical equivalent of the volume, V, while R_u, R_d and R_o will be the equivalent resistance of the upstream orifice, the downstream orifice, and the output tube respectively. The supply pressure, P_s is represented by a voltage V_s. The equivalent circuit is shown in Figure 4.5.3-1.

The signal input to the valve is a lateral cam movement y which results in a variation in the distance x as shown in Figure 4.5.3-2. In the equivalent circuit, the cam movement is equivalent to a variation in the resistance R_d. To estimate the bandwidth or frequency response of the bridge, visualize a small step change in the distance x. In the equivalent circuit this would correspond to a small step change in the value of R_d. Analysis of the electrical circuit shows that following the step change in R_d the capacitor C charges (or discharges) exponentially with a time constant equal to the capacity C times the equivalent resistance of the three resistors R_u, R_o, and R_d in parallel. Since the change in the resistance R_d is small, the value of R_d used in the calculation of the equivalent resistor can be an average. From this, a time constant τ can be found. This time constant is a direct measure of the bandwidth or cut-off frequency, f_c, of the circuit. The relationship is

$$f_c = \frac{1}{2\pi\tau}$$

Sometimes flapper valves are designed and used in such a fashion that the analysis is somewhat simplified from that considered above. Often the resistance R_o is so large in comparison to R_u and R_d that the resistor R_o in the equivalent circuit can be neglected. If the pressure in the chamber is small under all operating conditions and the supply pressure P_s sufficiently large, the upstream orifice runs under choked flow conditions. In this event, the voltage V_s and the resistance R_u can be replaced by a constant current generator. The equivalent circuit then reduces to a capacitor, C, in parallel with a resistance, R_d, the combination being fed by a constant current generator. In this simple situation, the bandwidth of the circuit is that frequency at which the capacitive reactance of the capacitor C equals the resistance of the orifice resistance R_d. Expressed as an equation this becomes:

$$f_c = \frac{1}{2\pi R_d C}$$

Let us now consider a specific example of a flapper-valve transducer operating under these conditions.

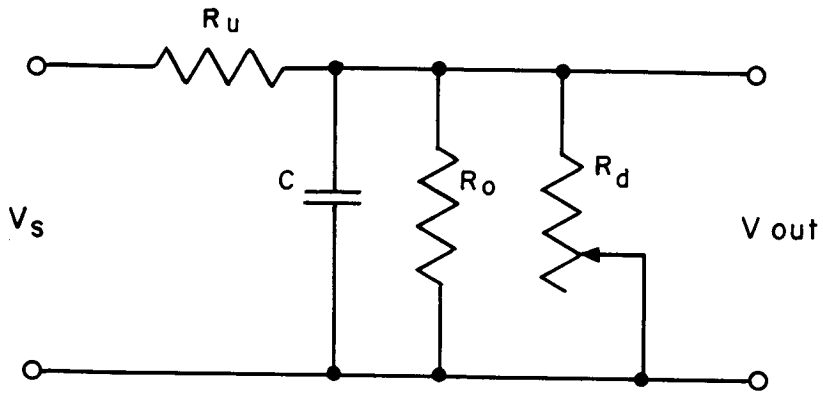

Figure 4.5.3-1 Equivalent circuit of a flapper valve.

A cross-sectional drawing of the valve to be considered is shown in Figure 4.5.3-2. The volume V is roughly 0.1 cubic inches. The amount of air flow which is taken for signal purposes is so small that it need not be considered in the analysis and the signal output connection is now shown.

The cam is contoured and experimentally the relationship between the chamber pressure and cam displacement is found to be essentially a straight line. The output pressure varies from about 0.21 psig to 1.25 psig, with the pressure output at the center position of the cam being about 0.75 psig. The supply pressure is 20 psig. Since the pressure in the chamber is always less than 1.25 psig, the upstream orifice always runs in the choked condition.

The time constant of the circuit can be readily found. Since the upstream orifice is choked, the fluid current into the volume can be found from Figure 2.2.5-7. This figure is a plot of pressure drop across an orifice with a constant supply pressure as a function of current through the orifice, for an orifice with a diameter of 1-inch and a flow coefficient of 1. Since the orifice is choked and the upstream pressure is 20 psi, the current for this 1-inch orifice is seen from Figure 2.2.5-7 to be 0.86 lbs/sec.

The actual current flowing through the orifice under consideration can be found by multiplying the 0.86 lbs/sec reference current by the actual diameter of the orifice squared and the flow coefficient of the orifice. The diameter of the orifice is .048 inches, and the flow coefficient for an orifice of this nature will be roughly 0.6. Multiplying, the actual fluid current flowing through the orifice is found to be 1.19×10^{-3} lbs/sec.

Since the upstream orifice is choked under all conditions, the flow through the downstream, or control, orifice will always be 1.19×10^{-3} lbs/sec. When the chamber pressure is 1.25 psi, the downstream orifice resistance is found by simply dividing 1.25 psi by 1.19×10^{-3} lbs/sec. This gives a resistance of 1050 ohms as the dc or steady-state resistance of the orifice. When the cam is moved through its full travel the resistance of the orifice is decreased, and the pressure in the chamber drops to 0.21 psi. In this case the steady-state resistance is equal to $0.21/1.19 \times 10^{-3}$, or 176 fluid ohms.

The pressure in the chamber is quite small, and it is seen from Figure 2.2.5-5 that for small pressure drops the incremental, or small-signal resistance of an orifice is approximately twice that of the steady-state resistance. The incremental resistances are the values which must be used in the calculation of the frequency response of the circuit. Consequently, the extremes of the incremental resistance for the flapper bridge are twice those found above. From the above steady state resistances, the incremental resistance of the orifice is seen to vary between 2100 fluid ohms and 352 fluid ohms.

Knowing the volume of the fluid capacitor and the parallel orifice resistance, the break frequencies can be found from Figures 2.2.6-3 and 2.2.6-4. This is done by finding those frequencies at which the capacitive reactance equals the orifice resistance. For the extreme values of the incremental orifice resistances, the break frequencies for these orifice resistances are found to be 260 cycles/second and 1,500 cycles/second. A plot of break frequency, or bandwidth, versus cam displacement is linear and is given in Figure 4.5.3-3.

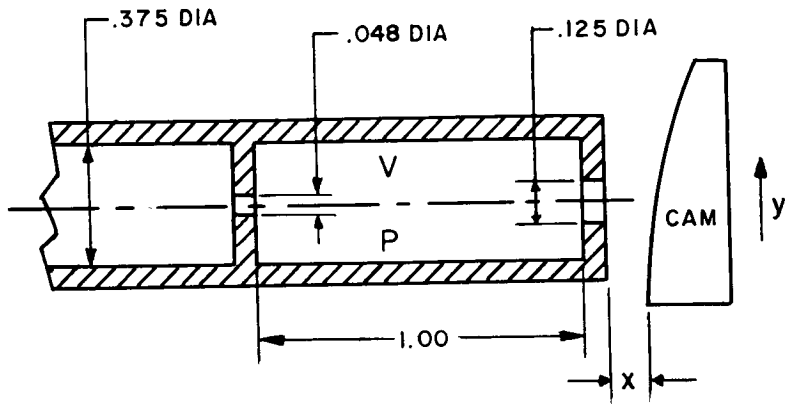

Figure 4.5.3-2 Cross sectional sketch of a flapper-valve transducer.

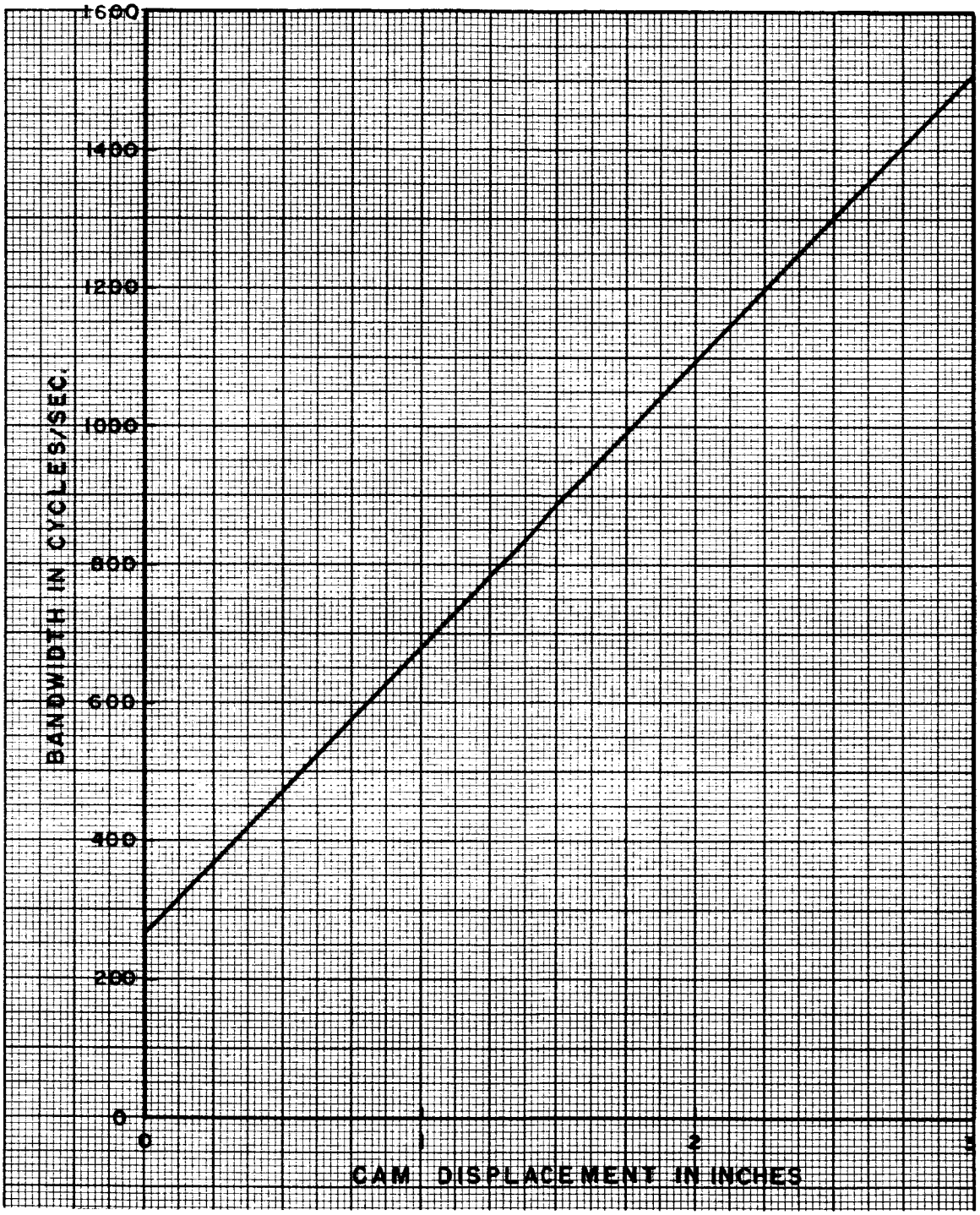

Figure 4.5.3-3 Frequency response of a flapper valve transducer.

4.5.4 Tube Terminating in Volume and Orifice

A typical fluid circuit would be a variable pressure source connected to an orifice by a small-tube, linear resistor. Variations in the pressure source would be the input signal. The output signal would be the pressure applied to the orifice.

In a practical gas circuit, the orifice might be one of the orifices of an active device. The linear resistor would be a separate component. Tubing of some sort would be used to connect the resistor and the orifice. The interconnecting tubing would have a finite volume, and consequently a fluid capacity. A sketch of the fluid circuit as visualized is shown in Figure 4.5.4-1. The volume and the orifice act as a capacitor, C, to ground shunted by the orifice resistance, R_o. The complete lumped equivalent circuit is shown in Figure 4.5.4-1, where R_1 represents the linear resistor.

The transfer function of this circuit is:

$$G(s) = \frac{1}{1 + sRC} \cdot \frac{R_o}{R_o + R_1} \qquad (1)$$

where R is the parallel combination of R_1 and R_o. In many cases, R_o will be much smaller than R_1. In this case, the transfer function becomes:

$$G(s) = \frac{R_o/R_1}{1 + sR_oC} \qquad (2)$$

The bandwidth or break frequency of this circuit is:

$$f_c = \frac{1}{2\pi R_oC}$$

In words, the bandwidth of the circuit extends from steady state up to the frequency at which the reactance of the tubing capacity becomes numerically equal to the incremental resistance of the orifice.

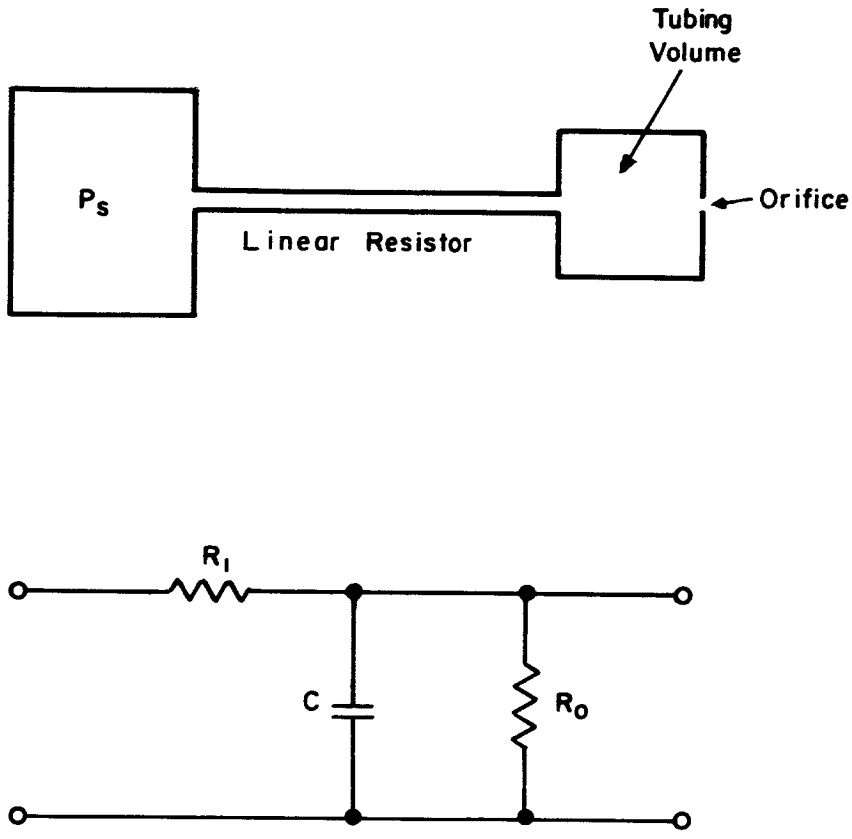

Figure 4.5.4-1 A typical fluid circuit and equivalent circuit.

4.5.5 Phase Delays Associated with Free Jets

In many fluid devices, a jet or fluid stream leaves one portion of the device, say an orifice, and travels some distance before interacting with some other portion of the device or another jet stream. This travel time represents a time delay, and associated with this time delay in a phase delay. The time delay, τ, is given by

$$\tau = L/\bar{u} \tag{1}$$

where L is the distance traveled by the fluid stream and $\bar{u}$ is the velocity with which the stream travels. The phase delay ϕ, associated with this delay is given by

$$\phi = 360\ fL/\bar{u} \tag{2}$$

where ϕ is in degrees, and the frequency f is in cycles per second.

In many air-operated, pure fluid devices the pressure drops across the orifices are such that jets leave the orifices of the device at near sonic velocity (13,600 inches per second). For the special case of an air stream traveling at sonic velocity, the phase delay is

$$\phi = .0264fL \tag{3}$$

This equation has been plotted in Figure 4.5.5-1 for travel distances between 1/10 inch and 1 inch. A useful plot is also obtained by assuming that the jet travels some given distance, say 1 inch, and considering a variety of velocities. Such a plot is given in Figure 4.5.5-2 where the phase delay in degrees per inch of travel is plotted as a function of frequency for a variety of fluid velocities.

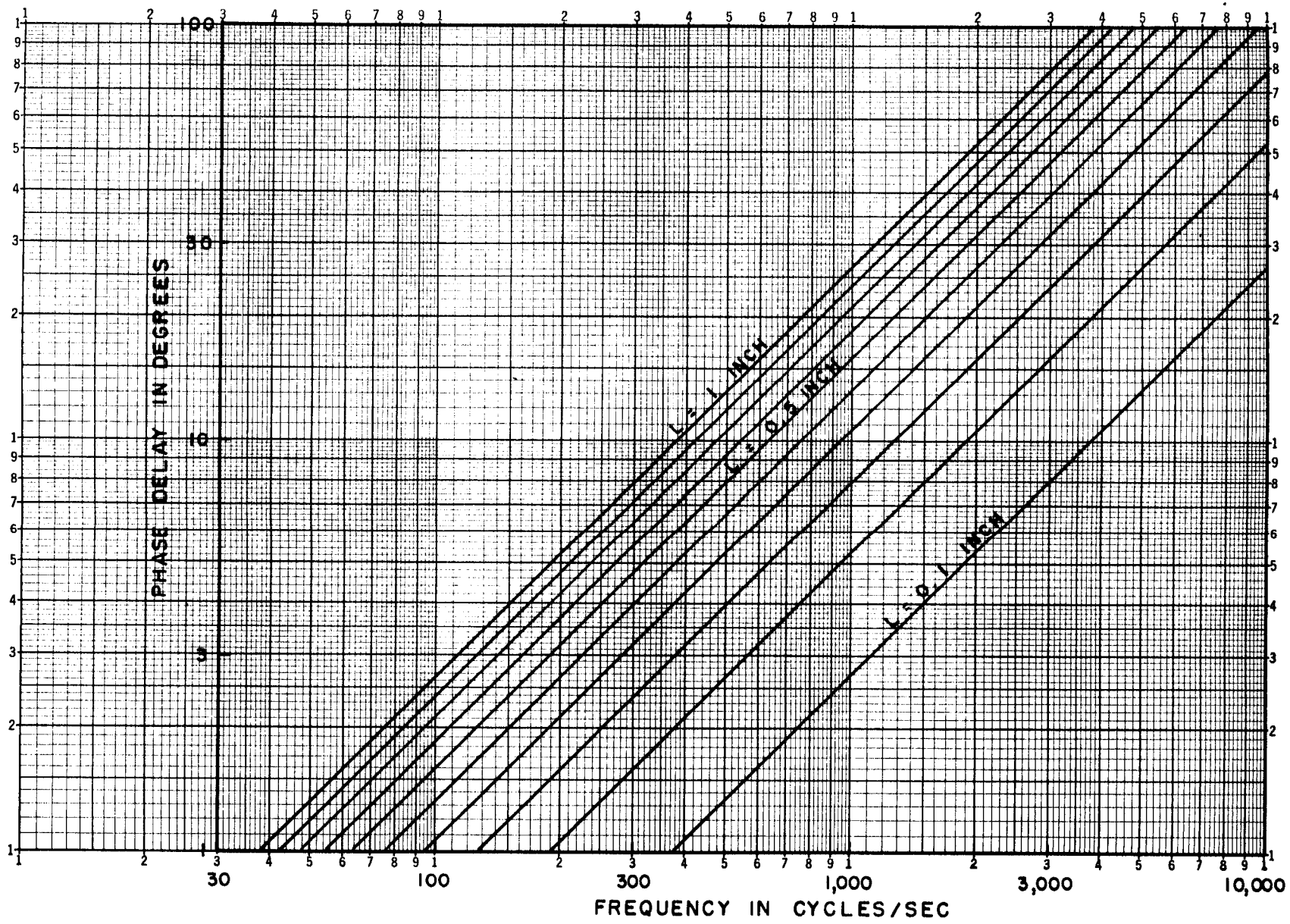

Figure 4.5.5-1 A plot of phase delay of free jets for various travel distances L. The jet is assumed to be moving at the speed of sound in air.

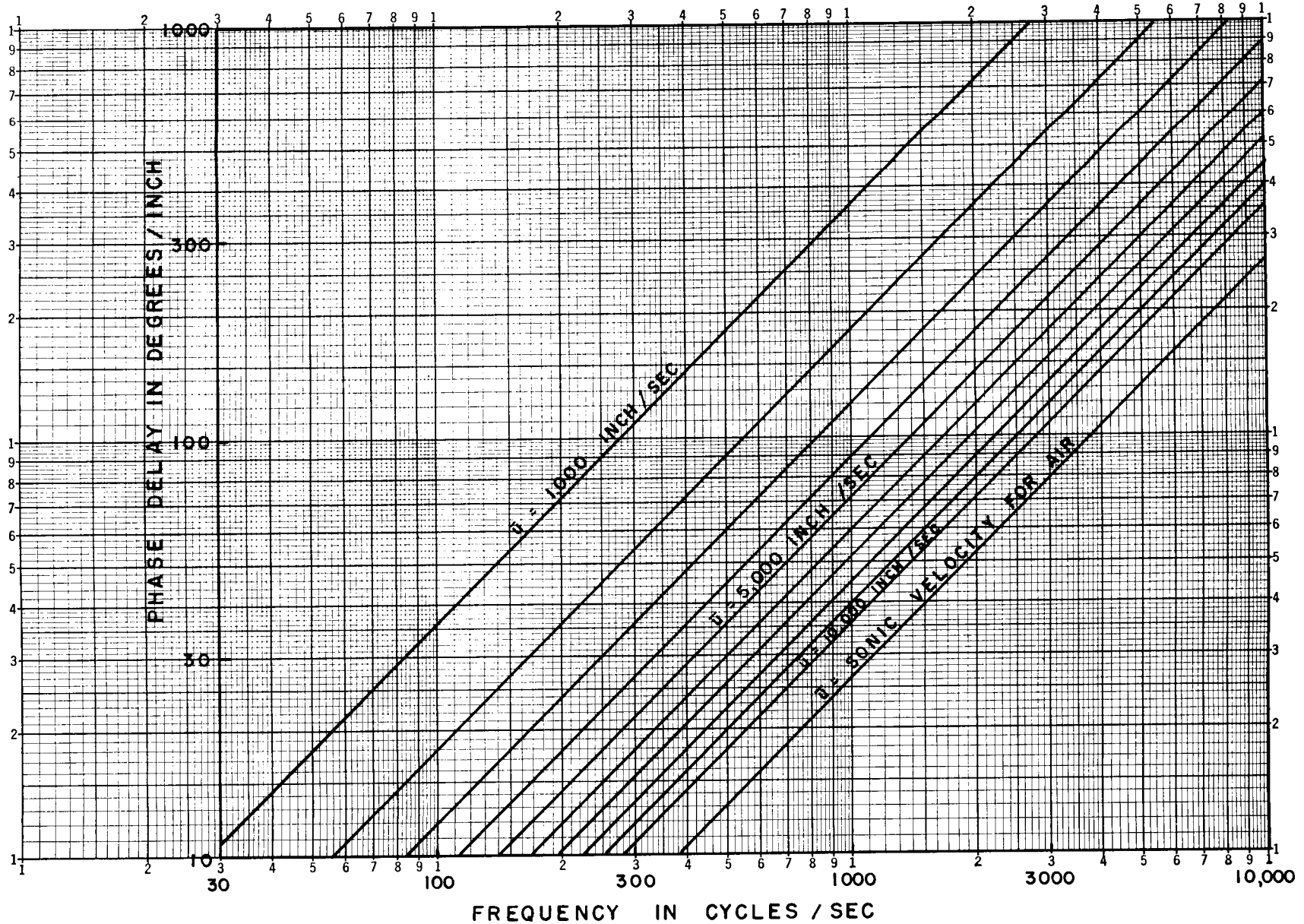

Figure 4.5.5-2 Phase delay of a free jet for various jet velocities.

4.6 Operational Amplifiers and Circuit Synthesis

4.6.1 Operational Amplifiers

An operational amplifier is simply a linear amplifier employing feedback. The input signal is fed to the amplifier through a resistor and the output is a constant times the input signal. The amplification factor is determined by the ratio of the feedback to the input resistor. The use of operational amplifiers in electronic control circuits has found widespread use, and will be equally important in fluid control systems.

The transfer characteristics of an operational amplifier are determined to a great extent by the characteristics of the feedback and input elements. If these elements are linear the gain of the amplifier will be linear, even though the elements, both active and passive, which compose the amplifier are nonlinear. Hence, the emphasis upon obtaining linear fluid resistors.

A great deal of effort has gone into the design and test of operational fluid amplifiers, particularly in the case of the Johnson Service Company who use the Transverse Impact Modulator as the active element in their amplifiers. As a result, the major problems have been solved and excellent operational fluid amplifiers are available. Their design has been discussed in Reference 6.

4.6.2 Circuit Transfer Functions.

A major problem in control circuits is the shaping of the circuit transfer functions such that the circuit is not only stable, but has adequate phase and gain margins. In electronic circuitry, a wide variety of circuitry is available. These provide the circuit designer with a selection of transfer functions which can be incorporated into the control system to give the proper shaping to the overall transfer function. Due to the lack of a pure-fluid, series capacitor, the vast majority of these circuits are not available to the fluid circuit designer. While inconvenient, this is not a major hinderance, since any desired transfer function can be approximated as closely as desired through the use of simple lead and lag circuits. These are obtained through using differentiators and integrators. Both types of circuits have been constructed and tested using pure fluid circuitry.

4.6.3 Integrators.

In electronics a commonly used type of integrator is simply a capacitor which is charged by a current generator. The voltage across the capacitor is used to drive a buffer amplifier. In pure fluid circuitry a different approach to integration is used. One method which has been successfully tried is the "Boot Strap Integrator." Such an integrator uses an operational amplifier, a capacitor to ground, and two summing resistors. A schematic of such an integrator is shown in Figure 4.6.3-1. The design of this circuit is discussed in Reference 6.

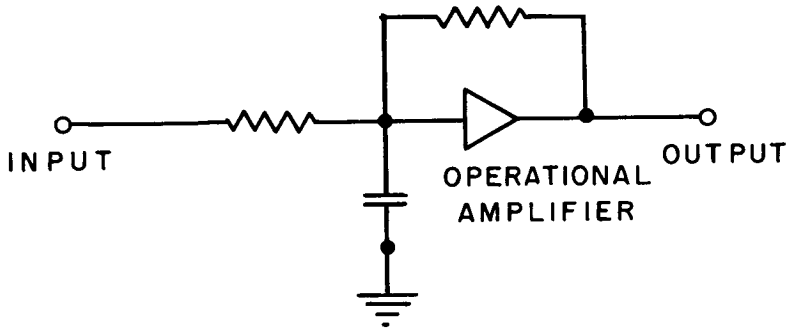

Figure 4.6.3-1 Bootstrap integrator.

4.6.4 Differentiators

A differentiating circuit utilizing an operational amplifier and the transfer function for the differentiating circuit are shown in Figure 4.6.4-1. This circuit is commonly found in electrical analog computers and control systems. Note that a series capacitor is required in the circuit.

In fluid circuits there is no series capacitor which does not involve moving parts. Therefore, in a pure fluid system differentiation must be obtained, or approximated, in some other fashion. One method is through the use of a time delay and a summing circuit. Such a circuit and the approximate transfer function for the circuit is shown in Figure 4.6.4-2.

This transfer function is readily derived. The transfer function of the delay, shown in the upper leg of the diagram in Figure 4.6.4-2, when expanded in a series becomes

$$Ae^{-s} = A(1 - s\tau + s^2\tau^2 + \cdots) \tag{1}$$

Let us consider the case where the delay of the circuit is such that

$$s\tau << 1 \tag{2}$$

When this condition holds the higher order terms in the expansion (1) can be dropped. In terms of frequency, the condition (2) becomes

$$\tau << \frac{1}{2\pi f} \tag{3}$$

In terms of the period $T = 1/f$, the condition is

$$\tau << \frac{T}{2\pi} \tag{4}$$

In words, this means that the delay used in the delay leg of the circuit shown in Figure 4.6.4-2 should be much less than the period, T, of the highest frequency wave which will be used in the circuit.

When the conditions outlined above hold the transfer function for the circuit under consideration become

$$G(s) = B - A + A\, s\tau \tag{5}$$

or

$$G(s) = B - A \quad 1 + \frac{A\, S\tau}{B - A} \tag{6}$$

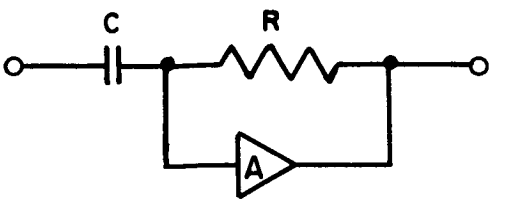

$$G(s) = \frac{ARCs}{\left[\frac{RCs}{1-A} + 1\right](1-A)}$$

Figure 4.6.4-1 A schematic and transfer function for a typical, electronic differentiating circuit.

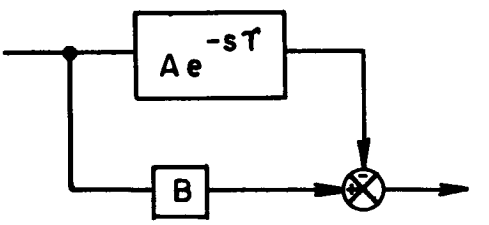

a. Delay and sum circuit

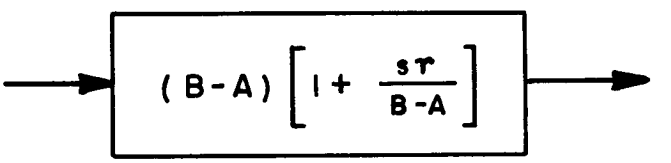

b. Transfer function of delay and sum circuit for small delays

Figure 4.6.4-2 A schematic and transfer function for a differentiating circuit.

This equation is of the form $1 + s\tau'$, which is the transfer function of a differentiating circuit with a corner frequency of $f_c' = 1/2\pi\tau'$, where

$$\tau' = \frac{A\,\tau}{B-A} \tag{8}$$

In terms of break frequencies, this becomes

$$f' = \frac{B-A}{A}\quad f_c \tag{9}$$

where the break frequency f_c is given by

$$f_c = \frac{1}{2\pi\tau} \tag{10}$$

Hence, over limited, but still useful, frequency ranges; differentiating circuits can be approximated through the use of a delay and a summing circuit. The delay could well be the time required for a signal to travel along a fluid tube of some sort, and the summing could be performed using an operational amplifier.

In order to make the gains A and B constant, the two legs involving the gain constant A and B would probably also use operational amplifiers.

5. APPLICATION TO TYPICAL FLUID CONTROL SYSTEM

5.1 Fluid System Description.

In this section the previously introduced concepts shall be applied to the analysis of a typical, fluid control-system. A block diagram of the control system is shown in Figure 5.1-1. In this Figure, a change in the electrical signal to the input transducer results in a change in the output pressure of the transducer. This pressure change is the input signal to the fluid amplifier. The output of the fluid amplifier is fed to a bellows, the output of which goes to a mechanical summing circuit. The output of the mechanical summer operates a valve-actuator package, which moves the load. A linear, position-feedback cam is attached to the load. This cam is a part of a flapper-valve transducer whose function is to linearly translate the position of the feedback cam, i.e. the load, into pressure. This pressure drives a fluid amplifier with a bellows output. This output is mechanically summed with the bellows from the input section of the circuit. This completes the feedback loop.

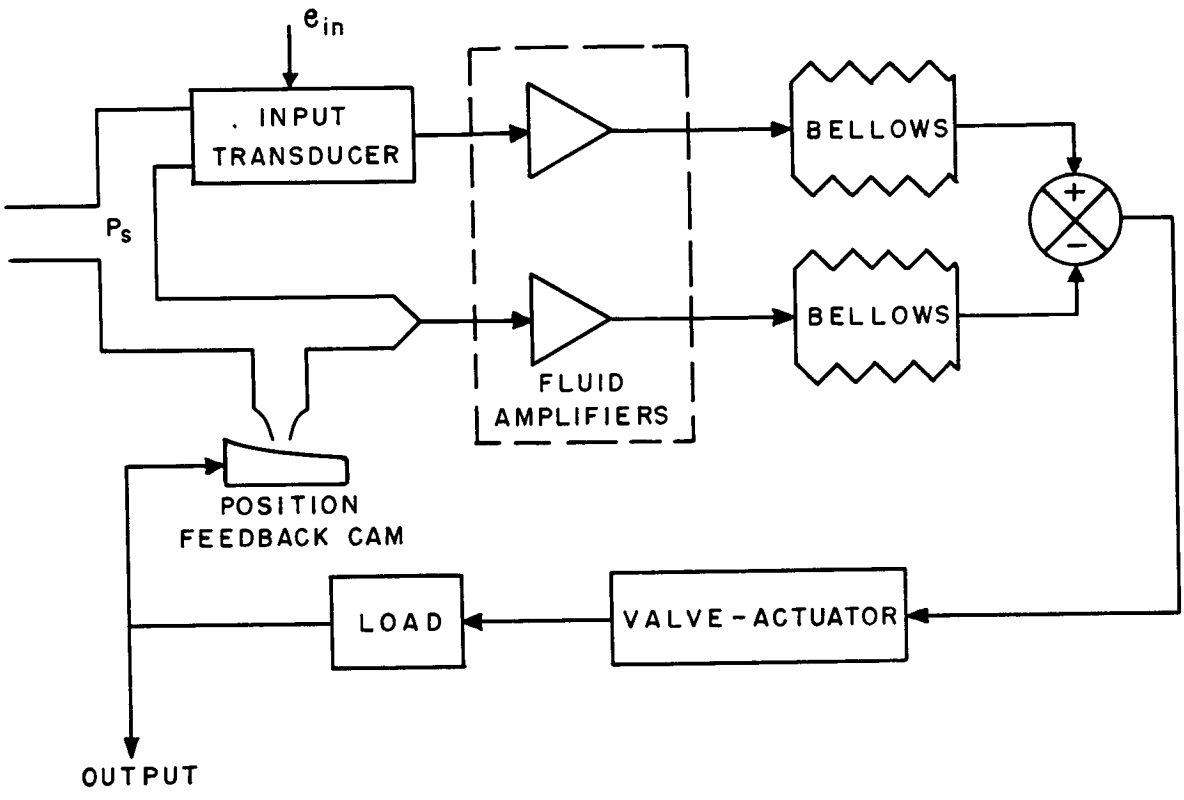

Figure 5.1-1 Fluid control system

5.2 Flapper-Valve Transducer.

The flapper-valve transducer was discussed in Section 4.5.3. As shown in that section, the equivalent circuit is a simple RC network whose transfer function is

$$G(s) = \frac{A}{1 + \tau_1 s} \tag{1}$$

The gain constant A is found by dividing the total, output-pressure change by the total cam displacement causing the pressure change, i.e.,

$$A = \frac{1.037}{3} = 0.346 \text{ psi/inch} \tag{2}$$

The time constant τ_1 depends upon the bandwidth of the circuit. For a central cam position, the break frequency is roughly 900 cycles per second. This corresponds to a time constant of 0.00018 seconds. The transfer function is hence

$$G(s) = \frac{0.346}{1 + 0.00018s} \text{ psi/inch} \tag{3}$$

at the mid cam position.

Let us consider the worst case, namely the narrowest bandwidth. This is seen from Figure 4.5.3-3 to be 260 cycles. This corresponds to a time constant of 0.00061 seconds. The transfer function is hence

$$G(s) = \frac{0.346}{1 + 0.00061s} \text{ psi/inch} \tag{4}$$

for this case.

5.3 Operational Amplifier

The closed loop gain of the operational amplifier is 11. As shown in previous sections, the output impedance of a typical impact modulator is roughly 10^5 fluid ohms. The output impedance of the operational amplifier will then be 10^5 fluid ohms divided by 11, or 9,100 fluid ohms.

Tests at the Johnson Service Company have shown that the bandwidth of an operational fluid amplifier is determined to a large extent by the load applied to the amplifier. In the particular case under consideration, the load is a metal bellows. A typical value for the volume of the bellows would be 0.1 cubic inch. The frequency-characteristics determining circuit of the operational amplifier then becomes 9,100 ohm resistor feeding a capacity representing the 0.1 cubic inch volume. From Figures 2.2.6-3 and 2.2.6-4, the break frequency of this circuit is seen to be 59 cycles per second. This corresponds to a time constant of 0.0027 seconds.

The force output of the bellows will depend upon the pressure within the bellows and the area of the bellows. Considering a bellows area of 2 square inches, the transfer function of the operational amplifier and the bellows becomes

$$G(s) = \frac{22}{1 + .0027s} \quad \text{lbf/psi} \qquad (1)$$

5.4 Valve-Actuator

The transfer function of a pneumatic valve-motor combination which is suitable for a nozzle actuation system was obtained from the Vickers Division of the Sperry Rand Corporation. This transfer function is shown in Figure 5.4-1 and gives the output rpm as a function of the input force in pounds. The first block shows a dead-band of plus and minus 5 pounds with a maximum input of 15 pounds. This, in the equivalent circuit, is transformed into an effective force which feeds a block with a transfer function of 19,200 RPM/sec-lb. The output of this block is an angular acceleration. This is integrated, giving an angular velocity which feeds into a dead-band of $\pm$1,650 rpm. The output of this is the output rpm of the motor. There is feedback around the integrator and the angular velocity dead-band as shown in Figure 5.4-1.

This transfer function, while not complex, includes dead-bands and an accurate analysis would require an analog computer simulation. For our purposes, the circuit analysis will be simplified by ignoring the dead-bands. This is not too unrealistic. The first dead-band, that is the effective force dead-band, is caused by springs in the valve and overlap of the valve. This dead-band could be reduced as much as desired by small changes in the design. Simply lapping the valve closer would be one such change. At the time of this writing it is not known what physically contributes to the rpm dead-band.

In our analysis the dead-bands shall be ignored and the resulting continuous transfer functions shall be used. The 19,200 rpm block is reduced to 320 revolutions/sec^2-lb, revolutions/sec^2 being a more convenient unit to use than RPM/sec.

The resultant equivalent circuit of the valve-motor combinations is shown in Figure 5.4-2. It is readily seen that the overall transfer functions between θ and F of Figure 5.4-2 is given by

$$\frac{\theta}{F} = \frac{1.33}{s(\tau_2 s + 1)} \quad \frac{\text{rev}}{\text{lb}} \tag{1}$$

where τ_2 is equal to 1/24th of a second. This corresponds to a break frequency of 3.8 cycles/second.

The motor will be used to drive (through gearing) a leadscrew, which will move the nozzle. The leadscrew must have a three-inch travel. A 5-threads/inch thread size has been tentatively selected, giving a total of 15 threads on the screw. Calling the angular rotation of the leadscrew θ_S, the transfer function between this and the linear output motion of the nozzle, Y, i.e., the linear travel of a nut on the leadscrew is given by

$$Y = k\,\theta_S \tag{2}$$

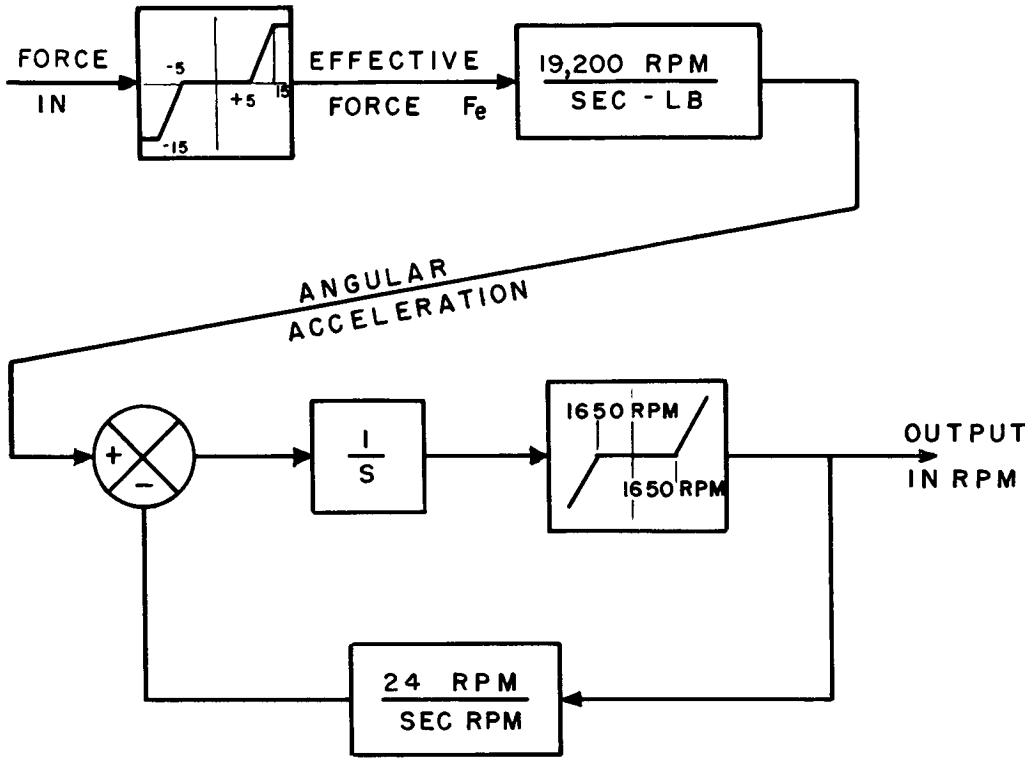

Figure 5.4-1 Equivalent circuit of valve-motor package

From the required 3-inch travel and 15 threads per inch, it is seen that the k of equation (2) is equal to 1/5, or

$$Y = 1/5\ \theta_S \tag{3}$$

From the above, plus considerations of power requirements and maximum speed requirements, it is seen that a gear ratio of 3/16 between the actuator and the leadscrew will be reasonable. Hence,

$$\theta_S = 3/16\ \theta \tag{4}$$

From equations (3) and (4) it is seen that

$$Y = \frac{3}{80}\ \theta \tag{5}$$

which is the transfer function between the linear output motion and the angular travel (in revolutions) of the motor. From this equation, and equation (1) above, the transfer function can be found between the input force which is applied to the valve and the displacement of the nut upon the threadscrew. This, is found to be

$$\frac{Y}{F} = \frac{.05}{S(\tau_2 S + 1)} \quad \frac{\text{inch}}{\text{lb}} \tag{6}$$

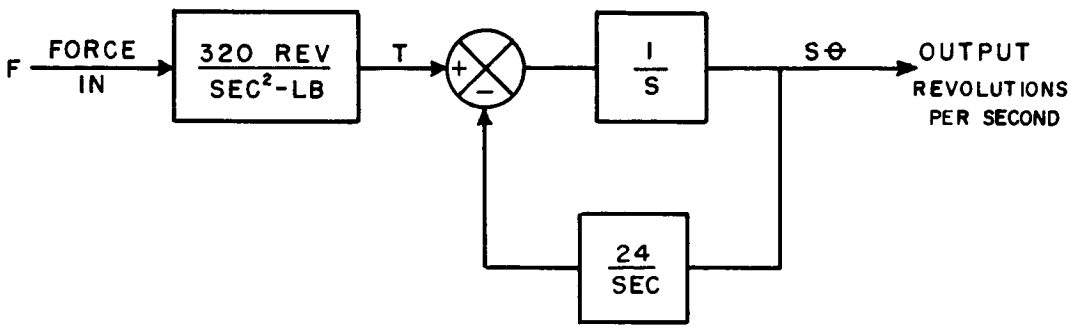

Figure 5.4-2 Simplified equivalent circuit of valve-motor package

5.5 Stability Analysis

The simplified equivalent block diagram of the control circuit is given in Figure 5.5-1. The block containing K_1 is the transfer function of the flapper-valve transducer. The frequency response characteristics of the operational fluid amplifier and the bellows is given by the block containing K_2; and for the circuit under consideration, has a cutoff frequency of about 59 cycles per second. The valve-actuator and load transfer function is represented by the block which is fed by the output of the mechanical summer.

The phase-gain characteristics of the transfer function for the open loop is plotted in Figure 5.5-2. It is seen from this plot that the circuit, as it stands, will have a gain margin of 46 db. and a phase margin of 80 degrees.

No rate feedback is shown in the control loop of Figure 5.5-1. Without a rate feedback of some sort, the response characteristics of the system would be unsatisfactory. The control loop analysed in this section is hybrid, i.e. it contains both pure fluid and mechanical components. The characteristics of the motor in the actuator package are such that a rate feedback cannot be taken directly from the pneumatic motor to the fluid amplifier. Rate feedback can be obtained by differentiating the output of the flapper-valve transducer and then summing this differentiated signal and the direct output of the transducer. This is shown in Figure 5.5-3. The fluid sum shown in this figure would be actually accomplished by applying two inputs to an operational amplifier.

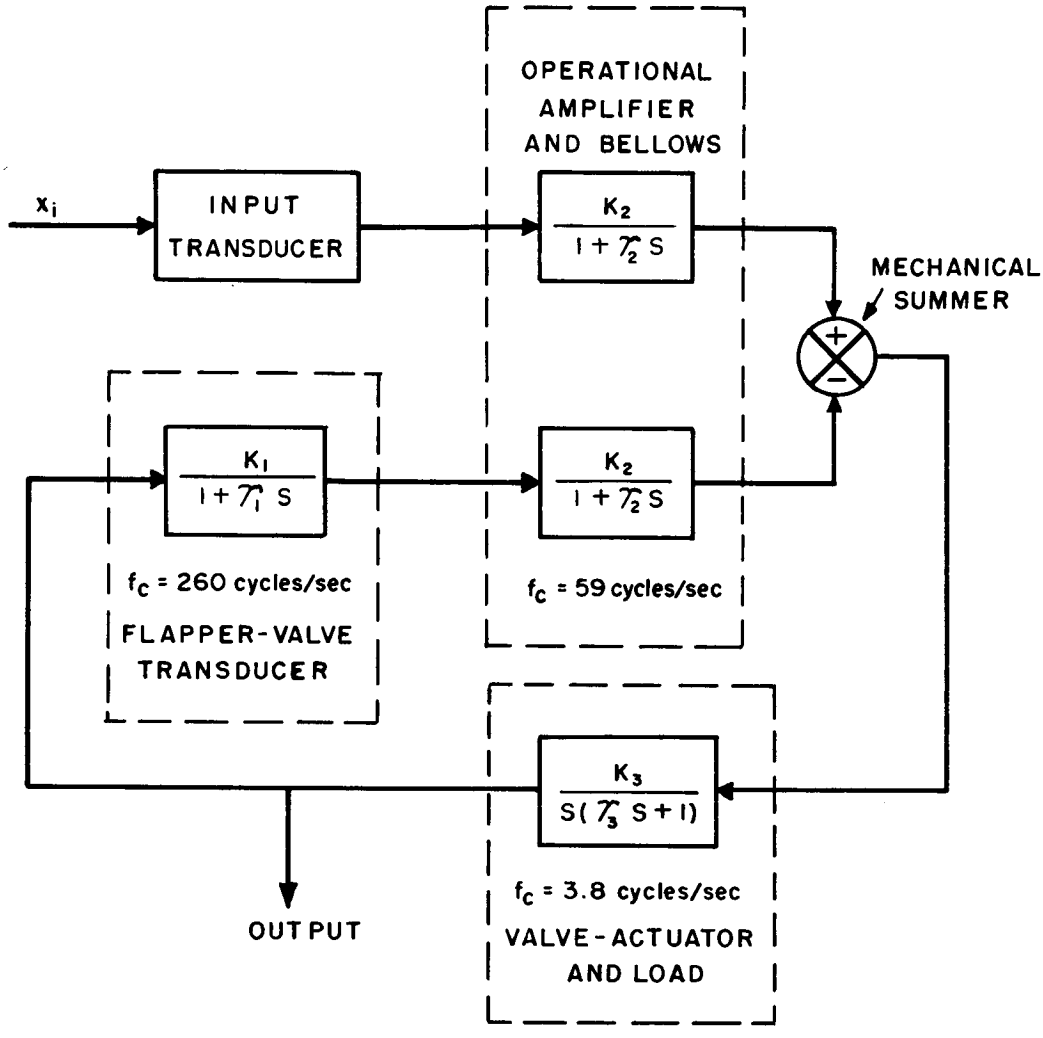

$K_1 = 0.364$ psi/inch
$K_2 = 22$ lbf/psi
$K_3 = 0.5$ in/lbf

$\tau_1 = 0.00061$ sec
$\tau_2 = 0.0027$ sec
$\tau_3 = 0.416$ sec

Figure 5.5-1 Block diagram of control system

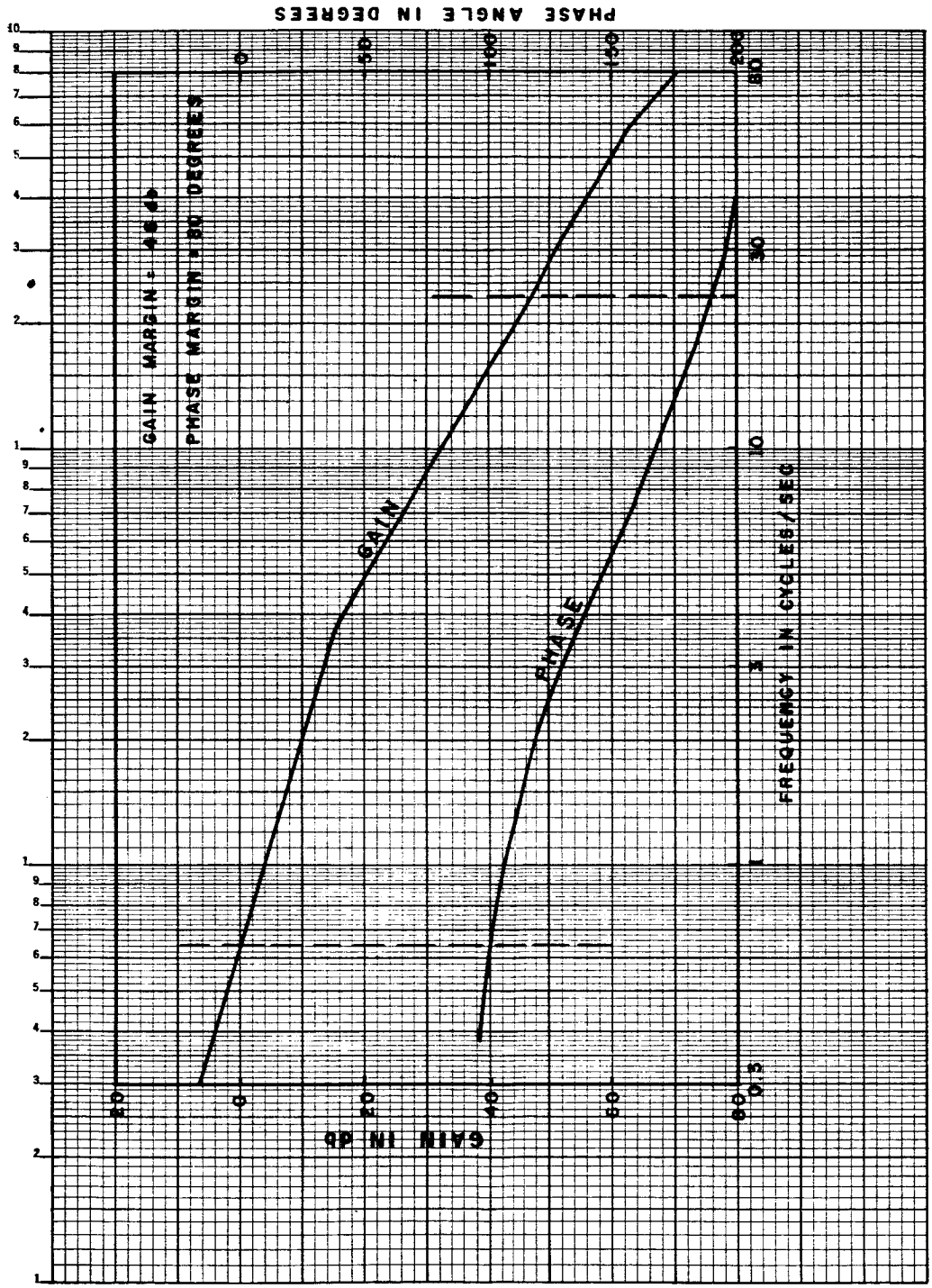

Figure 5.5-2 Bode Plot

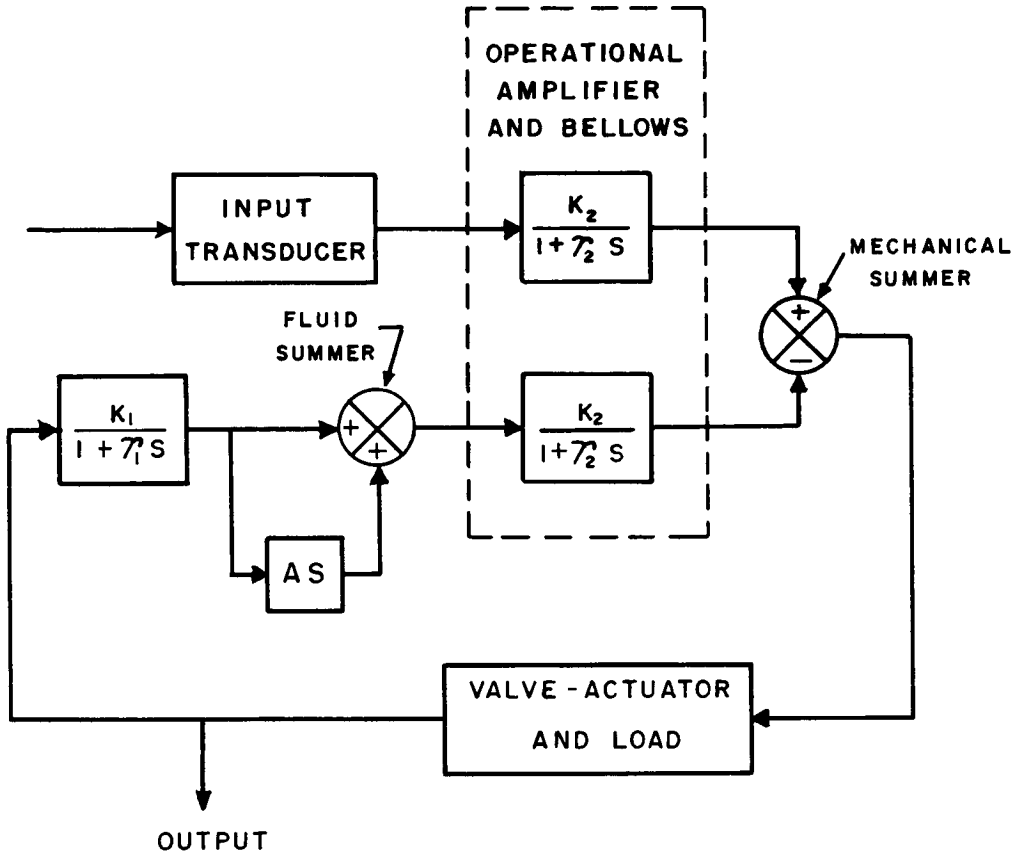

Figure 5.5-3 Rate Feedback Servo

NASA-Langley, 1965